INVESTIGATING THE ROLE OF SPINDLE CHECKPOINT MUTATIONS IN COLORECTAL CANCER

Laura Boyes

Thesis submitted for the degree of Doctor in Philosophy

The University of Edinburgh

2003

Dedication

For my family, particularly my mum, for all their love and support and for believing I could do it even when I didn't believe it myself.

Declaration

I declare that this thesis was composed entirely by myself and that the research presented is my own unless otherwise stated.

Laura Ann Boyes August 2003

The following publication derived from the research presented in this thesis:

Boyes L., Hardwick K., Dunlop M.G., Farrington S.M. (2003).
Functional analysis of colon cancer associated spindle checkpoint mutations in Saccharomyces cerevisiae. Proc. Amer. Assoc. Canc. Res., *44*:A114.

The following presentations derived from the research presented in this thesis:

Boyes L., Hardwick K., Dunlop M.G., Farrington S.M. (2003).
Functional analysis of colon cancer associated spindle checkpoint mutations in Saccharomyces cerevisiae. AACR 94th Annual General Meeting, Washington, US.

Boyes L., Reinhardt D., Dunlop M.G. and Farrington S.M. (2001).
Identification of mitotic check-point gene mutations in colon tumours.
EMBO Workshop on G2/M progression and associated checkpoints, Salamanca, Spain.

Boyes L., Reinhardt D., Dunlop M.G. and Farrington S.M. (2000).
The role of mitotic check-point genes in aneuploid colorectal tumours.
Proceedings of UK Molecular and Cell Biology Network - Genes and Cancer Conference, Warwick, UK.

Farrington S.M., **Boyes L.**, Reinhardt D. and Dunlop M.G. (2000).
Defects causing aneuploidy in Scottish colorectal cancer patients.
Scottish Society for Experimental Medicine, Western General Hospital, Edinburgh, UK.

Abstract

Genomic instability and more specifically aneuploidy, is a phenotype exhibited by the majority of colorectal tumours and is associated with poor prognosis. It has been hypothesised that mutations in genes involved in chromosome segregation and mitotic checkpoints may contribute to aneuploid phenotypes in colon tumours. In support of this hypothesis deletions and missense mutations in spindle checkpoint genes *BUB1* and *BUBR1* have previously been reported in non-diploid colon cancers with defective mitotic checkpoints, which also display chromosomal instability.

We identified a deleted *BUBR1* transcript in 25% of a panel of aneuploid colorectal tumours. The deletion, termed ΔE5, removes a protein domain that is conserved between BUB1 and BUBR1 in humans and yeast and in which mutations have previously been reported. We set out to determine the functional effects of this deletion in a yeast model system and *in vivo* with human cell lines.

Constructs of the deleted forms of the genes were created in the *S.cerevisiae* homologues, *BUB1* and *MAD3*. The functional effects of expressing the deleted Bub1p and Mad3p proteins in strains null for the respective gene were studied with respect to microtubule poison sensitivity, chromosome loss and spindle checkpoint activity. Parallel control experiments used full-length gene constructs. We show that cells expressing deleted proteins are more sensitive to microtubule poisons than those expressing the full-length protein. Both the *MAD3* and *BUB1 ΔE5* mutants show a chromosome loss phenotype indicative of a defect in chromosome segregation. We observed a more severe phenotype in *BUB1 ΔE5* deletion mutants, consistent with the chromosome loss phenotype seen in a *bub1* null strain. This suggests that *BUB1* may play a more significant role in mitosis than *MAD3* in the yeast system. Using an assay of individual cell growth in the presence of microtubule poisons, we show that the *MAD3* deletion mutant results in a defective mitotic checkpoint. An assay to specifically investigate spindle checkpoint function in the *BUB1 ΔE5* mutant, revealed a similar abrogation of the spindle checkpoint. Next, we investigated the ability of the mutant proteins to form spindle checkpoint complexes and found that both Mad3p and Bub1p ΔE5 proteins have reduced binding to Bub3p compared to the full-length protein. The proportion of the Mad3p ΔE5 protein found in

complexes with Cdc20p and Mad2p is also reduced. Furthermore, phosphorylation of the Bub1p ΔE5 mutant protein is markedly altered.

We initiated further experiments aiming to develop an in vivo system in diploid human cell lines to investigate the effect of the *BUBR1ΔE5* mutation on mitotic checkpoint function and spindle protein complex formation.

The data presented in this thesis show that mutations of *BUB1* and *BUBRI* identified in colorectal cancers, involving protein domains with considerable amino acid sequence similarities, substantially abrogate the spindle checkpoint and cause chromosome segregation defects in *S.cerevisiae*. These findings have relevance to understanding the nature of aneuploidy, chromosome mis-segregation and genomic instability in colorectal tumour cells.

Acknowledgements

The completion of this thesis has relied on help and support from many sources. I'd like to thank Malcolm Dunlop for donating some of his limited time and his unlimited bright ideas and Susan Farrington for masses of encouragement, for many an evening spent proofreading this thesis and for letting me play with her monster. There must also be big thanks to all the other members of the lab, too numerous to mention, over the past four years for plying me with gin and tonics, appreciating my cakes and generally keeping me sane during the tough times. Additional thanks must go to Sandy Bruce and Douglas Stuart for photographing and printing many yeasties and to Peter Teague and Andrew Carothers for statistical assistance.

I also extend a big thank you to all of the Hardwick group for making me feel at home in their lab while they must have been wondering if I would ever leave! Kevin for cheerfulness, advice and patience when faced with stupid questions, Michelle for teaching me about all things yeasty and generally being fab, Emma for late night sing-a-longs and Vincent and Vicky for keeping me amused with their belly dancing.

On a more personal note, thanks to the many friends who made my time in Edinburgh so much fun: Cherie for many a beer and footie match, and some of the most stonking hangovers ever; Ben and Jenny for feeding me, ER nights and lending me a telly when I needed it most and, as for Keith and Andrew, well, Go you Big Red Fire Engine. Also thanks to all the Nottingham gang for a record number of funny email conversations, for travelling miles to visit me and for their underhand tactics in canal boat racing although on that, I for one shall be keeping an open mind.

Thanks to Stuart for his love of football and of me, not necessarily in that order for selective thesis advice and keeping me company through the dark writing hours.

The biggest gratitude of all goes to my family; Mum, Peter, Stephen, Nikki, Dad, Lynn, Chloe, Holly, Nannie and Roo. Corny as it sounds, without you this thesis would never have been completed. Thanks to Peter and Stephen for sharing (and nurturing) my football (and Michael Owen) obsession, Nikki for taking me to the best bars where my little star Owen can be found and for making my pictures look less like mosaics, Mum for helping me keep the phone companies in business single handed and for being proud and Dad for many a holiday. Most of all, thank you all for making me stick at it, keeping me sane and an immeasurable amount of love, support and faith. You are the best.

Preface

You'll Never Walk Alone

When you walk through a storm
Hold your head up high,
And don't be afraid of the dark.
At the end of a storm,
There's a golden sky,
And the sweet silver song of a lark.
Walk on through the wind, Walk on through the rain,
Though your dreams be tossed and blown...
Walk on, walk on, with hope in your heart,
And you'll never walk alone...
You'll never walk alone.

Abbreviations

ALL	Adult leukaemia/lymphoma
AML	Adult myeloid leukaemia
APC	Adenomatous polyposis coli
APC/C	Anaphase promoting complex
ATL	Adult T cell leukaemia
ATLL	Adult T-cell leukaemia / lymphoma
BER	Base excision repair
BrdU	Bromodeoxyuridine
BUB	Budding uninhibited by benzamidazole
BUBR	BUB-related
C.elegans	Caenhorrhabditis elegans
CD	Conserved domain
CDK	Cyclin dependent kinase
CDKI	Cyclin dependent kinase inhibitor
CIN	Chromosomal instability
CML	Childhood myeloid leukaemia
COX	Cycloxygenase
CRC	Colorectal cancer
CRUK	Cancer research UK
cyc	Cyclin
dH_20	Distilled water
DMSO	Dimethyl sulphoxide
DNA	De-oxyribonucleic acid
dNTP	Deoxy nucleotide triphosphate
ECL	Enhanced chemiluminescence
E.coli	*Escherichia coli*
EDTA	Ethylenediaminetetra-acetic acid
EGFP	Enhanced green fluorescent protein
ES	Embryonic stem
FACS	Fluorescent activated cell sorting
FAP	Familial adenomatous polyposis
FCS	Foetal calf serum
GFP	Green fluorescent protein
GST	Glutathione S-transferase
HCl	Hydrochloric acid
HGU	Human genetics unit
HNPCC	Hereditary non-polyposis colorectal cancer
HNSCC	Head an neck squamous cell carcinoma
HPV	Human papilloma virus
HRP	Horse raddish peroxidase
HTLV	Human T-cell leukaemia virus
ICMB	Institute of cellular and molecular biology
LPP	Lambda protein phosphatase
MAD	Mitotic arrest deficient
MCC	Mitotic checkpoint complex

MCS	Multiple cloning site
MEN	Mitotic exit network
MIN	Microsatellite instability
MMR	Mismatch repair
MNNG	N-methyl-N'nitro-N-nitroguanidine
MPF	Mitosis promoting factor
MRC	Medical research council
NaOH	Sodium hydroxide
NER	Nucleotide excision repair
NSAID	Non-steroidal anti-inflammatory drugs
NSCLC	Non small-cell lung cancer
OD	Optical density
PAGE	Polyacrylamide gel electrophoresis
PBS	Phosphate buffered saline
PCR	Polymerase chain reaction
PEG	Poly ethylene glycol
PhIP	2-amino-1-methyl-6-phenylimidazo[4,5-b]pyridine
PTTG	Pituitary tumour transforming gene
RNA	Ribonucleic acid
RNAi	RNA inhibition
RT-PCR	Reverse transcriptase PCR
S.cerevisiae	*Saccharomyces cerevisiae*, budding yeast
S.pombe	*Saccharomyces pombe*, fission yeast
SDS	Sodium dodecyl sulphate
SIN	Septation initiation network
SNP	Single nucleotide polymorphism
SV40	Simian virus 40
TAE	Tris acetate EDTA
TEV	Tobacco etch virus
TRE	Tetracycline responsive element
tRNA	Transfer RNA
UTR	Untranslated region
UV	Ultra violet
WT	Wilm's tumour
YMM	Yeast minimal media
YPD	Yeast peptone dextrose
YPDA	Yeast peptone dextrose adenine

Table of Contents

List of Tables and Figures

Chapter 1: Introduction

1.1 Cancer

Cancer is the second biggest killer of humans after heart disease. 1 in 3 people will be diagnosed with cancer at some point in their lifetime and 1 in 4 will die from cancer (CRUK: www.cancerresearchuk.org/aboutcancer/statistics/?version=3). Cancer occurs more frequently in older people with 65% of cases occurring in the over 65s. Thus the incidence of cancer increases as advances in medical science reduce early mortality and prolong life expectancy.

1.1.1 Colorectal Cancer

Colorectal cancer (CRC), including cancers of the colon and rectum, is a major public health problem in developed countries. It is the third most commonly diagnosed cancer and the second most common cause of cancer mortality (CRUK: www.cancerresearchuk.org/aboutcancer/statistics/?version=3; ISD Scotland: www.show.scot.nhs.uk/isd/index.htm). There are 0.5 million cases world wide each year and 31,000 cases in the UK, with more than 20,000 deaths annually (Farrington, 2003). Despite improvements in research, surgery and clinical management, the number of cases of CRC in Scotland has increased by 22.8% in males and 2.4% in females between 1989-1999. The 5-year survival rate in Scotland is only 44.6% (ISD Scotland; www.show.scot.nhs.uk/isd/index.htm).

1.1.2 Environmental and Genetic Factors in Colorectal Cancer

Colon cancer is predominantly a disease of the Western world and age-standardised rates suggest that bowel cancer is fifteen times more common in industrialised countries than in developing countries (Burkitt, 1971; Parkin et al., 1999) indicating that there are environmental factors involved. Studies of migrants from countries with low incidence to those with high incidence show they attain cancer rates similar to their adoptive countries within a single generation (Haenszel, 1961; Stemmermann, 1970; McMichael and Giles, 1988). In most cases these migrants have accepted the dietary habits of their adopted countries indicating that differences in incidence rates may be explained at least in part by dietary factors. Numerous studies have examined the effects of diet and lifestyle on colorectal cancer

and these are extensively reviewed elsewhere (Gertig and Hunter, 1998; Potter, 1999).

To summarise these publications they suggest an association between the incidence of colorectal cancer and low dietary consumption of un-absorbable fibre and refined carbohydrate due to an increased bowel transit time and increase in faecal carcinogen concentrations (Burkitt, 1971; Willett, 1989; Trock et al., 1990; Levi et al., 1999). A recent study of 520,000 individuals in 10 European countries found an inverse relationship between dietary fibre intake and colorectal cancer and estimated a doubling of dietary fibre in populations with low fibre intake could reduce colorectal cancer risk by 40% (Bingham et al., 2003). In addition, some studies suggest a link between red meat consumption and colorectal carcinogenesis explained in terms of its fat content, bile acid production and development of carcinogens through cooking (Willett, 1989; Willett et al., 1990; Giovannucci et al., 1994; Levi et al., 1999). However these dietary studies are still speculative and further studies have questioned these correlations (Giovannucci et al., 1994; Goldbohm et al., 1994; Franceschi et al., 1997). Other factors have also been associated with an increased risk of colorectal cancer including alcohol consumption, lack of physical activity and smoking (Longnecker et al., 1990; Levi et al., 1999; Le Marchand et al., 1997). Long-term aspirin and Non-steroidal anti inflammatory drug (NSAID) intake has been shown to have a protective effect on colorectal cancer risk mediated through inhibition of cycloxygenase (COX) enzymes and induction of NF-κB anti tumour activity (Muscat et al., 1994; La Vecchia et al., 1997; Williams et al., 1999; Stark et al., 2001). Despite evidence that environmental factors are important in the development of CRC, the potential for manipulation of these factors for prevention needs to be more clearly defined.

The multifactorial aetiology of CRC involves genetic susceptibility as well as environmental factors. Recent advances in genetics and medicine have allowed significant progress in understanding the molecular events involved in CRC susceptibility and clinically impacting on the disease. Evidence suggests that 20-25% of CRC has a familial component and common genetic changes involved in sporadic CRC have also been elucidated (Fearon and Vogelstein, 1990). About 3% of CRC is associated with early onset syndromes due to mutations in high penetrance

genes (Bonelli et al., 1998; Dunlop et al., 2000; Farrington et al., 1998; Groden et al., 1991; Parkin et al., 1999).

Hereditary Non-polyposis colorectal cancer (HNPCC), is an early onset autosomal dominant condition accounting for almost 3% of cancers of the colon and is associated with germline mutations in Mismatch Repair (MMR) genes (Dunlop et al., 2000; Mecklin et al., 1995; Lynch and de la Chapelle, 1999; Aaltonen et al., 1993; Aaltonen et al., 1998). Affected family members inherit a mutant allele in one of the MMR genes; *MLH1, MSH2, MSH6* and more rarely *MLH3* and *PMS2* and one wild type allele. During early tumour development the wild type allele is somatically mutated, resulting in complete inactivation of the MMR system. This leads to a characteristic mutator phenotype in which short repeated sequences, microsatellites, which are more susceptible to mismatches, are altered in length and sequence showing a microsatellite instability (MIN) phenotype. The mutator phenotype leads to the rapid accumulation of somatic mutations which initiate and accelerate tumour progression. HNPCC patients therefore develop CRC prematurely at an average age of 45, more than 2 decades earlier than the general population (Peltomaki, 2001). The relative cancer risk for HNPCC carriers approaches 100% with a favourable five year survival rate of 65% compared to 44% for those with sporadic CRC (Dunlop et al., 1997; Sankila et al., 1996). Other early onset cancer syndromes are also associated with MMR and MIN defects including Turcots syndrome, characterised by the occurrence of brain tumours, colorectal cancers and adenomas (Turcot et al., 1959) and also Muir-Torre syndrome which manifests as the coincidence of sebaceous skin tumours and internal malignancy (Muir et al., 1967; Torre, 1968).

Familial Adenomatous Polyposis (FAP) is another high risk early onset CRC syndrome which results from germline mutations in the adenomatous polyposis coli (*APC*) gene and is characterised by hundreds to thousands of benign polyps which develop in the colon at an early age. The frequency and early onset of these polyps invariably results in the progression of one or more to malignancy. FAP is a relatively rare condition and germline *APC* mutation carriers account for less than 1% of CRC (Groden et al., 1991; Joslyn et al., 1991; Kinzler et al., 1991; Nishisho et al., 1991; Kinzler and Vogelstein, 1996; Bisgaard et al., 1994; Farrington and Dunlop, 2001).

Recently germline mutations have been identified in *MUTYH*, a Base Excision Repair (BER) gene in a multiple adenoma syndrome estimated to be responsible for 1-3% of CRC (Al Tassan et al., 2002; Jones et al., 2002; Sieber et al., 2003; Halford et al., 2003). Mutations in *MUTYH* are now thought to be involved in a polyposis syndrome due to defects in oxidative damage which is prevelant in the gut. This may promote unrepaired somatic lesions in genes such as *APC* producing the FAP-like phenotype. Interestingly the pathogenic mutations identified are bi-allelic and *MUTYH* mutations appear to act in a recessive manner to compromise BER and increase cancer risk (Jones et al., 2002).

Other hereditary disorders associated with colon cancer include Puetz-Jeghers syndrome, Cowden's disease and Juvenile polyposis (Liaw et al., 1997; Lynch et al., 1997; Howe et al., 1998). These syndromes and their occurrence are summarised in table 1.1.

Table 1.1 Hereditary Disorders Associated with Colon Cancer

Hereditary Disorder	Genes commonly involved	Proportion of heritable CRC	References
HNPCC	MLH1, MSH2, MSH6,	Up to 3%	Dunlop et al., 2000
Muir Torre	MLH1, MSH2	Very rare	Muir, 1966; Torre, 1997
FAP	APC, β-Catenin,	<1%	Farrington et al., 2002;
Multiple adenoma phenotype	MUTYH	1-3%	Halford et al., 2003
Peutz-Jehgers syndrome	STK1	<0.01%	Lynch et al., 1997
Cowden's disease	PTEN		Liaw et al., 1997
Juvenile polyposis	PTEN, SMAD4		Howe et al., 1998
Turcot syndrome	APC, MMR	Very rare	Foulkes et al., 1995

In addition to these early onset disorders, which account for only about 3% of CRC (Parkin et al., 1999), there is evidence that other somatic gene mutations arise during sporadic colorectal tumour development. The accumulation of these mutations through sequence mutation or chromosomal abnormalities is important in the initiation and progression of tumourigenesis from adenoma to carcinoma (Vogelstein et al., 1988; Lengauer et al., 1998; Fearon and Vogelstein, 1990; Kinzler and Vogelstein, 1996; Boland, 2000). A series of genetic alterations lead to progressive disregulation of the mechanisms controlling cell growth. It has been proposed that the mutation of at least five genes is necessary for the formation of a malignant tumour (Fearon and Vogelstein, 1990). The accumulation of the changes appears to be more important than the order in which they occur but some mutations are consistently associated with particular stages of the adenoma to carcinoma pathway such as early mutation of *APC* (Kinzler and Vogelstein, 1996; Boland, 2000). Mutation of *C-K-RAS* and mutation or loss through chromosomal rearrangements of *p53*, *DCC* and *APC* are frequently observed in CRC (Vogelstein et al., 1988; Delattre et al., 1989; Fearon and Vogelstein, 1990). These changes are accompanied by aneuploidy in most cases (Fearon and Vogelstein, 1990). This tumourigenesis model is summarised in figure 1.1.

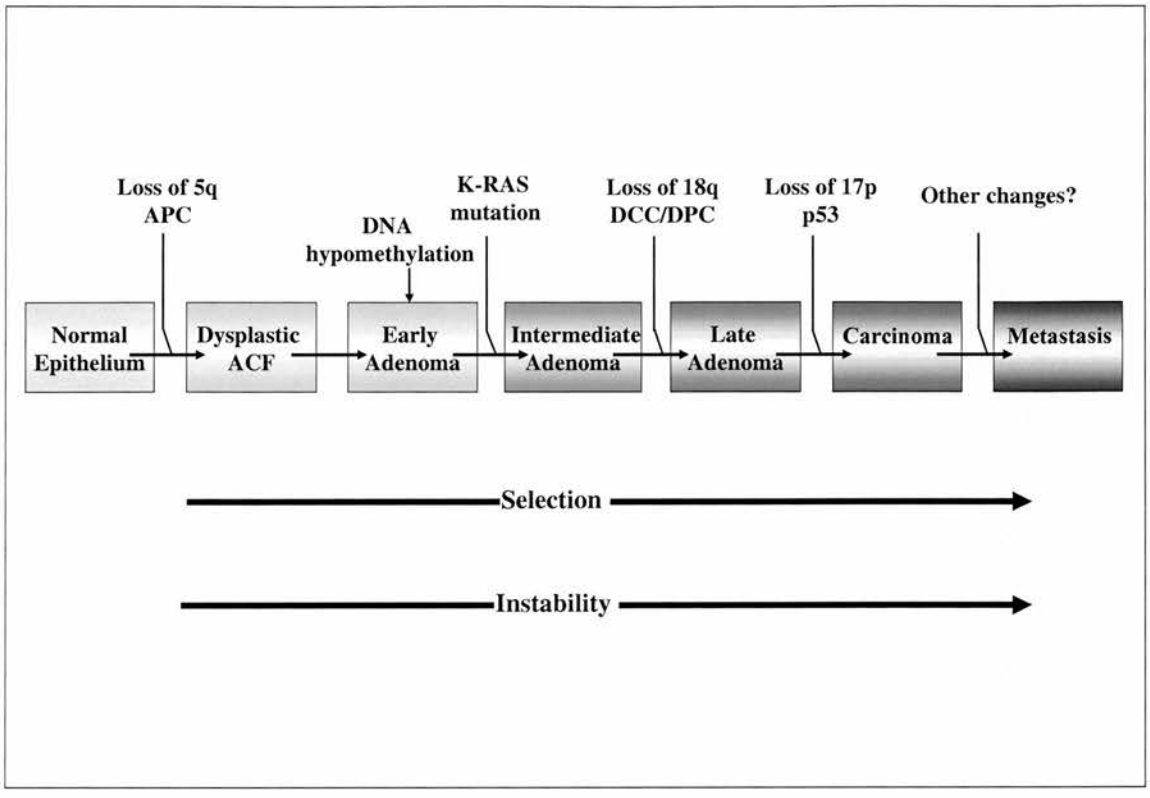

Figure 1.1 Genetic changes associated with the adenoma to carcinoma sequence of colorectal cancer.

Tumourigenesis proceeds through a series of genetic changes in oncogenes such as K-ras and tumour supressor genes such as APC, DPC and p53.The accumulation of sequential mutations causes the development of Aberrant Crypt Foci (ACF), the precursors of adenomas and progression through stages of adenoma development where tumours increase in size, dysplasia and villous content. The overall accumulation of changes is of greater importance than the order of changes. Both selection for growth advantage and genetic instability drive this process. (Figure adapted from Fearon and Vogelstein, 1990 and Kinzler and Vogelstein, 1996).

1.1.3 Selection and Mutation in Tumourigenesis

It is clear that the accumulation of genetic mutations is important in both familial and sporadic colorectal cancer but there is much debate on the mechanisms by which high frequencies of mutations accumulate in colorectal tumours. It is widely accepted that the progression from adenoma to carcinoma results from successive waves of clonal expansion and accumulation of genetic defects through cycles of cell division (Nowell, 1976). However, the relative importance of selection for growth advantage versus a mutator phenotype and genetic instability is still unclear. Loeb, originally proposed that early mutation of genes involved in protecting the stability of the genome, such as those involved in DNA repair or replication would invoke a mutator phenotype necessary for tumour progression (Loeb, 2001). A population of cells with a variety of mutations would result from the elevated mutation rate and cells with mutations in genes involved in the control of cell division, invasion, metastasis and apoptosis would preferentially survive selection pressures. This model would explain the disparity between the mutation rate in normal cells and the elevated frequency of mutations seen in CRC (Loeb et al., 1974; Peinado et al., 1992; Lengauer et al., 1998; Loeb, 2001). The presence of mutations in such mutator genes in both familial and a subset of sporadic CRC supports this theory (Borresen et al., 1995; Ma et al., 2000).

Contradictory to the mutator hypothesis, Tomlinson and Bodmer argue that selection for growth advantage is the initiating step in tumourigenesis and is sufficient alone to explain tumour formation (Tomlinson and Bodmer, 1999; Tomlinson et al., 1996). They provide evidence that mutations in cancer genes such as APC occur earlier in tumours than MMR defects and thus an increased mutation rate does not drive tumour initiation (Homfray et al., 1998). In this model mutations which confer the strongest selection advantage to the tumour cell rather than those which raise the intrinsic mutation rate are the most frequently seen in tumours. In support of the selection model it has been noted that an increased mutation rate may cause apoptosis (Cahill et al., 1999; Tomlinson and Bodmer, 1999) and also that mutations in Nucleotide Excision Repair (NER) and Base Excision Repair (BER), which would also confer a mutator phenotype, are rarely seen in sporadic tumours (Wu et al., 2003; Halford et al., 2003). This is disputed by further analysis of *APC*

mutation status in tumours showing MIN and those which are stable. A higher proportion of the MIN tumours harboured frameshift mutations in APC than the stable tumours, indicating *APC* mutation is a secondary event promoted by earlier mismatch repair defects (Huang et al., 1996).

It is likely that both a raised mutation rate through genetic instability and selection for a growth advantage contribute to CRC development but the relative contribution of these factors is unclear.

1.2 Genetic Instability in Colorectal Cancer

1.2.1 Microsatellite Instability Versus Chromosomal Instability

Genetic instability is a characteristic of almost all human tumours and is probably important in their initiation and progression (Lengauer et al., 1998). There are 2 types of genetic instability; DNA sequence or Microsatellite Instability (MIN) and Chromosomal Instability (CIN). The two types of instability rarely co-exist in tumours although some recent studies suggest they are not necessarily independent and there may be some overlap (Goel et al., 2003). MIN tumours are generally diploid with rates of gross chromosomal change similar to normal cells whereas CIN tumours are MMR proficient but are generally aneuploid with increased rates of chromosomal change. This indicates that either MIN or CIN provides the genetic instability to promote mutation and drive progression in each tumour (Orr-Weaver and Weinberg, 1998; Lengauer et al., 1997; Lengauer et al., 1998). Thus instability, be it microsatellite or chromosomal, increases as tumours grow and progress to malignancy in an exponential manner (Lengauer et al., 1998). This can lead to further genetic instability in the form of chromosome translocations and gene amplifications as genes involved in recombination and DNA double strand break repair such as *p53*, *ATM* and the *BRCA* genes become disrupted (Lengauer et al., 1998). In addition genetic instability can disrupt genes involved in recognising DNA damage and initiating apoptosis, such as *p53*, contributing further to the exponential effect. In fact the inactivation of protective apoptosis is probably an essential step in tumourigenesis. Genetic instability also has the effect of promoting heterogeneity

between different tumours and between individual cells of a single tumour, which presents a problem for cancer therapy (Lengauer et al., 1998).

DNA sequence instability is produced by defects in DNA repair and replication mechanisms such as NER, BER and MMR and results in changes in the nucleotide sequence of individual genes (Lemos et al., 2000; Dunlop et al., 2000; Peltomaki et al., 2001). Sporadic colorectal tumours with DNA sequence instability are relatively rare. About 13% of CRC have MMR defects and these show a characteristic microsatellite instability phenotype as discussed previously (Peinado et al., 1992; Lengauer et al., 1998).

Chromosomal Instability can be viewed cytogenetically as the loss, gain and translocation of chromosomes and is seen in the majority of CRC (Lengauer et al., 1998). CIN produces an imbalance in the number of chromosomes per cell, a phenotype known as aneuploidy (Nowak et al., 2002). The full significance of CIN in tumour progression has been debated. It has been argued that CIN may be a result of the abnormal growth and structure of a cancer cell rather than a cause. This is contradicted by evidence that MIN/MIN cell fusions remain chromosomally stable, arguing against non-specific factors (Lengauer et al., 1997). Additionally some precancerous colorectal lesions show aneuploidy suggesting it is an early event in tumour initiation (Fischbach et al., 1991). CIN is proposed as an alternative to specific gene mutation in the initiation of carcinogenesis by producing mass accumulation of gene mutations and accelerating loss of heterozygosity through chromosomal abnormalities. This is supported by the difficulty in the identification of cancer specific mutations, the lack of mutations seen in response to some carcinogens and the aneuploid nature of almost all tumours (Li et al., 2000). A two-stage model has been proposed whereby carcinogens or spontaneous mutation induce aneuploidy in normal cells through disruption of a mitotic, spindle or chromosome related gene. The aberrant chromosome segregation disrupts the spindle machinery and promotes karyotypic variation leading to an autocatalytic generation of aneuploidy and eventually to neoplastic transformation (Li et al., 2000).

1.2.2 Causes of Aneuploidy

Although the cause of MIN is well defined, the mechanisms which lead to CIN in CRC are not clear. The frequency of CIN and aneuploidy in colorectal tumours, particularly those with poor prognosis, provides good rationale for investigating its genetic causes (Baba et al., 2002; Duesberg and Li, 2003; Karelia et al., 2001; Risques et al., 2001). Unlike MIN, CIN is a dominant phenotype which cannot be abolished by fusion with a chromosomally stable cell suggesting it may result from gain of function type mutations (Lengauer et al., 1997). In cultured cells aneuploidy often occurs simultaneously to *p53* inactivation and G2/M phase cell cycle arrest occurs in p53 deficient cells. However, inactivation of *p53* does not affect chromosomal stability in non-CIN cell lines and is therefore likely that *p53* mutations exacerbate CIN but are not the underlying cause. This is supported by the occurrence of aneuploidy and CIN early in tumourigenesis whereas *p53* is inactivated much later (Lengauer et al., 1998).

Studies in yeast indicate many different genetic defects can produce a CIN phenotype including those involved in cell cycle checkpoints, chromosome condensation, sister-chromatid cohesion, kinetochore structure and function and microtubule formation (Murray, 1995; Nasmyth, 1996; Elledge, 1996; Paulovich et al., 1997; Kolodner et al., 2002). Examples of genes which when mutated may promote CIN in cancer are shown in Table 1.2 (adapted from Lengauer et al., 1998) and some examples are discussed below.

Table 1.2 Candidate Genes for the CIN Phenotype in Tumours

Protein Function	Genes involved
Chromatin Structure	
DNA methylation	*DNMT1, DNMT2, DNMT3A, DNMT3B*
DNA acetylation	*HD1, HD2, HDAC3*
Chromatin condensation	DNA topoisomerases (IIα, IIβ, TOP3), helicases
Centrosome	Aurora kinases, *PLK1*, *NEP1*, NIMA-related kinases
Microtubules	
Microtubule formation and motors	dynein and kinesin superfamilies, dynactin, tubulin
Microtubule associated proteins	MAP family, cytoplasmic linker proteins, *EB1*, *STT4*, G-proteins, ***CIN1, 2, 4***
Kinetochore	*CENP-A, B, C, D, E, F, G, INCENPs, CAS, CSE2*
Chromatid cohesion	
Cohesins	*SCC1*, ***SCC2***, *SB1.8*, ***SMC2***, *HCAP*, ***SMC4***, *MIS4, SA1*
Regulators of cohesion	*RCC1*, ***ASE1, PDS1, ESP1***
Cell Cycle Checkpoints	
Mitotic checkpoints	*MAD1, MAD2, MAD2B, BUB1, BUBR1,* ***BUB2***, *BUB3, MPS1L1(TTK), p55CDC,* ***DMA1,*** *CHFR, ROD, ZW10*
DNA damage checkpoint	*ATM, CHK1, CHK2, ATR, BRCA1, BRCA2, HsRAD51, XRCC1, XRCC2, XRCC3, p53*
Cell cycle regulators	mitotic cyclins, MAP kinases, CDKs and CDK inhibitors
Anaphase Promoting Complex	
Complex proteins	*APC158*, cullins *(APC2, CUL1, CUL3, CUL4, CUL5, CUL-2), CDC27/APC3, APC4, APC5, CDC16/APC6, APC7, CDC359, CDC23/APC8, APC11, CDC26*
APC/C Regulators	***HCT1/CDH1***, *CDC20/p55CDC, CDC5L*
Ubiquitination	*NEDD8, UBCH10*

Genes shown in **Bold** indicate yeast genes without a known human homologue.

Deregulation, duplication and altered distribution of centrosomes are often reported in tumours and can lead to abnormal chromosome segregation (Kramer et al., 2002). Abnormal numbers of centrosomes occur in breast, lung, prostate, colon, bladder, pancreatic and brain tumours, and have been associated with CIN phenotype in some of these (Kawamura et al., 2003; Salisbury et al., 1999; Pihan et al., 2001; Brinkley, 2001; Zhou et al., 1998; Sato et al., 2001). Multipolar spindles are also frequently observed in human tumours, probably as a result of these centrosome abnormalities. There have been numerous studies reporting the over-expression of centrosome-associated proteins in cancers. *STK15*, an aurora kinase involved in spindle assembly and centrosome maturation, is over-expressed and amplified in multiple human cancers (Zhou et al., 1998; Bischoff et al., 1998). Diploid mammalian cell lines in which STK15 is over-expressed have abnormal numbers of centrosomes, altered chromosome segregation and aneuploid phenotypes (Miyoshi et al., 2001; Zhou et al., 1998). Over-expression of polo-like kinase PLK1, involved in centrosome replication and dynamics, has also been reported in human tumours including gliomas and colorectal tumours (Takahashi et al., 2003; Dietzmann et al., 2001). BRCA1, associated with familial breast cancer, localises to and is phosphorylated at the centrosome during cell division suggesting it may have centrosome-associated functions (Salisbury et al., 1999). Inactivation of *p53* has also been shown to lead to abnormal centrosome number in mouse embryonic fibroblasts (Fukasawa et al., 1996) and $p53^{-/-}$ mice show centrosome abnormalities and aneuploidy suggesting *p53* may also play a role in centrosome mediated aneuploidy (Salisbury et al., 1999). However, centrosome abnormalities are also detected in chromosomally unstable pre-invasive carcinomas of the cervix, prostate and breast suggesting that centrosome defects, unlike *p53* inactivation, may be an early step in tumourigenesis and therefore although centrosome defects are probably an important factor in aneuploidy, *p53* is probably not the primary cause of these defects (Pihan et al., 2003). INCENP, a kinetochore protein involved in chromosome condensation, segregation and cytokinesis, is also over-expressed in a subset of colorectal cancer cell lines (Adams et al., 2001).

Thus it appears that yeast are providing us with many clues into the candidate genes involved in generating aneuploidy in cancer. However, progress is needed in

the identification and characterisation of further genetic mechanisms involved in the generation of aneuploid colorectal cancers.

1.3 The Cell Cycle in Cancer

The cell cycle is broadly divided into 2 phases; interphase and mitosis. During Interphase, the longer of the two phases, cells grow in size and replicate their DNA. Interphase can be divided into 3 sub-sections; Gap1 (G1), Synthesis (S) and Gap 2 (G2). Mitosis follows G2 and the cycle begins again. During the Gap phases cells prepare themselves for the action phases of S phase and mitosis through intense protein synthesis, for example. During S phase cells accurately replicate their DNA and cohesion, which attaches sister chromatids during mitosis, is established. In budding yeast the mitotic spindle is also assembled during S phase, but this occurs in mitosis in most eukaryotes including mammals. In mitosis the newly replicated sister chromatids attach to the spindle, are equally segregated and the cell physically divides to produce 2 daughter cells genetically identical to both the mother cell and each other.

1.3.1 Cyclins and Cyclin Dependent Kinases

The cell cycle is driven by altering levels and phosphorylation states of Cyclins (cyc), cyclin dependent kinases (CDK) and CDK inhibitors (CDKI). Different cyclins interact with CDKs to activate them at each phase of the cell cycle. The activated cyclin CDK complexes then phosphorylate key proteins to control cell cycle progression. This process is best understood in yeast where a single CDK, CDC28, interacts successively with a series of transiently expressed cyclins. In mammalian cells this is complicated by the involvement of multiple CDKs and cyclins. Most cells of the body are maintained in a quiescent state, G0 and only re-enter the cell cycle upon induction by a mitogenic growth signal. Cells in G0 retain low levels of cyclin D through active proteolysis. The levels of cyclin D accumulate in response to the release of growth factors and it interacts with CDK4 to stimulate re-entry into the cell cycle. The CDK4-cycD complex co-operates with a CDK2-cycE complex to phosphorylate the retinoblastoma protein (pRB). For this to happen the CDK2-cycE complex must be released from its inhibitor p27, which is

proteolytically degraded, a process initiated by activation of a ubiquitin ligase complex SCF^{Skp2}. Phosphorylation of pRB releases its inhibition of the E2F family of transcription factors and allows them to transactivate genes essential for S phase initiation and DNA replication (Molinari, 2000; Hartwell and Kastan, 1994).

The completion of DNA replication (and spindle formation in budding yeast) marks the end of S phase and entry into the second preparatory phase, G2.

A CDC2-cycB complex, also known as mitosis promoting factor (MPF) initiates mitosis. It is regulated by the availability of cyclin B, through synthesis and localisation and also by phosphorylation status. MPF is maintained in an inactive form in G2 by phosphorylation by the WEE1 kinase and only activates mitosis when dephosphorylated by CDC25 phosphatases. The cyclin-CDK complexes exert additional control on cell cycle progression through the phosphorylation and activation of other proteins, including CDKIs, to ensure their own destruction and progression to the next stage of the cycle. The cell cycle is summarised in figure 1.2.

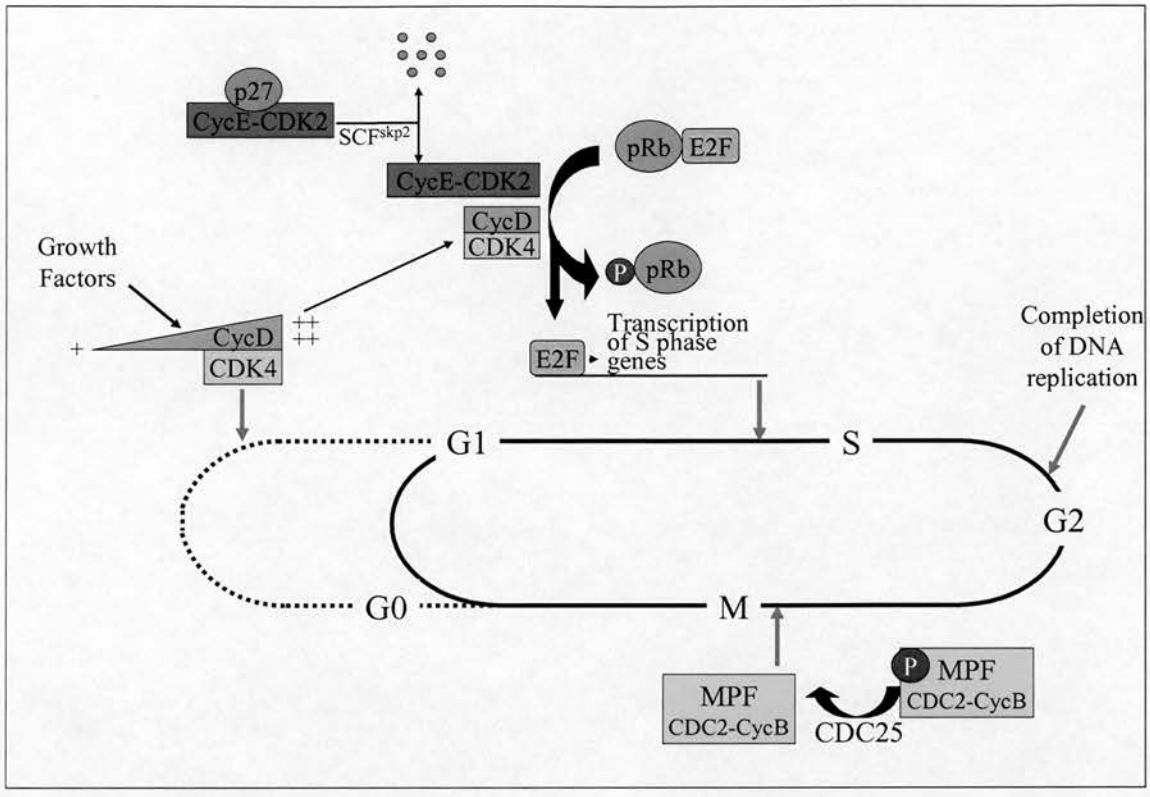

Figure 1.2 Cell cycle control

Progression through the cell cycle is controlled by a series of cyclins and cyclin dependent kinases. G0 is activated by an increase in levels of cyclin D and formation of a CycD-CDK4 complex. This complex is also involved in phosphorylation of pRb, releasing the transcription factor E2F to activate S phase gene transcription. Release of CycE-CDK2 from its inhibitor p27 by SCF^{skp2} is also required for E2F release. Mitosis is induced by CDC25 mediated dephosphorylation of Mitosis Promoting Factor (MPF), a complex of Cyclin B and CDC2.

Cell cycle genes are frequently mutated in various cancers. Cyclin B was found to be over-expressed in 26% of a subset of colorectal cancers analysed and its over-expression was found to initiate a CIN phenotype and alteration of the spindle checkpoint in yeast (Sarafan-Vasseur et al., 2002). Cyclins A and D are also frequently over-expressed in tumours (Yam et al., 2002; Molinari, 2000) and pRb is often altered in tumours particularly retinoblastomas and sarcomas and is impaired by tumour viruses such as Human Papilloma Virus (HPV) and Simian Virus 40 (SV40) (Molinari, 2000; Viallard et al., 2001). Cyclin E acts as a clinical indicator of poor prognosis when elevated in breast cancer patients and human CDC4, involved in the degradation of cyclin E is mutated in several tumour types (Clarke, 2002).

The cellular components involved in genome transmission and accurate cell division; the spindle, the centrosomes and DNA are all carefully monitored during their replication and segregation. Cell cycle regulation is exerted by the existence of checkpoints through out the cell cycle, which halt progression to the next stage of the cell cycle until certain criteria have been met. This ensures the stages of the cell cycle occur without error, only once and in the correct order, thereby maintaining the fidelity of cell division.

1.3.2 DNA Damage Checkpoints (G1/S and G2/M)

A DNA damage checkpoint operates at three stages of the cell cycle; G1, S phase and G2. It halts cell cycle progression or initiates apoptosis in response to DNA damage through complex mechanisms involving p53, ATM, ATR and the BRCA1 and 2 proteins. DNA lesions are recognised by the ATM and ATR proteins and, in response, p53 is upregulated, resulting in transcriptional activation of p53 dependent genes. These in turn activate CHK1 and 2 resulting in the phosphorylation and sequestration of CDC25 and sequestration of the CDC2-cycB complex in the cytoplasm causing checkpoint arrest. CHK1 and 2 activation is also important for BRCA1 phosphorylation, localisation and the DNA damage repair mechanisms. Many of these genes have been implicated in familial and sporadic tumours and *p53* in particular, is mutated in at least 50% of cancers (Molinari, 2000; O'Driscoll and Jeggo, 2003; Hoeijmakers et al., 2001).

1.3.3 Other Cell Cycle Checkpoints

Recent studies in mammalian cells suggest an additional checkpoint may exist at G1 which halts S phase in response to defects in histone synthesis and/or chromatin assembly. Newly replicated DNA is promptly assembled into nucleosomes which are important for the preservation of locus specific chromatin structure and chromatin-based epigenetic control of gene expression. It has been suggested that delayed or defective chromatin assembly causes stalling at replication forks, the generation of double strand breaks and activation of the G1/S DNA damage checkpoint. Thus mutations in chromatin assembly factor genes may be a further cause of CIN in cancers if they allow chromatin structure abnormalities to escape detection by the S phase checkpoint (Ye and Adams, 2003).

A further checkpoint exists at the S/G2 boundary which prevents mitotic spindle elongation for chromosome capture until DNA replication is complete. These two S-phase processes are usually co-ordinated by a timing mechanism as DNA replication takes only half the time of spindle formation. However, hydroxyurea inhibition of DNA replication arrests cells with short spindles and upon release, spindle elongation is delayed until the DNA is fully replicated. This checkpoint may also ensure cohesion, established in early S phase, is maintained until its degradation at anaphase of mitosis. This checkpoint is not yet well defined in mammalian cells but may involve many of the proteins involved in the G1 DNA damage checkpoint including ATR, BRCA1, BLM and CHK1 and 2, mutations in which are implicated in cancer pre-disposition syndromes. PDS1, a protein involved in mitotic progression may also be involved in this checkpoint and the PDS1 protein has been found to be dysfunctional in tumours (Smith et al., 2002).

DNA replication produces two sister strands of DNA which are tangled together or catenated. TOPO II removes these catenations to allow chromosomes to accurately condense. It has been proposed that a G2 checkpoint, separable from that involved in monitoring DNA damage, prevents completion of chromatid condensation in the absence of TOPO II and in response to catenation. Again, this checkpoint is thought to involve some of the G2/M DNA damage checkpoint proteins including ATR, CHK1 and BRCA1 proteins but utilises a distinct signalling

cascade to mediate cell cycle arrest. TOPO II activity is also required for sister chromatid resolution, to complete chromatid condensation and for sister chromatid separation in mitosis (Clarke and Gimenez-Abian, 2000).

Additional checkpoints operate during mitosis to ensure accurate chromosome segregation. These will be discussed in more detail later.

The cell cycle checkpoints are summarised in figure 1.3.

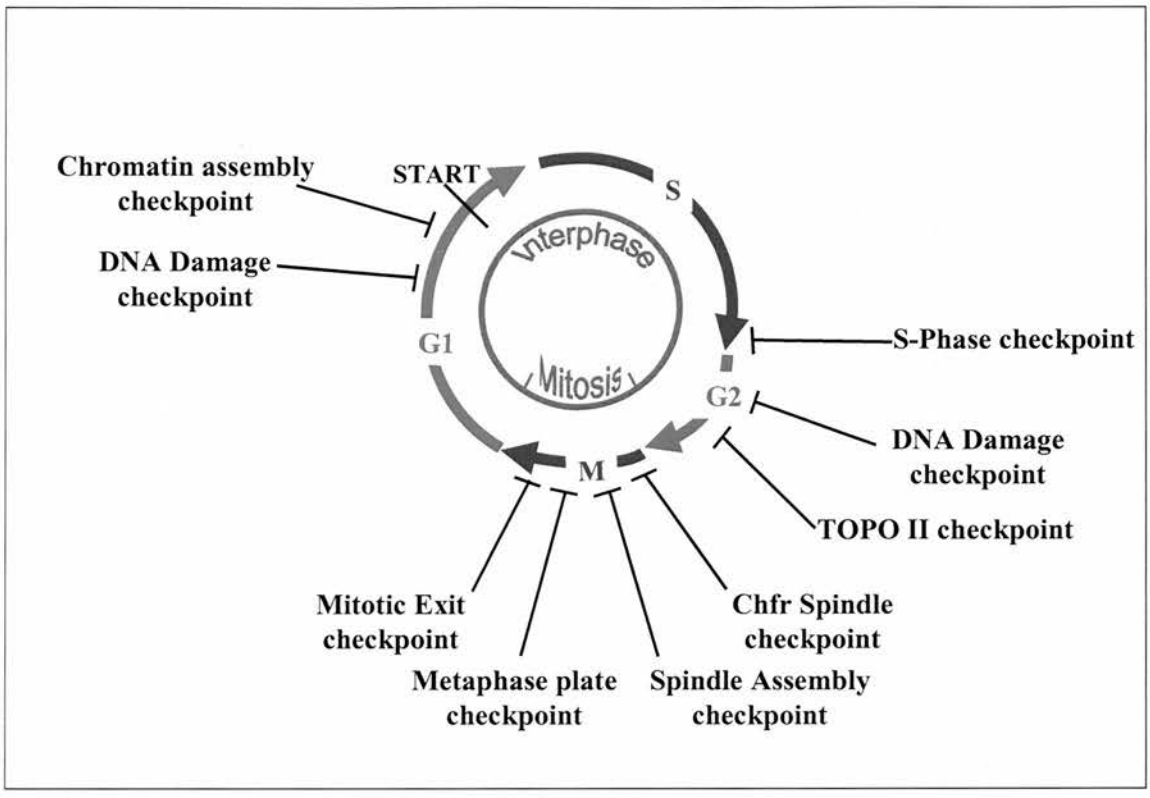

Figure 1.3 The cell cycle and its checkpoints

The cell cycle is controlled by a series of checkpoints which ensure an ordered progression through the stages of the cell cycle and maintenance of the fidelity of the genome. The cycle consists of two basic stages; Interphase and Mitosis. During G1 of interphase the cell prepares for cell division through intense protein synthesis. Once the start (or restriction point) of G1 has been passed the cell can no longer respond to external stimuli from the environment to halt division and progression to S phase and DNA replication is irreversible. After S phase activity the cell has a further preparatory phase, G2, before segregation of chromosomes and cell division during mitosis.

1.3.4 Proteolysis and the Cell Cycle

The cyclins, CDKs and CDKI proteins which ensure the accurate onset of each phase of the cell cycle also activate their own destruction. This cleverly ensures a precisely regulated order of events, where the proteins produced at each stage both initiate the next phase and ensure destruction of those required for the current phase, achieving a rapid and irreversible transition. For example in the G1/S transition cyclin E is activated by proteolytic destruction of its inhibitor p27. In turn CDK2-cycE initiates S phase DNA replication and also initiates onset of its own destruction to ensure the cell cannot return to G1.

Many of the cyclins involved in cell cycle progression, including p27 and cyclin E, are degraded by the addition of a ubiquitin chain destruction tag and degradation by the 26S proteasome. This process is summarised in figure 1.4.

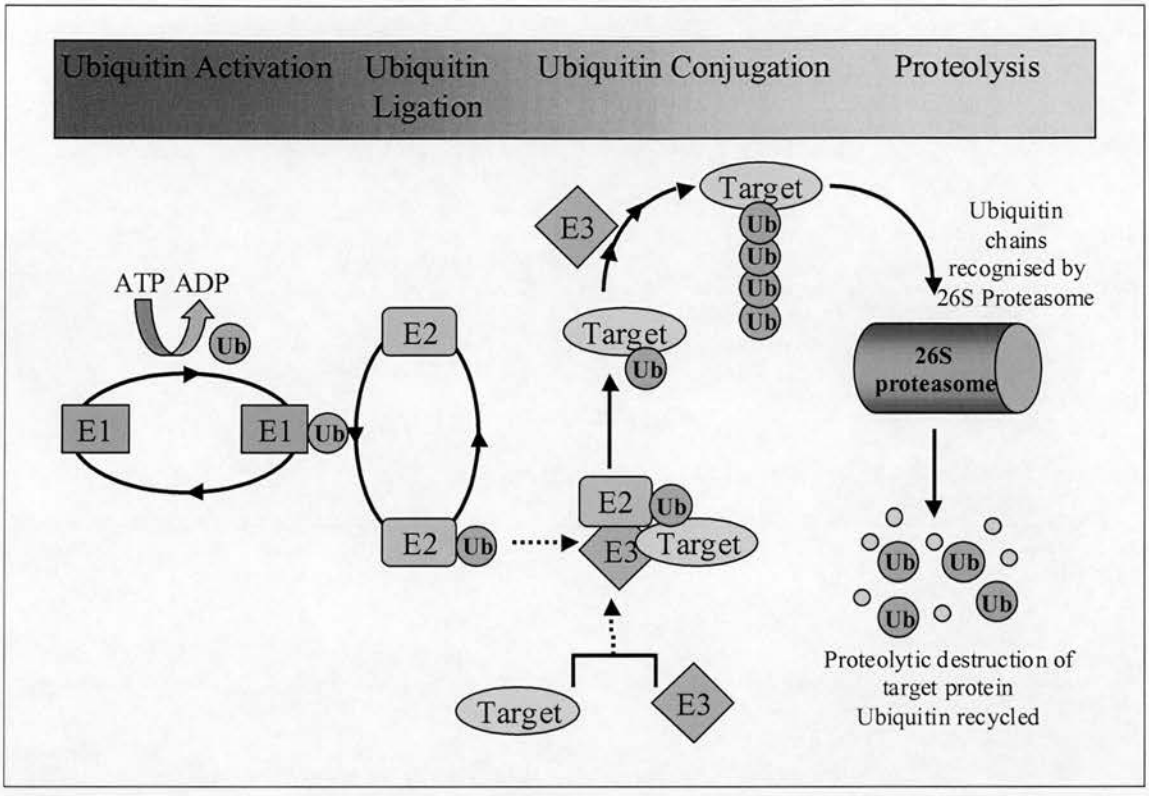

Figure 1.4 Ubiquitin mediated proteolysis

Cell cycle proteins are regulated by destruction by the 26S proteasome. To be recognised by the proteasome, target proteins must be tagged by a chain of ubiquitin molecules. This process involves a series of enzymatic reactions. An E1 ubiquitin conjugating enzyme actively binds to a ubiquitin molecule. This ubiquitin molecule is then transferred to an E2 ubiquitin ligase. An E3 ubiquitin conjugating enzyme transfers this to a target protein through interaction with both the target protein and the E2 enzyme. The E3 then catalyses the addition of further ubiquitin molecules to form a ubiquitin chain on the target protein. Ubiquitin tagged molecules are degraded by the 26S proteasome and the ubiquitin molecules are recycled.

Ubiquitin is activated by an E1 ubiquitin-activating enzyme by formation of a thioester bond between a cysteine residue on the surface of the E1 and the ubiquitin molecule. Active ubiquitin is then transferred to an E2 ubiquitin-conjugating enzyme forming a second high energy thioester bond. Finally an E3 ubiquitin-ligase enzyme interacts with the E2 and the target protein and catalyses formation of an isopeptide bond between the ubiquitin COOH terminus and a lysine residue on the target protein. The E3 enzyme then catalyses the addition of further ubiquitin molecules to the target protein to form longer ubiquitin chains which act as a marker for destruction by the 26S proteasome. The ubiquitin molecules are recycled to tag further proteins for destruction. Most cells contain a single conserved E1 enzyme but several related E2 enzymes and multiple E3 enzymes. Some E3 enzymes are made up of large multi-subunit complexes, including the SCF ligase complex, which degrades cyclins, and the anaphase promoting complex or cyclosome (APC/C) involved in degradation of important mitotic proteins (Doherty et al., 2002).

Proteins involved in ubiquitination and the proteolytic degradation pathway may also be candidate cancer and more specifically candidate CIN genes. SKP2, part of the SCF ubiquitin ligase complex is over-expressed in breast and gastric tumours (Signoretti et al., 2002; Masuda et al., 2002) and mice lacking SKP2 show centrosome defects and polyploidy (Nakayama et al., 2000). Genetic alterations have also been reported in several components of the APC/C in colorectal cancer cells. Expression of a truncation mutant form of the APC8 subunit in colon epithelial cells results in abnormal levels of APC/C targets and perturbed mitotic progression suggesting they have a deleterious role in CRC (Wang et al., 2003a). The protein c-CBL is another E3 ubiquitin ligase which targets receptor tyrosine kinases involved in growth factor initiation of the cell cycle, for degradation. *CHFR*, a mitotic checkpoint gene in which mutations have been reported in colorectal tumours, is also an E3 ubiquitin ligase (Scolnick and Halazonetis, 2000; Kang et al., 2002)

1.3.5 The Anaphase Promoting Complex: a 20S Subunit of the Proteasome

The anaphase promoting complex or cyclosome (APC/C) is key in co-ordinating the events of the cell cycle. It is a complex of proteins which act as an E3 ubiquitin

ligase and is involved in the destruction of mitotic cyclins and the initiation of sister chromatid separation. The complex was initially identified in 1995 as a large complex of 150 kDa with cyclin ubiquitination activity targeting cyclins A and B for destruction at the end of mitosis (Sudakin et al., 1995). Fractionation of the APC/C revealed it to be a 20S complex containing CDC16 and CDC27 which co localise to the centrosome and to the mitotic spindle during mitosis (Irniger et al., 1995; King et al., 1995; Tugendreich et al., 1995). It is a complex of 8-12 proteins including CDC26, cullin proteins APC1-8, APC10 and APC11 and homologues of the APC/C proteins have been identified in *S.cerevisiae* (Sudakin et al., 1995), humans (Jorgensen et al., 2001), *Xenopus levi* (Li et al., 1997), *Schizosaccharomyces pombe* (Yamashita et al., 1996), *C.elegans* (Furuta et al., 2000), *Drosophila* (Huang and Raff, 2002) and *Aspergillus* (Lies et al., 1998) suggesting the APC/C is conserved in all eukaryotes. The APC/C complex is an E3 ubiquitin ligase enzyme which targets proteins for destruction by the 26S proteasome, acting as a 20S subunit (King et al., 1995). The cell cycle specific target proteins contain at least one peptide motif either a destruction box (D-box), or a KEN box or both, often at the N-terminal and often other motifs also promote proteolysis. As many of the APC/Cs protein targets are involved in cell cycle regulation, the activity of the APC/C is itself carefully regulated. This is achieved by association with proteins which contain seven WD40 repeats in their carboxy terminus, such as Cdc20p and Cdh1p which were initially identified in budding yeast (Visintin et al., 1997) and *Drosophila* (Dawson et al., 1993; Dawson et al., 1995; Sigrist et al., 1995). These WD40 repeats are essential to mediate the interactions between APC/C and the regulatory factors. Cdc20p and Cdh1p have homologues in many organisms including *S. pombe* (Matsumoto, 1997; Yamaguchi et al., 1997; Kitamura et al., 1998; Kominami et al., 1998) and humans (Weinstein, 1997). These association factors activate the APC/C and also ensure specificity to the target protein, important for cell cycle progression. Mitotic kinases and phosphatases and spatial effects have also been shown to influence the activity of the APC/C.

The APC/C is present but inactive during interphase and is activated early in mitosis by the cyclinB-cdc2 complex or Mitosis Promoting Factor (MPF). The

stability of the MPF varies through out mitosis, suggesting that APC/C activity does likewise, both being deactivated at G1 (Wolf and Jackson, 1998).

One of the key functions of the APC/C is to induce chromosome segregation at anaphase. In *S.cerevisiae* this is achieved by proteolytic degradation of Pds1p which leads to the destruction of cohesin. This initiation of anaphase is achieved by association of the APC/C with a WD protein, Cdc20p, which activates its proteolytic function. This is described in more detail below. In budding yeast, *cdc20* mutants fail to destroy Pds1p and arrest at metaphase with unseparated sister chromatids. This phenotype can be bypassed by deleting the PDS1 gene producing chromosome segregation defects. These *cdc20/pds1* double mutants also have errors in spindle disassembly, cytokinesis and subsequent S phase entry suggesting Cdc20 is also required in late mitosis.

The APC/C is also responsible for degradation of Clb2p in late mitosis which initiates mitotic exit, cytokinesis and S phase entry. This degradation by APC/C relies on its interaction with another WD protein, Cdh1p. Budding yeast *cdh1* mutants have high levels of the Clb2p mitotic cyclin and are delayed in late mitosis due to errors in its proteolysis. Similar *Drosophila* fizzy related (fzr) mutants and fission yeast *cdh1* mutants also accumulate mitotic cyclins. Over-expression of Cdh1p and its homologues induces cyclin degradation indicating its importance for proteolysis. In *Xenopus* egg extracts either CDC20 or CDH1 can initiate cyclin B proteolysis indicating CDC20 may also be involved in APC/C mediated mitotic exit (Wolf and Jackson, 1998). Other APC/C substrates include Ase1p whose degradation prompts the initiation of spindle disassembly late in mitosis and Geminin, which inhibits DNA replication until mitosis is complete, is also degraded by the APC/C. Another example of the many roles of the APC/C in cell cycle regulation include its involvement in replication initiation at chromosomal replication origins (Wolf and Jackson, 1998).

The APC/C is further regulated by a polo-like kinase in budding yeast (Cdc5p), fission yeast (plo1p), *Xenopus* (PLX) and mammals (PLK). Mutants in CDC5 arrest with segregated chromosomes but chromatids do not digress to the cellular poles as Clb2p proteolysis is defective and in *Xenopus* egg extracts depletion of PLX prevents mitotic exit and cyclin B proteolysis. The polo like kinases phosphorylate APC/C

subunits in mammalian cells, initiating its degradation of cyclin B. However to do this they themselves must be phosporylated by MPF. The APC/C is negatively regulated by PKA, a cAMP-dependent protein kinase. PKA activity also fluctuates during mitosis, generally in an inverse manner to PLK's. Regulatory control is heightened by auto regulatory mechanisms by which Polo like kinases, CDC20 and MPF not only regulate APC/C activity but are also its targets. They contain destruction box motifs and accumulate through the cell cycle to peak at mitosis, after which they are destroyed by the APC/C. The accumulation, destruction and stability of the association factors are essential in regulating the APC/C and therefore ensuring mitotic control (Peters, 2002; Yen, 2002; Wolf and Jackson, 1998).

Alterations of APC/C subunit genes including *APC6* and *APC8* have been found in colorectal cancer cells. The experimental expression of the *APC8* truncation mutants resulted in increased levels of APC/C targets such as cyclin B1 and abrogation of mitotic progression (Wang et al., 2003a).

1.3.6 Sister Chromatid Cohesion and Chromosome Segregation

For accurate inheritance of a chromosome complement it is essential that the duplicated sister chromatids remain tightly associated until they are attached to the microtubule spindle. The chromatids then divide and promptly dissociate at anaphase for cell division to occur. This tight association is ensured through cohesin, a protein complex which assembles onto DNA during S phase and holds sister chromatids together until chromosome segregation at anaphase. Cohesin subunits vary between cell types but generally there are 4 subunits in budding yeast; two structural maintenance of chromosome proteins, Smc1p and Smc3p (Strunnikov et al., 1993; Michaelis et al., 1997) and two sister-chromatid cohesion proteins, Scc1p and Scc3p (Guacci et al., 1997; Michaelis et al., 1997). Additional protein factors are required to establish cohesin on chromatin (Ciosk et al., 2000). Homologues of these have been identified in other organisms including fission yeast (Birkenbihl and Subramani, 1995; Tomonaga et al., 2000) and vertebrates (Losada et al., 1998). Alternative subunits are involved in meiotic chromatids, thus vertebrates have three

Scc3 subunits; SA1 which predominates in somatic tissues, SA2 which is involved in *Xenopus* embryos and SA3 which is meiosis specific (Reviewed in Amon, 2001).

In 1999 Uhlmann et al., first showed that cleavage of one of the cohesin subunits, Scc1p is required for chromosome segregation (Uhlmann et al., 1999). They demonstrated that Scc1p is also cleaved at two sites showing sequence homology. Mutation of these two sites blocks cleavage of Scc1p and sister chromatid separation (Uhlmann et al., 1999). Replacement of one of the cleavage sights in Scc1p with a Tobacco-etch virus (TEV) protease site ultimately allowed chromosome separation through expression of the TEV protease, demonstrating that cleavage of Scc1p could induce sister chromatid separation (Uhlmann et al., 2000). Cleavage of Scc1p produces a 33kDa fragment which is cleared via the Proteasome-dependent N rule degradation pathway (Rao et al., 2001). Failure to destroy this fragment results in an increase frequency of chromosome loss, suggesting it may interfere with sister separation (Rao et al., 2001). Cohesin is also phosphorylated at serine residues adjacent to its cleavage sites by a polo kinase which is thought to promote its cleavage (Alexandru et al., 2001). Scc1p's cleavage and the dissociation from chromosomes both *in vitro* and *in vivo* depends on a protease Esp1p, often called Separin (Uhlmann et al., 1999). Further experiments by Uhlmann et al. demonstrate the C-terminal of Esp1 shows homology to cysteine proteases of clan CD and purified Esp1p can cleave recombinant Scc1p *in vitro*. Mutating the active site or addition of peptide inhibitors which covalently bind the active site of Esp1p prevent Scc1p cleavage (Uhlmann et al., 2000). During most of the cell cycle Esp1p is bound and inhibited by Pds1p, or Securin (Yanagida et al., 2000) ensuring Esp1 is localised to the spindle (Jensen et al., 2001). However, shortly before anaphase, Pds1p is ubiquitinated by the APC/C-Cdc20, targeting it for degradation by the 26S proteasome (Irniger et al., 1995; Cohen-Fix et al., 1996; Yamamoto et al., 1996). This destruction is dependent on association of Cdc20p with the APC/C (Hilioti et al., 2001). Esp1p is released from its inhibitor in an activated form which can cleave Scc1p. The cleavage of Scc1p causes cohesin to dissociate from sister chromatids, removing the force opposing poleward movement of chromatids and promoting sister separation (Ciosk et al., 1998; Uhlmann et al., 1999). This mechanism for chromosome segregation in budding yeast is summarised in figure 1.5.

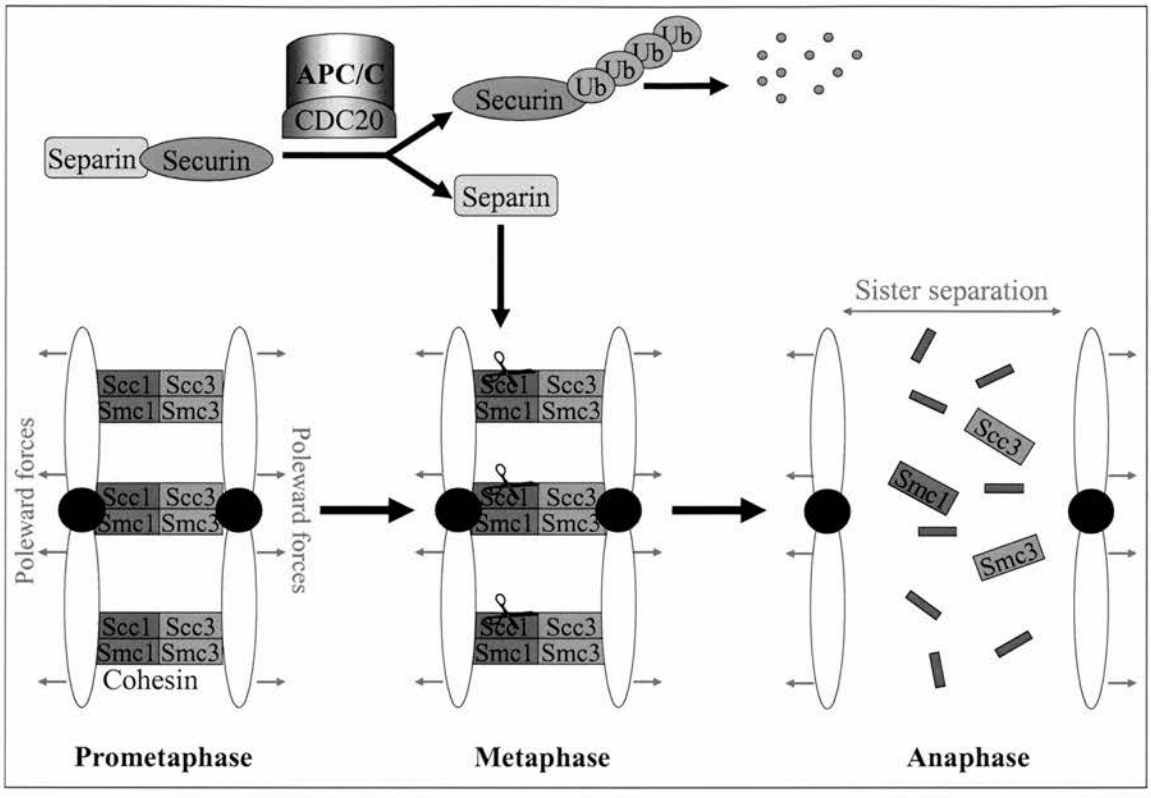

Figure 1.5 Chromosome segregation

Sister chromatids are attached together by a Cohesin complex of four proteins. At the metaphase to anaphase transition the Scc1 subunit of cohesin is cleaved and cohesin dissociates. The cleavage of Scc1 is achieved by the ubiquitination of the Separin inhibitor Securin by the APC/C-Cdc20 complex, targeting it for degradation. This releases Separin to allow it to cleave Scc1. The poleward forces acting on the chromosomes, due to the pull of microtubules on them, then cause the chromosomes to segregate to the poles of the cell in Anaphase.

This mechanism appears to be conserved in fission yeast (Tomonaga et al., 2000; Funabiki et al., 1996a; Funabiki et al., 1996b; Uzawa et al., 1990) and higher eukaryotes (Zou et al., 1999; Leismann et al., 2000). Studies in vertebrate cells show that cohesin associates with the centromeres of metaphase chromosomes but is lost during anaphase, consistent with this model (Losada et al., 2000; Waizenegger et al., 2000). Furthermore fragments of SCC1 are present during anaphase but not before and only after activation of APC/C-CDC20 and degradation of PDS1. Purified human ESP1 was shown to cleave SCC1 *in vitro*, when PDS1 is first removed by its preincubation with mitotic extracts with active APC/C-CDC20 (Waizenegger et al., 2000). Recent experiments have demonstrated degradation of PDS1 upon satisfaction of the spindle checkpoint in human cells and that the destruction of PDS1 can be halted upon re-activation of the checkpoint (Hagting et al., 2002). This destruction of PDS1 is also shown to be dependent on a KEN box in the amino terminal of PDS1 and a destruction box which inhibits sister chromatid segregation if mutated (Hagting et al., 2002). Further experiments in budding yeast and *Xenopus* suggest a similar mechanism operates in meiosis (Buonomo et al., 2000; Peter et al., 2001).

Esp1p and Pds1p also appear to have other mitotic functions including roles in spindle elongation (Jensen et al., 2001) and mitotic exit (Sullivan et al., 2001). Fission yeast mutants *scc1* and *scc2* have been shown to activate the spindle checkpoint and are hyper-sensitive to microtubule poisons suggesting cohesin subunits may also mediate microtubule-kinetochore interactions (Toyoda et al., 2002).

The human securin gene is identical to the oncogene *PTTG* (Pituitary Tumour Transforming Gene) which is highly expressed in some tumours including colorectal tumours (Heaney et al., 2000; Jallepalli and Lengauer, 2001). Over-expression of PTTG can transform cell lines (Zou et al., 1999), immortalises mouse fibroblasts and allows them to form tumours in nude mice (Jallepalli and Lengauer, 2001). Mouse and colorectal cancer cell lines in which PTTG is absent are viable but exhibit chromosome loss and sister chromatid separation defects (Jallepalli and Lengauer, 2001; Mei et al., 2001) consistent with a role for securin in tumourigenesis.

Furthermore RNA inhibition (RNAi) of human separin causes the formation of polyploid cells (Waizenegger et al., 2002).

1.3.7 Mitosis and Mitotic Checkpoints

During mitosis the newly replicated sister chromatids condense, line up on the equator of the cell and are equally segregated prior to cell division. Mitosis can be described in five stages; prophase, prometaphase, metaphase, anaphase and telophase or classed together as the G2/M progression. In prophase the duplicated centrosomes of the cell move to the poles of the cell and assembly of a bipolar microtubule spindle in the cytoplasm between them is initiated. The chromosomes condense and the nuclear envelope breaks down, initiating prometaphase during which the chromosomes line up along the equator of the cell and attach to the forming spindle producing a metaphase plate. The cells are now considered to be in metaphase. In anaphase the cohesin holding together the sister chromatids is degraded and they separate to the poles of the cell as the spindle elongates. Finally, in telophase adjacent chromosomes fuse to form the two daughter nuclei. The envelope reforms and the spindle forms a microtubule based midbody at the equator which participates in cytokinesis (Pines and Rieder, 2001; Cortez and Elledge, 2000).

At least 5 checkpoints are thought to monitor the stages of mitosis.

The earliest mitotic checkpoint regulates entry into prophase of mitosis in response to DNA damage through a p53 related mechanism discussed in 1.3 (Clarke and Gimenez-Abian, 2000; Taylor and Stark, 2001). Abrogation of this checkpoint causes gross chromosome rearrangements and aberrant chromosome segregation due to defects in genes such as *ATM, ATR, BRCA1 and 2*, and *p53*, all associated with both familial and sporadic tumours (Lengauer et al., 1998; Hartwell and Kastan, 1994).

The CHFR protein (checkpoint protein with forkhead-associated and ring finger domains) mediates the second checkpoint, at the prophase to prometaphase transition, and delays chromosome condensation in response to microtubule poisons which disrupt spindle formation and centrosome separation. CHFR is an E3 ubiquitin ligase which activates the checkpoint through ubiquitination of polo-like kinase 1 (PLK1) and delay of CDC2 activation (Kang et al., 2002; Chaturvedi et al.,

2002). The checkpoint was defective in 4 out of 8 human tumour cell lines examined, 3 of which do not express the CHFR protein and the other contains a missense mutation in the *CHFR* gene. Transfecting the wild type protein into these cell lines can restore the checkpoint, suggesting the abrogation of the checkpoint may contribute to tumourigenesis. However, only two of the cell lines with defective CHFR checkpoints exhibit aneuploidy, and then at only a low level and the frequency of CHFR inactivation in primary tumours has not yet been determined (Scolnick and Halazonetis, 2000; Cortez and Elledge, 2000). Additionally the *CHFR* gene is frequently methylated in tumours and cancer cell lines and evidence of age related methylation has been reported in colon cancer. Methylation was associated with loss of CHFR protein expression in cancer cell lines and treatment with demethylating agents restored its expression and checkpoint function. (Corn et al., 2003).

It has been hypothesised that in vertebrates, homologues of ROD and ZW10, initially identified in *Drosophila melanogaster*, may be involved in an additional branch of the spindle checkpoint monitoring congression to and alignment on the metaphase plate. *Drosophila* mutations in the genes coding for these proteins exhibit a similar but milder phenotype to *bub1* spindle checkpoint mutants, consistent with slightly later checkpoint failure. This was supported by the antibody depletion of homologues of these proteins in human cells, causing abnormal cell division and lagging chromosomes in anaphase. In addition, no ROD or ZW10 homologues have been identified in yeast, in which a true metaphase plate does not exist. These proteins also associate with dynein, a microtubule motor probably involved in chromatid congression to the metaphase plate but dynein cannot be detected at the kinetochores of *ZW10* or *ROD* mutants (Basto et al., 2000; Chan et al., 1999). It has been proposed that ROD and ZW10 activate metaphase arrest in response to metaphase plate defects and that dynein inactivates the checkpoint upon their repair by removal of the ROD/ZW10 complex from the kinetochore. Dynein is thought to have a similar switching off role in the spindle checkpoint by removal of key checkpoint proteins (Wojcik et al., 2001).

The spindle checkpoint delays the metaphase to anaphase transition allowing correct attachment of all sister chromatids to the bipolar microtubule spindle. A

combination of presence of unattached kinetochores, and lack of tension at unbound microtubules, initiates the assembly of protein complexes of the Mitotic Arrest Defective (MAD) and Budding Uninhibited by Benzimidazole (BUB) proteins initially identified in *S.cerevisiae.* These complexes inhibit the APC/C preventing the cleavage of cohesin, required for chromatids to move poleward (Hardwick, 1998). This checkpoint has been found to be defective in human colorectal cancer cell lines showing CIN. Mutations in human homologues of the *S.cerevisiae* genes, *BUB1* and *BUBR1* genes have also been identified and in a number of diploid colorectal tumour cell lines these mutations have been shown to induce CIN. (Cahill et al., 1998). The spindle checkpoint and its role in cancer is the focus of this thesis and will be discussed in detail later.

Gachet et al propose the existence of a distinct checkpoint at the metaphase to anaphase transition in *S.pombe.* The checkpoint is imposed by a stress activated MAP kinase (SAPK) which delays sister chromatid separation and mitotic exit in response to damage to the actin cytoskeleton and aberrant spindle pole alignment. Abrogation of this checkpoint may represent a further candidate which could be bypassed in human tumour cells (Gachet et al., 2001).

A separate mitotic exit checkpoint is functional, at least in yeast, at the anaphase to telophase transition inhibiting mitotic exit and cytokinesis in response to spindle damage, through a Bub2p protein network (Bardin and Amon, 2001). The Septation Initiation Network (SIN) in *Schizosaccharomyces pombe*, and the Mitotic Exit Network (MEN) in *Saccharomyces cerevisiae*, act to delay nuclear migration and cytokinesis in the presence of defects in the actin cytoskeleton and microtubule spindle. This checkpoint has not yet been established in mammalian cells although they do appear to delay mitotic exit in the presence of mis-orientated spindles (McCollum and Gould, 2001). Activation of the spindle checkpoint also inhibits mitotic exit into G1, through inhibition of cyclin B degradation by the APC/C. In a normal budding yeast mitosis the dephosphorylation of Cdh1p, Sic1p and Swi5p (the Mitotic exit network, MEN) by Cdc14/Tem1p allows Cdh1p to act as an association factor with the APC/C, activating the ubiquitination and proteolysis of cyclin B and thus mitotic exit. Bub2p is believed to act in a complex with Byr4p, forming a GTPase activating protein (GAP), hydrolysing Tem1-GTP and inactivating it in the

Cdc14/Tem1p complex. Thus Cdh1p cannot activate the APC/C and the retained high levels of Cyclin B and Cdc5p inhibit mitotic exit. In addition Pds1p probably has a role in inhibiting Cyclin B proteolysis and mitotic exit through inhibition of Cdh1p (Alexandru et al., 1999; Wang et al., 2000c)

The mitotic checkpoints are summarised in figure 1.6.

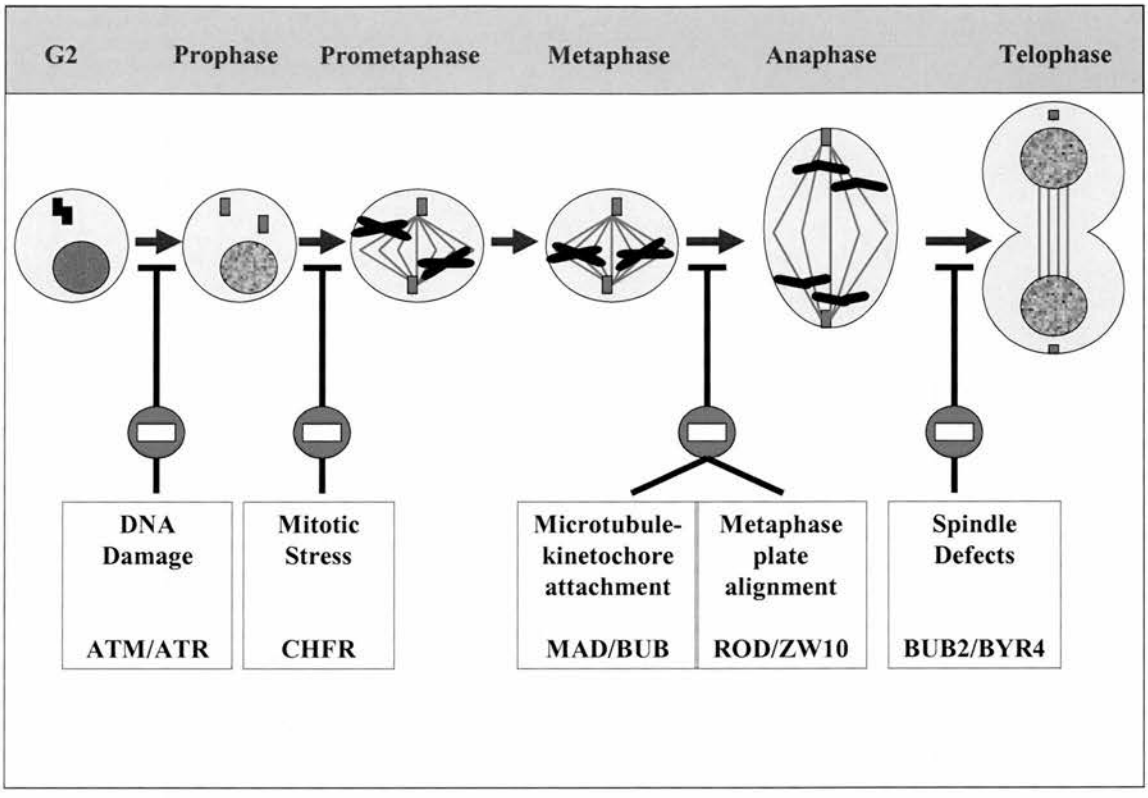

Figure 1.6 Mitosis and the mitotic checkpoints

Progression through the stages of mitosis is controlled by at least 4 checkpoints which block entry into the next stage if defects in the previous stage occur. This ensures the fidelity of chromosome segregation. Mitotic Checkpoint defects are common in cancers, allowing abberant chromosome segregation and aneuploidy.

The disruption of cell cycle checkpoints allow cells to bypass these tight growth controls. Checkpoint defects impart a growth advantage on the cell and can result in genetic instability, a characteristic phenotype of cancer. Cell cycle checkpoint defects can be seen to offer a solution to the genetic instability versus growth advantage debate as they impart both of these phenotypes on a cell which may explain the propensity for alterations in cell cycle genes and proteins in cancers (Molinari, 2000; Clarke and Gimenez-Abian, 2000). Furthermore, the recent identification of 'new' checkpoints may reveal further candidate genes involved in the induction of aneuploidy in tumours.

1.4 The Spindle Assembly Checkpoint

Insight into the mechanism of the spindle checkpoint has initially come from studies in the budding yeast, *Saccharomyces cerevisiae*. The Mad1, 2 and 3 and Bub1, 2 and 3 proteins, which act in the spindle checkpoint, were identified from yeast mutants which failed to arrest in mitosis in response to microtubule poisons (Li and Murray, 1991; Hoyt et al., 1991). The Mps1p (monopolar spindle) protein was identified later due to its essential nature, initially as a protein involved in spindle pole body duplication (Winey et al., 1991) but was later shown to be important in the spindle checkpoint (Weiss and Winey, 1996). Of the 7 spindle checkpoint components identified, 6 are known to act in a pathway to delay metaphase to anaphase transition in the presence of spindle and kinetochore defects whereas Bub2p acts in a distinct checkpoint to delay mitotic exit and cytokinesis (Alexandru et al., 1999).

1.4.1 Detection of Spindle Defects

The spindle checkpoint monitors the assembly of the mitotic spindle and bipolar attachment of the chromatids to microtubules and detects any defects in these processes, delaying chromosome segregation and anaphase until they are corrected. The checkpoint can detect a variety of errors including mass spindle disruption such as that caused by microtubule poisons, the presence of a single unattached kinetochore and defects in the centrosomes, centromeres and also microtubule motors. All these faults affect the attachment of kinetochores to microtubules

implying unattached kinetochores generate an inhibitory signal to halt mitosis (Rudner and Murray, 1996).

Kinetochores are multiprotein complexes which assemble on the centromeric DNA of the chromosome and are the site of interaction between the chromosome and the microtubule spindle (Rieder and Salmon, 1998). Attachment of the kinetochores to the mitotic spindle probably involves kinesin-like or dynein-like microtubule motors. Once the kinetochores attach to a microtubule emanating from each pole a tension is generated across the chromatids by the force pulling them towards the poles against the cohesin holding them together. This tension can be visualised as an increased distance between the kinetochores (Zhou et al., 2002a). There is evidence that the spindle checkpoint is activated in two ways. Firstly through detection of kinetochore unattachment and secondly due to a lack of the tension usually created on microtubules by their bipolar attachment to kinetochores.

The evidence that kinetochore attachment is important is that anaphase will not proceed until the last kinetochore on a lagging chromosome attaches to a microtubule as demonstrated in a rat kangaroo kidney cell line PtK1, but destruction of this remaining kinetochore by a laser microbeam, abolishes this delay. This suggests the presence of an unattached kinetochore is necessary to activate the checkpoint as tension on the sister kinetochores was absent in this case but anaphase still ensued (Reider et al., 1995; Rudner and Murray, 1996). Further experiments in PtK1 cells showed that MAD2 staining at kinetochores, indicative of spindle checkpoint activity relied on attachment not tension (Waters et al., 1998). Similarly, in maize, loss of MAD2 staining at kinetochores correlates with their attachment to spindle microtubules (Yu et al., 1999). In addition, some yeast mutants enter mitosis without undergoing chromosome replication yet have an intact checkpoint. These kinetochores cannot form bipolar spindle attachments but exit mitosis without delay, indicating lack of tension does not activate the checkpoint in these cells (Hardwick, 1998). A similar phenomenon is seen in mammalian cells where a single attached kinetochore lacking a sister, and therefore bipolar tension, does not activate the checkpoint (Rudner and Murray, 1996).

However, other evidence suggests that the spindle checkpoint monitors tension on microtubules, generated by their attachment to kinetochores, at least in meiotic cells and certain cell types. In insect spermatocytes, chromosomes attached to only one pole can arrest cells in mitosis for up to 9 hours. Application of tension at the mono-orientated chromosome using a micro needle induces premature anaphase (Li and Nicklas, 1995). These experiments introduced the idea that the absence of tension on unattached chromosomes might activate the spindle checkpoint. It is not clear whether tension and attachment are exclusive stimuli or in fact closely linked, as tension stabilises kinetochore-microtubule attachment and increases the number of attached chromosomes by slowing microtubule-kinetochore turnover (Rudner and Murray, 1996; Nicklas, 1997; King and Nicklas, 2000; Nicklas et al 2001; Zhou et al., 2002b). Thus application of artificial tension could have initiated the accumulation of microtubules at the kinetochore and inactivated the checkpoint through an attachment dependent mechanism (Li and Nicklas, 1995; Rieder and Khodjakov, 1997).

In contrast to Hardwick et al., 1998, Stern and Murray recently demonstrated that budding yeast cells which enter mitosis without prior DNA replication, and therefore have tension free kinetochores do arrest at the spindle checkpoint (Stern and Murray, 2001). Similar experiments which reduce tension across kinetochores but retain attachment by inhibiting DNA replication and sister chromatid cohesion also activate the checkpoint (Biggins and Murray, 2001). In meiotic budding yeast in which homologues were attached to the same pole and kinetochores lacked tension, anaphase onset was delayed but proceeded once bipolar attachment and tension were restored (Shonn et al., 2000). These studies indicate the importance of tension in spindle checkpoint activation.

Interestingly, upon treatment with nocodazole, which induces microtubule detachment, budding yeast cells exhibit a long term block at the spindle checkpoint whereas loss of tension induces only a delay. Perhaps the monitoring of tension and attachment at kinetochores have different functions. Kinetochore tension indicates bipolar attachment whereas attachment may be unipolar. Perhaps, a lack of tension indicates both sister kinetochores are attached to microtubules from the same pole causing the release of one kinetochore in search of a microtubule emanating from the

opposite pole (Zhou et al., 2002b). This is consistent with the nocodazole induced checkpoint delay noted in response to loss of tension compared to a prolonged block through lack of attachment.

Tension may also provide a stabilising mechanism for kinetochore microtubule attachment which may be important in chromosome alignment on the metaphase plate. This is indicated by the proteins involved in the tension response such as BUB1 and BUBR1 remaining at kinetochores longer than MAD2, which is involved in the unattachment response. This is also consistent with a further role for kinetochore tension in chromosome alignment at the metaphase plate (Hoffman et al., 2001; Skoufias et al., 2001; Zhou et al., 2002b).

Another hypothesis suggests tension may be the detection method in meiotic cells, whereas kinetochore attachment may dominate in mitotic cells, supported by correlation of MAD2 kinetochore staining with attachment in mitotic maize cells but with tension in meiotic ones (Yu et al., 1999).

Tension and attachment may represent different mechanisms of spindle checkpoint activation. The combination and type of detection methods probably vary between cell types and organisms. In higher eukaryotes both tension and attachment are probably monitored although their relative contributions to activating the checkpoint are not clear.

Attachment and tension may indicate two mechanisms of detecting free kinetochores with identical methods of checkpoint arrest or they could be independent mechanisms which recruit different protein complexes. This is supported by the localisation of human BUB1 and BUBR1 to kinetochores that have lost tension but of MAD2 only on loss of kinetochore microtubule attachment, a result of treatment with higher levels of microtubule poisons (Skoufias et al., 2001). Indeed in a previous study loss of tension at kinetochores was insufficient to universally recruit MAD2 (Waters et al., 1998). This suggests that there are 2 pathways of activation of the spindle checkpoint in higher eukaryotes, recruiting MAD2 in response to unattached kinetochores and BUBR1 and BUB1 upon loss of tension. This is consistent with the ability of both MAD2 and BUBR1 to inhibit the CDC20-APC/C complex and anaphase onset. However, *in vitro* evidence indicates

BUBR1 is a more potent inhibitor of APC/C than MAD2 (Sudakin et al., 2001; Tang et al., 2001; Fang, 2002). This is not consistent with the reduced intensity of arrest seen in response to loss of tension, thought to be mediated through BUBR1, compared to unattachment, mediated through MAD2. Further controversy is added, as in PtK1 cells the average amount of BUBR1 at metaphase chromosome does not fluctuate as the tension on them alters (Hoffman et al., 2001). In addition, BUB1 and BUBR1 respond differently to microtubule poison induced alterations in kinetochore attachment and tension disagreeing with their involvement in the same mechanism (Taylor et al., 2001). Furthermore, studies in PtK1 cells have observed a disruption in spindle checkpoint arrest in response to loss of tension upon injection of either BUBR1 or MAD2 antibodies. This suggests both BUBR1 and MAD2 respond to loss of tension and that there is overlap between the pathways, although this may be downstream of detection (Shannon et al., 2002).

Activation of the checkpoint through attachment results in alteration in chemistry at the kinetochore and attraction of the checkpoint signalling proteins. The mechanism of checkpoint activation by lack of tension is less clear. It is thought to involve tension-sensitive kinetochore protein phosphorylation (Gorbsky et al., 1995; Nicklas et al., 1995; Nicklas, 1997) and may involve a phosphorylated kinetochore protein recognised by the 3F3/2 antibody (Gorbsky and Ricketts, 1993; Nicklas et al., 1995; Campbell and Gorbsky, 1995; Nicklas, 1997). The 3F3/2 antibody recognises a phosphoepitope at the kinetochore during prophase and prometaphase but this signal, and presumably the phosphoepitope, is lost in the metaphase to anaphase transition. The 3F3/2 antibody stains unattached kinetochores but is much weaker at attached kinetochores in mitotic PtK1 cells (Gorbsky and Ricketts, 1993). In meiotic grasshopper and mantid spermatocytes the phosphorylated kinetochore epitope is shown to be regulated by tension (Nicklas et al., 1995; Nicklas, 1997). Application of tension to the kinetochores either by mitotic forces or through micromanipulation causes loss of the phosphoepitope and anaphase onset (Nicklas et al., 1995; Li and Nicklas, 1995; Nicklas, 1997). Injection of the 3F3/2 antibody to maintain the epitope, delays anaphase onset indicating the presence of the phosphorylated epitope activates the metaphase checkpoint (Campbell and Gorbsky, 1995) and suggests that phosphorylation of the epitope is the transmitter of tension related defects.

Recently, a third mechanism of checkpoint activation has been suggested. In budding yeast an aurora kinase Ipl1p was required for spindle checkpoint activation in response to loss of tension at kinetochores but not in response to unattachment (Biggins and Murray, 2001). In addition Ipl1p is important in establishing bipolar kinetochore attachment through re-orientation of sister chromatids. This is consistent with the theory that the transient mitotic block in response to abolition of tension is important in ensuring attachment is bipolar (Tanaka, 2002). Ipl1p may be involved in phosphorylation at the kinetochore in response to lack of tension, perhaps of the 3F3/2 epitope or of BUBR1 which is thought to be phosphorylated by AuroraB (Ditchfield et al., 2003). The vertebrate homologue of Ipl1p is auroraB.

In summary, it is likely that tension and unattachment both play a part in checkpoint activation and may reflect variation in the primary sensors of the checkpoint in response to different defects, in different cell types, or in different organisms. They may recruit different checkpoint proteins and also initiate different downstream pathways.

1.4.2 Spindle Checkpoint Proteins

The spindle checkpoint proteins are generally well conserved evolutionarily. They have been well studied in budding and fission yeast, *Xenopus*, mouse, humans, *Caenorhabditis elegans* and *Drosophila melanogaster* (He et al., 1998; Chan et al., 1999; Basu et al., 1999). Much of the early genetic and biochemical studies on the spindle checkpoint have been carried in budding yeast due to the availability of the genome sequence and genetic tractability of this model system. More recently this has been accompanied by extensive work in fission yeast and in higher eukaryotes which have allowed localisation studies and more complex biochemical investigations. A wealth of information is now published on the spindle checkpoint components and their interactions, although the mechanism of checkpoint activity is by no means fully elucidated. In this introduction I will briefly describe studies which have furthered our knowledge of the 6 spindle checkpoint proteins before discussing our current knowledge of the spindle checkpoint mechanism.

1.4.2.1 Mad1p

Homologues to budding yeast Mad1p have been identified in *Xenopus* (Chen et al., 1998), human (Campbell et al., 2001), fission yeast (Millband and Hardwick, 2002) and *C. elegans* (Kitagawa and Rose, 1999).

Mad1p is a coiled-coil phosphoprotein which is hyperphosphorylated upon checkpoint activation in budding yeast in a Mad2p, Bub1p and Bub3p dependent manner (Hardwick and Murray, 1995). In *in vitro* assays, Mad1p is phosphorylated by Mps1p and over-expression of Mps1p in *S.cerevisiae* causes hyperphosphorylation of Mad1p both in wild type and *mad* and *bub* mutant strains. This is accompanied by mitotic arrest in wild type strains only, suggesting that arrest is dependent on the other spindle checkpoint proteins, however Mad1p phosphorylation is not carried out by the Bub1p or Bub3p kinases (Hardwick et al., 1996). The immunodepletion of MPS1 in *Xenopus* prevents phosphorylation of MAD1, its localisation to the kinetochore and spindle checkpoint activation and thus it has been demonstrated that kinase activity of MPS1 is essential for these observations (Chen et al., 1998; Abrieu et al., 2001). Together these studies indicate that phosphorylation of MAD1 by MPS1 and recruitment of MAD1 to the kinetochore are probably early events in checkpoint signalling.

Residues 1-445 at the amino terminus of *Xenopus* MAD1 have been shown to be sufficient for targeting of MAD1 to kinetochores. This part of MAD1 does not bind to BUB1 or MAD2 and is a good candidate for direct interaction with a kinetochore protein (Chung and Chen, 2002). Human MAD1 is found at kinetochores during prometaphase but is lost from them at metaphase and anaphase upon microtubule attachment to kinetochores and metaphase plate alignment (Campbell et al., 2001). Residues 501-522 and 557-571 of human MAD1 form leucine zipper domains and are thought to mediate its interaction with MAD2 (Iwanaga et al., 2002).

MAD1 is a likely candidate for the 3F3/2 phosphoepitope, which is recognised upon lack of kinetochore tension and attachment and may act as a docking site for spindle checkpoint proteins. MAD1 shares some properties with the 3F3/2 epitope: the *Xenopus laevis* homologue of MAD1 localises to the kinetochore; in *S.cerevisiae* Mad1p is hyperphosphorylated when the checkpoint is activated and Mad1p recruits checkpoint proteins to the kinetochore (Hardwick and Murray, 1995). Thus MAD1

could provide a scaffold onto which other spindle checkpoint proteins assemble in response to lack of tension and attachment.

MAD1 resides predominantly at the nuclear pore complex throughout the cell cycle and associates with nucleoporins there including Nup53, Nup170 and Nup157. Spindle checkpoint activation results in changes in the interaction with the nuclear pore, release of MAD2 and Nup53 dependent hyperphosphorylation of MAD1 (Iouk et al., 2002). In higher eukaryotes the association of spindle checkpoint complexes with the nuclear pore may be important in detecting the onset of mitosis when the nuclear envelope disintegrates.

MAD1 complexes tightly with MAD2 both in *S.cerevisiae* and in *Xenopus* forming a constitutive complex which localises to free kinetochores in metaphase (Chen et al., 1998; Chen et al., 1999). The recruitment of MAD2 to free kinetochores is thought to be an important function of MAD1. *mad1* and *mad2* budding yeast mutants show similar benomyl sensitivity and elevated rates of chromosome loss indicative of their linked function (Warren et al., 2002).

Mad1p is also found in a signalling complex with Bub1p and Bub3p upon checkpoint activation in budding yeast (Brady and Hardwick, 2000) and the same complex of human proteins is detected *in vitro* (Seeley et al., 1999). Formation of this complex requires the Arg-Leu-Lys protein motif in Mad1p (Brady and Hardwick, 2000). In humans, this complex has kinase activity dependent on the BUB1 kinase motif resulting in autophosphorylation of BUB1 and phosphorylation of MAD1 (Seeley et al., 1999). The complex forms at mitosis during every cell cycle but is found at elevated levels upon checkpoint activation and may have an important signalling role in the checkpoint (Brady and Hardwick, 2000).

MAD1 has also been shown to be essential for BUBR1 localisation and phosphorylation at the kinetochore in *Xenopus* and for BUBR1 interaction with BUB3 and CDC20 in an effector complex (Chen, 2002). The role of these complexes will be discussed in more detail later.

1.4.2.2 Mad2p

Mad2p homologues have been identified in *S.pombe* (He et al., 1997), *Xenopus* (Chen et al., 1996), mouse (Pangilinan et al., 1997), *C. elegans* (Kitagawa and Rose, 1999) and 2 homologues have been identified in humans (Li and Benezra, 1996;

Pfleger et al., 2001; Chen and Fang, 2001). *Xenopus* MAD2 antibodies also recognise proteins at kinetochores in prometaphase *Drosophila* spermatocytes (Basu et al., 1998; Basu et al., 1999).

Localisation of MAD2 to free kinetochores by MAD1 is important for checkpoint function. *Xenopus* MAD2 was the first spindle checkpoint component to be localised to unattached kinetochores (Chen et al., 1996) in a MAD1 dependent manner (Chen et al., 1998) and this has also been observed in human HeLa cells (Li and Benezra, 1996) and in fission yeast (Garcia et al., 2001). In vertebrates MAD2 is detected on kinetochores following chromosome condensation but is lost upon chromosome alignment on the metaphase plate. MAD2 has also been shown to have a transient localisation at the kinetochore of 24-28 seconds in PtK1 cells using Fluorescence recovery after photo-bleaching (Howell et al., 2000). This turnover of MAD2 at kinetochores is thought to be important in its function as APC/C inhibitor. MAD2 has long been thought to be the major effector of the spindle checkpoint although recent studies have indicated that it is not the only inhibitor of the APC/C in the spindle checkpoint. Excess MAD2 can inhibit the APC/C and arrest cells at metaphase in many systems (Fang et al., 1998). Mad2p also interacts with Mad3p in budding yeast (Hardwick et al., 2000) and is found in a complex with BUBR1 and BUB3 in mammalian cells (Sudakin et al., 2001). Furthermore, MAD2 can exist in a tetrameric complex and as a monomer (Fang et al., 1998) and in both phosphorylated and unphosphorylated forms (Wassmann et al., 2003). These changes in turnover, concentration, complex formation, conformation and modification may all be important in MAD2's APC/C inhibiting activity.

This downstream function of MAD2 will be discussed in more detail later.

Over-expression of MAD2 generates a metaphase arrest (He et al., 1998). Upon depletion of MAD2, checkpoint arrested frog extracts exit mitosis prematurely, as do budding yeast *mad2* mutants (Chen et al., 1996; Chen et al., 1999). The human homologue of MAD2 is essential in the checkpoint and localises to the kinetochore in cells mitotically arrested with nocodazole (Li and Benezra, 1996). Mouse knockouts of MAD2 are embryonic lethal (Dobles et al., 2000) and $MAD2^{+/-}$ mice develop lung tumour at high rates indicating haploinsufficiency (Michel et al., 2001). These studies indicate the important role of MAD2 in the spindle checkpoint.

Additionally, a second homologue of MAD2, has been isolated in mammalian cells. The second human homologue, MAD2L2 shows 26% identity and 48% similarity to MAD2 in conserved regions, and is located on 1p36, a region frequently deleted in cancers. MAD2L2 may be involved in inhibition of anaphase to telophase transition by inhibiting proteolytic activity of Cdh1-APC/C, analogous to the role of MAD2 in the metaphase to anaphase transition (Pfleger et al., 2001). However, MAD2L2 does not bind MAD1 and its role in mitotic checkpoints remain unclear (Chen and Fang, 2001).

In summary, MAD1 is probably important for localising MAD2 to the kinetochore where MAD2 inhibits the APC/C through sequestering its association factor CDC20.

1.4.2.3 Mad3p /BUBR1

In human, mouse and *Xenopus,* BUBR1 is thought to be the homologue of budding and fission yeast Mad3p, although structurally Mad3p lacks the BUB1-like C-terminal kinase domain of BUBR1.

Mad3p shares significant homology with BUB1, and human BUBR1 is homologous to both BUB1 and Mad3p. Budding yeast Mad3p is homologous to yeast Bub1p in two conserved domains; CD1 showing 46% homology, containing the GIG domain involved in the CDC20 interaction; and CD2, 47% homologous, which binds Bub3p through E482 and the GLEBS domain (Hardwick et al., 2000). Human BUB1 and BUBR1 also contain these conserved domains and show 81% homology between the human protein domains (Cahill et al., 1998). Human BUBR1, unlike Mad3p also contains a kinase domain similar to that of BUB1, suggesting Mad3p may have lost a kinase domain during evolution. The conserved domains between the BUB1 and Mad3/BUBR1 proteins are shown in figure 1.7.

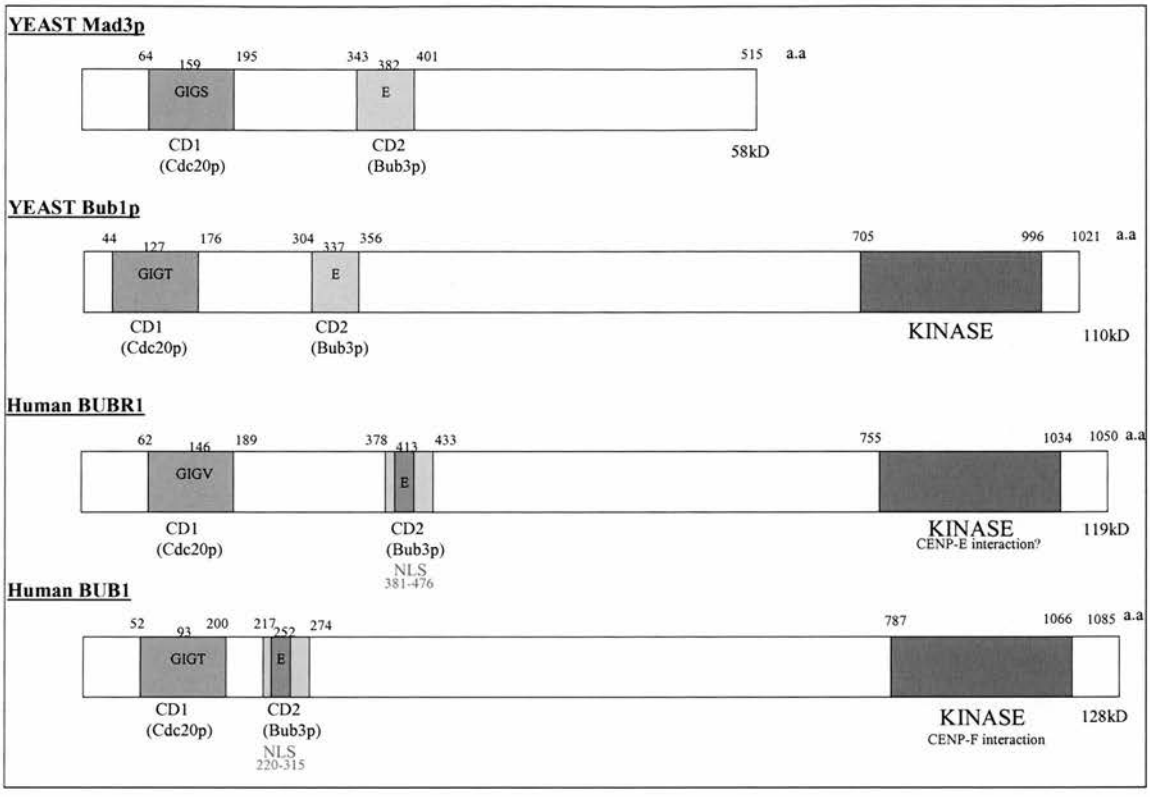

Figure 1.7 Homology between spindle checkpoint proteins

There is considerable homology between the Bub1p and Mad3p homologues in yeast and humans. The homology is particularly strong in two conserved functional domains which are important in interactions with other checkpoint proteins. Additionally the kinase domains of BUB1 and BUBR1 are probably involved in interactions with kinetochore associated proteins of the CENP family.

The yeast Mad3p and mammalian BUBR1 proteins form interactions with BUB3, CDC20 and MAD2 (Fraschini et al., 2001; Taylor et al., 1998). The interaction with BUB3 is thought to be important in the localisation of BUBR1 to kinetochores during the early stages of mitosis in humans and mice (Taylor et al., 1998; Jablonski et al., 1998). The *S.cerevisiae* Mad3p protein also complexes with Bub3p (Hardwick et al., 2000). The interactions with Mad2p and Cdc20p were also initially identified in *S.cerevisiae* (Hardwick et al., 2000; Wu et al., 2000; Sudakin et al., 2001) and a Bub3p-Mad3p-Mad2p-Cdc20p complex is thought to be important in APC/C inhibition during checkpoint activation in yeast (Fraschini et al., 2001). In human HeLa cells, BUBR1 is found in a complex with BUB3 and CDC20 (Tang et al., 2001; Sudakin et al., 2001). Sudakin et al., also identified MAD2 as part of this complex, although this is not found in the Tang study. All these studies agree that BUBR1 behaves as an inhibitor of APC/C-CDC20 in this complex. Mammalian BUBR1 has also been reported to interact with the APC/C subunits CDC20 and CDC27 (Wu et al., 2000). Interestingly, Mad3p has not been shown to inhibit APC/C activation in budding yeast (Hardwick et al., 2000). Inhibition of the APC/C-CDC20 is thought to be a major role of BUBR1 in the checkpoint which will be discussed in more detail later.

In mouse and human cells, BUBR1 is cytoplasmic during interphase but BUBR1 localises to kinetochores in human cells at prophase and remains there until anaphase (Chan et al., 1999). In mouse cells the localisation pattern is similar except it localises to the kinetochores at prometaphase (Taylor et al., 1998; Jablonski et al., 1998). In budding yeast Mad3p localises to the kinetochore when over-expressed (Hardwick et al., 2000). These observations are consistent with the role of Mad3p/BUBR1 as a spindle checkpoint protein.

The role of BUBR1's kinase domain is not clear. One study of human BUBR1 reports the kinase domain to be essential to BUBR1 function, as depletion or expression of a kinase-dead mutant form of human BUBR1 induced a mitotic defect producing aberrant cells with lagging chromosomes (Chan et al., 1999). However, in another study, recombinant human BUBR1 with a truncated kinase domain can bind and inhibit CDC20 *in vitro* as efficiently as the intact protein. Similarly, in *Xenopus*, kinase dead mutants of BUBR1 can still support checkpoint function, suggesting the

kinase domain may not be essential (Chen, 2002). BUBR1 is capable of autophosphorylation *in vitro* but is hyperphosphorylated by other kinases *in vivo* (Li et al., 1999).

The presence of a kinase domain in BUBR1 has suggested it may be a BUB1 homologue rather than a Mad3p homologue. However, Mad3p and BUBR1 share an N terminal extension containing a putative KEN box motif which is not seen in BUB1 proteins (Millband and Hardwick, 2002).

Xenopus BUBR1 was shown to be phosphorylated when localised to metaphase chromosomes but not when cytosolic, suggesting this modification may be important for the checkpoint (Chen, 2002). Human BUBR1 has also been reported to be hyperphosphorylated on spindle checkpoint activation (Chan et al., 1999; Li et al., 1999). Paradoxically, a later study reported phosphorylation of human BUBR1 during a normal mitosis and this is not increased upon treatment with microtubule poisons (Taylor et al., 2001). Co-localisation and immunoblot experiments in *Xenopus* egg extracts indicate that the presence of BUBR1 is important for kinetochore localisation of BUB1, MAD1, MAD2 and CENP-E (Chen, 2002). Both phosphorylation of BUBR1 and its localisation to kinetochores relies on MAD1 in *Xenopus* egg extracts indicating the complexity of interactions between the spindle checkpoint proteins at the kinetochore (Chen, 2002). In addition phosphorylation of BUBR1 is inhibited in mammalian cells by inhibition of Aurora B kinase (the yeast homologue of Ipl-1). This is accompanied by a reduction in the kinetochore localisation of BUBR1, MAD2 and CENP-E and inhibition of both the spindle checkpoint and chromosome alignment and indicates the importance of BUBR1 phosphorylation for its localisation and function (Ditchfield et al., 2003).

BUBR1 has also been shown to interact with the centromere associated kinesin-like motor protein CENP-E during mitosis. CENP-E is important in the establishment of bipolar attachments at metaphase and alignment on the metaphase plate and its interaction with BUBR1 may be important in monitoring this (Chan et al., 1998; Yao et al., 2000). This will be discussed in more detail later in this chapter.

Inhibition of BUBR1 in mammalian cells by antibody injection or RNAi, inhibits the spindle checkpoint (Chan et al., 1999; Ditchfield et al., 2003). In the RNAi

experiments the number of metaphase cells were reduced and many cells in anaphase exhibited lagging chromosomes (Ditchfield et al., 2003). These cells also exhibited defects in chromosome alignment. Inhibition of Aurora B kinase produces a similar phenotype, suggesting phosphorylation of BUBR1 is involved in chromosome alignment (Ditchfield et al., 2003). This is consistent with previous studies which describe a role for Aurora B, and the budding yeast homologue Ipl1p, in the correction of syntenic attachments (when sister chromatids are attached to the same pole), chromosome alignment and spindle checkpoint maintenance in response to a lack of tension (Biggins and Murray, 2001; Nigg, 2001). Potentially BUBR1 is important in some or all of these roles, indicated by its ability to interact with CENP-E and other microtubule associated proteins and its perceived role in linking lack of tension and the spindle checkpoint (Chan et al., 1998; Skoufias et al., 2001).

1.4.2.4 Bub1p

Bub1p is a serine-threonine protein kinase (Roberts et al., 1994; Taylor and McKeon, 1997) with known homologues in *S.cerevisiae* (Li and Murray, 1991; Hoyt et al., 1991), *S.pombe* (Bernard et al., 1998), *Xenopus* (Sharp-Baker and Chen, 2001), Human (Jablonski et al., 1998; Ouyang et al., 1998) and Mouse (Taylor and McKeon, 1997).

Bub1p contains the same two conserved domains as Mad3p; CD1 and CD2 (see Figure 1.7). The CD2 domain is known to interact with Bub3p, an interaction seen in budding yeast and mammalian cells (Roberts et al., 1994; Taylor and McKeon, 1997; Taylor et al., 1998). As it contains a CD1 domain, Bub1p might be expected to bind Cdc20p but although this is achieved *in vitro*, co-immunoprecipitation experiments isolate no Bub1p-Cdc20p complex in wild type budding yeast strains. However, a Bub1p-Cdc20p complex was found in *mad3* mutant extracts (Hardwick et al., 2000), suggesting Cdc20p has a higher affinity for Mad3p than Bub1p but that Bub1p may be able to carry out at least some of its functions when absent. Such redundancy between Bub1p and Mad3p would be explained by the homology between conserved domains of the proteins. Mad3p however, lacks homology to the C terminal region of Bub1p and would be unable to compensate for its kinase activities consistent with a more severe chromosome segregation defect in *bub1* than in *mad3* budding yeast mutants (Warren et al., 2002). This would not be true of the

human homologues of the proteins, as human BUBR1 has retained the kinase domain and thus may provide some redundancy with human BUB1. This is consistent with the identification of mutations in human *BUB1* and human *BUBR1* in tumours, whereas mutations in other checkpoint proteins, which do not share redundancy, may not be seen due to lethality. However, human BUBR1 and human BUB1 are not completely redundant as neither can maintain the checkpoint alone (Chan et al., 1999).

The protein kinase BUB1 binds to BUB3, an interaction first described in budding yeast (Roberts et al., 1994) but which also exists in mouse cells and is important in localisation of BUB1 to the kinetochore during mitosis (Taylor and McKeon, 1997; Taylor et al., 1998). BUB1 has also been identified in human cells and localised to the kinetochore in interphase, prophase and upon nocodazole activation of the spindle checkpoint (Ouyang et al., 1998). Contrary to these reports, studies by Jablonski et al. report that human BUB1 is loaded onto kinetochores during early prophase and remains there throughout mitosis with reduced concentrations from anaphase onwards (Jablonski et al., 1998). A similar phenomenon was observed in fission yeast (Bernard et al., 1998) and *Xenopus* (Sharp-Baker and Chen, 2001).

Over-expression of the protein kinase Bub1p in *S.cerevisiae* constitutively activates the checkpoint but does not accumulate hyperphosphorylated Mad1p, and is probably involved early in the signalling cascade (Farr and Hoyt, 1998). This is supported by studies in *Xenopus* in which MAD1, MAD2, BUB3 and CENP-E localisation all require BUB1 localisation to kinetochores (Sharp-Baker and Chen, 2001) indicating it may act as a scaffold onto which other proteins associate. However, other studies suggest Bub3p may act as this scaffold protein (Fraschini et al., 2001). This is consistent with the greater checkpoint defects seen in *bub1* and *bub3* budding and fission yeast mutants (Warren et al., 2002; Bernard et al., 1998). Perhaps BUB1 acts as a scaffold at the kinetochore in response to lack of tension and MAD1 acts similarly in response to unattachment. However BUB1 has been shown to localise specifically to the unattached kinetochore when chromosomes form unipolar attachments (Taylor et al., 2001) and thus may be involved in responses to both lack of tension and attachment.

BUB1 is a protein kinase with a conserved C-terminal protein kinase domain. Examination of the kinase activity of BUB1 has produced variable results. Bub1p has been found to be phosphorylated itself and Bub3p *in vitro* assays (Roberts et al., 1994) and can also phosphorylate MAD1 in humans (Seeley et al., 1999). The formation of the Bub1p-Bub3p complex is thought to stimulate Bub1p kinase activity (Roberts et al., 1994). However these observations are disputed in mouse studies (Martinez-Exposito et al., 1999) and *in vivo* phosphorylation of BUB3 by BUB1 has not been shown. In the *Xenopus* experiments mentioned above a kinase dead mutant of BUB1 is still fully functional in localisation of other checkpoint associated proteins to the kinetochore (Sharp-Baker and Chen, 2001). However, in another *Xenopus* study BUB1 kinase activity is required for metaphase arrest (Tunquist et al., 2002). Mutation of the kinase domain in budding yeast also caused a checkpoint defect (Roberts et al., 1994). Kinase activity has not yet been demonstrated in fission yeast (Vanoosthuyse and Hardwick, 2003) but kinase-dead mutants of Bub1p and truncation mutants lacking the kinase domain have a reduced spindle checkpoint function (Yamaguchi et al., 2003). Thus Bub1p kinase activity does not appear to be required for its localisation to the kinetochore, nor is it required to localise Mad2p to the kinetochore (Yamaguchi et al., 2003) although it has been shown to phosphorylate Mad2p.

Bub1p can autophosphorylate *in vitro* through its kinase activity (Roberts et al., 1994). One study shows *Xenopus* BUB1 is phosphorylated constitutively (Sharp-Baker and Chen, 2001) but another shows BUB1 fractions associated with metaphase chromosomes are substantially modified compared to cytosolic BUB1 suggesting phosphorylation of BUB1 may be important for checkpoint function (Chen, 2002). This phosphorylation of BUB1 is not due to BUBR1 kinase activity (Chen, 2002). Bub1p is hyperphosphorylated in mitosis in budding yeast (Brady and Hardwick, 2000) and upon spindle damage in humans (Taylor et al., 1998) and fission yeast (Yamaguchi et al., 2003). Fission yeast Bub1p has four putative CDK phosphorylation sites in its central region; T340, T423, T455 and S466 (Yamaguchi et al., 2003). Bub1p is phosphorylated throughout the cell cycle and is hyperphosphorylated upon checkpoint activation at these sites in a Cdc2p dependent manner. Elimination of this phosphorylation confers a reduced checkpoint activity

although Bub1p still localises to the kinetochore. Bub1p is also phosphorylated by other kinases at distinct sites (Yamaguchi et al., 2003) perhaps by the Mps1p homologue Mph1p (He et al., 1998). This is consistent with studies showing human BUB1 is also phosphorylated upon checkpoint activation (Taylor et al., 2001). Similar residues for CDK phosphorylation can be found in human, budding yeast, mouse, *Drosophila* and *Xenopus* BUB1, although the location of these are not conserved. *Xenopus* BUB1 has also been shown to be directly phosphorylated by CDC2 *in vitro* (Schwab et al., 2001). In both *Xenopus* and fission yeast, phosphorylation of BUB1 by CDC2 does not seem to affect its own kinase activity (Schwab et al., 2001; Yamaguchi et al., 2003). One hypothesis is that phosphorylation of Bub1p affects signalling to downstream effectors such as Mad3p (Millband et al., 2002) or may be required for interaction with other spindle checkpoint proteins in a similar way to the requirement of Mps1 for formation of Mad1p-Bub1p-Bub3p complex (Brady and Hardwick, 2000).

Thus it seems a BUB1-BUB3 complex is important at the kinetochore in response to lack of tension and possibly also to attachment, but the role of BUB1 kinase activity and the phosphorylation states are uncertain. BUB1 also interacts with MAD1, probably in the same complex as with BUB3 when the spindle checkpoint is activated. This complex is thought to be involved in signalling and formation of the APC/C inhibitory complex, although it is not actually a member of the effector complex (Brady and Hardwick, 2000; Seeley et al., 1999). This will be discussed in more detail later in this chapter.

Bub1p has recently been shown to interact with a centromere component Skp1p in budding yeast and this interaction is essential for the checkpoint response to lack of tension at kinetochores (Kitagawa et al., 2003). BUB1 has also been shown to interact with the adenomatous polyposis coli protein (APC; not to be confused with the Anaphase promoting complex or APC/C) and with CENP-F, both involved in microtubule dynamics and this will be discussed later .

1.4.2.5 Bub3p

BUB3 is a WD repeat structure protein with a propeller structure of 7 β sheet blades (http://alanine.ucdavis.edu/~dave/wilsonlab/). It is important in localisation of BUB1 and BUBR1 to the nucleus and the kinetochore through interaction with

their GLEBS motifs. *Xenopus* studies indicate BUB3 is diffusely localised throughout the nucleus during interphase but localises to kinetochore during early mitosis in *Xenopus* (Campbell and Hardwick, 2003), *Drosophila* (Basu et al., 1998), mice (Martinez-Exposito et al., 1999) and humans (Taylor et al., 1998). Mouse studies report BUB3 is recruited during prophase and lost as the chromosomes align on the metaphase plate, remaining only on lagging chromosomes (Martinez-Exposito et al., 1999). This is consistent with studies in *Xenopus* and *Drosophila* but in human cells BUB3 is lost from kinetochores at metaphase. In mammalian cells BUB3 is required for kinetochore localisation of BUB1 (Taylor et al., 1998). Bub3p is also involved in a signalling complex with Bub1p and Mad1p (Brady and Hardwick, 2000). BUB3 is essential to establish and maintain spindle checkpoint arrest in *Xenopus* egg extracts and addition of antibodies to BUB3 abrogates the spindle checkpoint but does not interfere with BUB3, BUB1 or MAD2 localisation at kinetochores consistent with its role in downstream signalling (Campbell and Hardwick, 2003). Mouse knock outs of BUB3 are embryonic lethal, indicative of its essential nature in the checkpoint (Kalitsis et al., 2000).

1.4.2.6 Mps1p

Mps1 (mono-polar spindles) is a protein kinase initially identified through its involvement in spindle pole body duplication in budding yeast (Winey et al., 1991). The involvement of Mps1p in the spindle checkpoint became apparent after the isolation of other spindle pole body mutants in which the spindle pole body fails to duplicate but cells arrest at the spindle checkpoint. This arrest is not seen in *mps1* mutants despite the presence of a monopolar spindle (Weiss and Winey, 1996). Subsequent experiments showed over-expression of Mps1p activates the spindle checkpoint in the absence of spindle damage (Hardwick et al., 1996).

Mps1p homologues have been identified in fission yeast (He et al., 1998), mouse (Fisk and Winey, 2001), humans (Stucke et al., 2002) and *Xenopus* (Abrieu et al., 2001). Studies in these organisms show MPS1 localises to the kinetochore and functions early in the spindle checkpoint, probably by the phosphorylation and recruitment of MAD1 and hence MAD2 to the kinetochore (Hardwick et al., 1996; Fisk and Winey, 2001; Abrieu et al., 2001; Liu et al., 2003a). Although kinase dead

MPS1 can still localise to the kinetochore itself, its kinase function has been shown to be essential for localisation of MAD1, MAD2 and CENP-E to the kinetochore in *Xenopus* and for checkpoint function (Abrieu et al., 2001). Human MPS1 is phosphorylated itself upon activation of the checkpoint and its activity is greatest when the checkpoint is switched on (Stucke et al., 2002). Human MPS1 is essential for spindle checkpoint activation but is not required for centrosome duplication as shown in yeast (Stucke et al., 2002) although it has been shown to localise to both centrosomes and kinetochores (Liu et al., 2003a).

Human MPS1 localises to nuclear pores and is required for spindle checkpoint activation in response to spindle and kinetochore defects in CENP-E defective cells. MPS1 is required for localisation of MAD1 and MAD2 to kinetochores but not for BUB1, BUBR1 or ROD suggesting it responds to reduced microtubule occupancy rather than kinetochore tension (Liu et al., 2003a). This is consistent with the hypotheses that MAD1-MAD2 respond to unattachment while BUB1-BUBR1 respond to lack of tension. MPS1 has also been shown to interact with the APC/C indicating additional checkpoint functions (Liu et al., 2003a).

A summary of the functions and homologues of the described spindle checkpoint proteins is shown in table 1.3.

Table 1.3: A Summary of Spindle Checkpoint Proteins and Functions

Protein	Interactions	Comments
MAD1		Coiled-coil phosphoprotein.
		Hyperphosphorylated upon checkpoint activation by Mps1.
		3F3 phosphoepitope?
	MAD2	Constitutive complex, localises to unattached kinetochores.
	BUB3 +BUB1	In signalling complex through Arg-Leu-Lys domain.
MAD2		Mouse knockouts are embryonic lethal.
		Shows hapolinsufficiency.
	MAD1	Constitutive complex, recruited to unattached kinetochores by MAD1 and required for MAD1 phosphorylation.
	CDC20	Complex inhibits APC/C.
	MAD3/BUBR1	In inhibitory complex with Cdc20?
MAD3/ BUBR1		BUBR1 has a C-terminal kinase domain.
		Phosphorylates APC.
	BUB3	Constitutive complex, recruited to kinetochores not under tension .
	MAD2	In inhibitory complex with CDC20 and possibly BUB3.
	CDC20	Complex inhibits APC/C.
	APC/C	Associates with APC/C subunits *in vitro*.
	CENP-E	Involved in detecting loss of tension and in checkpoint silencing?
BUB1		Serine Threonine protein kinase.
		Phosphorylates APC.
		Kinase domain not required for checkpoint arrest.
	BUB3	Direct binding, constitutive complex for kinetochore localisation.
	MAD1	In signalling complex with BUB3.
	CENP-F	Essential for CENP-E localisation.
BUB3		WD repeat protein resembling a β propeller.
		Knockout mice die early in embryogenesis.
		Phosphorylated by BUB1 *in vitro*.
	BUB1	Constitutive complex, recruits BUB1 to kinetochore.
	BUBR1	Constitutive complex, responds to lack of kinetochore tension and in Mitotic checkpoint complex (MCC) to inhibit APC/C.
MPS1		Serine threonine protein kinase.
		Involved in centrosome duplication .
		Phosphorylates MAD1.
		Over-expression activates the checkpoint.
APC/C		Proteolytic complex of 11 proteins.
		E3 Ubiquitin ligase.
	CDC20/CDH1	Initiates proteolytic degradation during the cell cycle.
		Specificity dependent on association factors.
CDC20		APC/C association factor.
	BUB3+MAD3+MAD2	Inhibits APC/C degradation of Pds1p.
APC		Regulates cytoplasmic pool of β-catenin.
	EB1	Stabilises and bundles microtubules.
	BUB1-BUBR1-BUB3	Phosphorylated by GSK3β and BUB1 and BUBR1.
CENP-E		Plus ended microtubule motor involved in chromosome alignment.
		Involved in checkpoint function and silencing.
		Conformation changes upon loss of kinetochore tension.
	BUBR1	Acts as motor-kinase complex to transduce loss of tension.
	BUB1?	BUB1 required for its kinetochore localisation.
CENP-F	BUB1	Interacts with kinase domain, recruited to kinetochore by BUB1.

1.4.3 Complexes at the Kinetochore

Three complexes of spindle checkpoint proteins exist constitutively in cells: MAD1-MAD2; BUB1-BUB3 and BUB3-MAD3. Upon activation of the spindle checkpoint by detection of lack of tension or attachment, these three complexes are recruited to the free kinetochore where they are thought to initiate spindle checkpoint activation and arrest chromatid separation. The localisation of the complexes to the kinetochore is thought to promote the formation of multiprotein complexes, phosphorylation effects and controlled turnover of essential proteins. Ultimately, there is initiation of a signalling complex which in turn produces inhibitory complexes to bind CDC20 and prevents it from activating the APC/C. The APC/C is inhibited from cleaving sister chromatid cohesion and separating the chromosomes, halting metaphase to anaphase progression. The inhibitory signal is conveyed from the initiating free kinetochore to all the kinetochores of the cell to generate an anaphase wait signal, possibly through soluble pools of non-kinetochore bound checkpoint proteins (Millband et al., 2002).

1.4.3.1 MAD1-MAD2 Complex

Mad1p complexes tightly with Mad2p both in *S.cerevisiae* and in *Xenopus* forming a constitutive complex. Studies in budding yeast and *Xenopus* indicate the complex forms independently of other checkpoint proteins and of cell cycle position (Chen et al., 1999; Chen et al., 1998). During mitosis this association seems to be important to recruit MAD2 to unattached kinetochores (Chen et al., 1998). The human homologue of MAD1 is also found at kinetochores during prophase but dissociates from them during metaphase and anaphase and upon microtubule attachment (Campbell et al., 2001). The crystal structure of this MAD1-MAD2 complex has been elucidated. It consists of an asymmetric tetramer in which the MAD1 monomers are elongated coiled coils to interact with MAD2. The C-terminal tails of MAD2 are hinged ligand binding elements which are regulated to interact with MAD1 or CDC20 in effector complexes (Sironi et al., 2002). This complex is highly stable.

The interaction between MAD1 and MAD2 is mediated via two leucine zipper domains in human MAD1 (amino acids 501-522 and 557-571). A polymorphism at amino acid 558 perturbs the coiled coil structure of MAD1 and reduces the

interaction with MAD2 4.5 fold (Iwanaga et al., 2002). This polymorphism may have relevance to cancer predisposition.

The MAD1-MAD2 complex has been reported to localise to the nuclear envelope during interphase in *Xenopus* (Chen et al., 1998). Biochemical and localisation studies in human cells and rats indicate that this complex actually localises to the nuclear pores (Campbell et al., 2001) and electron microscopy reveals human MAD1 localisation to the nuclear face of the nuclear membrane (Campbell et al., 2001). Biochemical studies with purified metaphase chromosomes from *Xenopus* egg extracts found little MAD1-MAD2 complex associated with them but that the amount of this complex increased greatly upon activation of the checkpoint with nocodazole (Chen, 2002).

Thus the MAD1-MAD2 complex probably exists constitutively in the cell, localising to the nuclear pore during interphase. At metaphase it is recruited to free kinetochores in response to a lack of tension on them. MAD1 is also phosphorylated by MPS1 either before kinetochore localisation or as a result of it and the phosphorylated MAD1-MAD2 complex may then act as a docking site for further checkpoint proteins and is involved in downstream checkpoint signalling functions.

1.4.3.2 BUB1-BUB3 Complex

The protein kinase Bub1p associates with Bub3p, an interaction first described in budding yeast (Roberts et al., 1994). A small stretch of amino acids in the N terminal of mouse BUB1 mediates an interaction with human BUB3 and is co-incident with the murine BUB1 kinetochore localisation domain suggesting it is interaction with BUB3 which localises BUB1 to the kinetochore during mitosis (Taylor and McKeon, 1997; Taylor et al., 1998). The interaction with BUB3 is important for BUB1 localisation to the kinetochore upon checkpoint activation and this has been observed in several species (Ouyang et al., 1998; Jablonski et al., 1998; Bernard et al., 1998; Sharp-Baker and Chen, 2001).

1.4.3.3 MAD3-BUB3 Complex

Studies show BUB3 is localised to the kinetochore in early mitosis in several organisms (Campbell and Hardwick, 2003; Basu et al., 1998; Martinez-Exposito et al., 1999; Taylor et al., 1998). BUB3 acts as a nuclear import and kinetochore

recruitment factor for MAD3 (and BUBR1) in the same way as it does for BUB1. A BUB3-MAD3 or BUB3-BUBR1 complex has been reported in humans, budding and fission yeast and *Xenopus* (Taylor et al., 1998; Roberts et al., 1994; Hardwick et al., unpublished data; Chen, 2002). MAD3 binds BUB3 through a CD2 domain conserved between MAD3 and BUB1 and between species, an interaction important for checkpoint function (Roberts et al., 1994; Amon, 1999; Hardwick et al., 2000) and kinetochore localisation in humans (Roberts et al., 1994; Amon, 1999). In *Xenopus* the interaction between BUB3 and BUBR1 was shown to be constitutive and to localise to the kinetochore upon checkpoint activation (Chen, 2002). Phosphorylation of BUBR1 may also be important for this localisation (Chen, 2002; Chan et al., 1999). Localisation of MAD3 to the free kinetochore by BUB3 is probably important to mediate interactions between MAD3 and the other checkpoint proteins in the effector complex. In support of this a Mad3p-Cdc20p-Mad2p complex cannot be isolated from *bub3* mutant budding yeast strains (Hardwick et al., 2000).

Thus studies in yeast and vertebrates have localised MAD1, MAD2, BUB1, BUB3 and MAD3 to unattached kinetochores during prophase and prometaphase, in at least three complexes: MAD1-MAD2, BUB1-BUB3 and MAD3-BUB3 (human BUBR1-BUB3). The recruitment of these three complexes to the kinetochore may be important to promote interactions between the proteins or post translational modification of them to activate the checkpoint.

1.4.4 Signalling Complexes

Experiments in *S.cerevisiae* have shown that a Mad1p-Bub1p-Bub3p complex is formed at a regulated time in the cell cycle and that treatment with nocodazole resulted in higher levels of this complex. Disruption of the RLK motif in Mad1p, which is necessary to form this complex, conferred a checkpoint defect showing the importance of the complex in normal checkpoint function. This indicates firstly that the Mad1p-Bub1p-Bub3p complex is involved in the spindle checkpoint and secondly that the checkpoint is activated every cell cycle, during the formation of kinetochore microtubule interactions, producing an anaphase wait signal. The formation of this complex is dependent on Mad2p, Bub3p and Mps1p but not on

Bub2p or Mad3p, suggesting roles for Mps1p and Mad2p in phosphorylating these proteins and localising them to the kinetochores respectively and indicative of a downstream role for Mad3p. The ability of the complex to form in strains containing only kinase dead Bub1p indicates the kinase activity of Bub1p is not essential for the complex, although Bub1p was found at lower levels in the complex in the kinase dead mutants (Brady and Hardwick, 2000). The same complex of human proteins is detected in vitro in which MAD1 and BUB1 are phosphorylated (Seeley et al., 1999).

This study is consistent with the hypothesis that Mad1p and Bub1p are important in a signalling complex from which Mad2p is released in an activated form to inhibit the APC/C, by interacting with Cdc20p, but do not actually exist in inhibitory complexes themselves (Musacchio and Hardwick, 2002).

1.4.5 Complexes Inhibiting the APC/C

Initial studies in yeast suggested Mad2p was the major effector in the spindle checkpoint. MAD2 has been shown to associate with the APC/C and to inhibit its ubiquitin ligase activity in *Xenopus* egg extracts (Li et al., 1997). MAD2 is rapidly turned over at kinetochores (Howell et al., 2000) and may be released from its kinetochore complex with MAD1 in a modified state, to inhibit Cdc20-APC/C, a complex which has been detected in yeast (Fang et al., 1998). This modification may involve oligomerisation, phosphorylation or interaction with other proteins. Oligomerisation has been seen in recombinant MAD2 *in vitro* (Fang et al., 1998), A monomeric point mutant of MAD2 still activates the checkpoint, suggesting oligomerisation is not the only method of checkpoint activation (Sironi et al., 2001). Structural analyses reveal MAD1 and CDC20 share a common MAD2 binding site and complex formation with peptides mimicking this site causes MAD2 to undergo a major conformational change which might also represent activated MAD2 (Luo et al., 2002). The crystal structure of the MAD1-MAD2 complex revealed that the tetrameric complex of MAD1-MAD2 is very stable. However, as a dimeric complex, MAD2 is slowly released to bind CDC20 (Sironi et al., 2002). High levels of MAD1 inhibit CDC20-MAD2 binding *in vitro* but MAD1 is required for formation of the CDC20-MAD2 complex *in vivo* in yeast. Thus it appears MAD2 recruitment to kinetochores is by formation of a tight tetrameric complex with

MAD1. This complex may be destabilised at the kinetochore to a dimeric complex through conformational changes, interaction with other proteins such as BUB1 and BUB3 or both. The 1:1 MAD1-MAD2 complex then slowly releases MAD2 allowing its efficient transfer to CDC20 and checkpoint arrest (Sironi et al., 2002).

The phosphorylation state of MAD2 may represent another checkpoint regulatory mechanism. Wassmann et al. recently showed that *in vitro* MAD2 is phosphorylated on multiple C-terminal serine residues in HeLa cells. This phosphorylation is cell cycle dependent and is lowest during spindle checkpoint activation. Mutation of the serine residues to aspartic acid residues, which mimic phosphorylation, prevents MAD2 binding to MAD1 and from complexing with APC/C-CDC20, preventing metaphase arrest in stable cell lines (Wassmann et al., 2003). C-terminal deletion mutants of MAD2 also show an aberrant spindle checkpoint response and are unable to interact with CDC20 and MAD1 (Fang et al., 1998; Sironi et al., 2001), the region having previously been shown to be involved in interacting with APC/C-CDC20 (Luo et al., 2000). NMR structural analyses have also indicated that MAD2 interacts with a common structural motif in CDC20 and MAD1 and that this interaction causes a structural rearrangement of the C-terminus of MAD2 (Luo et al., 2002; Sironi et al., 2002). These results have lead to a new hypothesis in which MAD2 is recruited to free kinetochores by association with MAD1, where it is phosphorylated, perhaps through formation of a MAD1-MAD2-BUB1-BUB3 signalling complex. Phosphorylation of MAD2 may represent a mechanism by which it could be released from the tight complex with MAD1 (Wassmann et al., 2003; Sironi et al., 2002). A dephosphorylation event would be required to allow MAD2 to interact with CDC20-APC/C and inhibit the destruction of cohesion. This model is supported by coimmunoprecipitation experiments in which only unphosphorylated MAD2 binds CDC20-APC/C (Wassmann et al., 2003). The phosphorylation of CDC20 has also been shown to be important for spindle checkpoint function through APC/C inhibition and disruption of one of four phosphorylation sites in CDC20 disrupts checkpoint response in *Xenopus laevi* (Chung and Chen, 2003).

Experiments in mammalian and *Xenopus* systems argue that BUBR1 is a more potent inhibitor of the APC/C-CDC20 than MAD2 and is therefore a more likely effector for the spindle checkpoint complex (Tang et al., 2001; Sudakin et al., 2001;

Chen, 2002). Two groups have recently isolated complexes with APC/C inhibitory activity from HeLa cells (Tang et al., 2001; Sudakin et al., 2001). Tang et al., purify a mitotic checkpoint complex (MCC) from nocodazole arrested HeLa cells containing BUB3, BUBR1 and CDC20. This complex was found to inhibit the activity of the APC/C at physiological mitotic concentrations and at concentrations lower than those required for MAD2 inhibition of the APC/C. This inhibition appeared to be mediated by preventing CDC20 associating with the APC/C and the inhibitory effects were less powerful on CDC20 already bound to the APC/C (Tang et al., 2001).

The second study by Sudakin et al., also isolated an APC/C inhibitory complex using a slightly different purification technique (Sudakin et al., 2001). The MCC isolated in this study contained BUB3 and BUBR1 and also MAD2. Again this complex was found to have superior inhibitory activity compared to recombinant MAD2 alone. Surprisingly this complex was present throughout the cell cycle but mitotic APC/C was significantly more sensitive to inhibition by the MCC than interphase APC/C. BUBR1 was found to associate preferentially with a phosphorylated form of the APC/C subunit CDC27. As APC/C subunits are often hyperphosphorylated during mitosis this suggests a method by which APC/C is sensitised to inhibition by the MCC. In addition it has been reported that BUBR1, MAD2 and CDC20 preferentially bind to mitotically phosphorylated APC/C (Fang et al., 1998; Kallio et al., 1998; Kotani et al., 1999; Wu et al., 2000). Further evidence shows the MCC activity is not affected by chromosomes *in vitro* and that it may be that the presence of unattached kinetochores which sensitises the APC/C to inhibition by the MCC (Sudakin et al., 2001).

A similar complex containing BUBR1, BUB3, CDC20 and MAD2 has been isolated from mitotic *Xenopus* egg extracts (Chen, 2002). Unlike in the study by Sudakin et al., this complex could not be isolated from interphase cells and the interaction between CDC20 and the other proteins was stronger in extracts prepared from nocodazole treated cells. Depletion of either MAD2 or BUBR1 severely reduced the amount of the other protein found bound to CDC20, although this could be due to defects in the formation of localisation complexes at the kinetochore (Chen, 2002).

Further immunoprecipitation studies on HeLa cell extracts detected two separate complexes containing CDC20; one in which CDC20 interacts with BUB3 and BUBR1 and one in which CDC20 interacts with MAD2 (Fang, 2002). The BUBR1-BUB3-CDC20 complex is shown to interact with APC/C and both MAD2 and BUBR1 are shown to inhibit the ability of CDC20 to activate APC/C *in vitro* but neither can inhibit a pre-formed APC/C-CDC20 complex, consistent with previous studies (Tang et al., 2001). Again this study agrees with those above that BUBR1 is a more potent inhibitor of CDC20 than MAD2 (at least 12fold) but the two inhibitory molecules act synergistically in that they can both inhibit the same pool of CDC20 (Fang, 2002). Further investigations indicate that the interaction between MAD2 and CDC20 promotes the inhibitory function of BUBR1 and vice versa, at least at certain concentrations (Fang, 2002). Thus both BUBR1 and MAD2 interact with and inhibit the CDC20 in the spindle checkpoint and these probably have an additive effect in the cell.

The evidence for the involvement of BUBR1 in APC/C-CDC20 inhibition in vertebrate systems is strong but in yeast cells the role for Mad3p in Cdc20p inhibition is less clear cut. Yeast two hybrid assays and immunoprecipitation experiments do reveal a Mad2p-Mad3p-Cdc20p complex which is essential for checkpoint function in wild type strains. Although the Mad3p-Mad2p and Mad3p-Cdc20p complexes are dependent on other checkpoint proteins, a Mad2p-Cdc20p complex can be isolated from *mad3* mutants which may indicate a lesser role for Mad3p in Cdc20p inhibition compared to Mad2p (Hardwick et al., 2000; Brady and Hardwick, 2000). The co-immunoprecipitation of the Mad2p-Cdc20p complex is only moderately affected in *bub3* and *bub1* mutants suggesting Bub3p may not be part of this complex (Hardwick et al., 2000). In a separate study, a Bub3p-Mad3p-Mad2p-Cdc20p complex has been isolated from budding yeast but the role of this complex in APC/C inhibition has not been investigated (Fraschini et al., 2001). Incidentally this complex is not dependent on kinetochores, consistent with previous studies by Sudakin et al. (Fraschini et al., 2001; Sudakin et al., 2001). Additionally, over-expression of Mad2p in budding yeast causes a spindle checkpoint arrest but no specific phenotype is associated with Mad3p over-expression (Millband and Hardwick, 2002). Human BUBR1 has been reported to bind the APC/C in mitotic

cells but there is no evidence to support this in its budding yeast counterpart (Chan et al., 1999; Hardwick et al., 2000). However, in fission yeast, a Mad2p-Mad3p-Bub3p-Cdc20p complex is also detected and Mad3p is essential for a checkpoint arrest initiated by over-expression of Mad2p consistent with a role for Mad3p in Cdc20p inhibition (Millband and Hardwick, 2002).

These studies have altered our previous ideas about how the checkpoint inhibited the APC/C in two ways. Firstly, it seems MAD2 is not the only inhibitor of the APC/C but a complex involving BUBR1 can also inhibit the APC/C and probably more efficiently than MAD2. Secondly, as the MCC can be isolated from interphase cells, it may not be recruitment of the spindle checkpoint complexes to the kinetochore which causes the MCC to form. A revised model might suggest the spindle checkpoint complexes which form at unattached kinetochores are important either in modifying the APC/C to sensitise it to inhibition by the MCC or in modification of the MCC itself. Another theory could be that the checkpoint proteins assembled at the kinetochore are important in establishing signalling and effector complexes which act locally to initiate an anaphase wait signal, perhaps through modification of the APC/C. This signal could then be communicated to the soluble pool of MCC to ensure each and every chromosome arrests. The local and diffuse signals could be mediated by different MAD2 and BUBR1 CDC20-inhibiting complexes which would be consistent with discrepancies in different studies and organisms.

MAD2 and BUBR1/Mad3p may work in combination in the checkpoint. Mad2p complexes with Bub3p, Mad3p and Cdc20p in budding yeast (Hardwick et al., 2000; Fraschini et al., 2001) and in vertebrate cells, probably acting to inhibit Cdc20p-APC/C activity and anaphase onset in both (Chen, 2002; Tang et al., 2001; Skoufias et al., 2001). The effects of MAD2-CDC20 and BUBR1-CDC20 interactions on APC/C inhibition have been reported to be additive (Tang et al., 2001; Fang, 2002). Alternatively they may act in response to different tension and attachment stimuli at the kinetochore; MAD2 in response to detachment and BUBR1 in response to a loss of tension (Skoufias et al., 2001; Waters et al., 1998). A further hypothesis is that one of the two CDC20 inhibitors acts at the kinetochore to inhibit CDC20 locally and that this in turn activates the other to inhibit CDC20 throughout the cell. Both

BUBR1 and MAD2 localise to unattached kinetochores but MAD2 has a short half-life there so may initially be activated there before it diffuses away and inhibits the cellular pool of CDC20 (Tang et al., 2001; Fang, 2002).

The differences between yeast and vertebrate systems could represent additional complexity required for higher eukaryotes. It is not a result of the lack of a kinase domain in Mad3p as BUBR1 proteins which have mutant or truncated kinase domains can still interact with CDC20 and activate the checkpoint in *Xenopus* and mammalian systems (Chen, 2002; Tang et al., 2001). BUBR1 is able to phosphorylate CDC20 in a cell cycle dependent manner but its kinase activity has no effect on APC/C function (Fang, 2002).

1.4.6 How do the Effector Complexes Delay the Metaphase to Anaphase Transition?

APC/C controls sister chromatid separation by initiating Pds1p destruction. This in turn activates the Esp1p protease to cleave Cohesin, removing the glue which holds sister chromatids together, thus allowing them to separate. To destroy Pds1p, APC/C must be associated with Cdc20p which activates it. Upon activation of the spindle checkpoint an inhibitory complex probably involving Mad2p and Mad3p binds and inhibits Cdc20p preventing its interaction with the APC/C and hence chromatid separation (Biggins and Murray, 1999; Hartman et al., 2000; Tanaka et al., 2000; Uhlmann et al., 2000).

Overlapping motifs have been identified in mammalian CDC20 which interact with APC/C and MAD2. A CDC20 truncation mutant able to bind MAD2 but not APC/C, induces the formation of multinucleated cells, by bypassing the checkpoint and these cells are more sensitive to microtubule drug induced apoptosis (Zhang et al., 2001).

In budding yeast over-expression mutants of Cdc20p avoid activation of the spindle checkpoint and no longer bind Mad proteins, suggesting Cdc20p has a greater affinity for APC/C than for Mad2p (Hwang et al., 1998).

Mammalian CDC20, p55CDC, has co-immunoprecipitated with the human homologue of MAD2 and components of the APC/C and injection of anti-p55CDC antibodies into mammalian cells induces metaphase arrest (Kallio et al., 1998). Additionally, human BUBR1 has been found to associate with the APC/C in

mitotically arrested cells, but not in interphase cells, through co-immunoprecipitation experiments (Chan et al., 1999).

In *Xenopus* cells MAD2 also interacts with the APC/C when the mitotic checkpoint is activated and injection of purified MAD2 induces metaphase arrest and inhibits the APC/C (Li et al., 1997).

Finally, recent experiments in human cells show human securin destruction is activated when the spindle checkpoint is satisfied by kinetochore attachment and that reactivation of the spindle checkpoint prevents securin degradation and sister chromatid separation (Hagting et al., 2002). This destruction of securin is dependent on destruction motifs within the protein which allow it to be targeted by the anaphase promoting complex- the KEN box and the D-box. Mutation of this D-box prevents sister separation and generates a *cut* phenotype where one cell can inherit both copies of the genome, consistent with aneuploidy in tumours (Hagting et al., 2002).

1.4.7 Additional Checkpoint Components in Multicellular Organisms

CENP-E is a kinetochore motor involved in chromosome alignment and is essential in maintaining kinetochore-microtubule attachments at monopolar chromosomes to allow them to become bipolar and align at the equator (Schaar et al., 1997; McEwen et al., 2001). Depletion of CENP-E in *Xenopus* egg extracts suggest it plays an essential role in activation of the spindle checkpoint in response to spindle damage (Abrieu et al., 2000). However CENP-E is also implicated in checkpoint silencing, as human CENP-E depletion by antibodies or antisense oligonucleotides causes chronic arrest of mitosis (Yao et al., 2000). CENP-E is a kinesin-like protein that undergoes microtubule dependent conformational changes, a mechanism which could convey alterations in kinetochore tension to BUBR1 to mediate both these effects.

In mammalian metaphase cells, CENP-E staining was observed in association with human BUBR1 in the mitotic cytosol and again with BUB1 at the kinetochore plate, and appeared stronger at unaligned chromosomes (Jablonski et al., 1998). CENP-E and BUBR1 levels are reduced upon kinetochore-microtubule attachment suggesting CENP-E may mediate the loss of tension at kinetochores to BUBR1. In support of this transducer function of CENP-E, *Xenopus* BUBR1 autokinase activity is stimulated by interaction with CENP-E *in vitro*, an interaction induced by free

kinetochores and important for recruitment of MAD2 (Mao et al., 2003). Antibody inhibition of CENP-E in *Xenopus* egg extracts inhibits its activation of BUBR1 kinase and abrogates checkpoint function (Mao et al., 2003). Localisation studies suggest sequential assembly of proteins at human kinetochores in the order BUB1, CENP-F, BUBR1; detectable at prophase prekinetochores, followed by CENP-E, thought to interact with all three of these proteins, detectable at prometaphase (Li et al., 1999). Thus human BUBR1 is likely to localise CENP-E to the kinetochore, where they may form a motor-kinase complex, allowing BUBR1 to monitor microtubule tension for checkpoint function and silencing (Chan et al., 1999).

In humans BUB1 and BUBR1 remain at kinetochores until late anaphase at reduced levels so perhaps a threshold level or modification of these proteins is necessary for checkpoint activation. In support of this, the phosphorylation state of human BUBR1 is dependent on the number of kinetochore microtubules attached to CENP-E (Li et al., 1999). This is consistent with the following model: BUBR1 recruits CENP-E to kinetochores where it could act as a sensor undergoing a conformational change in response to lack of tension. This could result in BUBR1 phosphorylation, possible induction of BUBR1 kinase activity and checkpoint activation (Jablonski et al., 1998; Chan et al., 1998; Chen, 2002). A further conformational change in the CENP-E-BUBR1 complex upon kinetochore tension may dephosphorylate or inhibit BUBR1 for checkpoint silencing.(Hoffman et al., 2001; Yen et al., 1991)

The interaction with CENP-E is thought to be mediated through BUBR1's kinase domain. As yeast MAD3 lack this domain it may be devoid of these CENP-E associated functions consistent with reduced chromosome loss rates in MAD3 mutants compared to other spindle checkpoint mutants (Chan et al., 1999). This is also supported by the lack of a known CENP-E homologue in yeast (Abrieu et al., 2000) and the ability of the kinase domain of BUB1, which shows similarity to BUBR1 kinase domain, to bind another kinesin motor, CENP-F (Jablonski et al., 1998).

CENP-F, is also involved in kinetochore assembly (Liao et al., 1995). Yeast two hybrid studies indicated that the kinase domain of BUB1 and the kinetochore localisation domain of CENP-F interact. Thus BUB1 may facilitate CENP-F binding

to the kinetochore, either by direct interaction or through phosphorylation or recruitment of intermediate proteins. CENP-F may then be important in the recruitment of human BUBR1 and CENP-E to the kinetochore. This may be part of BUB1's spindle checkpoint role or may represent a second role of BUB1 in kinetochore assembly; consistent with observations in yeast, that deletion of the BUB1 kinase domain can result in chromosome loss (Jablonski et al., 1998) and with severe chromosome segregation defects seen in budding yeast *bub1* mutants (Warren et al., 2002). Okp1p and Slk19p are possible *S.cerevisiae* homologues of CENP-F.

CENP-I has also been shown to be important in maintenance of spindle checkpoint arrest and for the localisation of MAD1, MAD2 and CENP-F to kinetochores (Liu et al., 2003b).

Overall, human BUB1 and human BUBR1 seem to have additional functions in kinetochore assembly that may link them with the spindle checkpoint and be important in localisation of checkpoint proteins to the kinetochore.

1.4.8 Adenomatous Polyposis Coli (APC) in the Spindle Checkpoint

The APC gene is involved in hereditary colorectal cancer and is somatically inactivated in the majority of colorectal tumours (Rosin-Arbesfeld et al., 2000).

Recent studies have clarified an additional role for APC, in microtubule presentation to the kinetochores and the detection of failure to do so through the spindle checkpoint. APC contains microtubule binding regions and is known to bind EB1, a protein which also interacts with microtubules (Berrueta et al., 1998; Munemitsu et al., 1994; Smith et al., 1994). APC localises to the ends of microtubules, and interacts with kinetochores at the outer kinetochore plate, stabilising the kinetochore-microtubule interactions and promoting microtubule polymerisation (Zumbrunn et al., 2001; Nakamura et al., 2001). APC co-immunoprecipitates with BUB1-BUB3 and BUBR1-BUB3 and is phosphorylated by them *in vitro* in the central and C-terminal portions of the protein which is interspersed with GSK3β phosphorylation sites. This is dependent on prior phosphorylation by GSK3β and other kinases. This phosphorylation may regulate attachment of kinetochores to microtubules, as phosphorylation of APC causes a decrease in its affinity for microtubules (Kaplan et al., 2001). Thus APC seems to have a role in the formation and stabilisation of microtubule-kinetochore interactions.

This may be linked to the spindle checkpoint or proposed kinetochore assembly functions of human BUB1 and BUBR1 or may be important in the repair of defects in the mitotic spindle or kinetochore. However, APC is not essential for the spindle checkpoint as *Min/Min* mouse embryonic cells have a functional mitotic arrest in response to microtubule disruption. APC mutations removing the C-terminal microtubule and EB1 binding domains but which leave the β–catenin associated regions unaffected, cause chromosomal instability in mouse ES cells, through aberrant chromosome segregation (Fodde et al., 2001; Kaplan et al., 2001). An N-terminal APC mutant mis-localised to the centrosome and compromised checkpoint arrest, perhaps due to an inability to bind microtubules. Thus APC truncation mutations may interfere with chromosome segregation and generate CIN in colorectal cancers, in addition to interfering with Wnt signalling. In this way APC mutations could impart both genetic instability and a growth advantage on the cell, accelerating tumourigenesis. In support of this, adenomas harbouring mutations in APC are more likely to grow and progress to invasive stages than those with ß-catenin mutations, perhaps due to an additional defect in microtubule capture. Plus many colorectal cancer cell lines with APC mutations described to date show a CIN phenotype (Fodde et al., 2001). APC mutations and aneuploidy are both frequent characteristics of colorectal tumours, and it now appears APC mutations may contribute to aneuploidy (Tighe et al., 2001). Additionally mutations in BUB1 and BUBR1 in tumours may affect APC phosphorylation and hence kinetochore-microtubule binding as well as spindle checkpoint function.

1.4.9 Checkpoint Silencing

As the last chromatid attaches to microtubules, creating microtubule tension and the chromosomes align on the metaphase plate, the sensor complexes dissociate from kinetochores. In HeLa cells, the concentration of BUB1, BUBR1 and MAD2 have been shown to decrease 3.7, 3.9 and 152-fold respectively upon kinetochore attachment (Zhou et al., 2002b). BUB3 kinetochore localisation is thought to drop at least 5 fold upon kinetochore attachment in *Xenopus* egg extracts (Campbell and Hardwick, 2003) and 3-5 fold in mice (Martinez-Exposito et al., 1999). This prevents the formation of the signalling complex MAD1-MAD2-BUB1-BUB3 and the effector complexes. This allows CDC20 to interact with the APC/C and activate

cohesin destruction. The chromosomes then separate and digress to the poles of the cell during anaphase (Chen et al., 1996; Chen et al., 1998; Jin et al., 1998; Li and Benezra, 1996; Taylor et al., 1998).

The mechanism by which these complexes dissociate is beginning to be investigated. The rapid turnover of MAD2 at kinetochores contributes to dissociation of the complexes (reviewed in Musacchio and Hardwick, 2002). Other proteins which have been implicated in spindle checkpoint function are thought to have a role in movement of proteins away from the kinetochore along spindle fibres. Consistent with this MAD2 has been reported to move onto spindles late in mitosis in fission yeast (Ikui et al., 2002).

Recent studies suggest dynein and dynactin are involved in the removal of kinetochore localised spindle checkpoint proteins when the checkpoint is inactivated. Dynein and dynactin are motor proteins which act on microtubules, transporting proteins along the spindle fibres from kinetochores to the poles of the cell and vice versa. They may act to assist transport of spindle checkpoint proteins including MAD2, BUBR1 and CENP-E from the kinetochore along the microtubule spindles towards the centrosomes, as inhibition of dynein and dynactin activity has been shown to prevent the transport of these proteins in PtK1 cells (Howell et al., 2001). Removal of these proteins upon kinetochore attachment is required to switch the checkpoint off (Wojcik et al., 2001; Howell et al., 2001). MAD2, BUBR1, CENP-E, the 3F3/2 phosphoantigen and ROD are continuously cycled while the checkpoint is active by removal from the kinetochore through a dynein dependent mechanism and replenished by an ATP-dependent mechanism (Howell et al., 2000; Wojcik et al., 2001). This continued remove and replenish cycle at free kinetochores would allow the checkpoint to be deactivated by inhibition of replenishment upon attachment of the final kinetochore, whilst the motor proteins would remove any checkpoint proteins remaining at the kinetochore. ZW10 and ROD are also thought to be involved in this process of silencing the checkpoint. These proteins are required to localise dynein to kinetochores, essential for checkpoint function, consistent with the model for checkpoint silencing (Howell et al., 2001). Thus ZW10 and ROD mutants would be expected to show prolonged activation of the checkpoint but actually

depletion of ROD and ZW10 prevents activation of the spindle checkpoint providing evidence of a parallel metaphase checkpoint (Chan et al., 2000; Basto et al., 2000).

CENP-E, another kinetochore motor protein has also been linked with checkpoint silencing. In cells depleted of human CENP-E chromosomes attached to microtubules stain brightly for MAD2 and the spindle checkpoint remains active (Yao et al., 2000; McEwen et al., 2001). CENP-E has also been shown to interact with BUBR1 and this complex may undergo a conformational change when kinetochores are under tension to inhibit BUBR1 checkpoint activity and switch off the checkpoint (Yao et al., 2000).

Increased localisation of dynein is seen at CENP-E depleted kinetochores, suggesting they compete for kinetochore binding sites and consistent with a role for CENP-E in checkpoint silencing and checkpoint function (Chan et al., 1999). However, CENP-E has also been shown to be have additional roles in checkpoint activation, maintenance and spindle checkpoint protein kinetochore localisation (Yao et al., 2000). These different functions may represent alternative conformations or separable pools of CENP-E.

Removal from the kinetochore of checkpoint protein complexes will halt activation of the spindle checkpoint and prevent formation of MCC and the checkpoint inhibitory complexes. However, for the checkpoint to be fully inactivated the existing effector complexes must dissociate. The break up of these complexes may be spontaneous or may be through an, as yet unidentified, assisted mechanism. There is a little evidence for assisted dissociation. Structural studies reveal the partial unfolding of MAD2 is required for dissociation of the MAD2-CDC20 complex. This is likely to inhibit or slow spontaneous break up, posing a kinetic barrier for dismantling the MCC (Luo et al., 2002; Sironi et al., 2002). Additionally, studies in PtK1 cells which possess two spindles show that the presence of an unattached kinetochore to one spindle does not inhibit anaphase onset on the other spindle (Rieder and Khodjakov, 1997). This suggests the inhibitory signals generated by the checkpoint can only travel a limited distance and this is consistent with an active mechanism for dissociation of inhibitory complexes in the cytosol (Yu, 2002).

1.4.10 A Summary of the Current Model for the Spindle Checkpoint

Current models of the spindle checkpoint propose that three complexes of checkpoint proteins exist throughout the cell cycle, MAD1-MAD2, BUB3-BUB1 and BUB3-MAD3 (or BUB3-BUBR1). On activation of the checkpoint in response to defects in chromosome attachment, these are recruited to kinetochores that have yet to bind microtubules; MAD1-MAD2 in response to the presence of unattached kinetochores and BUB3-BUB1 to loss of tension. Modification of these complexes, probably involving the kinase activities of MPS1 and possibly BUB1, result in the formation of a BUB3-BUB1-MAD1-MAD2 complex. From this signalling complex, MAD2 is released in an activated form, perhaps as an oligomer or through phosphorylation. Activated MAD2 then associates with CDC20 and probably MAD3/BUBR1 and APC/C, inhibiting APC/C mediated degradation of PDS1. PDS1 continues to inhibit ESP1 cleavage of the SCC1 cohesin subunit and the sister chromosomes remain joined. Thus the metaphase to anaphase transition is delayed (Brady and Hardwick, 2000).

Upon attachment of the last kinetochore to the bipolar spindle, the complexes are perceived to dissociate from the kinetochore and each other in some cases through spontaneous and assisted means. A reduced local concentration of MAD2 and MAD3/BUBR1 may allow CDC20 to be released and interact with APC/C, for which it has a higher affinity. APC/C-CDC20's proteolytic activity would be restored allowing it to degrade PDS1 and initiate anaphase. This model is summarised in figure 1.8.

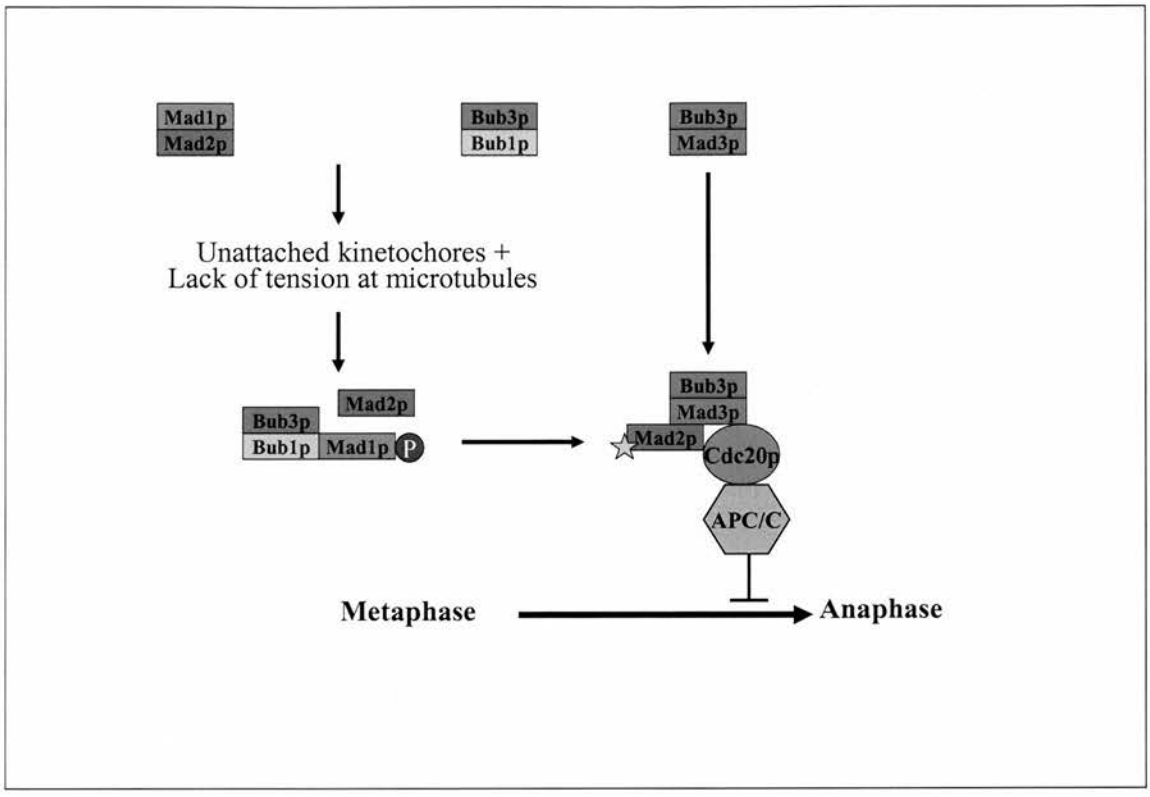

Figure 1.8 A model of the spindle checkpoint

Three constitutive complexes of spindle checkpoint proteins are recruited to free kinetochores. Their close localisation and possible modification catalyses formation of a signalling complex from which an activated form of Mad2p indicated by the star is released. This interacts with other checkpoint proteins to inhibit the Cdc20p from activating APC/C both locally at the kinetochore and throughout the cell. This generates the anaphase wait signal which delays chromosome segregation and the metaphase to anaphase transition.

1.5 The Role of the Spindle Checkpoint in Disease

Mutations in components of the mitotic spindle checkpoint have been implicated in tumourigenesis through the generation of aneuploidy. Defects in mitotic and meiotic spindle checkpoints may also be involved in birth defects, down syndrome, spontaneous foetal abortion and bone marrow failure (Matsuura et al., 2000; Nicklas, 1997; Shonn et al., 2000; Yamaguchi et al., 2003).

1.5.1 Defects in the Spindle Checkpoint

Knockout mice have been created for two spindle checkpoint components; *BUB3* and *MAD2*. *BUB3* mutant embryos fail to survive beyond day 6.5-7.5, accumulating mitotic errors from day 4.5, indicative of chromosome segregation defects. Treatments of null embryos with microtubule poisons show that the mitotic checkpoint is defective (Kalitsis et al., 2000).

MAD2 knockout mice grow normally to day 5.5 despite an absence of mitotic arrest response. The rapid cell division stage at E6.5 results in widespread chromosome mis-segregation and apoptosis in the absence of a functional checkpoint consistent with a role of spindle checkpoint defects in spontaneous abortion (Dobles et al., 2000).

Thus it appears knockout mutations in spindle checkpoint genes may be lethal at least in development. To address this, Michel et al generated cancer cell lines and murine primary embryonic fibroblasts deleted in one allele of *MAD2* and found that *MAD2* shows haploinsufficiency. *MAD2*$^{+/-}$ cells are checkpoint defective and show elevated levels of chromosome mis-segregation. *MAD2*$^{+/-}$ mice develop lung tumours suggesting mutations rendering checkpoint proteins null are lethal whereas partial disruption of the checkpoint may allow chromosomal instability while avoiding apoptosis and therefore contribute to tumourigenesis. The mice develop tumours in their lungs which is unexpected as mutations in spindle checkpoint genes are rarely found in lung tumours (Michel et al., 2001).

In *Xenopus*, partial depletion of BUB3 abrogates spindle checkpoint establishment and maintenance during mitosis but BUB3 is not required for maintenance of a meiotic metaphase arrest (Campbell and Hardwick, 2003). *Xenopus* BUB1 has been shown to be required for meiotic metaphase arrest (Tunquist et al., 2002) and immunodepletion of *Xenopus* BUB1 and BUBR1 interferes with localisation of other

checkpoint proteins (Sharp-Baker and Chen, 2001; Chen, 2002). These *Xenopus* experiments suggest mechanisms of checkpoint abrogation which may be responsible for the phenotypes seen in the mouse knockout mutants.

Studies of spindle checkpoint mutants show these proteins are not essential in yeast. Warren et al. examined the phenotypes of spindle checkpoint mutants and found that while all the spindle checkpoint mutants, excluding *bub2*, exhibited sensitivity to microtubule poisons and an elevated chromosome loss frequency, the extent of these phenotypes varied between the mutants, probably in relation to their contribution to checkpoint function (Warren et al., 2002). *bub3* and *bub1* were found to show the greatest checkpoint defects followed by *mad1*, *mad2* and *mad3* respectively, which all showed significantly reduced phenotypes. These experiments provide a system for quantifying the function of checkpoint proteins and their domains in budding yeast (Warren et al., 2002).

Although evidence in yeast suggests the proteins are not essential spindle checkpoint proteins do appear to be essential in mammalian systems and complete loss of their function is likely to be lethal. However, spindle checkpoint mutations which inactivate one allele or alter expression levels are likely to be less severe and may impact on diseases such as cancer.

1.5.2 The Spindle Checkpoint in Tumourigenesis

Over the last few years numerous studies have examined the role of spindle checkpoint defects in tumourigenesis and aneuploidy. The treatment of colorectal cancer cell lines with microtubule poisons show that those exhibiting CIN behave differently to those with MIN at the G2/M checkpoint. Cell lines of both types, arrested with DNA contents indicative of a G2 block and the MIN and normal cells maintained this block, resulting in a characteristic mitotic profile with a peak in mitotic index at 12-24 hours. However, CIN cells displayed an abnormal profile with no true peak and a lesser decrease in mitotic index indicative of an incomplete block and re-entry into mitosis. This suggests CIN cell lines harbour defects in mitotic checkpoints and some of these cell lines were shown to harbour mutations in spindle checkpoint genes (Cahill et al., 1998). Recent reports show some CIN cell lines to have an intact G2/M arrest in response to microtubule drugs, with reduced

maximum mitotic index compared to the MIN cells suggesting partial compromisation at the spindle checkpoint (Tighe et al., 2001). This could be due to mutations in genes less directly involved in the spindle checkpoint or in microtubule dynamics or spindle positioning. Indeed transfection of a truncated form of the APC gene into MIN cell lines does mimic the CIN response and APC truncation mutations are frequently found in CIN cell lines. Interestingly, studies of breast cancer cell lines show variation in the chromosomal instability observed with the highly unstable cell lines showing defective mitotic checkpoints, whereas those with moderate instability have intact checkpoints (Yoon et al., 2002) and this may account for the discrepancies observed between the Cahill and Tighe reports.

Analysis of spindle checkpoint genes in tumours has revealed fewer mutations than expected. In early studies, examination of the human *BUB1* gene in 19 CIN colorectal cancer cell lines, revealed heterozygous somatic mutations in two of the cell lines. The first, a G→A transition at a canonical splice donor site, results in a 197bp deletion at the RNA level, removing part of CD1 and the second involved a missense mutation substituting a tyrosine for a conserved serine. Over-expression of these mutant alleles in MIN cell lines produced a phenotype similar to CIN cell lines in response to microtubule poisons, indicative of a dominant negative effect. Over-expression of the wild type allele had no effect. Similarly co-expression of the wild type and mutant alleles abrogated the checkpoint. Analysis of the human *BUBR1* gene in the same panel of cell lines showed that all 19 cell lines produce the protein although two produce mutant RNA transcripts. The first of these resulted from a germline C→T transition substituting a methionine for a threonine in an unconserved region and the second was a somatic deletion of a T causing truncation of the protein in the kinase domain. Functional analysis of these was not reported (Cahill et al., 1998). No further mutations were found in these cell lines in any of the following spindle checkpoint genes; *MAD2, MAD2L2, MAD1, BUB3, TTK (MPS1), p55CDC20* (Cahill et al., 1999).

Since these early studies spindle checkpoint genes have been analysed in a variety of tumours for mutations and alterations in expression levels, particularly in cancers in which aneuploidy is common. These are summarised in table 1.4.

Many of the tumour cell lines examined were shown to be defective in checkpoint arrest (Cahill et al., 1998; Takahashi et al., 1999; Wang et al., 2002; Wang et al., 2000a; Saeki et al., 2002; Kasai et al., 2002; Ouyang et al., 2002; Hempen et al., 2003). Interestingly, many of the variants identified were altered in conserved domains and important functional domains of the protein supporting their pathogenicity (Hempen et al., 2003; Saeki et al., 2002; Ru et al., 2002). Deletions and truncating mutations were relatively rare (Cahill et al., 1998; Percy et al., 2000; Tsukasaki et al., 2001; Ohshima et al., 2000; Ru et al., 2002; Ouyang et al., 2002) but single base mutations were more frequent. Polymorphisms were frequently seen and combinations of these may confer an increased cancer risk. There is evidence that some spindle checkpoint gene polymorphisms do confer an increased cancer risk (Iwanaga and Jeang, 2002). Alterations in protein levels may also be important in cancer susceptibility and these may be a result of alterations in the promoter or untranslated regions of checkpoint proteins or methylation of checkpoint genes.

In addition, Adult T-cell leukaemia and lymphoma (ATLL) is caused by the human T-cell leukaemia virus type I (HTLV-I) which integrates randomly into the genome and produces an oncoprotein Tax that interacts with and inhibits MAD1, inducing chromosome instability (Jin et al., 1998).

Table 1.4: Spindle Checkpoint Genes in Tumourigenesis

Cancer type and number	Genes analysed	Results	% mt	Reference
19 Colon (CIN)	*BUB1*	1 missense mutation, 1deletion	10.5	Cahill et al.,
	BUBR1	1 missense mutation , 1 deletion	10.5	1998;
	MAD1	0 mutations	0	Cahill et al., 1999
	MAD2	0 mutations	0	
	MAD2L2	0 mutations	0	
	BUB3	0 mutations	0	
	TTK	0 mutations	0	
	Cdc20	0 mutations	0	
6 Colon (CIN)	-	All checkpoint Defective	-	Cahill et al.,1998
40 Colon	*BUB1*	0 mutations, 0 SNP	0	Jaffrey et al., 2000
32 Digestive tract	*MAD2*	0 mutations	0	Imai et al., 1999
	BUB1 CDs	1 missense mutation	3.1	
43 Gastric	*BUB1*	Protein expression upregulated in 84%	-	Grabsch et al.,
(81% aneuploid)	*BUBR1*	Protein expression upregulated in 68%	-	2003
	BUB3	Protein expression upregulated in 79%	-	
	All 3	Protein expression upregulated in 61%	-	
		Did not correlate with aneuploidy		
8 Gastric	*BUB1*	Several point mutations, unconfirmed at genomic level	-	Nakagawa et al., 2002
20 Lung NSCLC	*BUB1*	0 mutations, 1 SNP	0	Jaffrey et al., 2000
31 Lung HNSCC	*BUB1*	1 silent mutation, 0 SNP, all expressed protein	3.2	Yamaguchi et al., 1999
46 Lung	*MAD2*	0 mutations, some SNP, all expressed protein	0	Takahashi et al.,
	p55Cdc20	0 mutations, some SNP, all expressed protein	0	1999
9 Lung	-	4 checkpoint defective	-	Takahashi et al., 1999
88 Lung Mesothelioma	*BUB1* (not ex1)	1 missense mutation, 11 SNP, protein expressed in 31 cell lines tested	1.1	Sato et al., 2000
47 Lung Mesothelioma	*BUBR1*	0 mutations, frequent silent SNP, protein expressed in 31 cell lines tested	0	Sato et al., 2000
44 Lung	*BUB1*	0 mutations, some SNP	0	Haruki et al.,
	BUBR1	0 mutations, some SNP, protein upregulated	0	2001
	BUB3	1 missense mutation (5' UTR), some SNP	2.3	
60 Lung	*MAD2*	1 silent mutation, 1 missense SNP, reduced protein expression	1.7	Gemma et al., 2001
49 Lung	*MAD1*	2 missense mutations, several missense and silent SNP	4.1	Nomoto et al., 1999
8 Lung	*BUBR1*	Protein expression upregulated in all 8	-	Seike et al., 2002
4 Lung	*MAD1*	0 mutations, SNP	0	Tsukasaki et al., 2001
48 Breast	*MAD2*	1 silent mutation, 0 SNP	2.1	Gemma et al., 2001
21 Breast	*MAD2*	1 deletion mutation, 2 missense mutations (3' UTR), 0 SNP, altered protein expression in 3/13, upregulated in deletion	14.3	Percy et al., 2000
19 Breast	*BUB1*	0 mutations, 9 missense and silent SNP,	0	Myrie et al., 2000
	BUBR1	variable protein levels		
7 Breast	*BUB1*	0 mutations, some previously reported SNP	0	Ru et al., 2002
26 Breast	*MAD1*	2 missense, 1 silent mutations, SNP	11.5	Tsukasaki et al., 2001

Cancer type and number	Genes analysed	Results	% mt	Reference
7 Ovarian	*MAD2*	3 checkpoint defects + reduced MAD2 expression	-	Wang et al., 2002
22 Glioblastomas	*BUB1* *BUBR1* *BUB3*	1 silent mutation 9 silent mutations 4 missense SNP upstream of initiation codon	4.5 40.9	Reis et al., 2001
18 Giant cell Glioblastomas	*BUB1*	2 silent mutations	11.1	Reis et al., 2001
5 NPC	*MAD2*	2 checkpoint defective with reduced protein expression	-	Wang et al., 2000
86 Hematopoietic	*MAD1*	1 missense, 1 nonsense, 3 silent mutations, SNP	5.8	Tsukasaki et al., 2001
39 Prostate	*MAD1*	3 missense, 1 deletion, 1 silent mutation, SNP	12.8	Tsukasaki, 2001
5 Osteosarcoma	*MAD1*	0 mutations, SNP	0	Tsukasaki, 2001
17 Glioblastoma	*MAD1*	0 mutations, SNP	0	Tsukasaki, 2001
21 Bladder	*BUB1* *BUBR1* *BUB3* *TTK*	2 silent SNP 23 silent SNP, 13 missense SNP 0 SNP 4 silent SNP, 22 missense SNP	- - - -	Olesen et al., 2001
44 Bladder	*MAD2*	1 missense mutation, 3 silent SNP	2.3	Hernando et al., 2001
52 Bladder	*BUB1*	3 silent SNP	-	Hernando, 2001
9 Bladder	*BUB3*	0 SNP	-	Hernando, 2001
42 Sarcoma	*MAD2*	3 silent SNP	-	Hernando, 2001
10 Hepatocellular	*MAD2*	2 silent SNP	-	Hernando, 2001
58 Hepatocellular	*BUB1* *BUBR1* *MAD2L2* *Cdc20* *BUB3*	0 mutations, 2 missense SNP 0mutations, 2 silent, 1 missense SNP 0 mutations, 0 SNP 0 mutations, 1 silent 2 missense SNP 0 mutations, 0 SNP	0 0 0 0 0	Saeki et al., 2002
8 Hepatocellular	*BUB1*	All aneuploid, 5 Checkpoint defect, 0 mutations	-	Saeki et al., 2002
10 ATLL	*BUB1* *BUBR1*	1 missense mutation 3 missense, 1 deletion, 1 silent mutation	10 40	Ohshima et al., 2000
8 HTLV-1	*BUB1* *BUBR1*	0 mutations 1 nonsense mutation	12.5	Ohshima et al., 2000
6 ATL	*MAD1* *MAD2*	All checkpoint defective with MAD1 and MAD2 mislocalisation	-	Kasai et al., 2001
8 Leukemia	*BUB1*	2 deletion, 1 missense mutation	50	Ru et al., 2002
2 ALL	*BUB1*	1 heterozygous deletion mutation	50	Ru et al., 2002
2 Hodgkins Lymphoma	*BUB1*	2 deletion mutations	100	Ru et al., 2002
2 AML	*BUB1*	0 mutations	0	Ru et al., 2002
1 CML	*BUB1*	0 mutations	0	Ru et al., 2002
9 Oral cancer	Partial *BUB1*	0 mutations in exons 8,10,12,15 or kinase domain	0	Nakagawa et al., 2002
8 Thyroid	-	2 checkpoint defects	-	Ouyang et al., 2002
19 Thyroid	*BUB1* *BUBR1*	1 deletion mutation, 1 silent SNP 0 mutations, 1 silent SNP	5.3 0	Ouyang et al., 2002
4 aneuploid Pancreatic	-	All checkpoint defective	-	Hempen et al., 2003
18 Pancreatic	*BUB1* *BUBR1*	2 missense mutations in NLS 0 mutations	11.1 0	Hempen et al., 2003
23 various	*MAD1*	12 silent SNP, 9 missense SNP (affect not analysed), 12 with pathogenic missense SNP	-	Iwanaga et al., 2002

Together these studies suggest that spindle checkpoint gene defects are important in a subset of aneuploid cancers. Mutations appear to be rare in cancers which are largely influenced by carcinogens such as lung cancer (only 6 mutations in 523 cancers analysed) whereas they are more frequent in colon and digestive tract cancers (5/256 cancers), prostate cancers (5/39), leukemias (13/51) and breast cancers (7/140). This indicates alternative pathways of carcinogenesis may act in these two groups of tumours where spindle checkpoint mutations may act as an alternative mechanism to artificial carcinogens in the induction of CIN (Li et al., 2000).

Alternatively the rare occurrence of mutations, and the prevalence for missense mutations may reflect the essential nature of the spindle checkpoint proteins. Mutations which nullify the protein, such as large deletions or truncating mutations, may be lethal as shown in mouse knockouts. More subtle changes such as single amino acid changes and combinations of polymorphisms, may compromise the checkpoint, resulting in aberrant chromosome segregation and transformation. Most spindle checkpoint gene variants reported are single nucleotide polymorphism (SNP) and point mutations. Thus extensive studies into the occurrence of polymorphisms in spindle checkpoint genes in individuals with and without aneuploid tumours may clarify their role in cancer predisposition.

Variations in expression levels of spindle checkpoint proteins, seen in several of the tumours analysed, may also contribute to tumourigenesis through subtle effects. Mutations and polymorphisms have been identified in the untranslated regions of spindle checkpoint genes, including the 3' UTR and in the sequence between the Kozak sequence and the initiation codon, and although no functional work has been done on these, they may contribute to tumourigenesis by altering the protein expression levels. Alterations in the promoters or methylation status of the genes may also play a role.

Repeat sequence instability at the 2q locus containing the *BUB1* gene was found in 62.5% of colon cancers with 14.5% showing instability within the *BUB1* gene itself. Microsatellite instability in promoter regions has been linked to down-regulation of genes, with instability in coding sequences and introns appearing to influence gene transcription and suggests an alternative mechanism for

compromising the spindle checkpoint. No allelic instability was found in this region in Non-small Cell Lung Cancers (NSCLC) consistent with the infrequent involvement of the spindle checkpoint in lung cancers (Jaffrey et al., 2000)).

Alternatively, lethality of mutations may be avoided through overlapping functions between checkpoint proteins. There are several levels of redundancy in the spindle checkpoint. For example, the checkpoint proteins BUB1 and BUBR1 show good homology to each other and evidence suggests partial redundancy. In addition the checkpoint can be activated either by loss of attachment or tension and there are multiple checkpoint sensor and effector complexes. Furthermore some components of the spindle checkpoint have more than one homologue in human cells. There are two human homologues of MAD2, and BUBR1 was initially identified as a homologue of BUB1. Defects in only one of these might reduce checkpoint fidelity and generate low level aneuploidy insufficient to activate apoptosis and may contribute to carcinogenesis (Brady and Hardwick, 2000). Thus mutations in these would also allow compromisation but not elimination of the checkpoint, avoiding lethality. In addition, this homology may suggest a way in which polymorphisms in homologous proteins may combine to reduce checkpoint efficiency.

The avoidance of apoptosis is an important phenotype in cancer cells. Transfection of a dominant negative murine *BUB1, N-BUB1*, containing only the kinetochore localisation domain into HeLa cells suggests spindle checkpoint mutants may bypass apoptotic pathways. After treatment with microtubule poisons, the *N-BUB1* transfectants and parent cells both exhibited mitotic arrest but the *N-BUB1* cells exited mitosis prematurely and continued into a second mitosis, producing cells with 8N DNA content, indicative of irregular chromosome segregation. The parent cells however, were blocked at mitosis for a longer period before exiting with DNA contents less than 4N, indicative of apoptosis. It was hypothesised that spindle checkpoint mutations may allow cells to bypass both checkpoints and apoptosis in response to chromosome segregation abnormalities (Taylor and McKeon, 1997). However, this is not consistent with studies of *BUB3* and *MAD2* mutant mice, which undergo lethal mass apoptosis in embryonic stages, but this could reflect the intolerance for apoptosis in development. These mice were completely depleted of the proteins and mutations only affecting part of the protein function may achieve

this escape. Obviously the mutations shown to be involved in tumourigenesis must be able to avoid apoptosis but this may be due to the accumulation of mutations in apoptotic genes, such as *p53*, as a result of the chromosomal instability. *p53* is activated in response to microtubule poisons through MAP and ERK kinases, which are localised at unattached kinetochores and may induce G1 arrest and apoptosis to protect from aneuploidy (Sablina et al., 2001). Clarification of the mechanism involved in spindle checkpoint associated apoptosis will be needed before the contribution of spindle checkpoint mutations in bypassing apoptosis can be determined.

Finally, how do spindle checkpoint mutations fit into the sequential model of tumour progression shown in figure 1.1? Gascoyne et al., have very recently shown that in fibrosarcoma development the spindle checkpoint is active in mild fibromatosis but is abolished in aggressive fibromatosis and fibrosarcoma lesions (Gascoyne et al., 2003). This suggests spindle checkpoint inactivation occurs early in tumourigenesis, contributing to the chromosome instability required for tumour progression.

1.5.3 Spindle Checkpoint Mutations and Cancer Treatment

There is evidence that cells with defects in chromosome segregation, be it through spindle checkpoint protein abnormalities or otherwise, are more susceptible to certain chemotheraputic agents. MIN and CIN cell lines exhibit resistance to different types of carcinogens, with the MIN cells generating resistance to the alkylating agent N-methyl-N'nitro-N-nitroguanidine (MNNG) and treatment with a bulky adduct forming agent 2-amino-1-methyl-6-phenylimidazo[4,5-b]pyridine (PhIP) generating CIN cells with resistance to the drug. A MIN cell line transfected with a human *BUB1* mutant exhibited a CIN phenotype and was resistant to PhIP carcinogens which affected the parental MIN cell lines (Bardelli et al., 2001; Weitzel and Vandre, 2000). This demonstrates that cells with different types of instability are resistant to different drugs. Interestingly PhIP is the major dietary carcinogen in cooked meat and chicken, suggesting a diet rich in meat may contribute specifically to aneuploid tumours, a factor consistent with the frequency of aneuploid tumours in westernised societies (Bardelli et al., 2001). These variations in resistance to carcinogens may have important implications for development of chemotherapeutic agents.

It has been suggested that using a combination of mitosis arresting drugs with cytotoxic treatments which target cycling cells would affect only the checkpoint defective, tumour cells, leaving normal cells unharmed (Hardwick et al., 1996). Thus the identification of patients with mutations in these pathways could allow the tailoring of chemotherapy and treatment to those aneuploid tumours associated with poorer prognosis.

Although searches for mutations in checkpoint genes have resulted in a relatively small number identified in most cases, there is evidence that they do contribute to a subset of aneuploid tumours. Some mutations have been reported to date and most appear to be somatic but changes in the non-coding regions of checkpoint genes, combinations of polymorphisms and epigenetic alterations may also contribute to the loss of the checkpoint in sporadic and familial tumourigenesis. Clarification of the involvement of these in aneuploid colorectal cancer will ultimately aid the clinical surveillance, prevention and treatment of colon cancer. It is becoming increasingly likely that different genes are involved in subsets of cancers and that in the future, treatment may depend upon the genotype of the tumour. CIN cancers are probably a heterogeneous population with each CIN candidate gene being altered in a small proportion of aneuploid tumour cases. If a large number of genes are each responsible for a subset of cases, this may explain the frequency of aneuploid tumours. Thus by identifying the genotype of tumours we may be able to match the most suitable treatment to the patient. Unfortunately tailoring therapies to individual tumour genotype is expensive in terms of health service resources.

The advantage of genetic instability is that it differentiates cancer cells from their normal counterparts and may be utilised in therapy. As cancers with genetic instabilities harbour defects in cellular processes which maintain genomic integrity, they may be sensitive to particular chemical agents. For example NER defective cells are sensitive to UV light, *BRCA* mutant cells are hypersensitive to ionising radiation and cells with mitotic checkpoint defects are sensitive to taxanes including Paclitaxel and microtubule poisons (Lengauer et al., 1998; Jallepalli and Lengauer, 2001). Drugs such as taxanes and vinca alkaloids might act preferentially on cells with spindle checkpoint defects, i.e. tumour cells, by activating the spindle checkpoint and elevating missegration rates in tumours to the extent that cells are no

longer viable (Jallepalli and Lengauer, 2001). This is consistent with the increased sensitivity to microtubule poisons such as Benomyl seen in budding yeast spindle checkpoint mutants (Warren et al., 2002). Indeed studies have indicated that tumours over-expressing MAD2 may respond more successfully to treatment with microtubule poisons (Zhang et al., 2001). A nasopharyngeal carcinoma cell line over-expressing MAD2 was more sensitised to the microtubule poison vincristine perhaps through phosphorylation of apoptosis associated protein BCL-2 (Wang et al., 2003b). Prostate cancer cell lines with cell cycle checkpoint defects, were shown to be sensitive to the antiproliferative effects of the chemotherapeutic drug paclitaxel, although the cell cycle response at mitotic checkpoints and the speed of subsequent cell death by apoptosis varied in different cell lines (Lanzi et al., 2001). Thus it seems tumour cells with mitotic checkpoint defects may respond favourably to existing anticancer drugs.

Genetic instability may also be used to identify novel anti-cancer drugs and to target therapies to CIN tumours by exposing paired normal and tumour cell lines to different anti-tumour compounds and assessing cell death. In this way the paired cultures can be used to identify drugs with selective activity against CIN tumour cell lines. A technique based on this approach and incorporating fluorescent markers, is being used to identify new anticancer drugs using high throughput technology (Torrance et al., 2001).

1.6 Previous Work

Farrington and colleagues analysed a panel of thirty aneuploid colorectal tumours for mutations in human *BUB1* and *BUBR1* initially using RT-PCR. A novel alteration in human *BUBR1* was identified in ~20% of these tumours (Farrington et al., unpublished). This change is a 197bp deletion removing all of exon 5, in a conserved domain of the protein involved in interaction with CDC20 (CD1). The deletion is referred to as ΔE5 throughout this thesis. Alignment of the *BUB1* and *BUBR1* DNA sequences indicate the deletion shows identity to a *BUB1* mutation V400 previously reported in a colorectal cancer (Cahill et al., 1998). The same

change has been identified in a lymphoblastoid cell line from a family with early onset colorectal and other cancers. Karyotypic analyses of cell lines and peripheral blood lymphocytes from members of the family, revealed low level aneuploidy in a proportion of the samples, with both losses and gains of chromosomes being observed. A number of these cell lines were also investigated for functional defects at the G2/M check-point and preliminary results indicated that the mitotic index after spindle disruption was found to be aberrant when compared with control CIN and MIN tumour cell lines. Thus, initial results indicate that the change may play a major role in tumour formation, predisposing patients to the formation of aneuploid cells. Attempts to identify the genomic change associated with the altered cDNA transcript have not yet been successful, suggesting this may be a larger genomic deletion, well documented in cancer or possibly an alternative splicing effect.. The pathogenic effect of alternative splicing of the *WT1* gene is well documented in disease indicating alternatively spliced transcripts do impact on carcinogenesis (Lee and Haber, 2001; Philips and Cooper, 2000; Klamt et al., 1998; Kikuchi et al., 1998; Schneider et al., 1993). However, a recent study on alternative splicing in the human genome predicted none to occur in human *BUBR1* (Modrek et al., 2001).

The previously reported *BUB1* V400 mutation was shown to abrogate the spindle checkpoint consistent with induction of tumourigenesis (Cahill et al., 1998). These checkpoint defects would be expected to allow cells to accumulate chromosomal instabilities through a bypass of the checkpoint and consequently amass transforming mutations creating an aneuploid tumour.

1.7 PhD Aims and Methodology

The aim of this work has been to clarify the involvement of spindle checkpoint mutations in colorectal tumourigenesis. This has been approached in two ways:

1. Use of a budding yeast model system to investigate the effects of the *BUBR1ΔE5* and *BUB1V400* mutations on the spindle checkpoint and chromosome segregation.

S.cerevisiae has been used extensively in studies on spindle checkpoint function due to the availability of the complete genome sequence and genetic tractability of this model system.

The equivalent of the ΔE5 mutations were constructed in the *S.cerevisiae MAD3* and *BUB1* genes on plasmid constructs. These were transformed into *mad3* or *bub1* mutant strains and the transformants were analysed for sensitivity to microtubule poisons, spindle checkpoint activity and frequency of chromosome loss. The ability of the mutant spindle checkpoint proteins to interact with other checkpoint proteins and to form signalling and effector complexes was also investigated. The abilities of the mutant proteins to exert dominant negative effects were also analysed.

2. Further analysis of the *BUBR1* and *BUB1 ΔE5* deletions in human cells.

The ΔE5 mutations are ultimately to be investigated in human tumour cell lines. The human *BUBR1 ΔE5* deletion is to be constructed in plasmid form and used in over-expression studies in an inducible form in MIN cell lines. The ability of ΔE5 to abrogate the metaphase to anaphase checkpoint would then be investigated.

Construction of Green Fluorescent protein (GFP) fusions of the ΔE5 and wild type proteins would allow analysis of the effect of the deletion on the localisation and protein interactions of BUB1 and BUBR1. Additionally, antibodies to the N-terminal of BUB1 and BUBR1 were generated for use in immunofluorescence experiments.

Chapter 2: Materials and Methods

The following chapter documents the methods used during the work described in this thesis. Specific detail is also included in the relevant results chapters where appropriate.

2.1 General Information

Standard safety procedures and COSHH regulations have been adhered to through out this work in accordance with the MRC health and safety policies. Stock solutions and media marked with an asterisk(*) were prepared and sterilised by autoclaving by the MRC HGU technical services department. Those solutions marked with a hash($^{\#}$) were prepared by the solution and media preparation service at the Institute of Cell and Molecular Biology (ICMB), University of Edinburgh. Solutions and media were typically sterilised either by autoclaving for 15 minutes at 120°C and 15 pounds/inch^2 or by filtration, through 0.45 μm acrodisc syringe filters for small volumes (Gelman Sciences), or through 250 or 500ml 0.45μm filter units for larger volumes (Nalgene). Glassware was dry sterilised by baking in an oven at 250°C for 16 hours. The pH of solutions was adjusted by the addition of conc. HCl or Na OH as appropriate and monitored using a microprocessor pH meter (Hanna Instruments).

A list of Suppliers is shown in table 2.1

Table 2.1: List of Suppliers for Reagents and Chemicals

Supplier	Location	Items supplied
Roche	Lewes, UK	DNA polymerases, Restriction Enzymes
Fisher Scientific	UK	Chemicals
VWR	Poole, UK	Chemicals, Filter units
Melford	UK	Chemicals
Sigma	Dorset, UK	DNA Polymerases
New England Biolabs	Hitchin, UK	Restriction Enzymes, Ligase
Promega	Southampton, UK	Chemicals, Enzymes
Qiagen	Crawley, UK	DNA purification kits
Stratagene	Netherlands	Enzymes
Biogene	Kimbolton, UK	Growth Media Reagents
Difco	UK	Growth Media Reagents
Gibco BRL	UK	Growth Media Reagents
Oxoid	Basingstoke, UK	Growth Media Reagents
Nalgene	Nerijse, Belgium	Filter units
SLS	Strathclyde, UK	DNA Extraction Kits
Anachem	Luton, UK	SDS PAGE Apparatus
Cambio	Cambridge, UK	Molecular Biology Kits
USB Corporation	USA	Enzymes
Invitrogen	Paisley, UK	Competent Cells
Clontech	Oxford, UK	Plasmids
PE Applied Biosystems	Cheshire, UK	Enzymes
MWG Biotech	Milton Keynes, UK	Oligonucleotides

2.2 DNA Samples

The following samples were obtained directly as DNA samples. Where samples are prefixed with MD- this represents the laboratory identification code used.

2.2.1 Constitutional DNA from Colorectal Cancer Patients

Prof. M. Dunlop and Dr. S. Farrington have previously collected a panel of constitutional DNA from the blood, normal mucosa and tumours of patients with CRC. These were available as a laboratory resource and were used at a concentration of approximately 100ng/μl.

2.2.2 Plasmid Samples

Plasmid samples were originally obtained from a number of different laboratories and suppliers. These are shown in Table 2.2 alongside the source. Plasmids constructed by myself are listed and cloning strategy will be discussed in the relevant chapter.

Table 2.2: Plasmids Used in this Thesis

Plasmid Name	Description	Source
YCPLac22	Yeast/*E.coli* shuttle vector	Gietz and Sugino 1988
p423MET	Yeast/*E.coli* shuttle vector, methionine repressible promoter, over-expression plasmid	Mumberg et al 1994
p*MAD3*	*S.cerevisiae MAD3* Wild Type- YCPLac22	Warren et al 2002
p*MAD3-ΔE5*	*S.cerevisiae MAD3 ΔE5*- YCPLac22	This Study
p*MET:MAD3*	MET25 promoted *S.cerevisiae MAD3* Wild type over-expression	Warren et al 2002
pMET:MAD3-ΔE5	*S.cerevisiae MAD3 ΔE5* over-expression	This Study
p*BUB1*	*S.cerevisiae BUB1* Wild Type- YCPLac22	Warren et al 2002
p*BUB1-ΔE5*	*S.cerevisiae BUB1 ΔE5*- YCPLac22	This Study
p*MET:BUB1*	MET25 promoted *S.cerevisiae BUB1* Wild type over-expression	Warren et al 2002
pMET:BUB1-ΔE5	*S.cerevisiae BUB1 ΔE5* over-expression	This Study
pcDNA-3 *Myc hMAD3*	Human *BUBR1*- pcDNA-3 myc tagged	Taylor 2001
BVWT	Human *BUB1*- pBI-GFP	Cahill 1998
V400	Human *BUB1* Deletion mutant- pBI-GFP	Cahill 1998
V429	Human *BUB1*Missense mutant-pBI-GFP	Cahill 1998
pKS+ *V400*	Human *BUB1* Deletion mutant- pBluescript	This Study
pKS+ *V429*	Human *BUB1*Missense mutant- pBluescript	This Study
pKS+ *BVWT*	Human *BUB1*Wild Type- pBluescript	This Study
pKS+ *BUBR1*	Human *BUBR1*Wild Type- pBluescript	This Study
pBI *BUBR1*	Human *BUBR1*Wild Type- pBI-GFP	This Study
EGFP-*BUB1*	Human *BUB1* Wild type- EGFP-C1	This Study
EGFP-C1	GFP fusion vector	Clontech
PTet-On	Tetracycline regulatory element	Clontech
PTRELuc	Tetracycline responsive element coupled to luciferase	Clontech
pCMV-β	β-gal plasmid	Clontech
pTK-Hyg	Hygromycin resistant plasmid	Clontech

2.3 DNA and RNA Purification Protocols

2.3.1 Purification of DNA from Cell lines and Blood Lymphocytes

Isolation of genomic DNA from cell cultures and blood was carried out using a Nucleon II extraction kit (SLS) according to the manufacturer's instructions. This procedure was carried out in a class 2-containment hood.

2.3.2 Phenol Chloroform Extraction and Ethanol Precipitation

Solutions

1 x Tris EDTA (TE)*

10mM Tris (pH 7.7),

1mM Na_2EDTA (pH8.0)

3M Sodium acetate (NaOAc)

3M NaOAc-$3H_2O$

pH4

Phenol Chloroform extraction was carried out in a biological class 2 cabinet. An equal volume of phenol chloroform solution (Gibco BRL) was added to the DNA solution. This was inverted and spun for 5 minutes at 2000rpm in a Wifug lab centrifuge. Supernatant containing the DNA was carefully removed with a pipette. An equal volume of chloroform was then added to the supernatant, inverted and spun for 5 min at 2000rpm. The supernatant was again removed. Phenol chloroform was disposed of as liquid waste due to its hazardous nature.

For ethanol precipitation a 1:10 volume of 3M NaOAc (pH4) was added to the DNA solution along with 2-3 volumes of 100% ethanol. The solution was incubated for 30min at –70°C and then centrifuged for 15min at 2000rpm a Wifug lab centrifuge. The residual DNA pellet was re-suspended in an appropriate volume of 1 x Tris EDTA pH7.7.

2.3.3 Purification of DNA from Bacterial Plasmids

Plasmid DNA was extracted on small, medium and large scales using QIAprep miniprep, midiprep and maxiprep kits respectively (QIAGEN) according to the manufacturer's instructions.

For small scale DNA extraction from a large number of plasmid samples in 96well plates, a BioMek® 2000 workstation robot was used, operated by Dr. Stewart McKay (MRC, Human Genetics Unit, Edinburgh) according to the manufacturer's instructions.

2.3.4 Estimation of DNA Concentration

5µl of genomic and plasmid DNA samples were run on an agarose gel (see 2.4.4 for agarose gel electrophoresis) at stock concentration and 1:10 dilution and compared to DNA standards of known concentration (1µg/µl, 750ng/µl, 500ng/µl, 250ng/µl, 100ng/µl).

2.4 PCR Protocols

Manipulation of oligonucleotides and all PCR techniques were carried out in a biological class 2 cabinet designated for PCR. Equipment designated specifically for PCR use was employed to minimise contamination of PCR products.

2.4.1 Oligonucleotides for PCR

Primers were supplied by MWG Biotech as precipitates and resuspended in sterile dH_2O to a stock concentration of 1µg/µl. Amplification was performed using an Omnigene PCR system thermal cycler (Hybaid) under the following standard conditions: 94°C for 3 min for 1 cycle; 94°C for 1 min, 55°C for 1 min, 72°C for 1 min for 35 cycles; 72°C for 5 min for 1 cycle. Primers were specifically designed unless referenced (Tables 2.3 and 2.4).

Table 2.3: *S.cerevisiae* Oligonucleotides Used for PCR

Primer	Sequence 5'-3'	5' RE site
MAD3		
sec1 for	GATCGAGCTCCCTGCATTAAGCGACCCAATTAC	SacI
sec1 rev	GATCCGTCTCGGATGAAAAAGTTCTATGTACCAAAACC	BsmBI
sec2 for	GATCCGTCTCGCATCTCCTGAGAGAACTGGGGGAG	BsmBI
sec2 rev	GATCTCTAGAAATTGCCAAGACTTCTTCTAGCG	XbaI
BUB1		
sec1 for	GATCGAATTCTCTACTAATTAATGCTCAATAGCTGG	EcoRI
sec1 rev	GATCGCAGTGAAACAAATTTATATACCAAATCC	BtsI
sec2 for	GATCGCAGTGTTAATTATGAAGACAGACTCCGAG	BtsI
sec2 rev	GATCGGTACCACATCTGTTTCAGTAGTTTCTTTTATAGGCG	KpnI
seq prom	AACGCCTTTCGATTGCGGAAATGTG	
seq for	GATATGGAAACCTATAGGAACGATC	
seq f2	ACTAACATCCAACGCTTCCC	
seq f3	CCAGCTGCAGAATGGACGATGC	
seq rev	GGGGACAACGGGTGGCTGTGATG	
ycpLac22		
1f	CTGAATGAAGCCATACCAAACG	

Table 2.4: Human Oligonucleotides used for PCR

Primer	Sequence 5'-3'	5' RE site
BUBR1		
Sec1f	GATCGCGGCCGCATGGCGGCGGTGAAGAAGG	Not I
Sec1r	GATCGCAGTGTAATTTAAGCCAGAGATTGAG	Bts I
Sec2f	GATCGCAGTGTAACAATTCCAAGCTCGAGTGTCTCGGC	Bts I
Sec2r	GATCGTCGACTCACTGAAAGAGCAAAGCCC	Sal I
Sec1f(ii)	GATCCCGCGGGGATGGCGGCGGTGAAGAAGGAAGG	SacII
Sec2r(ii)	GATCCCCGGGGGTAGTGCATCTAAATGTGTCC	SmaI
1F	AAGGCCTGCAGCAGGACGAG	
1R	CTGCCCATGAGATATAGAACTGAGC	
2R	TTGAGAGCACCTCCTACACG	
3F	GAGTCTTCTGTACCACAACG	
3R	CACTGGTCAATAGCTCGGC	
4F	GGAGAAGATTTATGCAGG	
4R	CCTTCAAGGACATTATCTCATG	
5F	TCACAGGCTTCAGAAATGTAAC	
5R	CGTTCCTTTAACTTGAGG	
5xF	GCATTAAACGAGAATACC	
5xR	GAATTTATTCCTCAATTCACC	
6F	GGATATCGTCTAAATCGTG	
6R	ATACATGGTGATCATAAGAGAAC	
1xf	CCTCAAGGTGGGAAAGAGAG	
1xr	GATTGAGAAATCGAGGATCAC	
BUB1		
1F	ATGGACACCCCGGAAAATGTC	
1R	GAATATTCTGATTTAGAAATCG	
2F	CATGGCCTGCATTTCTAAG	
2R	AGCATCTTTGCTGGCCACTGC	
3F	GTGGAGACATCCCATGAGGATCT	
3R	AAACTGGGCTTCAAATGC	
4F	TGGGAATGGTTCAGGCAACG	
4R	GGATCTTCTGCAATGGCAGCG	
5F	AGCCCAAAACAGGCCTTGTCG	
5R	GTTCTGGAACTCCG	
6F	CTAAAGCCATCTATGCAGC	
6R	CAGTGTGATTTTTAAGGACTGTC	
1vf	CATGGACACCCCGGAAAATGTC	
1vr	GCATCTTTGCTGGCCACTGC	
Sec1f	GATCTCCGGAATGGACACCCCGGAAAATGTC	BspE1
Sec 2r	GATCGGATCCTTTTACATGGAAATATTCCATGGG	BamHI

2.4.2 Standard PCR

PCR reactions were performed either in a final volume of 50µl using the Expand Long Template PCR or AmpliTaq systems (Roche) or in a 25µl final volume using the Expand High Fidelity PCR system (Boehringer Mannheim).

Final reaction concentrations for the Expand Long Template system were 1xPCR buffer I, II or III as manufacturer's recommendations, 0.2mM dNTP's, 100ng each oligonucleotide primer, 100ng DNA and 2.5 Units of Expand High Fidelity PCR mix.

Final reaction concentrations for the AmpliTaq system were 1x AmpliTaq PCR buffer, 2.5mM MgCl2, 0.2mM dNTP's, 100ng each oligonucleotide primer, 100ng DNA and 1.25 units of AmpliTaq.

Final reaction concentrations for the Expand High Fidelity system were 1 x PCR buffer II, 0.2mM dNTPs, 100ng each oligonucleotide primer, 100ng DNA and 0.87 Units of Expand High Fidelity PCR mix.

2.4.3 Colony PCR

Bacterial plasmid DNA was analysed on a large scale in 96 well plates in 20µl AmpliTaq PCR reactions. Bacterial colonies were stabbed into PCR reaction reactions using a sterile p200 pipette tip. The colony was then streaked onto the appropriate square of a gridded L-Agar plate for growth and storage.

2.4.4 Gel Electrophoresis

Solutions

10 x Tris-Acetate EDTA (Kitaeva et al., 1997)*

2M Tris

5.7% w/v Glacial acetic acid

50mM Na_2EDTA (pH8.0)

Loading Buffer

100mM Na_2EDTA (pH8.0)

0.25% w/v Bromophenol blue

30% w/v Sucrose.

Standard agarose gels were prepared using 'Hi Pure' low EEO agarose (Biogene) and 1x TAE electrophoresis buffer. Separation of large fragments required low percentage gels (typically 1.5%) whereas smaller fragments were separated on higher percentage gels (typically 3%). If DNA fragments were being isolated from the gel for sequencing or plasmid construction, a 1-3% ultra pure Low Melting Point agarose (Gibco BRL) gel was prepared using 1x TAE electrophoresis buffer.

5-10µl standard PCR products were loaded onto the gel with 2µl of loading buffer. Size markers used were generally a 1kb ladder (Gibco BRL) or a 100bp ladder (Promega). The DNA was electrophoresed at 20-60V until the dye front was 1cm from the end of the gel although this varied with the size of fragments being investigated. The DNA was visualised by staining with ethidium bromide (Biorad) followed by UV trans-illumination using a Herolab trans-illuminator (Herolab, Wiesloch). Images were captured using a Herolab Camera and Easywin 32 version 2.00 software.

2.5 Cloning and Bacterial Culture

Media and additives

Luria Broth (L-broth)*

0.1% w/v Tryptone (Difco)

0.05% w/v Yeast extract (Difco)

171mM NaCl

Luria Agar (L-agar)*

0.1% w/v Tryptone (Difco)

0.05% w/v Yeast extract (Difco)

171mM NaCl

0.15% w/v Agar (Oxoid Ltd)

Ampicillin stock solution

20mg/ml ampicillin (Sigma)

Kanamycin stock solution

30mg/ml Kanamycin (Sigma)

2.5.1 Growth of Bacterial Cultures

Overnight cultures were prepared by inoculating 15ml cultures of L-broth containing 50μg/ml ampicillin or 30μg/ml kanomycin. They were incubated at 37°C and shaken at 225rpm for approximately 16 hours. These cultures were used for small-scale bacterial plasmid DNA extraction, to inoculate larger cultures for medium and large-scale bacterial plasmid DNA extraction (see 2.3.3) or to prepare glycerol stocks for long term storage (see 2.5.3).

2.5.2 Chemical Transformation into *E.coli*

Plasmids were transformed into either TOP10 (Invitrogen), DH5α (GibcoBRL) or SURE® (Stratagene) chemically competent *E.coli* strains. 1μl of plasmid minprep or ligation mixture was added to a 100μl aliquot of competent cells and incubated on ice for 1 hour. The cells were heat shocked at 37°C for 1 min and incubated again on ice for 2 mins. 200μl of SOC media (Invitrogen) was added and the cells incubated at 37°C with shaking at 200rpm for 1 hour. 100μl were plated onto L-agar plates with appropriate selection and these were incubated upturned at 37°C overnight. Colonies were analysed for the presence of the plasmid by colony PCR (see 2.4.3).

2.5.3 Colony Selection and Storage

Colonies growing on antibiotic selection plates, indicative of positive transformants, were picked using sterile p200 pipette tips. Presence of a correct sized insert was determined by Colony PCR amplification using appropriate primers as described above (2.4.3). Bacterial colonies were stabbed into PCR reactions before being streaked onto L-Agar selection plates marked with a 96 square grid, for

storage. The plates were incubated upturned at 37°C for approximately 16 hours and stored at 4°C.

Stocks for long-term storage were made by centrifugation of 1ml of overnight culture at 2000rpm for 5 mins in a Wifug lab centrifuge. The cell pellet was re-suspended in 1ml of L-Broth with 15% sterile glycerol (Sigma). The cell suspension was then transferred to a cryovial and stored at -70°C. Stored stocks were recovered by scraping off a small amount of the frozen stock, streaking out onto selection plates and incubating the plates upturned at 37°C overnight.

2.5.4 Restriction Digestion

Restriction digestion reactions were performed in a final volume of 50µl with final reaction concentrations of 1µg plasmid DNA or PCR product, 1x restriction enzyme buffer, 5µg BSA if recommended by manufacturer and 5 units restriction enzyme. The reaction was incubated at manufacturer's recommended temperature for 1-2 hours. In the event of a digestion with 2 enzymes being required, a compatible buffer was used as recommended by the manufacturer or if no buffers were compatible the digested DNA was ethanol precipitated between digests as above (2.1.2) and re-suspended in sterile dH_2O before the second digest.

For enzymes used, their suppliers, buffers and temperatures, see table 2.5.

Table 2.5: Restriction Enzymes Used for Cloning

Restriction enzyme	Recognition site (5'-3')	Buffer	Digestion conditions	Supplier
BspEI	T↓CCGGA	Buffer 3	37°C	NEB
Bts I	GCAGTG NN↓ CGTCAC↑NN	Buffer 4	37°C +BSA	NEB
AhdI	GACNNN↓NNGTC	Buffer 4	37°C +BSA	NEB
BsaBI	GATNN↓NNATC	Buffer 2	60°C	NEB
SacII	CCGC↓GG	Buffer 4	37°C	NEB
XbaI	T↓CTAGA	Buffer 2	37°C +BSA	NEB
BsmBI	CGTCTCN↓ GCAGAGNNNNN↑	Buffer 3	55°C	NEB
BstUI	CG↓CG	Buffer 2	60°C	NEB
KpnI	GGTAC↓C	Buffer L	37°C +BSA	Roche
SacI	GAGCT↓C	Buffer A	37°C	Roche
BamHI	G↓GATCC	Buffer B	37°C	Roche
EcoRI	G↓AATT C	Buffer H	37°C	Roche
XbaI	T↓CTAGA	Buffer H	37°C	Roche
SalI	G↓TCGAC	Buffer H	37°C	Roche
NotI	GC↓GGCCGC	Buffer H	37°C	Roche
SmaI	CCC↓GGG	Buffer A	25°C	Roche

2.5.5 Purification of Digested Fragments

Restriction Digests were visualised by agarose gel electrophoresis on a 1-3 % Ultra pure Low Melting Point agarose gel (Gibco BRL). DNA fragments of the required size were removed in slices of agarose using a clean scalpel blade. The DNA fragments were purified from the agarose using either a QIAquick gel extraction kit (QIAGEN) or an UltraClean DNA Purification Kit (CamBio), both according to manufacturer's instructions.

2.5.6 Ligation

Ligation reactions were carried out in a final volume of 20µl containing 5µl gel purified DNA fragment, 1-2µl digested plasmid DNA, 1x T4 DNA ligase buffer and 10 units T4 DNA ligase (New England Biolabs Inc.). Ligation reactions were incubated at 16°C for 16 hours.

2.6 Sequence Analysis

2.6.1 Purification of PCR Products

Small numbers of PCR products were cleaned for sequencing using a QIAquick PCR purification kit with a microcentrifuge (QIAGEN) according to manufacturer's instructions.

On a large scale (96-well plate format) PCR products were cleaned using Shrimp Alkaline Phosphatase and Exonuclease I. The final reaction volume was 8µl with 10 units of Exonuclease I (USB Corporation) and 2 units of Shrimp Alkaline Phosphatase (USB Corporation) and 400ng of DNA. The reactions were purified in a Omnigene PCR system thermal cycler (Hybaid) under the following conditions; 1 cycle at 37°C for 15mins, 1 cycle at 80°C for 15mins.

2.6.2 DNA Sequencing

All sequencing reactions were performed using ABI PRISM Ready Big Dye Terminator cycle Sequencing Kit with AmpliTaq DNA polymerase FS (PE Applied

Biosystems) and Applied Biosystems DNA sequencer models 373A, 377 or 3700 for 96 well format.

Sequencing of purified PCR products was carried out in 10µl reactions using 100ng purified DNA, 100ng primer and 4µl big dye terminator (PE Applied Biosystems). Amplification was performed on a PCR system thermal cycler (Hybaid) at 96°C for 30sec, 50°C for 15sec, 60°C for 4min for 25 cycles.

Sequencing of plasmid DNA was carried out in 20µl reactions using approximately 100ng plasmid DNA, 100ng primer, 4µl Big Dye (PE Applied Biosystems) and 0.36mM $MgCl_2$. Amplification was performed on a PCR system thermal cycler (Hybaid) at 96°C for 5min for 1 cycle, 96°C for 30sec, 55°C for 15sec, 60°C for 4min for 25 cycles. All sequencing reactions were stored at 4°C prior to precipitation

2.6.3 Precipitation of DNA from Sequencing Reactions

After amplification, standard precipitation of sequenced DNA was carried out by adding 55µl 95% ethanol and 2µl 3M NaOAC pH 4 to the sequencing reaction mix. The mixture was incubated on ice for 10min and then spun at 15000rpm in an IEC Micromax centrifuge for 30min. The DNA pellet was re-suspended in 70% ethanol and spun at 15000rpm for a further 10min. Ethanol was removed and the DNA pellet dried at room temperature ensuring complete evaporation of the alcohol. The cell pellet was stored at –20C.

For precipitation of DNA in 96 well format the above procedure was carried out as above except samples were incubated at room temperature for 30 mins. Plates were spun in a Sorvell RT6000 centrifuge at 2000rpm for 30 minutes and supernatant was removed by inverting the plate and pulse spinning the upturned plates on paper towels at 800rpm. 70% ethanol was added to the cell pellets down the side of each well and rapidly inverting the plate immediately. The pellets were dried by a further pulse spin at 800rpm in a Sorvell RT6000 centrifuge. Cell pellets were again stored at -20°C.

2.6.4 Gel Electrophoresis of Sequenced DNA

Precipitated cell pellets were re-suspended in 2-4μl loading dye (PE applied Biosystems) and heated at 90°C for 2min by Agnes Gallagher (MRC, Human Genetics Unit, Edinburgh). Samples were then incubated on ice until loading. Samples were analysed using Applied Biosystems DNA sequencer models 373A, 377 or in the case of analyses of samples in 96 well formats an ABI 3700 all according to manufacturer's instructions.

2.6.5 Analysis of Sequence Data

Raw sequence data was analysed using Sequencing Analysis Version 3.0 (PE Applied Biosystems). For alignment of multiple sequences of the same fragment, sequence data was imported into the Sequencher program Version 3.0.1 (Gene Codes Corp., Michigan). Up to 100 fragments at a time were aligned with the default assembly parameters adjusted to allow 75-85% minimum match. The relevant reference sequence was also imported from GenBank and incorporated in alignments to allow comparison of the sequenced fragments to the published sequence.

Alignments were trimmed of vector sequence and poor quality end sequences prior to further analysis. Individual base pairs highlighted by the Sequencher program as showing mutation, deletions or ambiguous sequence were then manually curated.

2.7 Saccharomyces cerevisiae Culture

2.7.1 *S.cerevisiae* Strains

The *S.cerevisiae* strains used during this work are listed in table 2.6. They are derived from either W303-1a (Rothstein) or S288c (Warren et al., 2002).

Table 2.6: *S.cerevisiae* Strains Used in this Thesis

Strain	Mating type	Genotype	Reference
KH 34	a	*ura3-1, leu2,3-112, his3-11, trp1-1, ade2-1, can1-100*	Hardwick et al 2000
KH 35	α	*ura3-1, leu2,3-112, his3-11, trp1-1, ade2-1, can1-100*	Hardwick et al 2000
YKH231	a	*ura3-1 leu2,3-112 his3-11 trp1-1 ade2-1 +CFIII URA3 SUP11*	Warren et al 2002
YPH278	α	*ura3-52, lys2-801, ade2-101, his3Δ200, leu2Δ1, CFIII, URA3, SUP11*	Warren et al 2002
YLB1	a	*Cdc20-(*myc*)$_{18}$::LEU2, ura3-1, leu2,3-112, his3-11, trp1-1, ade2-1, can1-100*	This Study
YLB2	α	*bub1Δ::HIS3, Cdc20-(*myc*)$_{18}$::LEU2, ura3-1, leu2,3-112, his3-11, trp1-1, ade2-1, can1-100*	This Study
YLB4	α	*mad3Δ::URA3, Cdc20-(*myc*)$_{18}$::LEU2, ura3-1, leu2,3-112,his3-11, trp1-1,ade2-1,can1-100*	This Study
KH228	a	*BUB3-(*myc*)$_{13}$::*G418*, ura3-1, leu2,3-112, his3-11, trp1-1, ade2-1, can1-100*	Hardwick et al 2000
KH238	a	*bub1Δ::HIS3, BUB3-(*myc*)$_{13}$::*G418*, ura3-1, leu2,3-112, his3-11, trp1-1, ade2-1, can1-100*	Hardwick et al 2000
YRJ 10	a	*mad3Δ.2, BUB3-(*myc*)$_{13}$::*G418*, ura3-1, leu2,3-112, his3-11, trp1-1, ade2-1, can1-100*	Hardwick et al 2000
YRJ111	a	*mad3Δ::URA3, ura3-1, leu2,3-112, his3-11, trp1-1, ade2-1, can1-100, CFIII URA3 SUP11*	Warren et al 2002
YRJ112	a	*bub1Δ::HIS3, ura3-1, leu2,3-112, his3-11, trp1-1, ade2-1, can1-100, CFIII URA3 SUP11*	Warren et al 2002
YCD280	α	*ura3-52 lys2-801 ade2-101 hisΔ200 leu2Δ1 bub1-1::HIS3 +CFIII URA3 SUP11*	Warren et al 2002
YMB111	a	*ura3-1 leu2,3-112 his3-11 trp1-1 ade2-1 mad1Δ::URA3 +CFIII URA3 SUP11*	Hardwick et al 2000
YMB113	a	*ura3-1 leu2,3-112 his3-11 trp1-1 ade2-1 mad2Δ::URA3 +CFIII URA3 SUP11*	Hardwick et al 2000
KH304	α	*Cdc20-(*myc*)$_{18}$::LEU2,mad1Δ::URA3 ura3-1, leu2,3-112, his3-11, trp1-1, ade2-1, can1-100*	K. Hardwick
YMB003	a	*bub3Δ::LEU2, ade2-1, trp1-1, can1-100 leu2,3-112, his3-11, ura3-1*	K Hardwick
KH40	a	*cin1Δ::HIS3, ade2-1, trp1-1, can1-100 leu2, his3-11, ura3-1*	Hardwick et al 2000

2.7.2 *S.cerevisiae* Media

Media used and its components are listed in table 2.7.

Table 2.7: S.cerevisiae Media

Media	Components
YPDA[#]	1% w/v Yeast Extract 2% w/v Bacto-peptone 2% w/v Glucose 0.003% w/v Adenine sulphate
YPD	1% w/v Yeast Extract 2% w/v Bacto-peptone 2% w/v Glucose 0.001% w/v Adenine sulphate
YMM	0.67% w/v Yeast Nitrogen Base w/o amino acids 2% w/v Glucose 1 Pellet Sodium Hydroxide/l
Sporulation	0.3% w/v Potassium Acetate 0.02% Raffinose
Low Adenine media	0.67% w/v Yeast Nitrogen Base w/o amino acids 2% w/v Glucose 1 Pellet Sodium Hydroxide/l 6mg/l Adenine 90mg/l each of Adenine, Tryptophan, Histidine, Lysine, Methionine, Uracil 220mg/l Leucine 87mg/l each of Cysteine, Isoleucine, Serine, Alanine, Glutamic acid, Arginine, Threonine, Glutamine, Tyrosine, Asparagine, Glycine, Phenylalanine, Aspartic acid, Proline, Valine
Selective media	YMM Plus amino acids required from: 90mg/l each of Adenine, Tryptophan, Histidine, Lysine, Methionine, Uracil 220mg/l Leucine 87mg/l each of Cysteine, Isoleucine, Serine, Alanine, Glutamic acid, Arginine, Threonine, Glutamine, Tyrosine, Asparagine, Glycine, Phenylalanine, Aspartic acid, Proline, Valine

For solid media 2% w/v agar was added prior to autoclaving.

2.7.3 *S.cerevisiae* Supplements

Supplements used are listed in table 2.8.

Table 2.8: *S.cerevisiae* Supplements

Supplement	Stock Solution	Final Concentration mg/l
Benomyl (Sigma)	30mg/ml in DMSO	10-15
Nocodazole (Sigma)	10mg/ml in DMSO	15
Hydroxyurea (Sigma)	100mg/ml in dH_2O	5000

2.7.4 *S.cerevisiae* Growth Conditions

Wild type *S.cerevisiae* were grown at 30°C either upturned on solid media or in liquid media on shaking platforms to provide aeration. To maintain selection for plasmid DNA and/or for auxotrophic markers inserted on the genome, cells were grown on selective media lacking appropriate amino acids.

2.7.5 Storage of *S.cerevisiae* Strains

Strains were stored for short periods on solid media at 4°C and longer term at -80°C in YPD supplemented with 20% v/v glycerol.

2.7.6 Lithium Acetate Transformation

Solutions

5M LiOAc

1M Tris pH7.4

500mM EDTA

LiOAc mix

100mM LiOAc

10mM Tris pH7.4

1mM EDTA

Filter sterilised

PEG mix

40% PEG 2000

100mM LiOAc

10mM Tris pH7.4

1mM EDTA

Filter sterilised

A 5ml culture of the strain to be transformed was grown in selective media overnight at 30°C. The culture was diluted in YPDA to attain a 50 ml culture an OD_{600} of 0.15 and grown for 4 hours at 30°C to a log phase culture with an OD_{600} of 0.3-0.6. The culture was centrifuged at 2000rpm for 5minutes, washed in 1ml LiOAc mix and transferred to an eppendorf tube. This culture was centrifuged again at 5000rpm for 30 seconds and washed again in 1ml LiOAc mix. The centrifugation was repeated again and the cells resuspended in 500µl LiOAc mix.

1-2µl of the DNA to be transformed and 15µl of salmon sperm carrier DNA (10mg/ml) were added to a 100µl aliquot of the LiOAc yeast cell mix. In addition one transformation was set up without DNA as a negative control. 700µl of PEG mix were added to this and mixed gently by pipetting before incubating at room temperature for 30 minutes. The transformation mix was then heat shocked at 42°C for 15 minutes. The mix was pelleted by centrifugation at 5000rpm for 30 seconds, the supernatant removed and the pellet resuspended in 200µl of YPDA. The transformation was plated onto selective media and incubated upturned at 30°C until colonies were visible. Mixed colonies were picked and streaked onto selective media before use in subsequent assays.

2.7.7 G2/M Arrest by Growth in Nocodazole

Nocodazole is an inhibitor of tubulin polymerisation which causes depolymerisation of the microtubule spindle and initiates the spindle checkpoint arresting cells at the G2/M transition.

A 5ml culture of *S.cerevisiae* cells was grown overnight in selective media or YPDA at 30°C to stationary phase. The culture was diluted in 50ml YPDA to attain an OD_{600} of 0.2 and grown for 4 hours at 30°C to mid log phase, OD_{600} 0.3-0.6. Nocodazole (Sigma) was then added to the culture to give a final concentration of 15mg/l and the cultures were incubated at 23°C for 3-4 hours.

The arrested culture was centrifuged at 3000rpm for 5 minutes and the supernatant removed. The cell pellet was resuspended in 1ml of sterile dH_2O and transferred to a screw cap eppendorf. The cells were centrifuged again at 5000rpm for 30 seconds, the supernatant was removed and the cell pellet sizes were equalised by eye before storing at –80°C.

2.7.8 S-phase Arrest by Growth in Hydroxyurea

Hydroxyurea is an inhibitor of a deoxynucleotide synthesising enzyme and therefore blocks DNA synthesis. It was used in these experiments to synchronise cells by arresting them at S-phase.

A 5ml culture of *S.cerevisiae* cells was grown overnight in selective media or YPDA at 30°C to stationary phase. The culture was diluted in 50ml YPDA to attain an OD_{600} of 0.2 and grown for 4 hours at 30°C to mid log phase, OD_{600} 0.3-0.6. Hydroxyurea (Sigma) was then added to the culture to give a final concentration of 5mg/ml and the cultures were incubated at 23°C for 3-4 hours. Hydroxyurea arrests were usually preformed concurrently with Nocodazole arrests in order to synchronise cells with and without activated spindle checkpoints.

The arrested culture was centrifuged at 3000rpm for 5 minutes and the supernatant removed. The cell pellet was resuspended in 1ml of sterile dH_2O and transferred to a screw cap eppendorf. The cells were centrifuged again at 5000rpm for 30 seconds. The supernatant was removed and the cell pellet sizes were equalised by eye before storing at –80°C.

2.7.9 Mating of Haploid Strains

S.cerevisiae strains of opposite mating types (a and α) were streaked onto YPDA and grown overnight at 30°C. A sterile toothpick was used to pick small amounts of each strain and mix together on a drop of sterile dH_2O water on a YPDA plate. The

mating mix was incubated at 30°C for 4 hours and examined for zygote cells indicative of mating.

2.7.10 Growth of Diploid Yeast Strains

4 hours after mating of haploid strains, zygotes were picked with a Singer Instruments MSM System Series 300 micromanipulator and grown either on YPD or on selective solid media. The colonies were tested for diploid status using a mating test. Diploid cells fail to mate with both the a and α tester strains. The cells were then grown in liquid sporulating media at room temperature for 3-7days. The cells were then examined by light microscopy for sporulation and tetrad formation.

2.7.11 Tetrad Dissection

1ml of the sporulated culture was centrifuged at 8000rpm for 1 minute and resuspended in a 190µl of sterile dH_2O and 10µl β-glucoronidase (76,800 Units/ml), (ICN Biomedicals Inc.) was added and mixed gently. The cells were incubated at room temperature for 10-15 minutes until the walls of the tetrad appeared to be digested. 20µl of tetrad mix was dripped onto YPDA and the tetrads were dissected using a Singer Instruments MSM System Series 300 micromanipulator and grown at 30°C until colonies were visible. The tetrads were replica plated onto selective plates to identify and isolate the required strain genotype.

2.7.12 Benomyl Sensitivity Assay

Methyl 1-(butylcarbamoyl)-2-benzimidazolecarbamate or benomyl is an inhibitor of microtubule polymerisation which arrests wild type cells at the spindle checkpoint. Spindle checkpoint mutants escape this arrest and divide with incorrectly formed spindles leading to cells with lethal chromosome defects (Li and Murray, 1991).

Transformants were freshly streaked out onto selective plates and incubated upturned at 30°C overnight. Small amounts of the streak outs were resuspended in 200µl of sterile dH_2O in the first row of a 96-well plate. The cells were diluted 1:10 and 1:100 into the second and third rows of the plate with gentle mixing. The

serially diluted cells were stamped onto YPD plates supplemented with 0, 10, 12.5 and 15μg/ml Benomyl (Sigma) using a sterile stamper. The plates were incubated upturned at 23°C for 3 days and growth compared and recorded photographically.

2.7.13 Microcolony Assay

Microcolony assays were carried out as previously described (Li and Murray, 1991). Small amounts of freshly streaked out transformants were picked using a sterile toothpick and streaked onto a YPD plate supplemented with 10μg/ml Benomyl. A Singer Instruments MSM System Series 300 micromanipulator was then used to isolate 25 individual cells on the benomyl plate. The individual cells were counted at 2 hourly intervals over a total of 12 hours to assess growth. The plate was incubated upturned at 23°C between counting. The mean number of cells at each time point was calculated, discounting any cells which remained single and unbudded throughout, assuming they were dead when isolated.

2.7.14 Liquid Culture Budding Assay

Liquid culture assays were carried out as described previously (Farr and Hoyt, 1998). Freshly streaked transformants were grown and arrested in nocodazole as in 2.7.7. 1ml samples of the culture were taken before addition of nocodazole (0 hours) and at 4, 6 and 8 hours after addition of nocodazole. The samples were centrifuged at 5000rpm for 5minutes and the supernatant removed. The cells were fixed by addition of ice cold ethanol while vortexing to prevent the cells aggregating. The samples were stored at –20°C until they were scored.

The cells were centrifuged again and the supernatant removed. They were washed 3x in sterile cold 1x PBS before sonicating for 2x 15 seconds using a Sonics and Materials Inc. Vibra-Cell™ sonicator.

Cells were viewed using a Zeiss Axioscope II fitted with an automated CCD camera and images were captured using SmartCapture^{VP} (Digital Scientific). Image capture and counting used a 63x oil DIC lens. The number of multi-budded cells in a 200-cell population were counted and the proportion of multi-budded cells was calculated as an indicator of spindle checkpoint function. Multi-budded cells

represent those which have been unable to arrest at the checkpoint and continue to bud are also unable to undergo cytokinesis resulting in 3 or more buds.

2.7.15 Colour Minichromosome Loss Assay

The chromosome loss assays were performed as described by Hieter et al., 1985. 5ml cultures were prepared in selective media from freshly streaked out cultures and incubated with constant shaking at 30 °C overnight. The cultures were diluted in 5ml YPDA to an OD_{600} of 0.3 and grown with constant shaking for 4 hours to an OD_{600} of approximately 0.6. The number of cells in the culture were counted with a haemocytometer and the culture diluted in YPDA to a concentration of approximately 2500 cells per ml. 200µl of the diluted culture were plated onto low adenine solid media and the plates were incubated at 30°C for 3 days until visible colonies formed. The plates were then incubated at 4°C for up to 2 weeks to allow the red and white sectoring to develop. The numbers of colonies were then counted and the number of less than half red colonies and the number of at least half but not entirely red colonies were recorded. Further details on this assay appear in chapter 4.

2.8 Protein Biology

Solutions

Lysis Buffer

50mM HEPES pH 7.6

125mM KCl

0.1% Triton X-100

1mM Na Vanadate

1mM $MgCl_2$

1mM EGTA

0.1mM PMSF (added immediately before use from fresh 0.1M Stock)

1 complete mini EDTA-free protease inhibitor tablet (Roche) per 10ml

1.5M Tris-HCl pH8.8

1.5M Tris-HCl pH 6.8

Resolving gel mixes (24ml)

Component	10%	15%
30% Acrylamide	8ml	12ml
2% bis-acrylamide	1560µl	1032µl
1.5M Tris-HCl pH8.8	6ml	6ml
10% SDS	240µl	240µl
dH_2O	8.2ml	4.728ml
10% ammonium persulphate to polymerise	240µl	240µl
Temed to polymerise	24µl	25µl

Stacking gel mix (150ml)

25ml 30% Acrylamide

20ml 2% Bis-acrylamide

18.75ml 1M Tris-HCl pH6.8

86.25ml dH_2O

0.1% ammonium persulphate and 0.1 % Temed to polymerise

10x Running Buffer

250mM Tris Base

1.9M Glycine

1% w/v SDS

Sample Buffer

80mM Tris-HCl pH6.8

100mM DTT (added immediately before use from 1M stock)

10mM EDTA

2% w/v SDS

10μg/ml LPC (leupeptin, pepstatin and chymostatin)

2mM PMSF (added immediately before use from fresh 0.1M Stock)

Bromophenol blue as required

20% v/v Glycerol

10x Transfer Buffer

1.5M Glycine

200mM Tris

Towbin Buffer

25mM Tris

192mM Glycine

0.1% SDS

20% Methanol

Blotto

5% w/v Marvel dried milk powder

1x PBS

0.02% v/v Tween

(0.5M NaCl for Bub1-G antibody)

PBST

1 x PBS

0.02% v/v Tween 20

(0.5M NaCl for Bub1-G antibody)

PBS[#]

2.8.1 Crude Extraction of Total Cellular Protein from Yeast

Cell pellet samples of arrested or stationary phase cultures were defrosted on ice and resuspended in 300µl of sample buffer containing protease inhibitors. Approximately 200µl of beads (0.5mm zirconia/silica beads, BioSpec Products, Inc.) were added and the mixture was "bead-beated" for 1 minute at 4°C, incubated on ice for 5minutes and "bead-beated" again for 1minute at 4°C. The sample was heated to 95°C for 5 minutes before centrifugation at 13,000 rpm for 1 minute. The crude protein preparation was loaded on SDS Polyacrylamide gel for analysis and excess was stored at –80°C.

2.8.2 Co-immunoprecipitation

25 or 50 ml cultures were grown and cell pellets were collected by centrifugation before being lysed in 800µl of lysis buffer by bead beating in a bead beater (Biospec Products). Approximately 200µl of beads (0.5mm zirconia/silica beads, BioSpec Products, Inc.) were added and the mixture was "bead-beated" for 1 minute at 4°C, incubated on ice for 5minutes and "bead-beated" again for 1minute at 4°C. The samples were centrifuged at 13000rpm for 1 minute at 4°C and the supernatants retained. DTT was added to a final concentration of 1mM before 2 further clarifying spins were performed. After the final spin a 30µl sample was removed and stored at –80°C as the total protein input into the IP, referred to in the chapters as the total. Affinity matrix and antibody were added as appropriate. These were typically either 30µl 50:50 slurry Protein A Sepharose^{TM} CL-4B (Amersham) washed 3 times in lysis buffer, plus 4µl of antibody or 30µl of c-myc antibody coupled beads (c-myc (9E10) AC sc-40 AC mouse monoclonal IgG_1, Santa Cruz Biotechnology) washed 3 times in lysis buffer. Immunoprecipitations were incubated at 4°C with rotation for 2 hours before pelleting the beads by centrifugation at 8000rpm for 1 minute. A 30 µl sample of the supernatant was taken and stored at –80°C representing the unbound protein fraction and referred to in the chapters as the supernatant. The beads were washed 3 times in 500µl of lysis buffer before being transferred to a clean tube and washed twice with PBS. The last of the PBS was removed and 55µl of sample buffer

was added to the beads which were then heated to 95°C for 5 minutes prior to loading on SDS-PAGE gels.

2.8.3 SDS Polyacrylamide Gel Electrophoresis

SDS polyacrylamide gels were poured between 2 glass plated separated by spacers and assembled in a pouring rig (Anachem). The base of the gel was sealed with a 1cm plug of 0.05% agarose. The resolving gel solution was prepared, poured between the plates and overlaid with water-saturated butan-1-ol. The gel was left to set at room temperature after which the butanol was washed off with water. the stacking gel was poured and an appropriate comb inserted to create the loading wells. Once the gel had polymerised the comb was removed and the wells were washed with dH_2O. The gel was firmly fixed into the electrophoresis apparatus (Anachem) and the chambers filled with 1x Running Buffer. Protein samples and appropriate molecular weight markers were then loaded and the gel was run at 180 volts for 45 minutes for small gels or for 30 volts for 16 hours followed by 300 volts for 2-3 hours for large gels, or until the coloured loading dye had run off the end of the gel.

2.8.4 Western Blot Analysis

Gels were removed from plates, the stacking gel and agarose removed and soaked in transfer buffer for 5 minutes. 4 pieces of 3MM paper and 1 piece of Hybond nitrocellulose membrane (Amersham) were cut to approximately the size of the gel and also soaked in transfer buffer. The paper membrane and gel were assembled into a sandwich as per transfer equipment manufacturer's guidelines (Pharmacia Biotech) in which the sandwich was stacked in the order negative (black) terminal, foam plate, 2x 3MM paper, Gel, Membrane, 2x 3MM paper, foam plate, positive (white) terminal. The proteins were transferred in a wet transfer tank (Pharmacia Biotech) at 65volts for 1½ hours.

Transfer was confirmed by temporary staining of the membrane with Ponceau Stain (Sigma) at room temperature for 5 minutes. The position of the protein molecular weight markers was recorded using a biro on the membrane and the

membrane was cut up for antibody treatment. Ponceau stain was removed by washing in 1x PBST.

The membrane was blocked by incubating at room temperature in Blotto for 30 minutes with shaking, to prevent non-specific protein interactions. Primary antiserum was diluted into sufficient fresh Blotto to cover the membrane as indicated in table 2.8. Membranes were incubated in primary antibody at 4°C overnight with constant shaking. The membrane was washed twice in 1x PBST at room temperature with constant shaking for 5 minutes each time. HRP conjugated secondary antiserum was diluted into a further volume of fresh Blotto and applied to the membrane. Incubations in secondary antibody were carried out at room temperature with constant shaking for 1 hour. The membrane was then washed twice again with 1x PBST as before.

2.8.5 Immunodetection with Enhanced Chemiluminescence

(Delhommeau et al., 2002)

Equal Quantities of ECL reagents 1 and 2 (Sigma) were mixed on a sheet of SaranWrap™. The excess fluid was blotted off the membranes using 3MM paper and they were placed protein side down onto the ECL mix, ensuring the membrane was uniformly covered. The membranes were incubated in the ECL mix for 1 minute at room temperature before excess ECL was removed by blotting on 3MM paper. The membranes were assembled on a glass plate and wrapped in saran wrap before being exposed to Kodak ML autoradiography film typically for 15 seconds, 1 minute, 5 minutes and 1 hour.

2.8.6 Antibodies to *S.cerevisiae* Proteins

Antibodies used are shown in table 2.9.

Table 2.9: Antibodies to *S.cerevisiae* Proteins

Antibody	Source	Description	Use	Reference
Anti-Mad3p GG	Rabbit Polyclonal	Raised against full-length protein fused to GST.	Western Blots 1:500	Hardwick et al 2000
Anti-Bub1p G	Rabbit Polyclonal	Raised against amino acids 1-216 fused to GST.	Western Blots 1:250. Use 0.5M NaCl in Blotto and PBST	Brady and Hardwick 2000
Anti-Bub1p 12/99	Rabbit Polyclonal	Raised against amino acids 1-216 fused to GST.	Co-Ips 1:200	Hardwick et al 2000
Anti-Mad2p	Sheep Polyclonal	Raised against full-length protein fused to GST.	Western Blots 1:500	Hardwick et al 2000
Anti-Mad1p R	Rabbit Polyclonal	Raised amino acids 27-310 fused to GST.	Western Blots 1:500. Use 0.5M NaCl in PBST	Hardwick et al 1995
Anti-Mad1p S	Sheep Polyclonal	Raised amino acids 58-215 fused to GST.	Western Blots 1:500 Co-Ips 1:200. Use 0.5M NaCl in PBST	K Hardwick
Anti-Myc A14	Rabbit Polyclonal	Raised against c-myc protein tag.	Western Blots 1:1000	Santa Cruz Laboratories
Anti-Myc 9E10	Mouse Monoclonal	Raised against c-myc protein tag.	Western Blots 1:1000	Berkley antibody company
Anti-Rabbit IgG-HRP	Donkey	Horse Radish Peroxidase linked whole antibody.	Western Blots 1:5000	Amersham
Anti-Sheep IgG-HRP	Donkey	Horse Radish Peroxidase linked whole antibody.	Western Blots 1:5000	Abcam
Anti-Mouse IgG-HRP	Sheep	Horse Radish Peroxidase linked whole antibody.	Western Blots 1:5000	Amersham

2.8.7 Protein Phosphatase Treatment

Protein extracts showing additional modified bands by western blot analysis were treated with Lambda protein phosphatase (LPP) to identify phosphorylation effects. 30µl of total cell extract or bead fraction from co-immunoprecipitation experiments were resuspended in a total reaction volume of 50µl containing 1x LPP reaction buffer, 1x $MnCl_2$ and 400 units of LPP enzyme (Sigma) as indicated by the manufacturers' instructions. The reactions were incubated at 30°C for 30 minutes. A control sample in which the enzyme was absent was also incubated under the same conditions. The phosphatase treated and untreated samples were then analysed by SDS PAGE and western blotting for modifications.

2.9 Calculation and Statistics

The results presented graphically generally show either the mean of three experminetal repetitions (for microcolony and liquid culture assays) or the total cumulative data from three experimental repetitions. Statistical analysis was generally performed on the total cumulative results of three repetitions of an experiment. Where error bars are shown in the liquid culture assay results they represent +/- one standard deviation about the mean.

Peter Teague and Andrew Carothers advised as to the suitability of statistical analyses, providing statistical assistance. Results from individual experiments were analysed by Chi-squared analysis, further details of which are provided in chapter 4.

The chromosome loss assays and liquid culture assays were also analysed by Mantel Haenszel tests, a derivative of Chi-squared analysis which takes account of the variation between the three experimental repetitions by using the variance of each set in the final statistical analysis. Further details of this test are also provided in Chapter 4.

2.10 Biological Material

2.10.1 Cell Lines

The cell lines used in the course of this PhD are listed in table 2.10.

Table 2.10: Summary of Cell lines

Cell Line	Cell type	Media (Gibco BRL)	Reference
HCT116	Colorectal Carcinoma	McCoys	Papadopoulos et al,. 1994
LoVo	Colorectal Carcinoma	RPMI	Liu et al., 1995b
DLD1	Colorectal Carcinoma	RPMI	Dexter et al., 1979
SW480	Colorectal Carcinoma	L-15	Leibovitz et al., 1976
HeLa	Ovarian tumour	DMEM	Scherer et al., 1952
HRT 18	Colorectal Carcinoma	RPMI	Lee et al., 1981
F9	Mouse Embryonic carcinoma	DMEM	Bernstine et al,. 1978

2.10.2 Maintenance of Cell Lines

Media, Solutions and Additives

Freezing medium

8% w/v Dimethylsulphoxide (DMSO) in new-born calf serum

Tissue Culture Medium

RPMI/ McCoys/ L-15/DMEM (Gibco BRL)

10% Foetal Calf Serum (FCS)

1% w/v Penicillin and Streptomycin*

Phosphate Buffered Saline*

0.1M $NaH_2PO_4.H_2O$

0.1M $Na_2HPO_4.7H_2O$

pH7.4

Trypsin Versene TV*

50% w/v Trypsin

50% w/v Versene

Table 2.11: Tissue Culture Additives

Additive	Stock Concentration	Final Concentration
Geneticin (Gibco BRL)	50mg/ml	500μg/ml
Hygromycin (Sigma)	50mg/ml	2mg/ml
Doxycycline (Sigma)	20 mg/ml	2μg/ml

Cells were cultured at 37°C, 5% CO_2 in humidified incubators. All tissue culture was carried out under sterile conditions in a class 2-containment hood. Sterile flasks, plates, glassware, solutions and other consumables were used.

Frozen stocks of cell lines were thawed rapidly in warm water before transferring to 5ml of appropriate tissue culture media. Media was initially changed after 24hours to remove traces of DMSO followed by feeding and passaging as required. Cells were detached from culture flasks using either a cell scraper or by washing with PBS and incubating with 1-3ml TV for 3 minutes. Fresh media was then added accordingly. To retain the cell lines as a renewable source at least 3x 10^6 were split from the main culture, centrifuged at 1200rpm in a Wifug lab centrifuge and the cell pellet resuspended in 1.5ml of freezing medium. The cells were then sequentially frozen at –70 and –140°C.

2.10.3 Transfection of Adherent Cells

Transfection of DNA into adherent cells was carried out using FuGene Reagent (Roche) for generation of stable cell lines such as pTet-On stable cell lines or LIPOFECTIN® reagent (GibcoBRL) for transient transfection for example with pCMV-β and pTRE-Luc to assay pTet-On activity. Both were used as per manufacturer's instructions using the method below.

Initially, $2x10^5$ cells were plated into each well of a six-well plate and left overnight or until ~60% confluent. 1μg of DNA was diluted into 100μl Opti-MEM reduced serum media (Gibco BRL). 5μl of FuGene6 or Lipofectin was diluted into a further 100μl of Opti-MEM. These mixes are left to stand at room temperature for 30-45 minutes. The 2 solutions are combined and incubated at room temperature for 10-15 minutes. Meanwhile, cells are washed with serum-free Opti-MEM. For transfection with Fugene6, the FuGene6 mixture was added directly to the cells. However for Lipofectin transfection, 800μl of Opti-MEM was added to the Lipofectin mixture, which was then added to the cells. The cells are incubated at 37°C for 6 hours, after which the media was replaced with appropriate media containing 10% FCS. After 72 hours Geneticin/Hygromycin selection was added for stable transfections or cells were assayed for gene activity for transient transfections.

Cells were maintained under selective conditions, which killed the appropriate control cells. Individual resistant clones were isolated by dilution cloning at 2-6 weeks post antibiotic selection. Mixed cell populations were counted, diluted and plated into 96-well microtitre plates at estimated concentrations of 1, 2 and 3 cells

per well. Plates were examined for colony formation after 1-2 weeks and those with single colonies were perceived to have originated from a single cell. When colonies covered the base of the microtitre well they were washed and removed with TV to 24-well plates. These were upgraded to 6 well dishes when appropriate cell numbers were produced.

2.10.4 Luciferase Reporter Assay

Stable pTet-On cell lines were transiently co-transfected with pTRE-Luc and pCMV-β. Luciferase assays were used to establish activity of the inserted pTet-On plasmid using a Promega Luciferase Assay system as per manufacturer's instructions summarised below.

Stable cell transfectants in 6-well plates were washed twice in PBS and incubated at room temperature in 500 µl of 1x Reporter Lysis Buffer. Cells were removed in the lysis buffer using a cell scraper and transferred to an eppendorf. The extracts were mixed by vortexing for 15 seconds and centrifuged at 14,000 rpm for 15 seconds to pellet cells. The supernatant was removed to a fresh tube and stored at –70°C.

To assay luciferase activity 20µl of cell extract was mixed with 100µl of luciferase assay reagent in a luminometer tube, both at room temperature and luminescence was quantified for 30 seconds using a luminometer (EG&G Berthhold Lumat LB 9507).

2.10.5 β-Galactosidase Assay

To normalise for cell number and transfection efficiency, β-galactosidase assays were carried out on the luciferase assay cell extracts. This assayed activity of co-transfected pCMV-β using a *β*-Galactosidase Enzyme Assay System with Reporter Lysis Buffer (Promega). 50µl of cell extract was added to 50µl of 2x assay buffer and incubated at 37°C for 30 minutes before adding 150µl of 1M Sodium Carbonate to stop the reaction. Reporter lysis buffer was used as a negative control. β-galactosidase activity was quantified by measuring the OD_{405} using a Lab systems Multiskan MS plate reader.

Chapter 3: Construction of *S.cerevisiae BUB1 ΔE5* and *MAD3 ΔE5*

3.1 Introduction

Previous work in our laboratory has involved the screening of a panel of 30 aneuploid colorectal tumours by RT-PCR for *BUB1* and *BUBR1* variants. We identified an identical deletion in *BUBR1* in transcripts from 6 of these tumours. The deletion removed part of a highly conserved domain, CD1 thought to be important in spindle checkpoint protein interactions (Hardwick et al., 2000). Clarification of the genomic structure of *BUBR1* revealed the whole of exon 5 was removed in the deletion and thus it was termed ΔE5. However extensive analysis of genomic DNA from the tumours harbouring *BUBR1ΔE5* mutation has so far failed to reveal any splice site defects or intronic variants, although analysis is ongoing. Long range PCR techniques on the genomic DNA tumour samples were unfortunately inconclusive, so the involvement of large deletions and rearrangements has not been eliminated. Thus clarification of the nature of the deletion requires further characterisation at the genomic and protein levels to identify the specific genomic alteration involved. At the transcript level, the deletion is predicted to produce a frameshift and a stop codon would occur 43 base pairs upstream of the end of the deletion. This would truncate the protein to one containing the first 128 amino acids of BUBR1 followed by an additional 14 post frameshift amino acids. However the limited availability of antibodies to the N terminal of BUBR1 and diminishing tumour material has impaired investigations into the effect of ΔE5 at the protein level (Susan Farrington, unpublished).

Another possibility is that the deletion of exon 5 is an alternative splicing effect. The evidence would suggest that such an alternative splicing phenomenon is likely to be pathogenic as the homologous region of the BUB1 protein is deleted in colon cancers which are defective in cell cycle checkpoints and exhibit CIN (Lengauer et al., 1997; Cahill et al., 1998) and similar transcripts cannot be detected in control lymphocyte RNA (Susan Farrington, unpublished). In addition computerised

analyses using genomic and cDNA sequence data to predict alternatively spliced transcripts showed no evidence for alternative splicing in *BUBR1* (Modrek et al., 2001). Thus, if this was an alternative splicing effect with no functional significance we would expect it to appear in a large proportion of normal and tumour tissue, yet numerous analyses of spindle checkpoint gene transcripts in tumours have not revealed this variant (Percy et al., 2000; Sato et al., 2000; Haruki et al., 2001). Additionally, alternatively spliced gene variants have already been implicated in human disease including CD44 which is aberrantly spliced in colon adenomas (Ghigna et al., 1998) and splice variants of ATM which have been shown to affect its function (Teraoka et al., 1999).

As stated, the equivalent of the ΔE5 mutation has previously been reported in *BUB1* in colon cancer, removing the same part of a conserved domain. In this case the deletion V400 was due to a genomic defect in a splice donor site, detected in the tumour DNA and the mutation was shown to abrogate spindle checkpoint function when exogenously overexpressed in human cell lines (Cahill et al., 1998).

The aim of this thesis was thus to investigate the hypothesis that these *BUBR1* and *BUB1* mutations are causally involved in the development of aneuploidy in colorectal cancer. To address this hypothesis I used the yeast model system *S.cerevisiae* to analyse the effect of the ΔE5 mutations on the spindle checkpoint and chromosome stability. Many of the studies of the spindle checkpoint have been carried out in the budding yeast *Saccharomyces cerevisiae*. In addition *S.cerevisiae* is easily manipulated genetically and experiments assessing spindle checkpoint function in yeast mutants are well established.

The first step in this analysis was the generation of the *BUBR1ΔE5* mutant constructs in the *S.cerevisiae* homologue of the gene. Human BUBR1 was initially identified as a BUB1 related protein as it shares significant homology to BUB1 in two conserved domains CD1 and CD2 and at the C terminal kinase domain (Cahill et al., 1998a). However, functional analyses indicate BUB1 and BUBR1 have very different roles in the spindle checkpoint. BUBR1 shows homology to both *S.cerevisiae* Bub1p and Mad3p and there has been some debate over which of these is the budding yeast homologue of BUBR1. Indeed both Mad3p and Bub1p bind to Bub3p like BUBR1 but Mad3p and BUBR1 have both been shown to be involved in

Cdc20p inhibition in the spindle checkpoint effector complex (Tang et al., 2001; Sudakin et al., 2001). Thus it is now widely accepted that Mad3p is the yeast orthologue of BUBR1 (Taylor et al., 1998). However in view of this uncertainty and in the light of identification of an identical causative mutation in *BUB1* in colon cancer, I have constructed the ΔE5 mutation in both *S.cerevisiae MAD3* and *BUB1*.

Hardwick et al have previously constructed YCPLac22 yeast-*E.coli* shuttle vector cassettes containing the full-length *BUB1* and *MAD3* genes under the control of wild type promoters (Hardwick et al., 2000; Warren et al., 2002). These full-length constructs were used to generate the ΔE5 mutant constructs and were also used as controls in subsequent assays, along with the empty YCPLac22 vector. The aim was to use these vectors to assess the functional ability of the ΔE5 proteins in yeast *bub1* and *mad3* null mutants which normally exhibit spindle checkpoint defects and an increased rate of chromosome loss. These phenotypes can be eliminated by complementation with the full-length proteins and thus the YCPLac22 based MAD3 and BUB1 constructs were used to investigate whether ΔE5 retained this ability and thus checkpoint function.

In addition full-length and deletion constructs were used to generate p423MET constructs in which the *MAD3* or *BUB1* genes are under the control of methionine repressible promoter, allowing them to be over-expressed. Over-expression constructs have previously been used to examine the ability of mutant proteins to form spindle checkpoint complexes, specifically with BUB3 (Warren et al., 2002). The ΔE5 constructs generated were used in similar experiments to determine the ability of the ΔE5 proteins to form spindle checkpoint complexes.

Thus the generation of ΔE5 constructs under the control of wild type promoters expressing endogenous levels and the methionine inducible promoter for over-expression levels were thought to be an essential way of analysing the functional effect of ΔE5 in the yeast model system.

3.2 Methodological Overview

3.2.1 Generation of Wild Type Constructs

ΔE5 constructs under the control of their intrinsic wild type promoters were prepared from p*MAD3* and p*BUB1* using PCR mutagenesis methods as described below and named p*MAD3-ΔE5* and p*BUB1-ΔE5*.

3.2.1.1 Polymerase Chain Reaction

Expand Hi fidelity PCR as described in 2.4.2 was used to amplify the two sections sec1 and sec2, flanking the area of ΔE5 using the yeast section primers (for details of primers see section 3.3.2). The p*MAD3* and p*BUB1* plasmids (2.2.2) were used as templates and these comprised YCPLac22 vector cassettes containing the full-length *MAD3* or *BUB1* coding sequence driven by the respective wild type promoters (Hardwick et al., 2000; Warren et al., 2002). Correct amplification of the sections was confirmed by agarose gel electrophoresis as described in 2.4.4 and sequencing of the PCR reactions as described in 2.6 to determine accuracy of the PCR.

3.2.1.2 Restriction Digestion

The amplified sections sec1 and sce2 were digested with appropriate internal restriction enzymes compatible to the sites in the primer sequence (Bts1 for *BUB1* and BsmB1 for *MAD3*) as described in 2.5.4. The digested fragments were purified as described in 2.5.5.

After ligation of sec1 and sec2 (see below) this insert was digested with enzymes compatible to external restriction sites (EcoR1 and Kpn1 for *BUB1* and Sac1 and Xba1 for *MAD3*) and gel purified as described in 2.5.4 and 2.5.5. Digests with two enzymes were performed sequentially with an ethanol precipitation step between to remove incompatible buffers. Additionally the full-length constructs p*MAD3* and p*BUB1* were digested with the same enzymes and the vector backbones were also gel purified in the same way (2.54, 2.55).

3.2.1.3 Ligation

The fragments of sec1 and sec2 were ligated together as described in 2.5.6 to produce the insert for the cassette. The insert of sec1 and sec2 and original vector p*MAD3* or p*BUB1* were then digested as described above with restriction enzymes at external sites. The purified insert was then ligated into the purified vector as described in 2.5.6.

3.2.1.4 Chemical Transformation into *E.coli*

Ligation reactions were transformed into *E.coli* as described in 2.5.2 and plated onto selective media containing ampicillin.

3.2.1.5 Colony Selection

Positive transformants were selected as described in 2.5.3 and analysed by colony PCR (2.4.3). Positive transformants were fully sequenced to confirm the deletion and ensure the sequence was error free, as described in 2.6.

3.2.2 *MAD3 ΔE5* and *BUB1ΔE5* Over-expression Construct

The *MAD3 ΔE5* over-expression construct was generated to examine spindle checkpoint protein function which will be described in chapter 5. The over-expression vector used, p423MET, is a yeast-*E.coli* shuttle vector with a methionine-repressible MET25 promoter. Altering methionine concentration controls transcription of the inserted gene. Maximum gene induction, approximately 50-fold, is achieved in methionine free media but under standard conditions and media, the plasmid is leaky producing 2-3 fold over-expression of the insert (Warren et al., 2002).

The over-expression construct was generated from p*MAD3-ΔE5* using simple cut and paste techniques. The previously generated ΔE5 construct p*MAD3-ΔE5* was digested with appropriate enzymes for the sites flanking the coding sequence, Bam H1 and EcoR1. The over-expression vector p423MET was also digested with the same enzymes, both as described in 2.5.4. These sites were chosen as they removed the entire coding sequence but not the promoter regions and cut only once in both the vector sequence and the *MAD3* coding sequence. The selected restriction sites retained the frame of the protein for correct transcription and translation.

The vector backbone and ΔE5 insert were purified as described in 2.5.5. They were then ligated as described in 2.5.6. Ligation reactions were transformed into *E.coli* (2.5.2) and positive transformants were selected by colony PCR (2.5.3) before being fully sequenced (2.6) as described above.

pMET:BUB1-ΔE5 was generated with the help of Kevin Hardwick in parallel with these experiments.

The full-length *BUB1* and *MAD3* over-expression construct p*MET:BUB1* and p*MET:MAD3* have previously been constructed by Warren et al and were used along with the empty p423MET vector as controls in subsequent functional assays.

3.3 Results

3.3.1 Identification of the ΔE5 Region in the Yeast *BUBR1* Orthologues

Previously published alignments of the human and budding yeast proteins were used to identify the region deleted by ΔE5. Two alignments have been published and these are not identical (Cahill et al., 1998; Hardwick et al., 2000). The ΔE5 start site predicted by these two alignments would be different. Thus the start site used was between these two predictions, retaining all the strongly conserved residues predicted in the disputed area.

ΔE5 removes 197 base pairs and would be predicted to cause a frame shift and protein truncation. A similar effect is seen if the equivalent 197 base pairs of the yeast protein are deleted. In Mad3p a stop codon is produced through the frameshift 45 base pairs down stream of the deletion site predicting a protein fragment containing only the 137 N terminal amino acids plus 15 amino acids after the frameshift. In BUB1 a stop codon is produced 6 base pairs downstream of the deletion removing most of the protein and leaving only the N terminal 118 amino acids plus 2 amino acids after the frameshift.

As the genomic alteration associated with ΔE5 is not known and ΔE5 may in fact be due to an alternative splicing effect the area removed from the full-length constructs was removed in frame. Additionally previous experiments in budding yeast had studied the effects of N terminal portions of Bub1p and Mad3p on spindle checkpoint function (Warren et al., 2002). N terminal protein fragments of Bub1p containing amino acids 1-210 and 1-367 were shown to exhibit similar spindle checkpoint defects to null mutants. Similar results were obtained for truncation mutants of Mad3p containing only the first 60, 87 or 236 amino acids (Hardwick et al., 2000). Thus truncation mutants containing 120 amino acids of Bub1p or 152 amino acids of Mad3p, including some new amino acids would be predicted to have similar detrimental effects on checkpoint function. Thus an in frame 198 base pair section containing amino acids 140-205 of Mad3p was targeted for removal and amino acids 121-186 were removed from Bub1p. This was a circumspect strategy as

any effect seen upon removing the section in frame is likely to be amplified in the event of a protein truncation. The alignments and areas deleted in ΔE5 are shown in figure 3.1.

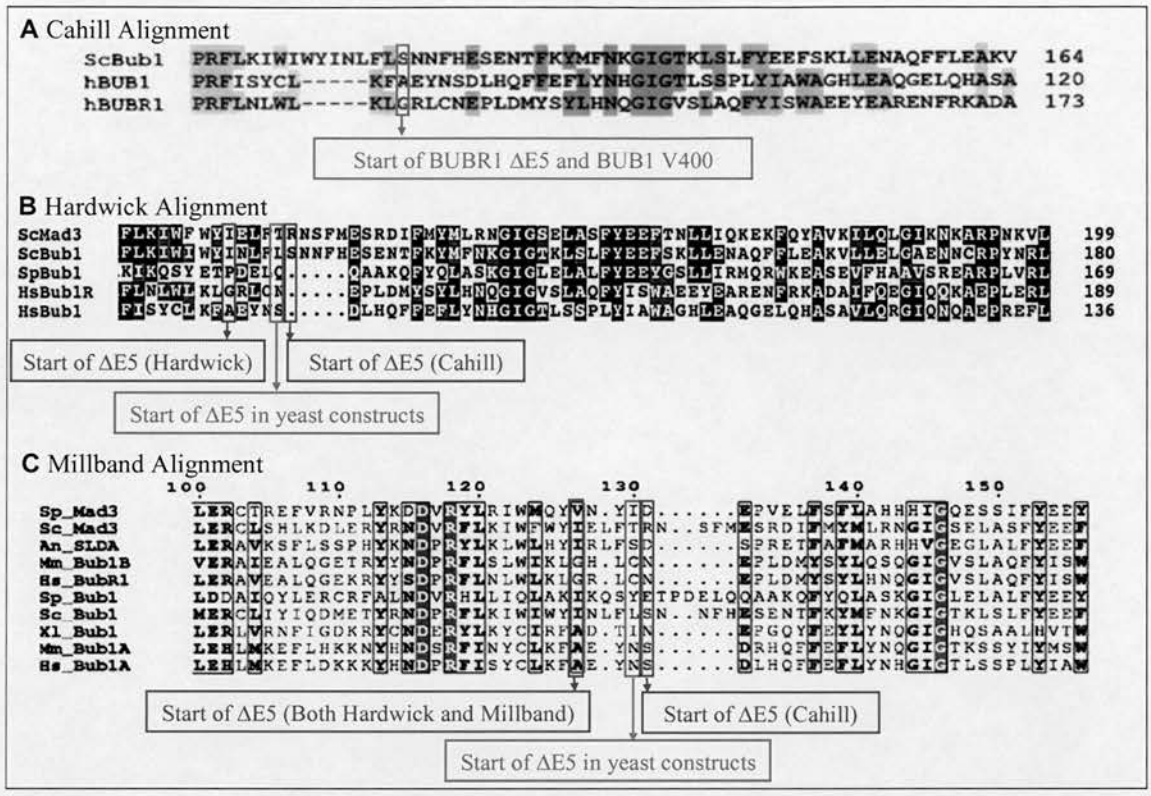

Figure 3.1 Alignment of BUB1 and BUBR1 homologues and position of ΔE5 in yeast constructs

Alignments of homology region 1 by Cahill et al and Hardwick et al were used to identify the equivalent region to ΔE5 in yeast (Hardwick et al., 2000; Cahill et al., 1998). A) shows the position of BUBR1ΔE5 and its equivalent in BUB1, V400. It also indicates the predicted ΔE5 start site in S. cerevisiae according to Cahill et al.

B) The ΔE5 start sites identified using different alignments are indicated by the coloured boxes. Purple indicates the position of ΔE5 in human BUB1 and BUBR1 and the position of the equivalent start site in yeast identified using the Hardwick alignment. Using the Cahill alignment to identify the equivalent start site in S. cerevisiae Bub1p corresponds to the position indicated in blue in the other homologues. The area deleted in the yeast cassettes constructed is shown in red and represents a compromise between the two alignments.

C) Since the construction of the ΔE5 plasmids a further alignment has been published by Millband and Hardwick comparing homologues from additional species. This alignments varies slightly from the previous Hardwick alignment and demonstrates that the exact site of ΔE5 may alter as sequence data from further BUB1 and BUBR1 orthologues becomes available for alignment (Millband and Hardwick 2002).

3.3.2 Primer Design

PCR mutagenesis methods were used to construct the mutant form of the *BUB1* and *MAD3* genes. Primers with specific restriction endonuclease recognition sites were designed to flank ΔE5. The primers used to produce the flanking sections of MAD3 and BUB1 were 1for and 1rev, and 2for and 2rev, producing section one and section two. The details of these primers are summarised in table 3.1.

Table 3.1 Sections Generated for ΔE5 Construction

Section	Forward primer	Reverse primer	5' restriction site	3' restriction site	Size Base pairs
MAD3 sec1	MAD3 sec1for	MAD3 sec1rev	Sac1	BsmB1	226
MAD3 sec2	MAD3 sec2for	MAD3 sec2rev	Xba1	BsmB1	569
BUB1 sec1	BUB1 sec1for	BUB1 sec1rev	EcoR1	Bts1	642
BUB1 sec2	BUB1 sec2for	BUB1 sec2rev	Kpn1	Bts1	1140

The endonuclease sites on the external primers matched the internal sites in the full-length gene constructs towards the 5' and 3' ends to allow the deletion to be ligated into the vector cassette once constructed. The internal primers contained sites recognised by restriction enzymes which cut downstream of their recognition sites allowing the area of the deletion to be removed exactly. This primer design and the important restriction sites are shown in figure 3.2.

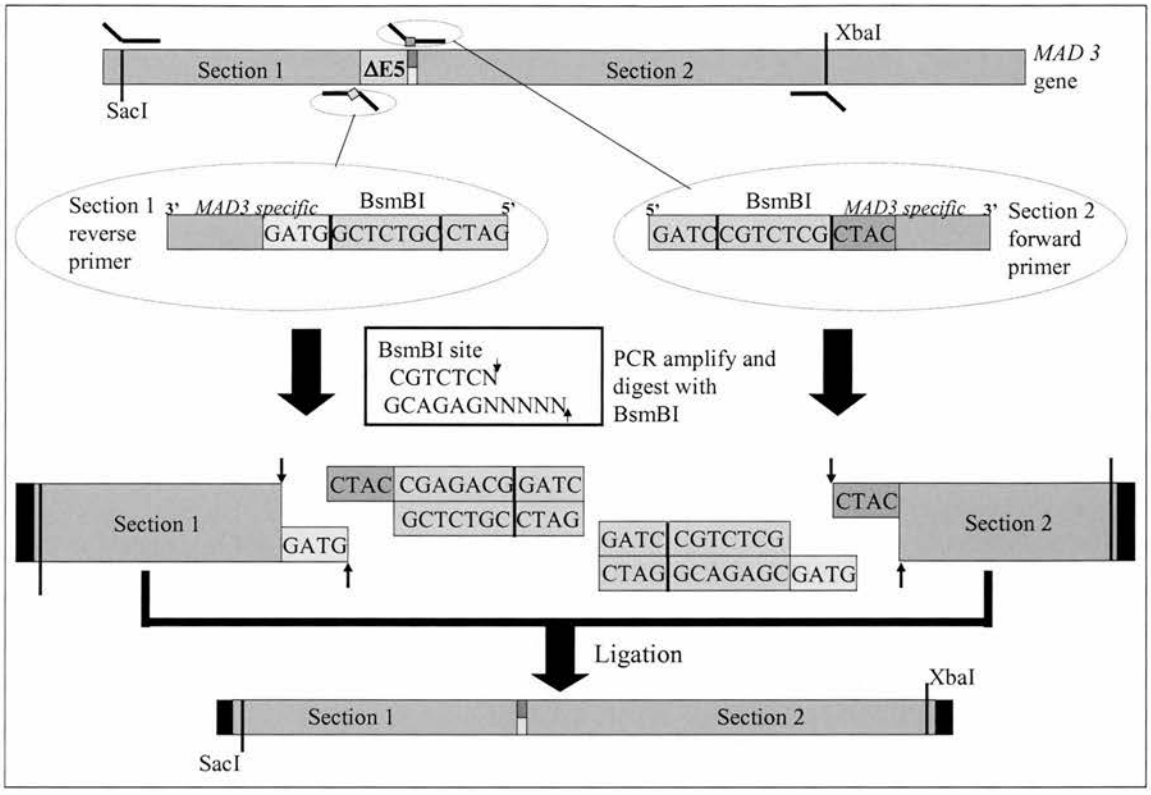

Figure 3.2 Primer design and construction of the ΔE5 deletion section

This figure summarises the procedure used for the MAD3 construct. The section primers were designed to contain recognition sites for the restriction enzyme BsmB1 which cuts upstream of the site. PCR was used to generate two sections flanking the deletion with these recognition sites at the 3' end of section 1 and the 5' end of section 2. Digestion with these enzymes produced two sections with compatible overhangs. The primers were designed such that the overhangs formed the 4 bases immediately after the ΔE5 section. Thus when the sections were ligated, the exact area of ΔE5 was removed in the resulting fragment. A similar procedure was used for BUB1 although the Bts1 restriction site was used for this as the BUB1 coding sequence includes a BsmB1 restriction site.

3.3.3 Cloning Strategy for the generation of *BUB1ΔE5* and *MAD3ΔE5* constructs

The Expand Hi fidelity PCR method was used to amplify the two sections either side of the deletion as described in chapter 2. The section PCRs were visualised using agarose gel electrophoresis, sequenced and gel purified using the Qiagen method described. The sections were then digested with appropriate internal enzymes, BsmB1 for *MAD3* and Bts1 for *BUB1* and sections one and two were ligated together producing products of 773 and 1750 base pairs respectively. The ligation products were digested with the enzymes recognising the external restriction sites. The full-length constructs were also digested with these enzymes and the vector backbones were gel purified. The ligated insert sections were then ligated into the vector backbone and the new ligation reaction was transformed into bacterial cells. This cloning strategy is summarised in figure 3.3.

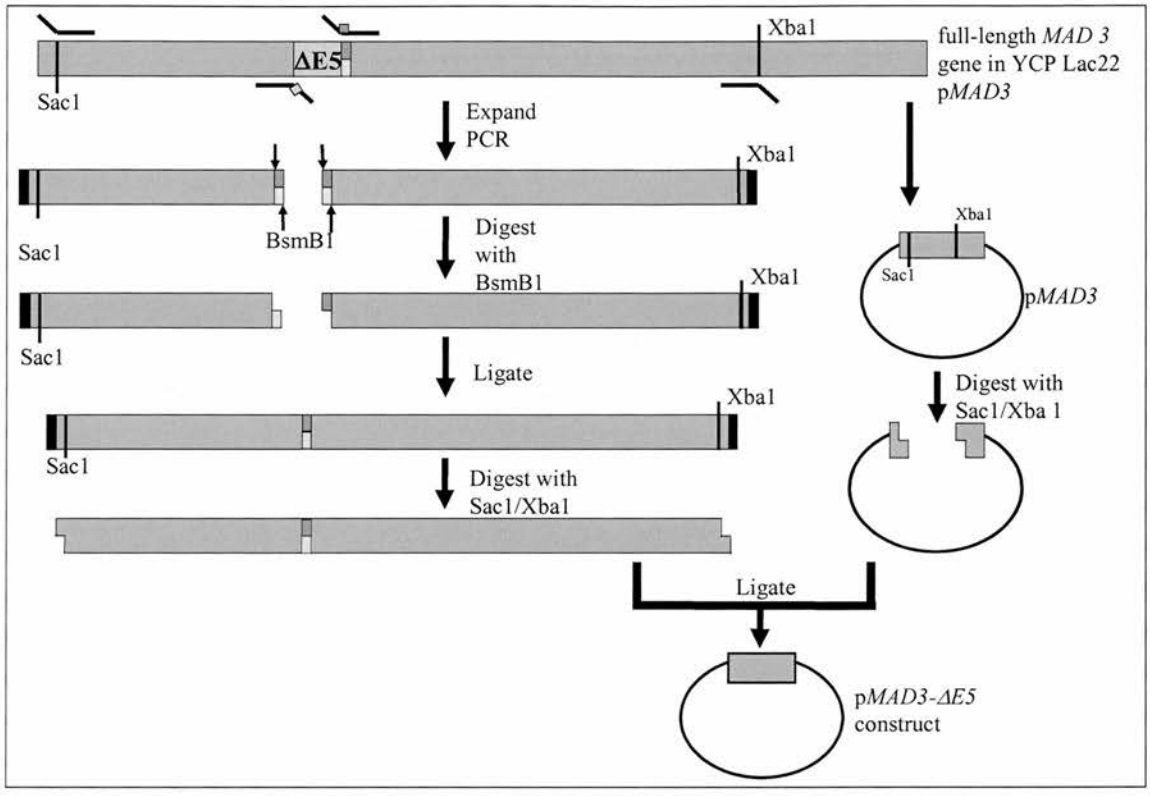

Figure 3.3 Cloning Strategy for Sc pMAD3 ΔE5

The newly constructed deletion section and the full-length construct were digested with the same enzymes and the vector backbone was gel purified. These were then ligated together to produce the ΔE5 construct. A similar strategy was used for p*BUB1-ΔE5* using restriction enzymes EcoR1 and Kpn1. The enzymes chosen were specific single cutters within the coding sequence flanking the area of ΔE5.

Positive transformants were isolated and analysed by colony PCR and initially visualised on agarose gels before sequencing. Positive transformants indicated by sequencing of the colony PCR reactions were grown on a small scale, DNA was isolated by miniprep and the recombinant gene was fully sequenced to ensure the deletion site formed correctly and the DNA sequence was error free. A comparison of the sequence of the recombinant genes and the full-length constructs are shown in figure 3.4.

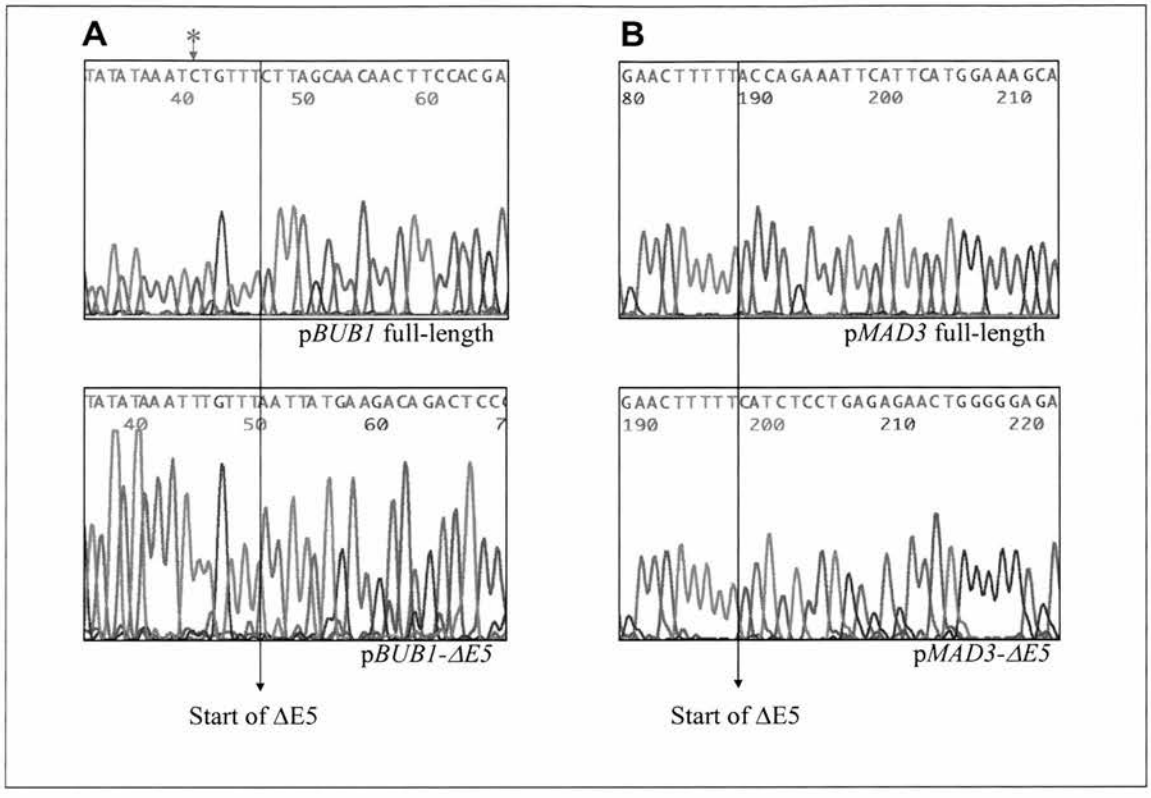

Figure 3.4 Sequencing of the Recombinant ΔE5 plasmids

A Sequencing of the S. cerevisiae *BUB1* full-length and ΔE5 plasmids showing the start site of the deletion, indicated by the black arrow. The red asterisk indicates a silent variant acquired in the *BUB1* full-length coding sequence during culture and preparation. This variation was not present in the original plasmid stock and hence is not seen in the deletion. However as it is a silent variant it would be unlikely to affect protein function.

B Sequencing of the equivalent *MAD3* full-length and ΔE5 constructs for comparison of the sequence following the deletion.

3.3.4 Generation of *MAD3 ΔE5* Over-expression Construct

The recombinant YCPLac22 *ΔE5* plasmids were used to generate over-expression constructs containing the *MAD3* and *BUB1 ΔE5* genes. The recombinant *MAD3 ΔE5* gene was excised from the p*MAD3-ΔE5* vector by digestion with restriction enzymes BamH1 and EcoR1 to produce a 1363 base pair deletion fragment. The fragment was ligated into over-expression vector p423MET digested with the same enzymes, the ligation mix was transformed into *E.coli* and positive transformants were isolated and checked by fully sequencing as before. This cloning strategy is summarised in figure 3.5.

pMET:BUB1-ΔE5 was generated with the help of Dr Kevin Hardwick from p*BUB1-ΔE5*.

Diagrams of all the constructs generated are shown in figure 3.6.

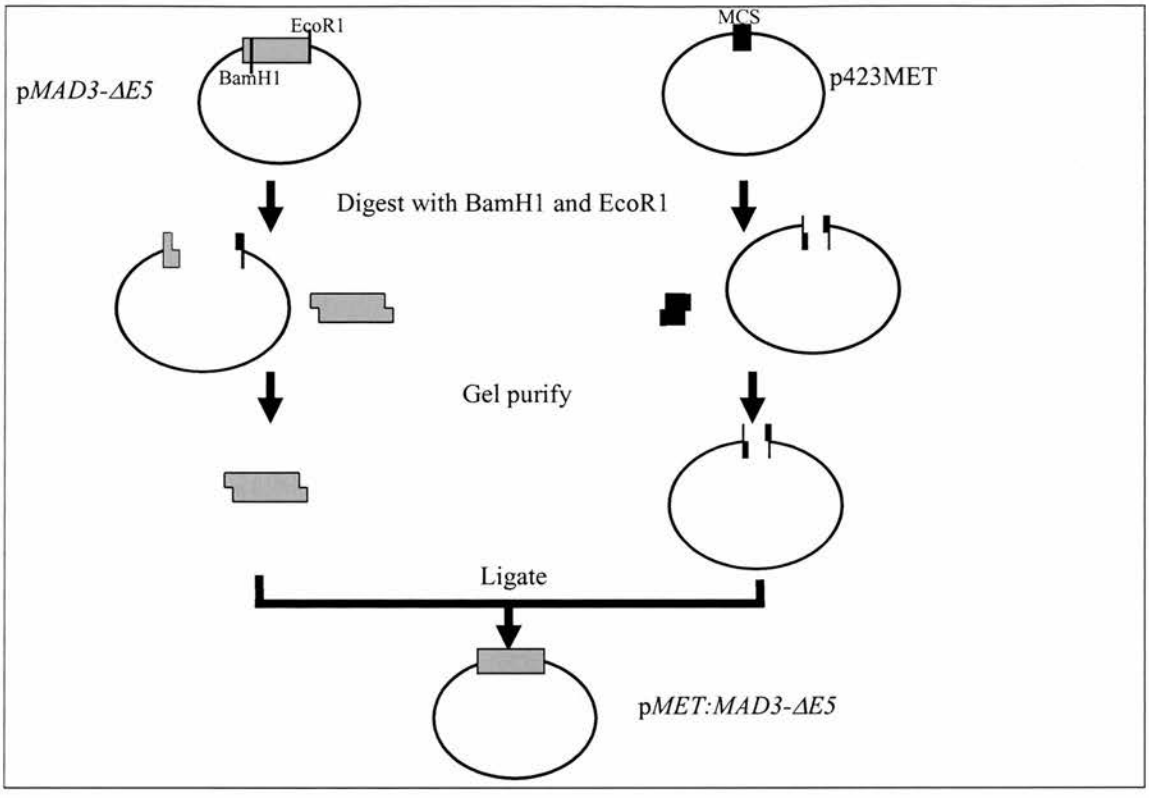

Figure 3.5 Cloning Strategy for the MAD3 ΔE5 over-expression construct

The MAD3-ΔE5 over-expression construct was generated using restriction digestion and ligation techniques as shown.

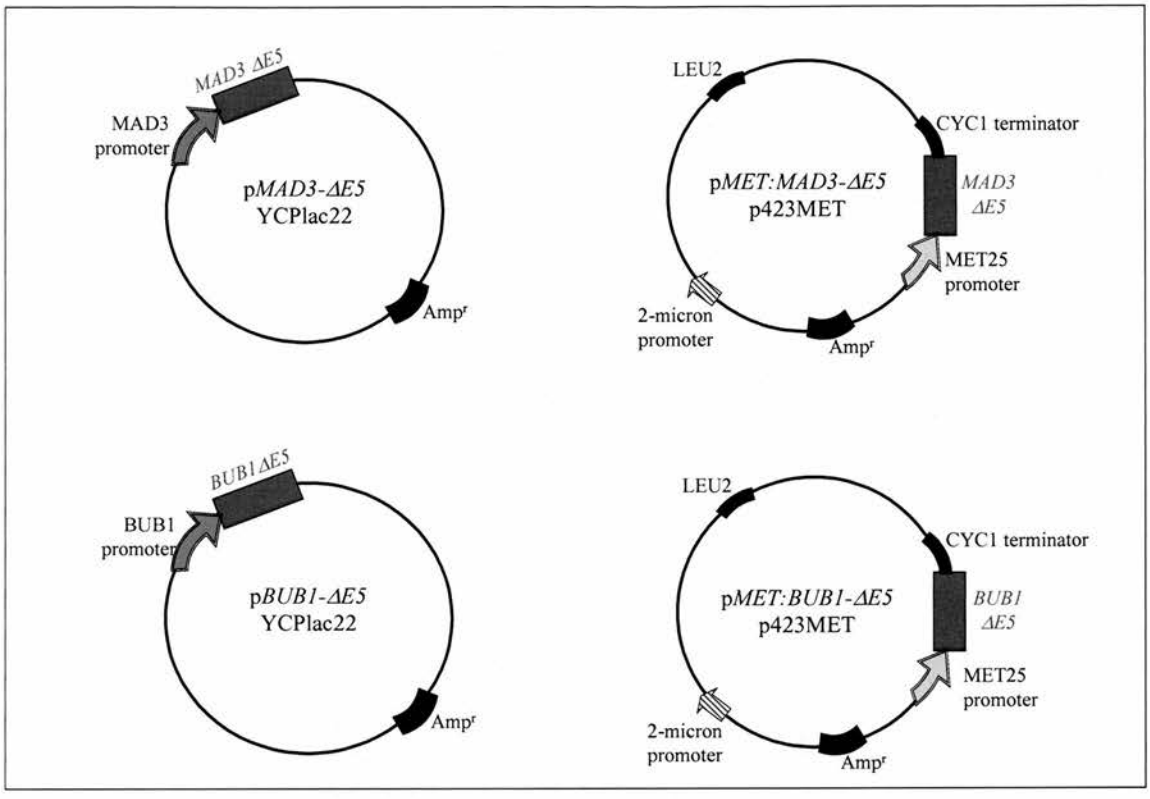

Figure 3.6 Diagrams of the ΔE5 constructs generated in this study

3.4 Discussion

The deletion ΔE5 identified in aneuploid colorectal tumours removed a domain of BUB1 related proteins conserved from yeast to man. Hardwick et al and Cahill et al have both published alignments of BUBR1 with homologues in other species. Cahill et al initially identified BUBR1 as a BUB1 related protein and aligned homologous regions of the protein with human BUB1 and *S.cerevisiae* Bub1p (Cahill et al., 1998). Later Hardwick et al repeated the alignment to include *S.cerevisiae* Mad3p and S.pombe Bub1p (Hardwick et al., 2000). These alignments are slightly different. To establish the area homologous to that removed by ΔE5 in yeast Mad3p and Bub1p, I used each alignment in turn to identify the start point of *BUBR1ΔE5* and the BUB1 equivalent V400 as indicated in Figure 3.1. I examined those residues whose inclusion differed between the two alignments and decided to remove only those which were unconserved. This retained all the conserved amino acids whose deletion was predicted in only one of the two alignments. Specifically, the Cahill alignment states the deletion begins just after a Leucine residue in *S.cerevisiae* Bub1p. By marking the start of BUBR1ΔE5 after a WLKL motif on the Hardwick alignment we can see there is a discrepancy between these two predicted areas. Of the 5 residues between the two predicted start sites (IELFT in *S.cerevisiae* Mad3p), the Glutamic Acid (E) and the Leucine (L) are conserved between several species. Additionally the Phenylalanine (F) is conserved between *S.cerevisiae* Bub1p and Mad3p. Thus these residues were not deleted in the constructs. However, the Threonine (T) residue is not conserved in any of the other species and thus was removed in the deleted portion. Thus the starts of the ΔE5 deletions are one amino acid upstream of that predicted by Cahill et al.

Most recently Millband and Hardwick have aligned Mad3p and Bub1p homologues from many species including S.pombe, *S.cerevisiae*, mouse, human, Xenopus and Aspergillus (Millband and Hardwick, 2002). This alignment is more extensive and is largely similar to the previous Hardwick alignment. The threonine upstream of the ΔE5 start site predicted by the Cahill alignment is unconserved in all these additional species. However, the positions of some of the homologues are

slightly different. It seems that the presence of a gap in the homologues of higher eukaryotes leads to increasing variation in alignments as orthologues from more species are included. Thus the exact position of the ΔE5 region may be altered as homologues of BUB1 and BUBR1 are identified in other organisms and as more alignments become available.

The deletions were constructed in frame, as described earlier. As the genomic change associated with the deletion has not been identified and the size of the protein produced is also unknown we have been unable to ascertain whether the protein is truncated due to a frameshift effect after the deletion. Additionally, ΔE5 removes an entire exon and therefore may be due to an alternative splicing effect and this may be predicted to retain the sequence in frame. Thus 198 base pairs were removed in ΔE5 corresponding to 66 amino acids and preserving the frame of the coding sequence.

These measures represent prudence in the construction of the ΔE5 constructs, as truncation mutants have been shown to abrogate spindle checkpoint function and those removing large numbers of conserved amino acids would be predicted to have a similar detrimental effect (Hardwick et al., 2000; Warren et al., 2002).

Although the full relevance of the deletion constructed in yeast would be clearer with greater knowledge of the behaviour of ΔE5 in tumours these constructs can be used to give a clearer understanding of the possible functional consequences of the deletion. The nature of the ΔE5 mutation in tumours is being further investigated using long range PCR of genomic DNA to search for the genomic change in the tumours which cause the deletion of exon 5 in the messenger RNA and this work has so far been inconclusive. Sequencing of the entire 13 kilobases of intronic sequence surrounding exon 5 is also in progress to address our understanding of the deletion at the genomic level. In addition we have recently generated antibodies to the first 25 amino acids of the N terminal of BUB1 and BUBR1 and these could be used to establish the size of the mutant BUBR1 protein and any truncation effect.

Two cloning strategies were used to generate constructs described in this chapter; one using PCR based techniques and the other using restriction digestion and ligation techniques. The cloning strategies used were both fairly successful, although isolation of positive clones typically took several attempts. The PCR based method

used to construct p*MAD3-ΔE5* and p*BUB1-ΔE5* was more troublesome than that used for the over-expression constructs and at least 5 attempts were required to yield positive clones. I briefly attempted other PCR based techniques such as overlapping PCR but this was unsuccessful despite 3 attempts and the recombinant ΔE5 constructs were eventually created using the method described.

Once generated, the clones were fully sequenced to verify the deletion and to ensure the remainder of the coding sequence was error free. This identified several variants in the sequences. The p*MAD3-ΔE5* plasmid was found to contain 3 single base changes including one nonsense mutation predicted to cause truncation of Mad3p to just 60 amino acids. These errors were also present in the full-length clone stock. The errors were removed using restriction digestion of fragments of the ΔE5 plasmid and a new error free full-length plasmid and ligation of appropriate sections. The p*MAD3-ΔE5* plasmid used in the subsequent functional assays was error free.

Two variations were identified in the p*BUB1-ΔE5* sequencing out with the deletion site which did not appear to be present in the wild type construct. Unfortunately numerous attempts to separate the ΔE5 deletion from these variants, using similar digestion and ligation techniques as those used for p*MAD3-ΔE5*, were unsuccessful. However, after discussions with Dr Hardwick it was concluded that the nature of these alterations suggested they were unlikely to significantly affect checkpoint function and thus would not interfere with functional assays on ΔE5. The first of these was AAC→AGC converting an asparagine to a serine at amino acid 334 in CD2. According to homology alignments this residue is actually a conserved serine in Mad3p, S. pombe Bub1p and in human BUB1 and BUBR1 suggesting it will have no effect on protein function. An ATA→ATG converted an isoleucine to a methionine at amino acid 293, which is a conservative change, and an ACA→ACG had no effect on the threonine residue 268. These are unlikely to have a significant effect on protein function as they both occur in unconserved regions of the protein.

Sequencing of the full-length *BUB1* clone after p*BUB1-ΔE5* had been generated revealed a single base alteration which had not been present in either the original stock nor in the ΔE5 construct made. This was a silent change at nucleotide 349 converting a TTT codon to a TCT, still encoding Phenylalanine. The high number of

variants seen in the sequencing results was surprising as high fidelity Expand Taq enzyme was used for all the PCRs. We hypothesised it may be a result of the type of electrocompetent *E.coli* cells which were used, TOP 10 cells. These are very efficient cells for transformations but do not have any measures in place to prevent rearrangements of carrier plasmids. This may have been a factor in the incorporation of incorrect nucleotides in the numerous cell division cycles during preparation of *E.coli* cultures for isolation of plasmid DNA and for glycerol stocks. Subsequent cloning experiments utilised SURE® cells, which are engineered to carry inactivating mutations in the pathways catalysing gene rearrangements in an attempt to reduce the number of variants created.

The constructs generated by the work in this chapter were vital in functional assays to determine the effect of ΔE5 on spindle checkpoint function. The constructs in which *MAD3* and *BUB1 ΔE5* were under the control of their wild type promoters were used in strains null for either *BUB1* or *MAD3* in assays investigating their affect on checkpoint function, chromosomal instability and the generation of aneuploidy. The over-expression constructs were used to investigate the effect of ΔE5 on checkpoint protein interactions and spindle checkpoint complexes.

The results of these functional analyses are described in chapters 4 and 5.

Chapter 4: ΔE5 Abrogates Spindle Checkpoint Function and Confers a Chromosome Loss Phenotype in *S.cerevisiae*

4.1 Introduction

The overall aim of this chapter was to determine the effect of ΔE5 on spindle checkpoint function using the constructs described in chapter 3, p*MAD3-ΔE5* and p*BUB1-ΔE5*.

4.1.1 Spindle Checkpoint Mutants Exhibit a Marked Sensitivity to Microtubule Poisons

Benomyl (Methyl 1-(butylcarbamoyl)-2-benzimidazolecarbamate) is an inhibitor of microtubule polymerization. Treatment with microtubule poisons at concentrations of 10-15μg/ml considerably lengthens the cell cycle in wild type cells in which the spindle checkpoint is functional, due to a slowed assembly of the mitotic microtubule spindle and activation of the spindle checkpoint. Spindle checkpoint mutants do not exhibit this delay and exit mitosis with incomplete spindles leading to aberrant chromosome segregation, the accumulation of lethal chromosome defects and cell death. Thus yeast spindle checkpoint mutants show a decreased growth ability on media containing benomyl and the *mad* and *bub* null mutants were initially identified through this marked sensitivity (Li and Murray, 1991; Hoyt et al., 1991).

Recently the benomyl sensitivity of *bub* and *mad* null mutants have been directly compared. Cells containing mutations in *BUB1* and *BUB3* showed an order of magnitude greater benomyl sensitivity than *mad1*, *mad2* or *mad3* mutants. This indicates that the checkpoint proteins contribute different roles to the maintenance of cell viability via the spindle checkpoint and may also reflect other mitosis-related functions, in kinetochore structure or cell cycle progression for example (Warren et al., 2002).

Complementation of the null *bub* and *mad* strains with exogenously expressed full-length Bub1p or Mad3p rescues this sensitivity phenotype by restoring checkpoint function. The empty YCPLac22 vector does not achieve this rescue, acting as a negative control (Warren et al., 2002). These full-length constructs and the empty vector can therefore be used as positive and negative controls in this characteristic spindle checkpoint assay to assess spindle checkpoint function in the ΔE5 mutants.

This assay has previously been used to clarify function and important regions of spindle checkpoint proteins by mutating conserved residues and domains and testing their benomyl sensitivity. Specifically MAD3 mutants replacing the conserved GIGS domain with four alanine residues or the conserved Glutamic acid residue 382 to a lysine, both show marked benomyl sensitivity. In the GIGS mutants this is equivalent to that seen in a null mutant and in the E382K mutant it is slightly less severe. This indicates the relative contributions of these conserved amino acids to Mad3p checkpoint function (Hardwick et al., 2000).

Thus this assay was essential to primarily determine whether the ΔE5 deletion conveys a spindle checkpoint defect and disrupts the function of Mad3p and Bub1p in the checkpoint.

However, benomyl sensitivity may also represent defects in tubulin and other microtubule spindle related components, perturbed microtubule dynamics and inappropriate cell cycle progression (Stearns et al., 1990; Stearns and Botstein, 1988; Hoyt et al., 1990).

Thus further assays were required to confirm that the defects observed were related to abrogation of the checkpoint and not a result of disruption of additional protein functions of Bub1p and Mad3p.

4.1.2 Null *mad3* Mutants Initially Divide Faster in Microcolony Assays

Li and Murray initially identified the Madp proteins through the isolation of benomyl sensitive mutant cell populations. However, as stated above, this would

include structural microtubule mutants as well as those involved in feedback control (Li and Murray, 1991). To distinguish between these structural mutants and mutants with defective spindle checkpoints, microcolony assays were used. These assays involve the isolation of individual cells and monitoring their growth on benomyl containing solid media over a 12 hour period. Wild type cells divide slowly initially before undergoing adaptation to the microtubule poison allowing an increased rate of growth. The mutants harboring defects in spindle checkpoint control initially divide more rapidly due to a bypass of checkpoint arrest but later accumulate lethal defects slowing their growth rate and resulting in the limited viability seen in the benomyl sensitivity assay. Cells harboring mutations in structural microtubule components such as *tub* and *cin* mutants behave very differently in microtubule assays, budding only once and arresting as a single large bud. This is of particular importance as some of the spindle checkpoint proteins are believed to have additional microtubule related functions which may contribute to the benomyl sensitivity phenotypes of mutants. Again the characteristic null *mad3* phenotype can be rescued by plasmid expression of full-length Mad3p but not by expression of the equivalent empty vector.

Thus by exogenously expressing the Mad3ΔE5 protein in the *mad3* null strain I have assessed the functional effect of ΔE5 on Mad3p spindle checkpoint function. In addition the microcolony assay will distinguish those mutations effecting checkpoint function from those effecting microtubule structure and clarify the effect of ΔE5. This assay was important to distinguish spindle checkpoint disruption by ΔE5 from an effect on microtubule structure.

This microcolony assay is not suitable for examining the effect of ΔE5 on spindle checkpoint function in *bub1* mutants as they are hypersensitive to benomyl compared to *mad3* mutants. This results in a high level of cell death in *bub1* mutants after only a few hours even at low concentrations of benomyl (see figure 4.11 and appendix 5). Thus an alternative liquid culture assay was used to investigate the spindle checkpoint affect of ΔE5 on Bub1p function.

4.1.3 Null *bub1* Mutants Show a Characteristic Budding Phenotype in Liquid Culture Assays

This liquid culture assay has been used as an alternative to the microcolony assays described above to examine the effect of BUB1 mutations on spindle checkpoint function (Warren et al., 2002). In this assay, synchronized cultures are grown in liquid media containing nocodazole, a benomyl related compound used as an alternative in liquid media due to technical considerations. The resulting cell populations are vigorously sonicated to separate cell clusters and examined microscopically. Almost 100% of wild type cells arrest at mitosis as large budded cells whereas up to 60-70% of *bub1* mutants progress through mitosis unperturbed to produce at least one further bud showing a characteristic multi-budded phenotype (Hoyt et al., 1991).

Warren et al effectively used this assay to show that truncating mutants containing only the first 367 amino acids of Bub1p displayed a similar multi-budded phenotype to a *bub1* null mutant. Mutants containing the N terminal 608 amino acids, amino acids 211-1021, a K733R substitution and an E333K substitution also exhibited multi-budded phenotypes of varying severity, indicating the important residues of Bub1p involved in spindle checkpoint function.

To summarise, these experiments suggest amino acids 1-608 are sufficient to maintain Bub1p spindle checkpoint function, the kinase domain of Bub1p is not required and amino acids 211-367 may be particularly crucial. The phosphorylation of E333 is also thought to be important to checkpoint function whereas the K733R substitution is likely to disrupt function due to a destabilizing effect on the Bub1p protein (Warren et al., 2002).

Thus null *bub1* mutant strains can be used in rescue experiments as the multi-budded phenotype can be rescued by addition of the full-length BUB1 plasmid but not by the empty vector. The liquid assay will be used to test the ability of the BUB1ΔE5 to rescue the null multi-budded phenotype, indicating its influence on spindle checkpoint function and identifying if any defects associated with benomyl sensitivity are also associated with multi-budded phenotypes indicative of aberrant spindle checkpoint function in *BUB1ΔE5*.

4.1.4 Spindle Checkpoint Mutants Exhibit Increased Rates of Chromosome Loss

The association of the ΔE5 mutations with aneuploid tumours raises questions about the effect of the mutation on chromsome stability. Chromosome loss phenotypes have previously been associated with *mad1*, *mad2* and *mad3* spindle checkpoint mutants in budding yeast when challenged with microtubule poisons (Li and Murray, 1991). *bub1* and *mad2* mutants also exhibit chromosome loss in the absence of spindle damage (Pangilinan and Spencer, 1996) as do *S. pombe bub1* mutants (Bernard et al., 1998), *Drosophila bub1* mutants (Basu et al., 1999) and *C. elegans mdf-1* and *mdf-2* mutants (Kitagawa and Rose, 1999).

Specific chromosome loss assays have been devised to efficiently test this phenotype. The *S.cerevisiae* chromosome loss assay utilizes the $Ade2_{ochre}$ strain which harbors a mutation in the 5AIR carboxylase enzyme involved in the purine biosynthesis pathway. Cells thus accumulate a red pigmented intermediate, resulting in colonies which are red in colour. Addition of a SUP11 minichromosome encoding the ochre-suppressing tRNA allele ade2-101 restores the enzyme and leads to white colonies. Chromosome segregation defects resulting in mis-segregation of the minichromosome are observed as reversion of the cells to red. Thus rates of chromosome loss can be calculated by examining the red-white sectoring phenotype exhibited. The rate of chromosome loss is standardized against the number of cell divisions by scoring the number of colonies which are at least half sectored, representing loss of the minichromosome at the first division, as a proportion of the total number of colonies counted. Red colonies are not included in the total count, as they have undergone a chromosome loss event prior to the start of the assay at plating (Hieter et al., 1985; Spencer et al., 1990). This assay is summarized in Figure 4.1.

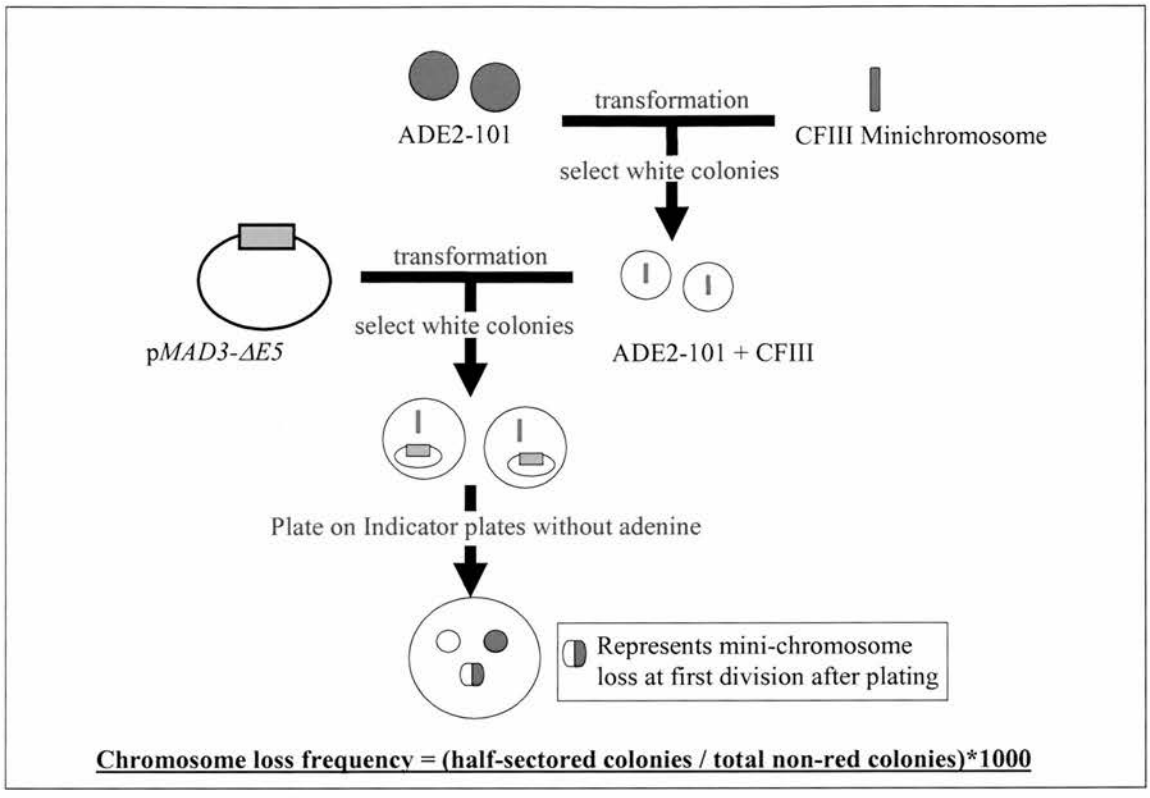

Figure 4.1 Colour colony chromosome loss assay

The chromosome loss assay uses the ADE2-101 strain which harbours an ochre mutation in ADE2 gene producing pigmented red colonies. Transformation of this strain with the CFIII ochre suppressing minichromosome restores the purine biosynthesis pathway producing white colonies.

This strain is transformed with test plasmids and plated onto indicator plates lacking adenine to activate the purine biosynthesis pathway. Any cell in which the mini-chromosome has been lost due to mis-segregation appear red. For each test strain, the number of half sectored colonies which are at least half red and the total number of colonies which are not entirely red are scored. Rates of chromosome loss in units of losses per thousand divisions are calculated as shown.

In this assay null *bub1* and *mad3* mutants exhibit increased rates of chromosome loss compared to wild type strains. Supplementation of the null strains with the appropriate full-length gene construct restores checkpoint function and reduces chromosome loss rates to wild type levels. Addition of the empty vector does not achieve this rescue. Thus using the empty YCPLac22 cassette as a negative control and the full-length p*MAD3* and p*BUB1* vectors as positive controls, I have investigated the ability of p*MAD3-ΔE5* and p*BUB1-ΔE5* to restore checkpoint function to null strains and rescue this phenotype. This addresses the ability of the ΔE5 proteins to function in the spindle checkpoint and whether the mutations can be responsible for mis-segregation of chromosomes.

Warren et al have shown that chromosome loss rates vary between different spindle checkpoint mutants and that this correlates with the benomyl sensitivity phenotype. Thus the rates of chromosome loss are indicative of mis-segregation due to aberrant spindle checkpoint function. Additionally, they examined the effects of deletions and mutations in *BUB1* on the chromosome loss phenotype. They report increased rates of chromosome loss for all the mutants analysed although the degree of increase varied between the mutants and suggested functional domains at both the N and C termini of Bub1p are important in chromosome segregation (Warren et al., 2002).

This assay is of particular interest for *BUBR1ΔE5* and the equivalent mutation found by Cahill et al, *BUB1 V400* due to their involvement in colon cancers. Current hypotheses suggest aneuploidy in tumours is generated by errors in chromosome segregation so an assay measuring the frequency of such mis-segregation events in cells harbouring tumour associated mutations will help to clarify both the contribution of these mutations to tumourigenesis and ultimately the mechanism by which such an effect may be mediated. This may also provide an assay system for evaluating the contribution of tumour associated variants identified in the future.

These are all well established assays in yeast which have been used to assess the effect of mutations and truncations on the spindle checkpoint function of the Madp and Bubp proteins. Although most of these studies have been involved in isolating

important domains of spindle checkpoint proteins and deciphering their specific functions, the principals can be easily applied to cancer associated mutations.

Thus the results described in this chapter describe the use of the ΔE5 constructs in these assays to investigate their effect on spindle checkpoint function and chromosome segregation, and to ascertain whether the ΔE5 mutant phenotypes are consistent with a role in the generation of aneuploidy and ultimately, tumourigenesis.

4.2 Methodological Overview

4.2.1 Transformation into Null Strains

The YCPLac22 empty vector, full-length p*MAD3* and p*MAD3-ΔE5* constructs were each transformed into the *mad3* null mutant strain YRJ111 via the lithium acetate procedure as described in 2.7.6. Similarly YCPLac22, p*BUB1* and p*BUB1-ΔE5* were transformed into the *bub1* null mutant strain YRJ112. Positive transformants were selected on media lacking tryptophan and mixed colonies were streaked onto new selective plates before use in the described assays. Each assay was performed on at least 3 independent occasions, using a new transformation for each repetition.

The YCPLac22 and full-length constructs were used as negative and positive controls respectively. Additionally the wild type strain (KH34) and untransformed null strains (YRJ111 and YRJ 112) were included in at least one of the repetitions to validate the controls.

4.2.2 Benomyl Sensitivity Assays

Benomyl sensitivity assays were carried out as described in 2.7.12. The assays were generally performed in duplicate with two mixed populations assayed per transformation. The sensitivity of the transformants were tested at several concentrations of benomyl, typically 10, 12.5 and 15μg/ml and also on benomyl free media to ascertain their growth under unchallenged conditions. Two plates were prepared for each benomyl concentration.

4.2.3 Microcolony Assays

Microcolony assays were performed on the *mad3* + p*MAD3*, p*MAD3-ΔE5* and YCPLac22 transformants as described in 2.7.13 (Li and Murray, 1991).

4.2.4 Liquid Culture Assays

Liquid culture assays were performed on the *bub*1 + p*BUB1*, p*BUB1-ΔE5* and YCPLac22 transformants as described in 2.7.14 (Hoyt et al., 1991).

4.2.5 Chromosome Loss Assays

Chromosome loss assays were performed using both the MAD3 and BUB1 transformants as described in 2.7.15 (Hieter et al., 1985; Spencer et al., 1990). Overnight cultures were grown in selective media lacking tryptophan to select for the YCPLac22 plasmids and uracil to select for the minichromosome. The cultures were then diluted to an OD of 0.3 and grown in non-selective media for 4 hours before further dilution, typically 1 in 2500 and plating on indicator plates lacking adenine.

4.2.6 Calculations and Statistics

For each of the assays described, three experimental repetitions were performed. Due to the large volume of data acquired, the data presented in this chapter is representative of that observed in each of the repetitions. Further details of individual experiments are presented in the appendix.

In the microcolony assays, the mean number of cells and buds per microcolony was calculated for 25 cells for each experiment. The mean of the three repetitions has been calculated and this data is displayed graphically.

In the liquid culture assays the proportion of multi-budded cells with more than 2 buds was calculated as a percentage of the total number of a 200-cell population. Again the mean of the three repetitions is presented here graphically with variation indicated as error bars showing the standard deviation between the individual repetitions. The 200 cell counts (not percentages) for each repetition were pooled and the total numbers of multi-budded cells observed in the 600-cell populations were compared in pairs as shown in the table below.

In the chromosome loss assays, the sample size (total number of colonies) for each transformant population and each experimental repetition varies. Thus the original counts of half sectored/non-red colonies are shown to indicate the sample size. The chromosome loss rate per thousand divisions was calculated using:

$$\text{Chromosome loss rate} = \frac{\text{number half sectored colonies}}{\text{total number non-red colonies}} * 1000$$

These figures were calculated for each of the individual experiments and for the total of the three repetitions as an alternative to the standard method of calculating the mean to allow for the differences in sample size between repetitions. This total chromosome loss rate is presented in the figures.

Both the liquid culture assays and the chromosome loss assays were analysed statistically in paired data sets (e.g. vector compared to deletion).

Sample	No. half-sectored colonies	No. non-red colonies	Total number colonies
Vector	a	n_1-a	n_1
DeletionΔE5	c_1-a	n_2-(c_1-a)	n_2
Total	c_1	c_2	N

The expected value for **a** was calculated by the product of the relevant row and column totals divided by the total sample size. For example the expected number of half-sectored colonies for the Vector population would be :-

$$\text{Expected} = \frac{c_1 * n_1}{N}$$

Each of the three experimental repetitions for the pair were analysed and totalled according to the Mantel-Haenszel analysis :-

$$\text{Mantel-Haenszel statistic } t = \frac{\Sigma\text{Observed} - \Sigma\text{ Expected}}{\sqrt{\Sigma}\text{ Variance}}$$

Where variance is calculated by:-

$$\text{Var} = \frac{n_1 * n_2 * c_1 * c_2}{N^2 (N-1)}$$

This test is similar to a chi-squared analysis but is more powerful as it also considers the variation between the three experimental repetitions and the direction of the differences observed between populations. If all the experimental repetitions show differences in the same direction (e.g. the proportion of half-sectored colonies in the vector is always higher than in the deletion) the t^2 value should equal the value obtained by adding the chi-squared values from the three individual experiments together. The probabilities associated with the t values obtained were calculated using Minitab.

Chi-squared was used to analyse the data within individual experimental repetitions for chromosome loss assays and liquid culture assays and this is presented in the appendices.

Chi-squared analysis was performed at 1 degree of freedom using the formula below:

$$\chi^2 = \Sigma \frac{(\text{Observed} - \text{Expected})^2}{\text{Expected}}$$

For Chi-squared statistical analyses the probability of statistical significance (p values) was calculated using Microsoft Excel. P values of less than 0.05 were considered statistically significant (5% confidence interval) unless otherwise stated.

4.3 Results

The results presented here are representative of at least three duplicate experiments using fresh transformants. The statistical analysis have generally been carried out on the three experimental repetitions or occasionally the mean of the three data sets where stated. The data presented generally shows the cumulative data from the three repetitions or the mean where stated. Further data from individual experiments and statistical analysis of these is presented in the appendix at the end of this thesis.

4.3.1 MAD3ΔE5 Mutants are as Benomyl Sensitive as Null *mad3* Mutants

To address the hypothesis that ΔE5 abrogated the function of Mad3p in the spindle checkpoint, the ability of p*MAD3-ΔE5* to rescue the benomyl sensitivity phenotype associated with the null *mad3* mutant was investigated. Figure 4.2A shows the benomyl sensitivity shown by the null *mad3* mutant strain, YRJ111, as indicated by the reduction in yeast colony size and abundance compared with the wild type KH34 strain. This is due to the accumulation of lethal chromosome defects in a proportion of the null cells. The mutants are more sensitive to higher concentrations of benomyl. The YPD plates without benomyl act as a control to ensure any reduced viability on the benomyl plates is not due to an intrinsic growth defect.

Figure 4.2B shows the phenotypes of the null *mad3* strain separately transformed with either the empty YCPLac22 vector, p*MAD3-ΔE5* or the full-length construct p*MAD3*. A sensitivity equivalent to that in the null mutant is seen in the YCPLac22 transformant, acting as a negative control. The addition of the control full-length p*MAD3* construct rescues this sensitivity phenotype and restores viability to a level equivalent to the wild type strain.

The p*MAD3-ΔE5* transformant does not achieve this rescue and exhibits a similar limited viability on benomyl to that seen in the YCPLac22 transformant. The benomyl sensitivity of this mutant indicates the Mad3ΔE5p protein does not perform

its spindle checkpoint function as well as the full-length protein. Additionally there seems to be little difference in the sensitivity phenotype of the ΔE5 mutant and the empty vector suggesting the ΔE5 mutation removes all the checkpoint function of Mad3p, rendering it null. The experiment was repeated in triplicate with fresh transformants. The results shown in figure 4.2 show results from one experiment but are representative of all the results obtained and photographs of individual experimental repetitions are presented in Appendix 1 at the back of this thesis.

Thus the benomyl sensitivity assay suggests that the Mad3 ΔE5 mutation would abrogate the spindle checkpoint in cells which harbour it. This is consistent with the hypothesis that the ΔE5 variant could induce the chromosome mis-segregation and genetic instability phenotypes associated with tumourigenesis.

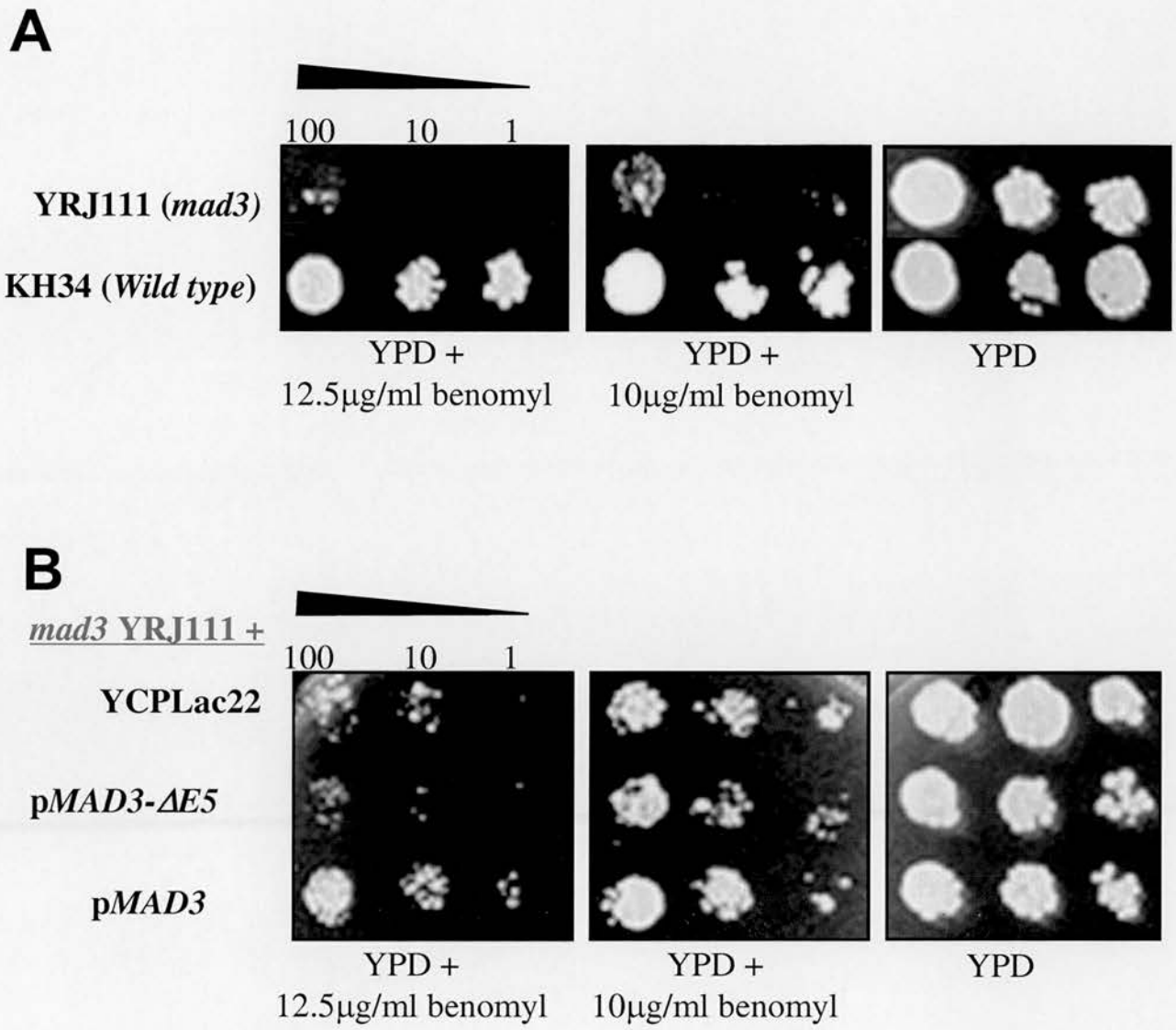

Figure 4.2: MAD3 benomyl sensitivity assay results

A The null *mad3* mutant YRJ111 shows a benomyl sensitivity phenotype which is not present in the wild type strain.
B This phenotype can be rescued by expression of the full-length protein from the p*MAD3* construct. The empty YCPLac22 vector does not achieve this rescue. The p*MAD3-ΔE5* construct cannot achieve this rescue either suggesting the Mad3ΔE5p protein cannot maintain checkpoint function.
The sensitivity is shown at 3 dilutions 100, 10 and 1 times.

4.3.2 BUB1ΔE5 Confers an Intermediate Benomyl Sensitivity Phenotype

The null *bub1* mutant shows a benomyl sensitivity phenotype much greater than that seen in the null *mad3* mutant. This is indicative of a greater role for Bub1p in the spindle checkpoint. Bub1p is also thought to be involved in additional mitotic functions such as in kinetochore assembly whose disruption may contribute to the benomyl sensitivity phenotype.

Figure 4.3A shows the extent of the benomyl sensitivity phenotype seen in the *bub1* mutant and 4.3B shows that this phenotype can be rescued by the full-length protein by exogenously expressing the p*BUB1* construct. The ScBUB1ΔE5 does not fully achieve this rescue although the benomyl sensitivity phenotype it confers is not as severe as that seen in the null mutant when transformed with the empty vector. This suggests the BUB1ΔE5 mutation does compromise the checkpoint although partial function is retained. This retained function of Bub1p could be mediated through the C terminal kinase domain which is absent in Mad3p, consistent with the differing phenotype conferred by MAD3ΔE5 and perhaps with additional functions of Bub1p in mitosis via its C terminus. This is particularly interesting as previous analysis of BUB1 mutants indicate the C-terminal domain is required for full protein function (Warren et al., 2002).

This may have relevance to the relatively small number of mutations in spindle checkpoint genes observed in tumours. Severe spindle checkpoint mutations that remove checkpoint function entirely may induce a similar lethality to that seen in *BUB3* and *MAD2* knockout mice. Thus only those mutations which compromise checkpoint function may avoid this lethality, while inducing the chromosome instability phenotype which drives tumourigenesis.

The set of results shown in these figures are representative of all the experimental repetitions and photographs of individual experiments are presented in appendix 2 at the back of this thesis.

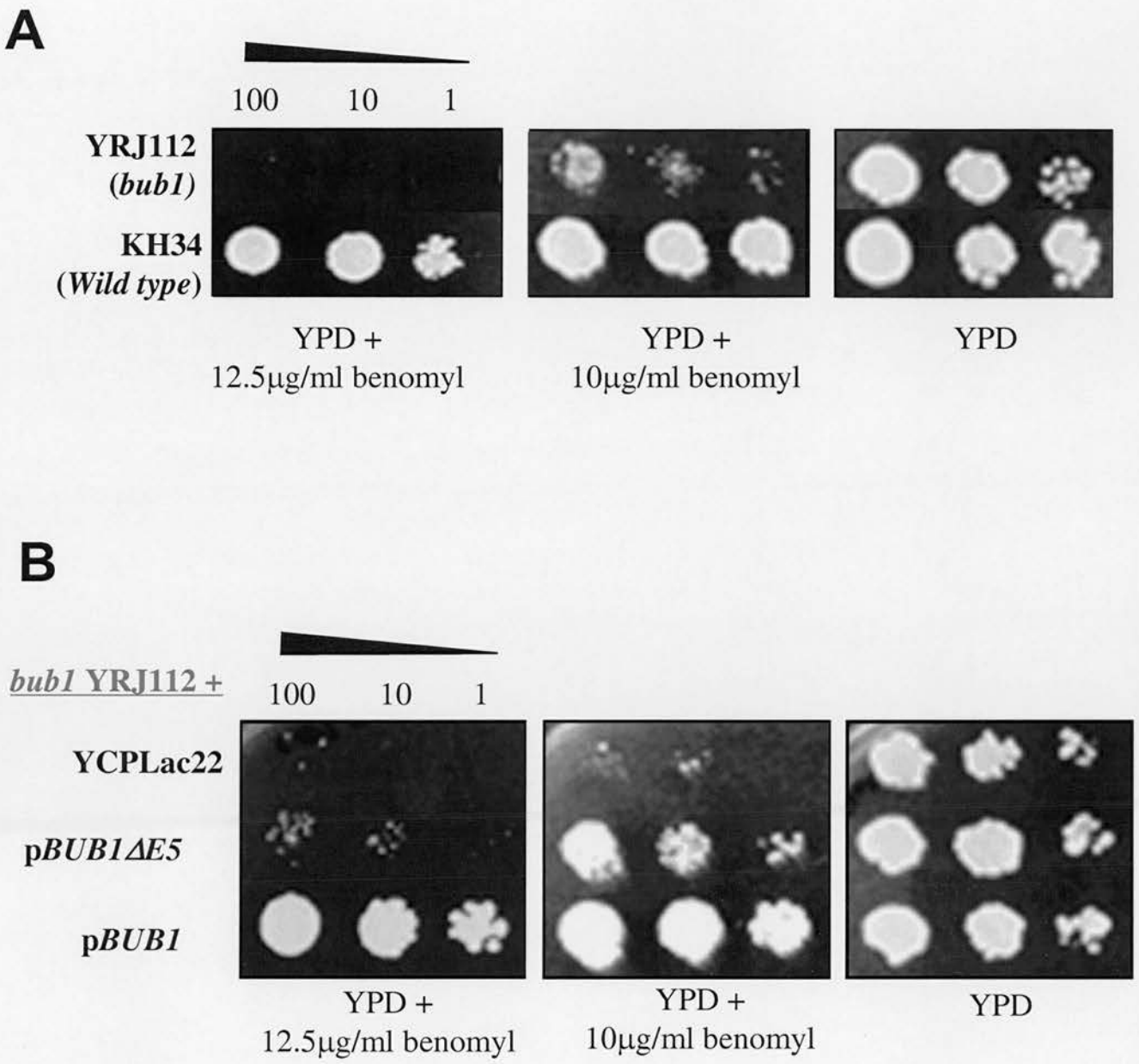

Figure 4.3: BUB1 benomyl sensitivity assay results

A The null *bub1* mutant YRJ112 shows a severe benomyl sensitivity phenotype which is not present in the wild type strain.
B This phenotype can be rescued by expression of the full-length protein from the p*BUB1* construct. The empty YCPLac22 vector does not achieve this rescue. The p*BUB1-ΔE5* construct cannot fully achieve this rescue but is less sensitive than the null strain suggesting the BUB1ΔE5 protein can support partial checkpoint function.

4.3.3 MAD3 ΔE5 Abolishes Spindle Checkpoint Function

As benomyl sensitivity phenotypes can be attributed to other mitosis related defects, such as in structural microtubule components, microcolony assays were used to determine whether the benomyl sensitivity of MAD3ΔE5 was due to a spindle checkpoint defect or to interference in other mitotic functions.

Microcolony assays were initially carried out on wild type, *mad3* null strain and a *cin1* microtubule structural mutant to verify the assay. The individual and mean numerical results of the three experimental repetitions are shown in table 4.1 and the mean of these experiments is displayed in figure 4.4. Further details of individual repetitions are shown in appendix 3.

Table 4.1 Microcolony assay optimisation

The data below shows the results from each of three experimental repetitions, A, B and C. Each repetition analysed the growth of 25 microcolonies of each strain over 12 hours and the mean number of cells per microcolony was calculated. The mean of these three experiments was calculated and is presented in figure 4.4.

Time	**Mean cell number per microcolony**											
(Hrs)	**Wild Type**				***cin1***				***mad3***			
	A	B	C	Mean	A	B	C	Mean	A	B	C	Mean
0	1	1	1	1	1	1	-	1	1	1	1	1
2	1.72	1.35	1.72	1.60	1.84	1.31	-	1.58	2.08	1.84	1.88	1.93
4	2.56	2.18	2.16	2.3	2	1.64	-	1.82	3.08	2.6	2.84	2.84
6	3.6	3.12	2.8	3.17	2	1.95	-	1.98	4.44	3.68	4	4.04
8	4.92	5.06	4.12	4.7	2	2	-	2	5.72	5.08	5.52	5.44
10	5.96	8.12	6.04	6.71	2.08	2	-	2.04	6.46	7.96	6.76	7.06
12	10.48	10.23	8.04	9.58	2.16	2.05	-	2.11	8.68	11.4	7.68	9.25

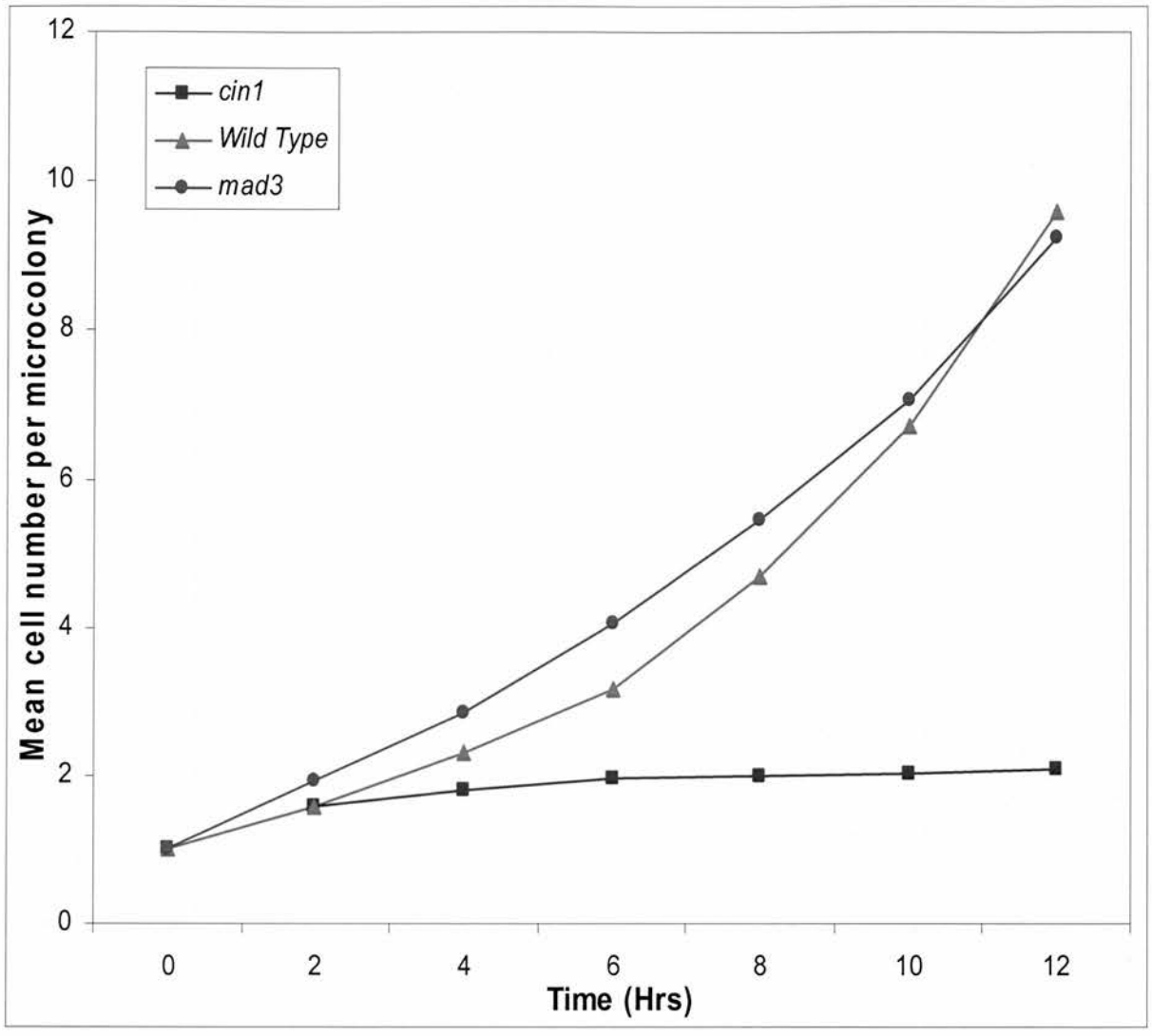

Figure 4.4: MAD3 microcolony assay optimisation

In microcolony assays, wild type strains initially arrest at the checkpoint showing a slow rate of growth. After prolonged treatment with microtubule poisons, the cells adapt showing an increased growth rate. Spindle checkpoint mutants such as *mad3* exhibit no initial arrest, dividing faster than wild type cells but accumulate lethal defects, resulting in reduced growth rate upon prolonged exposure. Structural mutants such as *cin1* arrest as a double bud due to defects in cytokinesis.

The mad3 null strain initially shows an increased rate of growth compared to wild type due to defective growth arrest at the spindle checkpoint. This increased growth rate is not sustainable in the mutant however as a proportion of the cells accumulate chromosomal abnormalities leading to cell lethality. Thus the rate of growth in the null mutant begins to fall. However, the wild type strain grows slowly initially due to the mitotic block at the spindle checkpoint but after several hours the cells adapt to the presence of the microtubule poison, perhaps through metabolism of the poison and thus are able to adapt to the block and continue to grow and divide. This results in an increased growth rate compared to the null strain upon prolonged exposure and also explains the greater viability of the wild type strain in the benomyl sensitivity assays.

The results of the three repetitions of the microcolony assay are shown in table 4.2 for the *mad3* null mutants transformed with the MAD3 constructs and the mean of these are presented in figure 4.5.

Table 4.2 Microcolony assay results

The data below shows the results from each of three experimental repetitions, A, B and C. Each repetition analysed the growth of 25 microcolonies of each transformant over 12 hours and the mean number of cells per microcolony was calculated. The mean of these three experiments was calculated and is presented in figure 4.5.

Time	**Mean cell number per microcolony**											
(Hrs)	***mad3* + YCPLac22**				***mad3*+ p*MAD3***				***mad3*+p*MAD3-ΔE5***			
	A	B	C	Mean	A	B	C	Mean	A	B	C	Mean
0	1	1	1	1	1	1	1	1	1	1	1	1
2	1.92	1	1.75	1.56	2.04	1.41	1.74	1.73	1.91	1.14	1.70	1.58
4	3.16	1.73	2.25	2.38	2.88	2	2.13	2.34	3	1.59	2.65	2.41
6	5.16	2.46	3.292	3.64	3.88	2.12	2.83	2.94	4.5	2.38	3.26	3.38
8	7.52	3.45	4.542	5.17	4.88	2.94	3.78	3.87	6.18	3.57	4.91	4.89
10	11.36	4.18	5.208	6.92	7.36	3.29	5.65	5.43	8.86	4.81	6.63	6.77
12	14.2	4.82	5.917	8.31	9.84	4.35	6.87	7.02	12.41	6.67	8.87	9.32

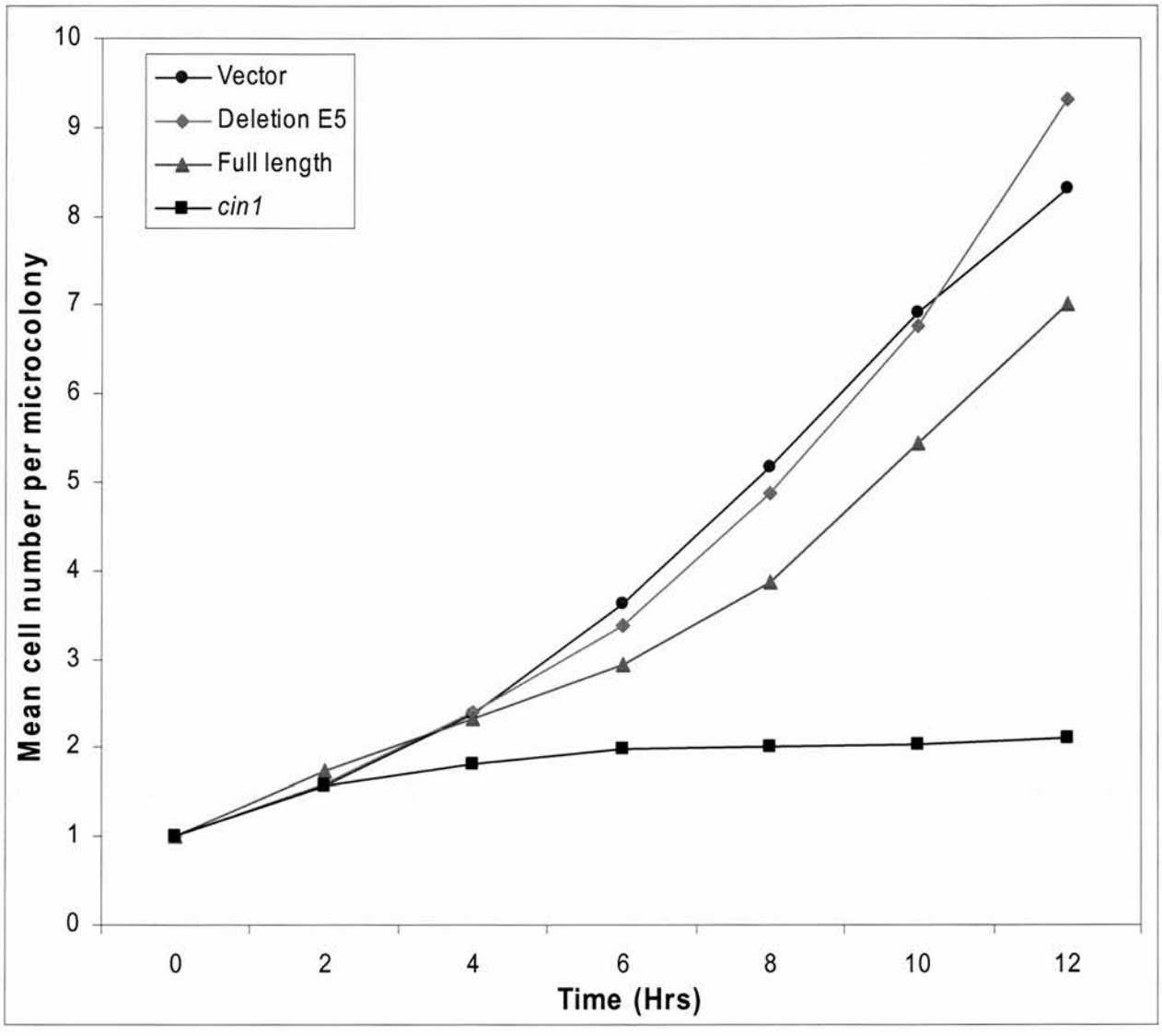

Figure 4.5: MAD3 microcolony assay results

The vector and full-length transformants show similar phenotypes to the null *mad3* and wild type strains respectively as shown in figure 4.4.The ΔE5 transformant shows a similar phenotype to the null strain indicative of a spindle checkpoint defect.

A comparable growth rate pattern to the null mutant is seen in the *mad3* YCPLac22 transformant. The full-length *mad3* transformant shows a similar pattern to the wild type strain, verifying these as controls. MAD3ΔE5 shows a growth pattern similar to the null strain consistent with a reduced spindle checkpoint function. MAD3ΔE5 shows an increased growth rate at the early time point of treatment in a similar way to the null strain but maintains this increased growth rate longer than the null mutants suggesting spindle checkpoint function may not be fully abolished and thus the cells may not accumulate lethal defects at such an increased rate. Alternatively this may reflect a general effect on cell growth.

The quantitative behaviour of the transformants is variable between experiments although the MAD3ΔE5 transformants behave similarly relative to the vector and full-length in each of the repetitions (see appendix 4). Therefore this assay is analysed qualitatively to compare the behaviour of the ΔE5 mutant with the behaviour of the control full-length, vector and structural mutant controls but statistical analysis has not been performed.

These variations in behaviour make it difficult to draw any firm conclusions about the proportion of MAD3 function which is abolished by ΔE5 but they consistently show a deleterious effect of ΔE5 on spindle checkpoint function. Significantly, the pattern of growth in the MAD3ΔE5 mutants does not resemble that of the structural microtubule mutant *cin1*. This suggests the benomyl sensitivity phenotype of the MAD3ΔE5 mutant is attributable to a defect in spindle checkpoint function and not any structural component of the spindle.

4.3.4 BUB1 ΔE5 Shows a Multi-budding Phenotype in Liquid Culture Assays, Consistent with Spindle Checkpoint Abrogation

The extreme benomyl sensitivity phenotype seen in the bub1 null mutants makes them unsuitable for analysis by microcolony assay. Many attempts were made to optimise this assay for use with the bub1 null mutants at various concentrations of benomyl (see appendix 5) but the behaviour of the mutants was inconsistent and eventually I decided an alternative assay was required to specifically analyse spindle checkpoint function in BUB1ΔE5.

Liquid culture assays were used as an alternative to analyse the budding behaviour of the *bub1* mutants after spindle checkpoint activation with nocodazole. Under normal growth conditions (zero hour time point) spindle checkpoint mutants will behave similarly to checkpoint functional cells, cycling from a single cell to a double bud and rarely showing a multi-budded phenotype as shown in figure 4.6. However, when challenged with microtubule poison for 6 hours or more wild type cells arrest at the spindle checkpoint as a single large budded cell. The null mutants transformed with full-length BUB1 acted comparably to wild type cells. However, spindle checkpoint mutants are unable to arrest at the metaphase to anaphase transition and thus continue through the checkpoint to produce at least one further bud exhibiting a multi budded phenotype. On analysis, the ΔE5 transformants also exhibit this multi-budded phenotype indicative of spindle checkpoint failure. Photographic examples of the characteristic phenotypes shown by the three transformed populations after 6 hours of nocodazole treatment are shown in figure 4.7. A similar phenotype is seen after 8 hours of nocodazole treatment (see figure 4.8).

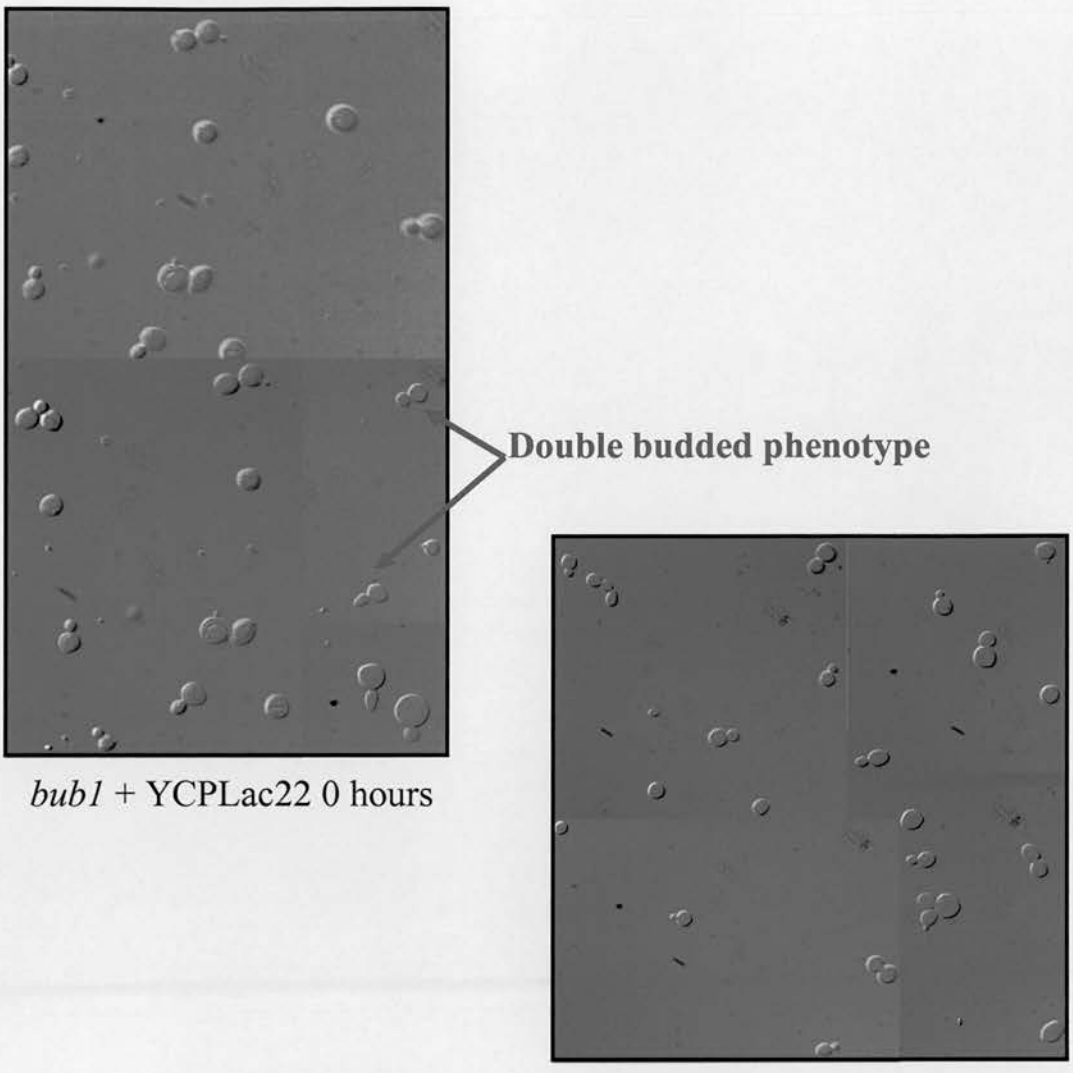

bub1 + YCPLac22 0 hours

bub1 + p*BUB1* 0 hours

bub1 + p*BUB1-ΔE5* 0 hours

Figure 4.6 BUB1 liquid culture assay results after 0 hours treatment with nocodazole

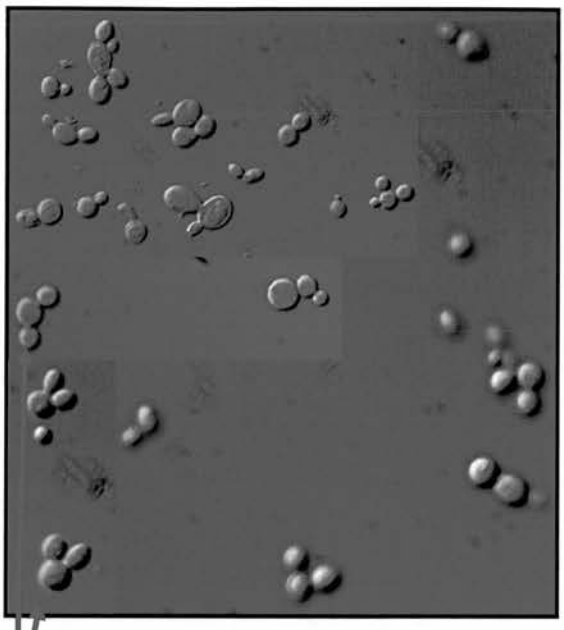

bub1 + YCPLac22 6 hours

Multi-budded phenotype

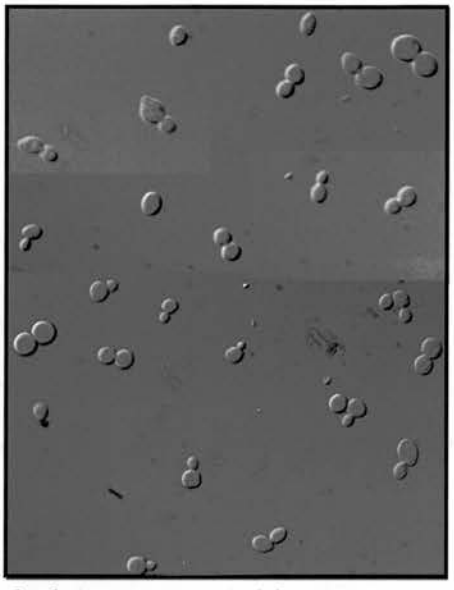

bub1 + p*BUB1* 6 hours

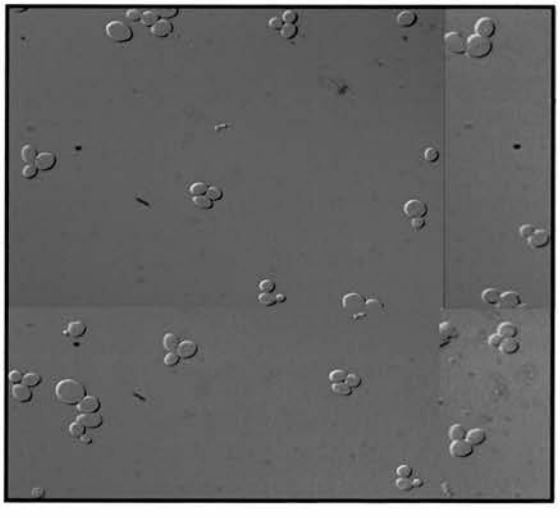

bub1 + p*BUB1-ΔE5* 6 hours

Figure 4.7 BUB1 Liquid culture assay results after 6 hours treatment with nocodazole

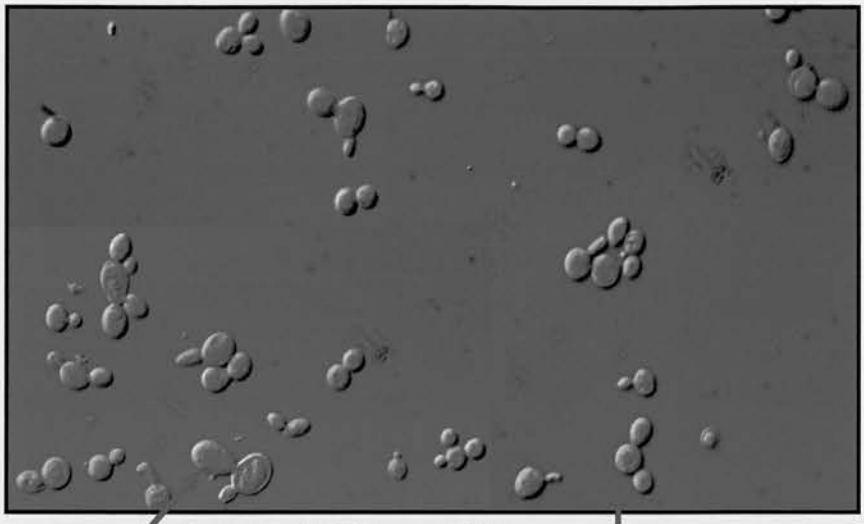

bub1 + YCPLac22 8 hours

Multi-budded phenotype

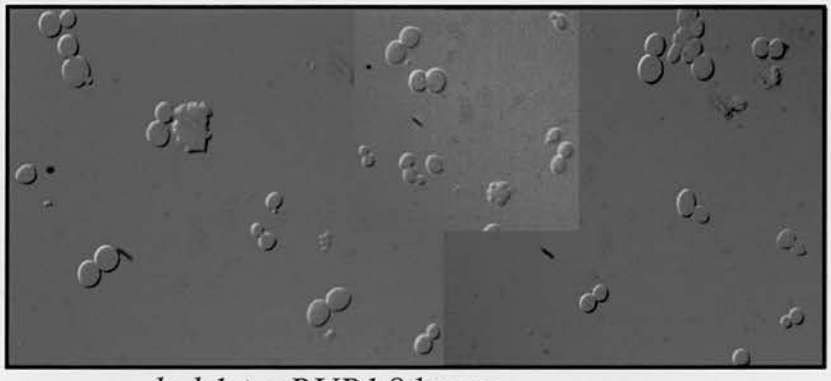

bub1 + p*BUB1* 8 hours

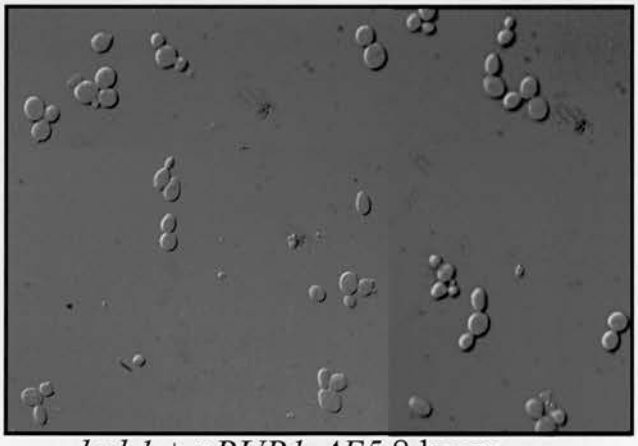

bub1 + p*BUB1-ΔE5* 8 hours

Figure 4.8 BUB1 liquid culture assay results after 8 hours treatment with nocodazole

The efficiency of spindle checkpoint function was quantified by scoring the number of cells showing a multi-budded phenotype as a proportion of a 200 cell population for each of the *bub1* transformants, YCPLac22, *BUB1ΔE5* and full-length *BUB1*. These experiments were repeated three times and the individual and total results are presented in table 4.3A with the individual and mean percentages of multi-budded cells shown in table 4.3B. Statistical analysis of the three repetitions is shown in figure 4.9 where the mean percentages of multi-budded cells are also presented graphically. The results of the individual repetitions are presented graphically in appendix 6 later in this thesis with statistical analysis in appendix 7.

Table 4.3 Liquid culture assay results

A The table below shows the number of multi-budded cells in a 200 cell population of each transformant in three repetitions of the liquid culture assay and in the total 600 cell population of these three repetitions. The means of these three assays are shown graphically with Mantel haenszel statistical analysis in figure 4.9. Chi squared statistical analysis of the individual experimental counts are shown in Appendix 7.

Time (Hrs)	**Number of multi-budded cells**											
	***bub1* + YCPLac22**				***bub1* + p*BUB1-ΔE5***				***bub1* + p*BUB1***			
	A	B	C	Total	A	B	C	Total	A	B	C	Total
0	3	6	5	14	10	5	8	23	4	1	5	10
6	64	53	52	169	66	37	43	146	9	3	9	21
8	57	46	65	168	47	34	45	126	2	5	9	16

B The table below shows the percentage of multi-budded cells in each transformant population in three repetitions of the liquid culture assay and the mean of these values. The mean values are presented graphically in figure 4.9 with Mantel Haenszel statistical analysis of the total counts. Graphical representations of the percentage of multibudded cells for the individual experiments are shown in Appendix 6.

Time (Hrs)	**Percentage of multi-budded cells**											
	***bub1* + YCPLac22**				***bub1* + p*BUB1-ΔE5***				***bub1* + p*BUB1***			
	A	B	C	Mean	A	B	C	Mean	A	B	C	Mean
0	1.5	3	2.5	2.33	5	2.5	4	3.83	2	0.5	2.5	1.67
6	32	26.5	26	28.17	33	18.5	21.5	24.33	4.5	1.5	4.5	3.5
8	28.5	23	32.5	28	23.5	17	22.5	21	1	2.5	4.5	2.67

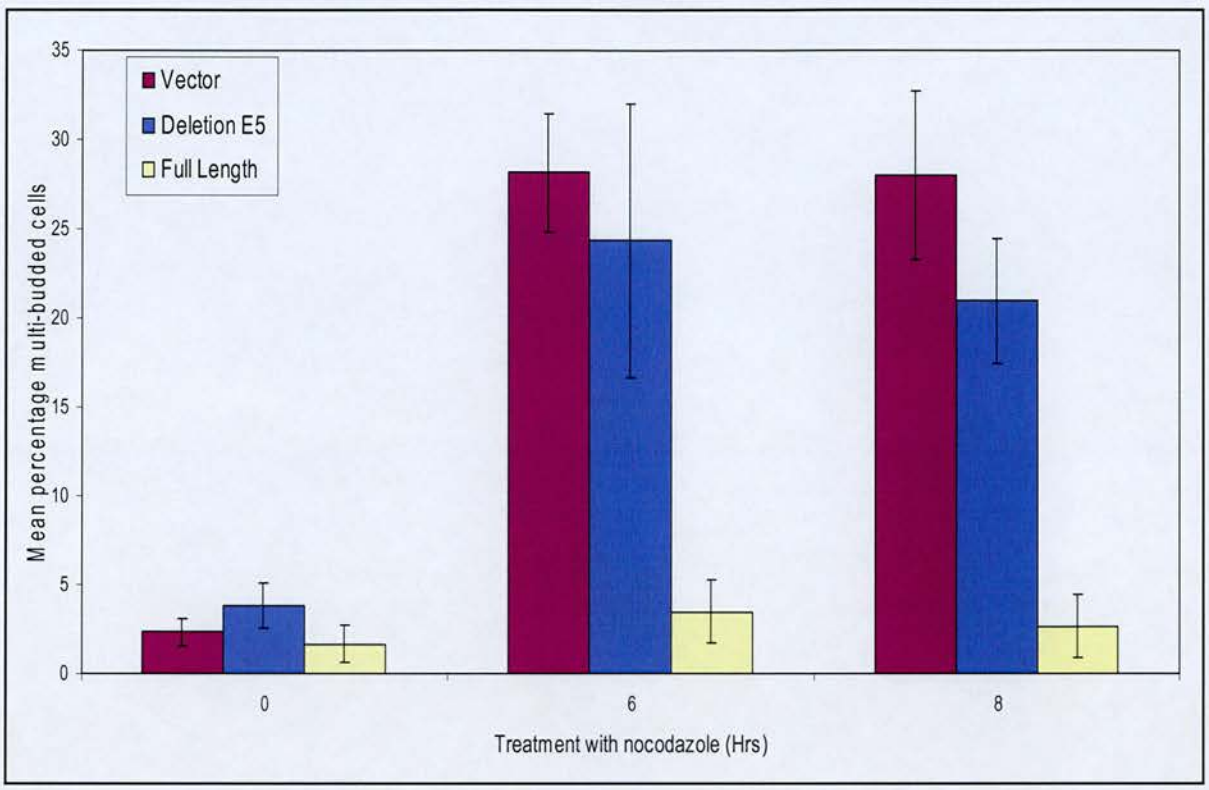

p values Mantel Haenszel Analysis (3 d.f.)	0.404	**0.034**	**0.0424**
	0.606	0.752	0.5708
	0.729	**0.0224**	**0.0166**

Figure 4.9 BUB1ΔE5 liquid culture assay results

The mean percentage of multi-budded cells for each transformed population (over 3 experimental repetitions) are presented in the graph above. Error bars indicate ± 1 standard deviation (0.763, 3.329 and 4.770 for vector at 0,6 and 8 hours; 1.258, 7.654 and 3.5 for deletion at 0, 6 and 8 hours and 1.041, 1.732 and 1.756 for full-length at 0, 6 and 8 hours).
The p values for Mantel Haenszel analyses of paired data sets are indicated below the graph with statistically significant values in red. This statistical test analyses the data from all three repetitions.
Both the vector and ΔE5 transformed *bub1* strains show an increased multi-budded phenotype after nocodazole treatment indicative of aberrant spindle checkpoint function.

Prior to nocodazole treatment both the vector and full-length transformant populations produce low proportions of multi-budded cells which do not significantly differ ($t = 0.346$, $p=0.729$). After treatment with nocodazole the proportion of multi-budded cells remains low in the full-length population indicative of spindle checkpoint arrest. A significantly higher percentage of vector transformants show a multi-budded phenotype after prolonged 6 or 8 hour arrest in nocodazole than full-length transformants ($t = 2.2819$ $p=0.0224$, $t =2.397$ $p=0.0166$, after 6 and 8 hours respectively). Thus the full-length and vector transformants act as suitable controls behaving in a manner consistent with previous reports for wild type and null strains.

The ΔE5 transformant shows a similar phenotype to the vector and full-length prior to nocodazole treatment. However, the proportion of multi-budded cells is significantly increased compared to the full-length transformant after 6 or 8 hours treatment with nocodazole consistent with the hypothesis that ΔE5 confers a spindle checkpoint defect ($t =2.120$ $p= 0.034$, $t =2.030$ $p=0.0424$ after 6 and 8 hours respectively). The severity of the multi-budded phenotype does not significantly diverge from that of the vector transformant ($t =0.316$ $p=0.752$, $t =0.567$ $p=0.571$). Thus these data do not provide any evidence to support the partial function of Bub1ΔE5p in the spindle checkpoint as suggested by the benomyl sensitivity data but they are consistent in that they demonstrate that BUB1ΔE5 harbours a spindle checkpoint defect.

4.3.5 MAD3ΔE5 is Associated with a Defect in Chromosome Segregation and an Increased Level of Chromosome Loss

The benomyl sensitivity phenotypes of the ΔE5 mutants and the results of the microcolony and liquid culture assays suggest they are able to escape checkpoint arrest despite defects in chromosome capture caused by the depolymerisation of microtubules. This lead to the hypothesis that the ΔE5 mutations allow cells to undergo aberrant mitoses which may lead to errors in chromosome segregation and the chromosome instability associated with aneuploid tumours.

In yeast, spindle checkpoint mutants have previously been shown to have elevated rates of chromosome loss due to mis-segregation events through colour colony chromosome loss assays. This assay allows quantification of the frequency of chromosome loss in different spindle checkpoint mutants thus clarifying the effect of the mutations on chromosome segregation defects.

Thus the constructs YCPLac22, ΔE5 and full-length were used in the ADE101 indicator strain to assess chromosome number. Raw data of the relative chromosome loss rates seen in the wild type and null *mad3* strains and the vector, ΔE5 and full-length transformants are shown in tables 4.4 and 4.5. The total results of three experimental repetitions are presented graphically with statistical analysis of the three data sets in figure 4.10. Similar graphs and analysis of individual experiments appear in appendix 9 and 10. Additionally, photographic representations of the sectoring phenotypes shown by the transformant populations from one repetition are shown in figure 4.11 and further photographs are shown in appendix 8.

Table 4.4 MAD3 chromosome loss colony counts

The number of half sectored colonies as a proportion of non-red colonies for each experiment is shown below. This also indicates the sample size for each transformant.
These counts are combined to produce a total ratio of half sectored colonies to total non-red colonies for each strain and transformant. The loss rates of these total counts are presented in figure 4.10 with Mantel Haenszel statistical analysis of the three data sets.

Experiment	**Proportion of half sectored colonies**				
	mad3	**Wild Type**	***mad3*** **+ YCPLac22**	***mad3*** **+ p*MAD3-ΔE5***	***mad3*** **+ p*MAD3***
A			13/9934	22/11854	3/6668
B	15/3751	10/19159	69/18492	65/17775	18/11937
C			25/6008	16/6224	3/8266
Total	15/3751	10/19159	107/34434	103/35853	24/26871

Table 4.5 MAD3 chromosome loss rates

Chromosome loss rates were calculated using the proportions listed in table 4.4 for each experiment. The loss rates for each mutant using the total data is shown in figure 4.10. The loss rates and Chi-squared statistical analyses of individual experiments are presented in Appendix 9 and 10.

Experiment	**Chromosome loss rate per thousand divisions**				
	mad3	**Wild Type**	***mad3*** **+ YCPLac22**	***mad3*** **+ p*MAD3-ΔE5***	***mad3*** **+ p*MAD3***
A			1.309	1.856	0.450
B	3.999	0.522	3.731	3.657	1.508
C			4.161	2.571	0.36
Total	3.999	0.522	3.107	2.873	0.893

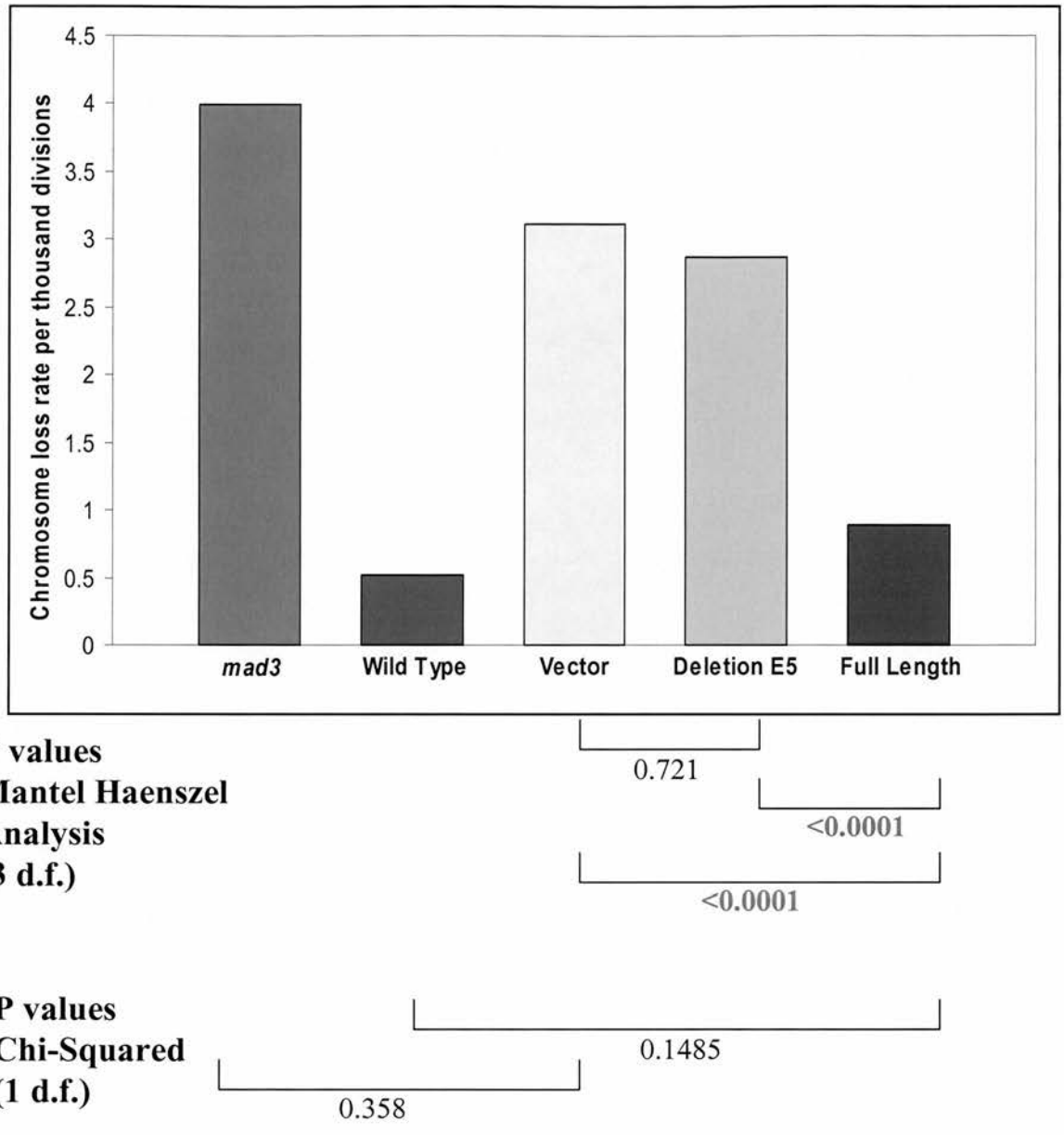

Figure 4.10 MAD3 chromosome loss assay results

The graph illustrates the rate of chromosome loss in losses per thousand divisions. The values shown are an accumulation of three individual experiments, results of individual repetitions and their individual chi-squared statistical analyses are shown in the appendix.

The p values of the Mantel Haenszel analysis comparing pairs of mutants across all three repetitions are shown below the graph with statistically significant values in red.

The vector and full-length loss rates are comparable to the *mad3* null mutant and wild type control strains respectively as shown by chi-squared analysis. ΔE5 shows an increased chromosome loss rate similar to the vector alone indicative of aberrant spindle checkpoint function and a chromosome segregation defect.

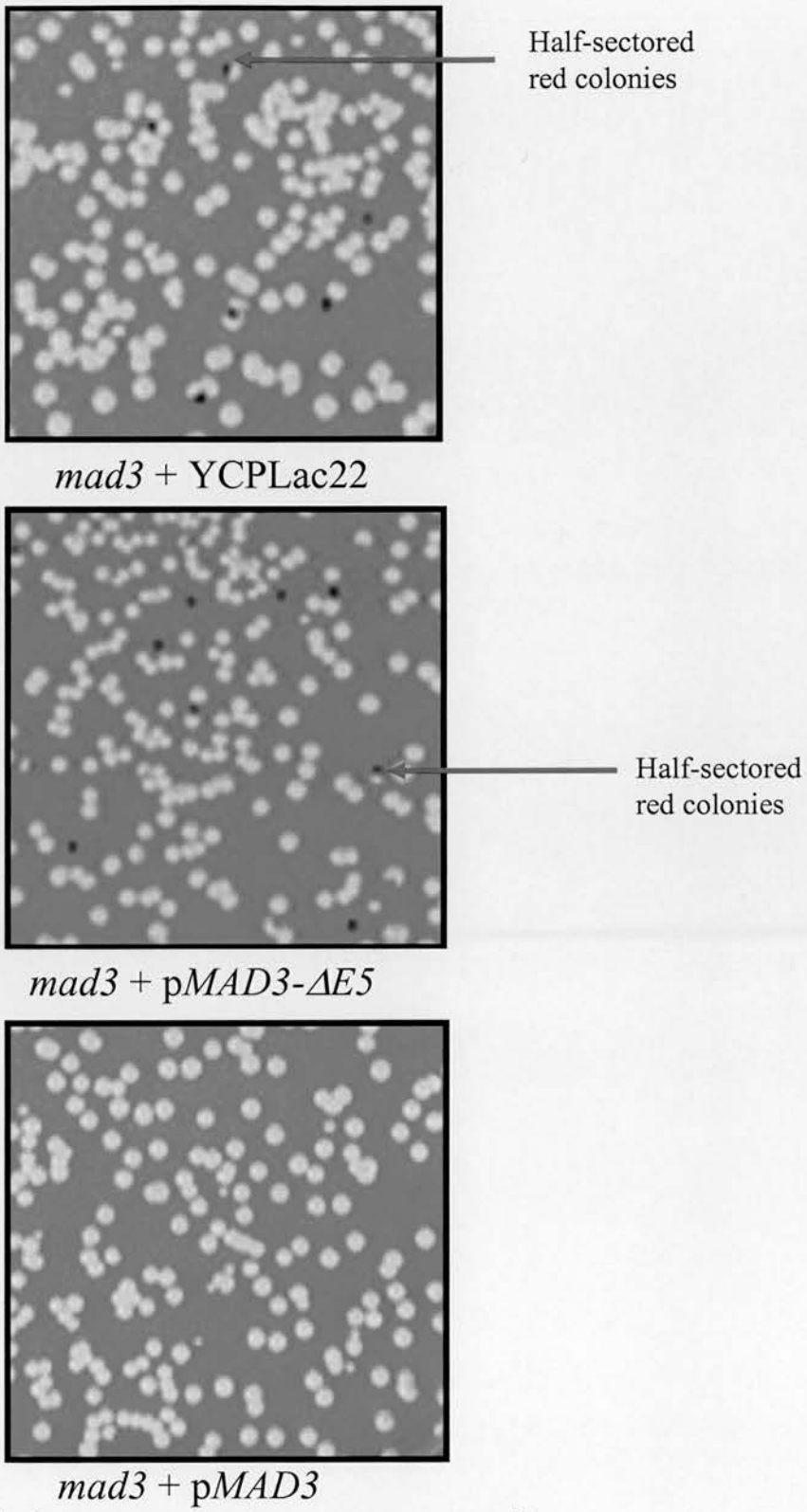

Figure 4.11 MAD3 chromosome loss assay results

A high rate of chromosome loss is seen in the vector transformant which is rescued in the full-length transformant. The deletion does not achieve this rescue indicating it harbours a spindle checkpoint defect.
This increased chromosome loss rate is indicated by the half red sectored colonies.

The *mad3* null mutants have been reported to exhibit an increased rate of chromosome loss compared to wild type strains. My analysis of these strains revealed differences in rates of chromosome loss in the wild type and *mad3* null strains, consistent with previous chromosome loss experiments (Warren et al., 2002; K. Hardwick, unpublished). These were compared to the loss rates of the control full-length and vector transformants and Chi-squared analysis revealed no significant difference between the loss rates of mad3 and vector (χ^2 = 0.844 p=0.358) or between wild type and full-length (χ^2 =2.088 p=0.148) indicating the vector and full-length behave comparably to the null and wild type strains as controls. However, the rate of chromosome loss between the vector and full-length transformants are highly statistically significantly different indicating the power of the assay (t = 5.854 p<0.0001). Chi squared analysis was used here as the loss rates of the null *mad3* mutant and wild type strain were tested only once.

The rate of chromosome loss in ΔE5 is significantly different to the full-length transformant (t = 5.303 p<0.0001) indicative of a defect in chromosome segregation. This is consistent with the hypothesis that ΔE5 initiates a chromosomal instability phenotype and that this may be associated with the aneuploid phenotype observed in colorectal tumourigenesis.

The loss rate seen in ΔE5 is not significantly different to that seen in the vector alone (t = 0.357 p = 0.721), which is consistent with the similar benomyl sensitivities of these two transformant populations. These data suggest MAD3ΔE5 is unable to function in the spindle checkpoint, providing no rescue of the null *mad3* phenotype. Thus removal of the ΔE5 region seems to have rendered the Mad3p protein non-functional. This could be a result of removal of important functional domains of Mad3p or may indicate the tertiary structure of Mad3p has been disrupted. The exact effect of ΔE5 at the protein level was investigated further as described in chapter 5.

Overall these data indicate MAD3ΔE5 induces a benomyl sensitivity phenotype, abrogates spindle checkpoint function and is associated with defective chromosome segregation. These phenotypes are consistent with the hypothesis that ΔE5 induces chromosomal instability and aneuploidy, phenotypes associated with colorectal cancer. Thus these yeast functional assays support the role of BUBR1ΔE5 in colorectal tumourigenesis.

4.3.6 BUB1ΔE5 is Associated with an Intermediate Chromosome Loss Phenotype

Null *bub1* mutants are also associated with a very severe chromosome loss phenotype in *S.cerevisiae*. The phenotype is much greater than that seen in *mad3* mutants suggesting that *bub1* has a greater role in chromosome segregation. This may be mediated through its role in the spindle checkpoint and/or through additional mitotic roles.

The rates of chromosome loss in the *bub1* null mutants transformed with vector alone and the full-length construct are comparable to those previously reported for *bub1* null mutants and wild type strains (Warren et al., 2002). The numerical results of the chromosome loss assays are shown in table 4.6 and 4.7. Photographic representations of the sectoring phenotypes are shown in figure 4.12. The total loss rates are displayed graphically in figure 4.13 with statistical analysis. The equivalent results and analyses of individual repetitions are presented in appendix 11-13 at the back of this thesis. As was found for the MAD3 assay, the loss rates of the vector and full-length transformant populations significantly differ, indicating the power of the assay ($t = 23.181$ $p<0.0001$). The loss rate of the BUB1ΔE5 transformant is significantly increased compared to the full-length transformant indicative of a spindle checkpoint defect ($t = 17.692$ $p<0.0001$). Additionally, this ΔE5 loss rate significantly differs from that of vector alone ($t =2.332$ $p=0.0198$). This intermediate phenotype of BUB1ΔE5 suggests it retains some function in chromosome segregation, perhaps through the C terminal kinase domain of the protein. This is in agreement with the initial benomyl sensitivity data described earlier. However, as no convincing intermediate phenotype is seen in the liquid culture assay analysing spindle checkpoint function, this intermediate loss rate may be achieved through retention of a protein domain involved in chromosome segregation which is separate from the spindle checkpoint functions of Bub1p.

Table 4.6 BUB1 chromosome loss colony counts

The number of half sectored colonies as a proportion of non-red colonies for each experiment is shown below. This also indicates the sample size for each transformant.
These counts are combined to produce a total ratio of half sectored colonies to total non-red colonies for each strain and transformant. These loss rate was calculated for these total counts and is presented in figure 4.13.

Experiment	Proportion of half sectored colonies		
	bub1 + YCPLac22	*bub1* + p*BUB1-ΔE5*	*bub1* + p*BUB1*
A	64/2184	59/1346	10/4331
B	83/1660	90/4109	21/8208
C	62/2270	115/4465	2/7008
Total	209/6114	264/9920	33/19547

Table 4.7 BUB1 chromosome loss rates

Chromosome loss rates were calculated using the proportions listed in table 4.6 for each experiment. The loss rates for each mutant using the total data is shown in figure 4.13. The individual loss rates and statistical analyses of individual experiments are presented in Appendix 12 and 13.

Experiment	Chromosome loss rate per thousand divisions		
	bub1 + YCPLac22	*bub1* + p*BUB1-ΔE5*	*bub1* + p*BUB1*
A	29.304	43.834	2.309
B	50.00	21.903	2.558
C	27.313	25.756	0.285
Total	34.184	26.613	1.688

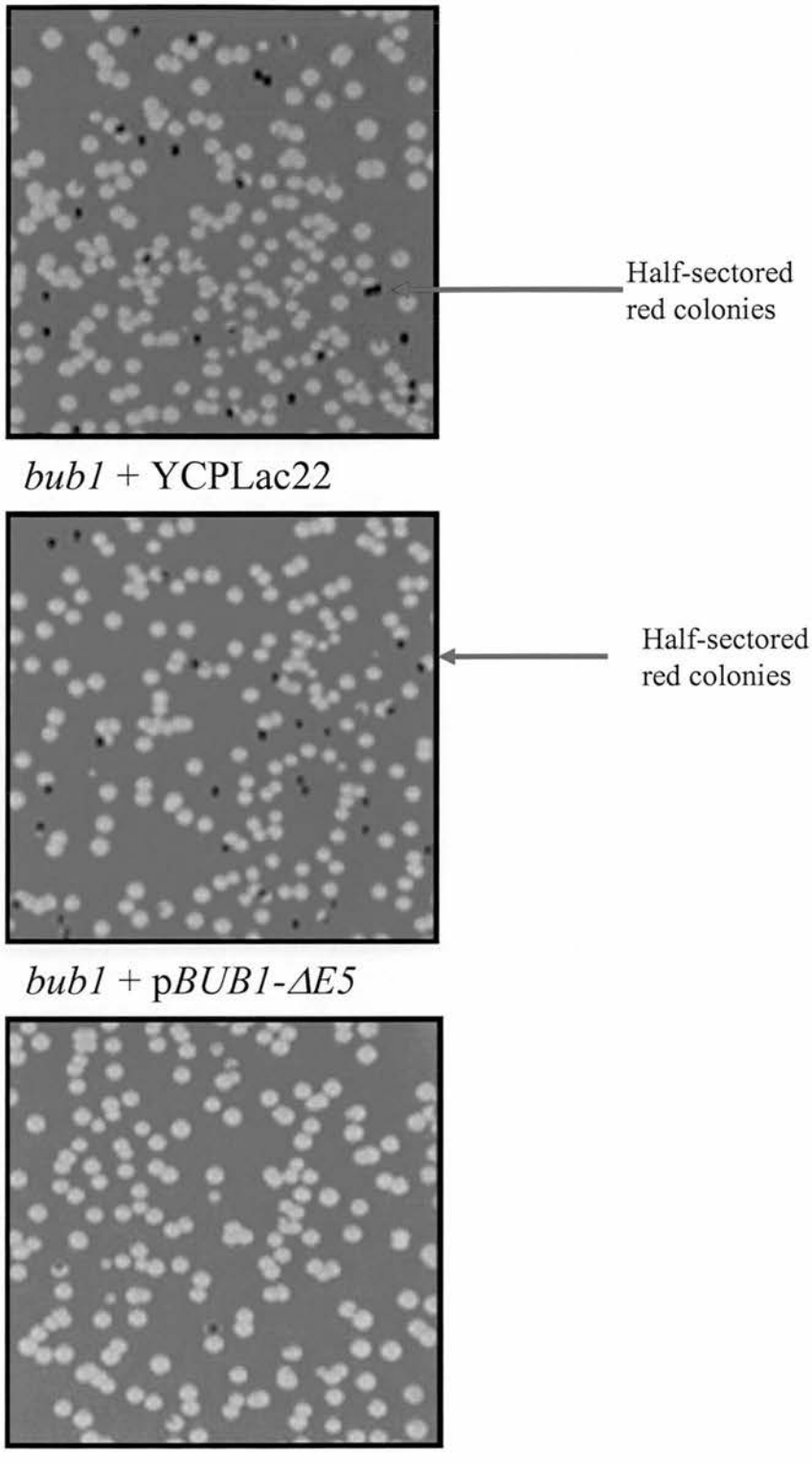

Figure 4.12 BUB1 chromosome loss assay results

A high rate of chromosome loss is seen in the vector transformant which is rescued in the full-length transformant. The deletion does not achieve this rescue indicating it harbours a spindle checkpoint defect.
This increased chromosome loss rate is indicated by the half red sectored colonies.

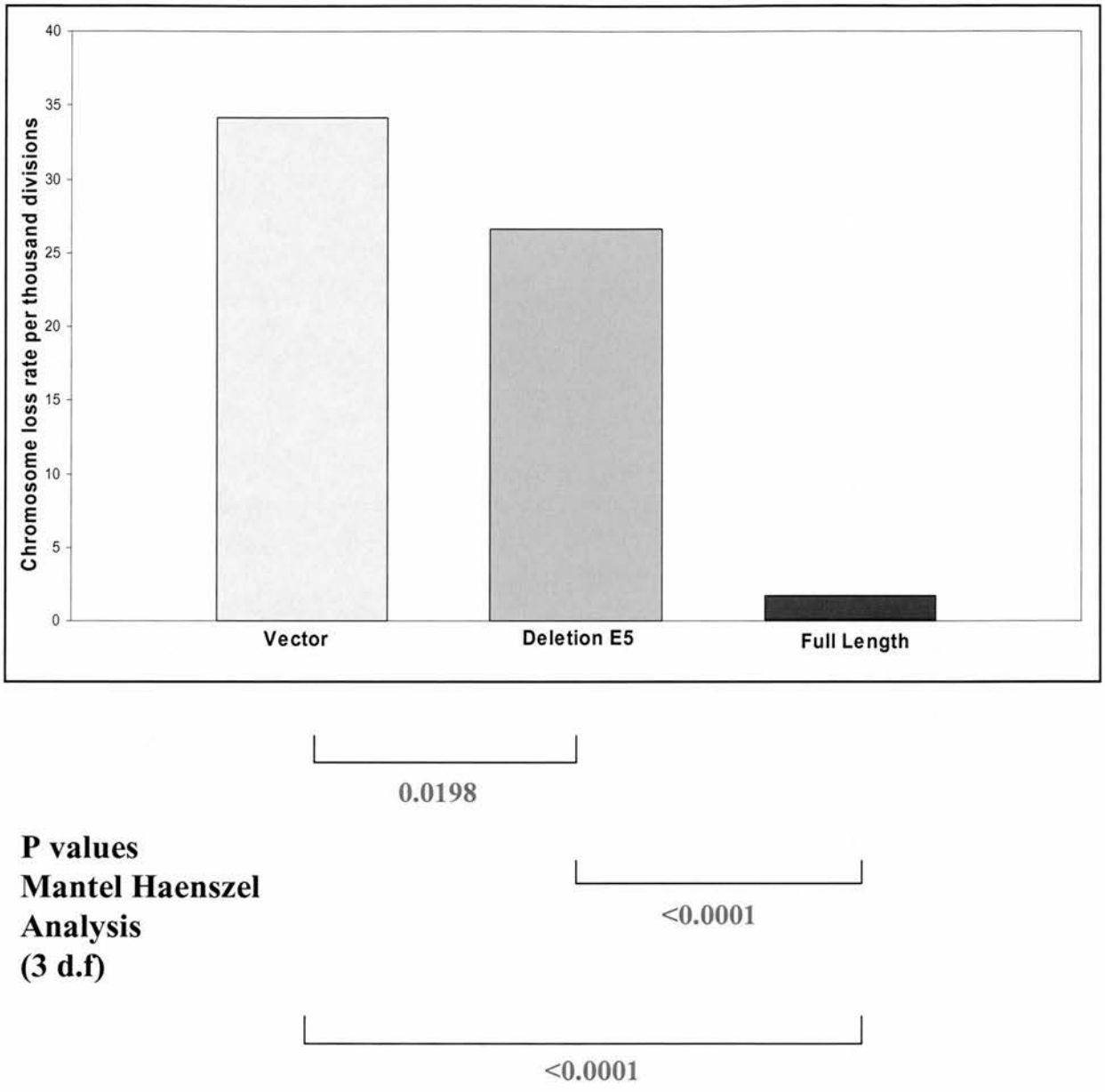

Figure 4.13 BUB1 chromosome loss assay results

The graph illustrates the rate of chromosome loss in losses per thousand divisions. The values shown represent an accumulation of three individual experiments, results of individual repetitions and their statistical analyses are shown in the appendix. The p values of the Mantel Haenszel analysis comparing pairs of mutants (at 1 degree of freedom) are shown below the graph with statistically significant values in red. This statistical test analyses data from all three experiments.

ΔE5 shows an increased chromosome loss rate but this is less severe than the vector alone, indicative of a partial defect in spindle checkpoint function.

4.4 Discussion

The results presented in this chapter show that MAD3ΔE5 confers a benomyl sensitivity phenotype associated with a spindle checkpoint defect in *S.cerevisiae* and results in an increased rate of chromosome loss, indicative of a defect in chromosome segregation. These phenotypes are equivalent in severity to those seen in a null *mad3* strain signifying a complete loss of Mad3p function by removal of the ΔE5 region.

The MAD3ΔE5 mutation has thus been shown to produce a spindle checkpoint defect and chromosomal instability in *S.cerevisiae* which has relevance to the understanding of aneuploidy in colorectal tumours harbouring this mutation in *BUB1* and *BUBR1*. It is hypothesised that these mutations abrogate the spindle checkpoint in colorectal cells and invoke a chromosomal instability phenotype, accelerating the accumulation of mutations required for tumourigenesis. This is supported by the increased rate of chromosome loss seen in the MAD3ΔE5 *S.cerevisiae* mutants.

In addition, the benomyl sensitivity and checkpoint deficient phenotypes of the ΔE5 mutants suggest they are able to bypass the spindle checkpoint despite errors in chromosome attachment due to destruction of the microtubule spindle. This may impart a growth advantage on the cells which may act as an accelerator of tumourigenesis. This is supported by the increased growth rate exhibited by the MAD3ΔE5 mutants in the microcolony assay. In yeast cells this checkpoint bypass eventually leads to a reduced viability when challenged with microtubule poisons. However, it is envisaged that in human cells a small population of cells may acquire mutations in those genes which allow them to avoid this lethality such as those involved in apoptosis for example. These could then be preferentially selected and may continue to accumulate mutations at an accelerated rate to promote carcinogenesis. Interestingly, the initial microcolony assay indicated that after 24-26 hours on benomyl containing media, the MAD3ΔE5 mutants exhibit 2-fold increased mean numbers of cells per microcolony compared to the equivalent vector alone transformants. Thus our hypothesis that the ΔE5 mutation fulfils both the mutation and selection for growth advantage criteria important for tumourigenesis is supported by these experiments in *S.cerevisiae*.

These experiments also provide a useful insight into the role of Mad3p in the yeast spindle checkpoint. The loss of function phenotype exhibited by MAD3ΔE5 can be attributed in part to the removal of the 66 amino acids by ΔE5, however the remaining C terminal amino acids of Mad3p would be predicted to retain partial protein function. Previous reports show there are two major functional protein domains in Mad3p (CD1 and CD2) and mutation of either domain causes a benomyl sensitivity phenotype (Hardwick et al., 2000). Removal of CD2 in a truncation mutant also confers a spindle checkpoint defect as shown by microcolony assays, indicating both domains are required for full checkpoint function (Hardwick et al., 2000). CD2 function would not be expected to be affected by ΔE5 as it is situated out with the area. However the results presented in this chapter disprove this hypothesis, showing that spindle checkpoint function is abolished by removal of the ΔE5 domain alone. Thus CD2 function seems to be dependent on CD1. This is consistent with previous reports in which mutation of the GIGS domain in Mad3p to four alanine residues (AAAA) produced a benomyl sensitivity phenotype equivalent to that seen in a null strain (Hardwick et al., 2000). However, a CD2 mutant, E382K, in which a conserved residue of CD2 is altered, shows a less severe benomyl sensitivity phenotype than the null strain. Thus mutation of CD1 is sufficient to nullify the protein function of Mad3p whereas mutation of CD2 is not. One explanation for this phenomenon is that CD1 mediates the major spindle checkpoint function of Mad3p and disruption of this domain abolishes checkpoint function, whereas CD2 may be associated with a secondary Mad3p function and thus checkpoint proficiency is only reduced when CD2 is mutated. Alternatively, the structure of the Mad3p protein may be affected by the mutation of CD1 both in the AAAA and the ΔE5 mutant. This may reduce protein stability and ultimately protein concentration or may affect the tertiary structure of Mad3p, either of which could manifest itself as protein dysfunction and spindle checkpoint abrogation. The nature of ΔE5 on protein stability and the formation of protein-protein interactions has been further investigated and will be described in Chapter 5.

Overall, these results suggest the area removed by ΔE5 is essential for spindle checkpoint function and its removal is sufficient to destroy checkpoint function. This destruction of Mad3p function produces a benomyl sensitivity phenotype and an

elevated frequency of chromosome segregation defects, consistent with the established role of Mad3p in the checkpoint. Thus the deletion of ΔE5 in Mad3p has provided us with important insight into the role of this region and ultimately of Mad3 in the spindle checkpoint.

The BUB1ΔE5 mutant shows a similar phenotype to MAD3ΔE5 in *S.cerevisiae*. BUB1ΔE5 shows severe benomyl sensitivity and chromosome loss phenotypes associated with a spindle checkpoint defect. This is again consistent with the hypothesis that the BUBR1ΔE5 and BUB1V400 mutations found in colorectal cancers induce a chromosomal instability phenotype and accelerate tumourigenesis. There is substantial evidence that aneuploidy is important in tumourigenesis (Fischbach et al., 1991). The characterisation of *S.cerevisiae* BUB1ΔE5 has relevance to the equivalent mutation in both human BUB1 and BUBR1, as BUBR1 shows homology to both yeast BUB1 and MAD3 and includes a C-terminal kinase domain, similar to BUB1, which is absent in MAD3.

Previous studies with human cell lines containing the BUB1V400 mutation show they have a compromised ability to arrest at mitosis, although the severity of this defect is uncertain (Cahill et al., 1998; Tighe et al., 2001). This arrest is specifically associated with aneuploid tumour cell lines and absent from diploid lines. Exogenous over-expression of the wild type BUB1 protein restores this checkpoint arrest indicative of a causative role of the BUB1V400 mutation in the generation of aneuploidy (Cahill et al., 1998a). That the BUB1V400 mutation is important in aneuploid tumourigenesis is supported by the functional analysis of BUB1ΔE5 in *S.cerevisiae* reported here. These studies of BUB1V400 in the human cell system and the similar mitotic checkpoint deficient and chromosomal instability phenotypes seen in the equivalent yeast BUB1 and MAD3 mutants, further support the pathogenic nature of BUBR1ΔE5.

In addition to the obvious relevance of these results to tumourigenesis, they provide important information about the yeast Bub1p protein and its role in mitosis. Like the MAD3ΔE5 mutant, BUB1ΔE5 shows similar phenotypes to the corresponding null mutant indicative of abrogated checkpoint function and mitotic defects. However, consistent with previous experiments, the phenotype in the BUB1

mutant is more severe. This is thought to be due to additional functions for BUB1 in the spindle checkpoint and mitosis.

Interestingly, the BUB1ΔE5 benomyl sensitivity and chromosome loss phenotypes are intermediate in severity between the null and wild type strains, suggesting ΔE5 does not destroy all of Bub1p's function. However, there is no evidence that the spindle checkpoint defect is anything less than a total abolishment. This could be due to a limitation of the liquid culture assay or may suggest the mitotic functions retained by Bub1ΔE5p are not spindle checkpoint associated. The reduced severity of the benomyl sensitivity and defective chromosome segregation phenotypes in ΔE5 compared to the null mutant may represent some function of Bub1p in kinetochore assembly or structure, which would contribute to these phenotypes but would not be apparent in the liquid culture assay. This additional function of Bub1p may be mediated by the C-terminal kinase domain of the protein which has previously been shown to be uninvolved in checkpoint function (Warren et al., 2002). This hypothesis is also supported by the null spindle checkpoint phenotype seen in the MAD3ΔE5 mutant which lacks the C terminal kinase domain. Additionally, previous studies of kinase domain truncation mutants show they exhibit elevated chromosome loss rates but achieve spindle checkpoint arrest as efficiently as wild type strains, consistent with a chromosome segregation role of Bub1p's kinase domain which is separable from its checkpoint function (Warren et al., 2002). Studies in fission yeast show some Bub1p is retained at kinetochores until cytokinesis, again indicating an additional role for Bub1p after the metaphase to anaphase transition (Bernard et al., 1998).

However, the spindle checkpoint defect exhibited by *bub1* null and ΔE5 mutants is far more severe than that seen in the respective *mad3* mutants. Thus the greater severity of the benomyl sensitivity and chromosome loss phenotypes of *bub1* mutants are partly attributable to defects in Bub1p's spindle checkpoint function. This supports the greater role for Bub1p in the spindle checkpoint than Mad3p, also supported by previous studies of chromosome loss rates and spindle checkpoint function in BUB and MAD mutants (Warren et al., 2002).

The differing severity of phenotype between MAD3ΔE5 and BUB1ΔE5 suggests ΔE5 is having a different effect at the protein level in the two proteins. Thus the ability of the mutant ΔE5 proteins to form spindle checkpoint protein complexes was examined in order to clarify the mechanism through which ΔE5 affects spindle checkpoint function. The results are discussed in the next chapter.

The ΔE5 and V400 mutations identified in colon cancer cells are heterozygous in nature and may exert a dominant negative effect on the wild type protein. The experiments so far have investigated the effect of the yeast mutation in strains otherwise null for the protein. Thus in an attempt to clarify the dominant negative nature of the ΔE5 proteins, the effect of p*MAD3*-ΔE5 and p*BUB1-ΔE5* on chromosome segregation and benomyl sensitivity was examined by transforming the plasmids into wild type strains. This is also addressed in Chapter 5.

Chapter 5: The ΔE5 Proteins are Defective in the Formation of Spindle Checkpoint Protein Complexes

5.1 Introduction

The results presented in chapter 4 describe the affect of the ΔE5 mutations on spindle checkpoint function. ΔE5 appears to abrogate the spindle checkpoint and induce a chromosome mis-segregation phenotype. The severity of these defects varies between the MAD3ΔE5 and BUB1ΔE5 mutants. In subsequent experiments I wanted to investigate the underlying defect leading to this phenotype. One hypothesis is that removal of the ΔE5 domain destabilises the Mad3p and Bub1p proteins and that the resulting reduced protein concentration impairs checkpoint function. Alternatively, the removal of the ΔE5 domain may have disrupted specific interactions between Mad3p and Bub1p and other spindle checkpoint proteins which are important for correct checkpoint function. The differing severity of the BUB1ΔE5 and MAD3ΔE5 mutants suggest the underlying mechanism of checkpoint disruption may be different in the two mutants.

Thus the experiments described in this chapter set out to investigate the effect of the ΔE5 mutation on the formation of spindle checkpoint protein complexes. Specifically, the affinity of the interactions of the ΔE5 proteins for Bub3p, Cdc20p, Mad1p and Mad2p were investigated. The effect of ΔE5 on protein phosphorylation was also studied. Both BUB1 and BUBR1 proteins are known to be phosphorylated upon spindle checkpoint activation (Chan et al., 1999; Chen, 2002; Taylor et al., 1998) and Bub1p is also shown to be phosphorylated in a budding yeast mitosis (Brady and Hardwick, 2000). Inhibition of the phosphorylation of BUBR1 by aurora B kinase abrogates spindle checkpoint function and localisation of the spindle checkpoint proteins (Ditchfield et al., 2003). The role of phosphorylation in the checkpoint is discussed further in chapter 1. Thus we hypothesised that the ΔE5 proteins may be aberrantly phosphorylated and this may be responsible for the defects in spindle checkpoint function exhibited by the ΔE5 mutants.

The effect of ΔE5 at the protein level was investigated in three ways. Firstly the mutant proteins expressed at wild type levels were visualised in yeast total cellular extracts using standard polyacrylamide gel electrophoresis (PAGE) and western blotting techniques. This aimed to verify that the mutant proteins were of the predicted size and to examine the stability of the mutant proteins relative to their full-length counterparts. The phosphorylation status of the mutant proteins was also investigated using total cellular extracts.

To investigate the ability of the mutant proteins to form interactions with specific checkpoint proteins; Bub3p, Cdc20p, Mad1p and Mad2p additional co-immunoprecipitation experiments were combined with PAGE and western blotting. The affinity of these interactions relative to their full-length counterparts were quantitated by a combination of densitometry and comparison of serially diluted fractions. Over-expression constructs were used in these co-immunoprecipitation experiments to investigate the formation of checkpoint complexes, as the expression levels from the wild type promoters were difficult to visualise with the antibodies available. For these experiments the methionine promoters were not induced but the leaky nature of the system increased the concentration of the exogenously expressed protein approximately 2-3 fold. Similar over-expression plasmids in which spindle checkpoint proteins are expressed from a methionine repressible promoter have previously been used to analyse the interactions of wild type spindle checkpoint proteins (Warren et al., 2002). Strains in which checkpoint proteins were myc-tagged were also used to assist in co-immunoprecipitation of Bub3p and Cdc20p for which antibodies to the native proteins were unavailable.

Mad3p is known to form interactions with Bub3p and Cdc20p and these are thought to be important for spindle checkpoint function (Hardwick et al., 2000). The interaction with Cdc20p is mediated by conserved domain 1 (CD1), part of which is removed by ΔE5. However, the second conserved domain, CD2 is thought to mediate the interaction of Mad3p with Bub3p and the primary structure of this domain is not altered in the ΔE5 mutant. Thus the hypothesis was that the ability to interact with Cdc20p would be reduced in the Mad3ΔE5p protein but the interaction

with Bub3p may be unaffected. In checkpoint arrested wild type strains, the Mad3p-Cdc20p complex is also associated with Mad2p and thus the effect of the ΔE5 mutation on the formation of this Mad3p-Cdc20p-Mad2p complex which is thought to be important for checkpoint function, was also investigated (Hardwick et al., 2000). Mad2p has also been found to associate with a Mad3p and Bub3p complex (Fraschini et al., 2001) and this was also investigated in the mutant.

The effect of ΔE5 on the interactions of Bub1p was also analysed. The formation of a Mad1p-Bub1p-Bub3p complex is important in spindle checkpoint function (Brady and Hardwick, 2000) so the ability of Bub1ΔE5p to form these interactions has been investigated. Other data has indicated that a truncating mutant containing amino acids 1-210 does not co-immunoprecipitate with Bub3p whereas those containing amino acids 1-367 and 1-608 do, suggesting amino acids 211-367 of Bub1p are important in the interaction with Bub3p (Warren et al., 2002). Additionally the 1-608 truncation mutant is the only one to retain interaction with Mad1p suggesting amino acids 368-608 are involved in Mad1p binding. The area removed by ΔE5 includes neither of these domains suggesting these interactions should be unperturbed. However, the results in chapter 4 demonstrate that BUB1ΔE5 does induce a spindle checkpoint defect and, as disruption of the Mad1p-Bub1p-Bub3p complex also abolishes spindle checkpoint function (Brady and Hardwick, 2000), this suggests that this may be the underlying mechanism behind BUB1ΔE5 spindle checkpoint inactivation. Bub1p has also been shown to interact with Cdc20p in a yeast 2-hybrid assay and in Mad3p the interaction with Cdc20p is thought to be mediated by CD1 (Hardwick et al., 2000), a domain conserved in Bub1p and removed by ΔE5. Thus it was hypothesised that the ability of Bub1ΔE5p to interact with Cdc20p would be compromised in the ΔE5 mutant protein and this has also been investigated.

Finally, the methionine repressible over-expression constructs were induced in chromosome loss assays to investigate the ability of the mutant proteins to interact with Bub3p. Over-expression of Bub1p and Mad3p by MET423 promoters have previously been reported by Warren et al to induce chromosome loss phenotypes in

wild type strains, due to sequestering of Bub3p from functional spindle checkpoint complexes (Warren et al., 2002). This effect is seen with full-length constructs but is absent when using the p423MET vector alone. Thus to investigate the efficiency of Bub3p interaction with the ΔE5 proteins, the ΔE5 over-expression plasmids were used in chromosome loss assays with full-length MET and p423MET vectors as positive controls. The aim was to clarify the ability of the ΔE5 proteins to interact with Bub3p and also to understand how the predicted dominant negative effect of the equivalent human mutations may be mediated.

Previous investigation into over-expression phenotypes have aided identification of specific amino acid domains which mediate interactions with Bub3p. Specifically, N-terminal truncation mutants of Bub1p (containing amino acids 1-211) do not display an elevated chromosome loss rate, indicating this area does not interact with Bub3p. The main area for Bub3p interaction was identified as amino acids 211-367 of Bub1p consistent with the parallel co-immunoprecipitation studies (Warren et al., 2002). The area removed by ΔE5 is amino acids 121-186 of Bub1p and thus is unlikely to be involved in Bub3p interaction. Hence over-expression of the ΔE5 protein from the p423MET plasmid would be predicted to induce a similar elevated chromosome loss phenotype to that seen in the full-length plasmid, through sequestering of Bub3p and spindle checkpoint disruption. However as described in chapter 4 deletion of ΔE5 in Bub1p both abolishes spindle checkpoint function and induces a chromosome loss phenotype which may be mediated in part by abrogation of the Bub1p-Bub3p interaction.

The full-length Mad3p protein also induces a chromosome loss phenotype when over-expressed due to sequestering of Bub3p. Two hybrid experiments indicate amino acids 308-409 mediate the interaction between Mad3p and Bub3p. In Mad3ΔE5p the area removed, amino acids 140-205, is again out with the area predicted to interact with Bub3p (Hardwick et al., 2000). However, spindle checkpoint function has been shown to be abolished in the *S.cerevisiae* MAD3ΔE5 mutant suggesting the Bub3 interaction may be affected. Thus the ability of over-expressed Mad3ΔE5p and Bub1ΔE5p to interact with and sequester Bub3p were also investigated in wild type strains. Again this is important in clarifying the effect of the heterozygous BUBR1ΔE5 and BUB1V400 mutations in colorectal tumours.

These over-expression experiments are particularly interesting as over-expression of spindle checkpoint proteins is associated with certain cancers, and may act by sequestering other spindle checkpoint proteins, preventing their usual spindle checkpoint interactions important for function. Indeed over-expression of spindle checkpoint proteins in *S.cerevisiae* induces a chromosome loss phenotype (Warren et al., 2002). The expression level of the mutant ΔE5 protein in human tumours has not yet been investigated but if over-expressed, sequestering of Bub3p by mutant Bub1p may be a factor in checkpoint deficiency. These experiments also have specific relevance to the human mutations, BUB1V400 and BUBR1ΔE5, as both are heterozygous and sequestering of Bub3p, preventing interaction with wild type proteins may allow them to exert a dominant negative effect.

To further investigate the ability of the ΔE5 mutations to exert a dominant negative effect wild type strains were transformed with the plasmids in which MAD3 and BUB1 were under the control of their wild type promoters. Chromosome loss assays were again utilised to analyse the ability of the mutant protein to sequester the wild type pool of Bub3p when expressed at twice the wild type concentration.

The combination of these experiments were essential to elucidate the mechanism of checkpoint disruption by ΔE5 at the protein level and to clarify the dominant negative manner of checkpoint disruption in human cells.

5.2 Methodological Overview

5.2.1 Production of New Strains YLB1, 2 and 3

A number of new strains were essential for co-immunoprecipitation analyses to analyse the interactions between Mad3p and Cdc20p and Bub1p and Cdc20p. This required strains containing myc-tagged Cdc20p as no anti-Cdc20p antibodies were available and strains which were also deleted for Mad3p and Bub1p, to ensure all the protein detected was interacting with the exogenously expressed protein, allowing the extracts from the full-length and ΔE5 transformants to be accurately compared. New strains YLB1, YLB2 and YLB3 were created by mating of appropriate existing strains as described in 2.7.9. YLB1 and YLB2 were both created from crosses between KH304 and YRJ112. YLB3 was isolated from a cross between KH304 and YRJ10. Zygotes were isolated from these crosses as described in 2.710 and tetrads were dissected and selected from these as described in 2.7.11.

5.2.2 Lithium Acetate Transformations

Lithium acetate transformations were carried out as described in 2.7.6. A summary of the transformations relevant to the work in this chapter are shown in table 5.1 below.

Table 5.1: Transformations for Analysis of Protein Interactions

Strain	Strain properties	Transformed plasmids	Selective media	Experimental Use
YRJ111	*mad3Δ*	p*MAD3*, p*MAD3-ΔE5* YCPLac22	URA, TRP	Preparation of total cellular extracts to examine protein expression, stability and modification by phosphorylation of ΔE5 compared to the full-length protein.
YRJ112	*bub1Δ*	p*BUB1*, p*BUB1-ΔE5* YCPLac22	URA, TRP	
YKH231	Wild Type Chromosome loss strain	p*MAD3*, p*MAD3-ΔE5* YCPLac22 p*BUB1*, p*BUB1-ΔE5*	URA, TRP	In chromosome loss assays to assess the dominant negative effect of ΔE5 proteins when expressed at same level as wild type protein.
YPH278	Wild Type Chromosome loss strain	p*MET:MAD3*, *pMET:MAD3-ΔE5* p423MET p*MET:BUB1*, p*MET:BUB1-ΔE5*	URA, HIS	In chromosome loss assays to analyse interaction with Bub3p and dominant negative effect when ΔE5 proteins are over-expressed. Control in co-immunoprecipitations.
YLB1	Cdc20-myc	p423MET p*MET:BUB1*, *pMET:BUB1*-ΔE5	HIS	In co-immunoprecipitation experiments to analyse interaction between Bub1p and Cdc20p
YLB2	Cdc20-myc, *bub1Δ*	p423MET p*MET:BUB1*, p*MET:BUB1*-ΔE5	HIS	In co-immunoprecipitation experiments to analyse interaction between Bub1p and Cdc20p
KH238	Bub3-myc, *bub1Δ*	p423MET p*MET:BUB1*, p*MET:BUB1*-ΔE5	HIS	In co-immunoprecipitation experiments to analyse interaction between Bub1p and Bub3p
YLB3	Cdc20-myc, *mad3Δ*	p*MET:MAD3*, p*MET:MAD3*-ΔE5 p423MET	HIS	In co-immunoprecipitation experiments to analyse interaction between Mad3p and Cdc20p
YRJ10	Bub3-myc, *mad3Δ*	p*MET:MAD3*, p*MET:MAD3*-ΔE5 p423MET	HIS	In co-immunoprecipitation experiments to analyse interaction between Mad3p, Bub3p and Mad2p.
MB003	*bub3Δ*	p*BUB1*	HIS	In phosphorylation analysis

Positive transformants were streaked onto fresh selective plates before use in the following assays.

5.2.3 Preparation of Total Cell Extracts

Total cellular extracts were prepared as described in 2.8.1 and analysed by PAGE as described below.

5.2.4 SDS Polyacrylamide Gel Electrophoresis (PAGE)

The total cellular extracts and protein fractions from the co-immunoprecipitation experiments were loaded onto polyacrylamide gels and the proteins were separated by electrophoresis as described in 2.8.3. Large 10% gels were used to analyse Bub1p fractions as the full-length protein is approximately 120kDa and smaller 12.5% or 15% gels were used for Mad3p analysis as Mad3p is approximately 60kDa in size.

5.2.5 Western Blotting

The proteins were transferred to nitrocellulose membrane as described in 2.8.4 and probed with the appropriate antibodies as listed in table 2.9. 0.5M NaCl was added to blots probed with anti-Bub1p and anti-Mad1p antibodies to reduce the amount of non-specific background binding.

5.2.6 Enhanced Chemiluminescence (Delhommeau et al., 2002)

Protein bands were visualised by ECL as described in 2.8.5. The protein bands were quantitated by densitometry using Biorad quantity one software and by comparison of diluted fractions.

5.2.7 Lambda protein Phosphatase Treatment

Protein samples showing modification in western blot analyses were treated with lambda protein phosphatase and analysed by western blot analysis to confirm that any additional bands were due to protein phosphorylation, as described in 2.8.7.

5.2.8 Co-immunoprecipitation

Protein interactions were analysed by co-immunoprecipitation experiments as described in 2.8.2. For analysis of Bub1p interactions, extracts from strains containing myc tagged Bub3p or Cdc20p (YLB1, YLB2, KH238) transformed with the BUB1 over-expression constructs were incubated with protein A Sepharose

beads and anti-Bub1p 12/99 antibody. Bub1p (~118kDa) was then detected by western blotting and probing with anti-Bub1p G antibody, myc-Bub3p (~78 kDa) using anti-myc 9E10 antibody and Mad1p (~90kDa) using either anti-Mad1p R or S as described in 2.8.3-2.8.5. Mad3p interactions were similarly analysed by incubating cell lysates from myc-tagged Bub3p or Cdc20p strains (YLB3 and YRJ10) transformed with the MAD3 over-expression constructs with c-myc 9E10 antibody coupled beads. Western blots were then probed with anti-Mad3p GG to detect Mad3p (~58kDa), anti-Mad2p to detect Mad2p (~36kDa) or anti-MYC A14 antibody to detect myc-Bub3p or myc-Cdc20p (~180kDa).

The relative amounts of protein co-immunoprecipitated from the ΔE5 and full-length cellular extracts were quantitated using a combination of densitometry methods and comparing serial dilutions of fractions.

5.2.9 Chromosome Loss Assays

Chromosome loss assays were performed on KH231 transformants and KH278 over-expression transformants as described in 2.7.15. Overnight cultures were prepared in minimal media lacking appropriate selection as listed in table 5.1. Cultures were diluted and grown in YPD and plated onto indicator plates. The indicator plates used for the over-expression experiments lacked methionine to induce expression from the met423 promoter.

5.2.10 Benomyl Sensitivity Assays

Benomyl sensitivity experiments were carried out in parallel with the chromosome loss experiments as described in 2.7.12.

5.2.11 Preparation of Cultures for Protein Analysis

Transformants were grown overnight in selective media as described in 2.7.4. These cultures were either used directly for preparation of total cellular extracts or were diluted in YPDA and used in preparation of G2/M nocodazole arrested cultures as described in 2.7.7 or S-phase arrested cultures as described in 2.7.8. These cultures were used in co-immunprecipitation experiments to analyse protein interactions.

5.3 Results

5.3.1 pMAD3-ΔE5 and pBUB1-ΔE5 Produce Proteins of Appropriate Size which are as Stable as their Full-length Counterparts

The vectors in which *MAD3* and *BUB1* were under control of their wild type promoters were transformed into *mad3* and *bub1* null strains respectively. The transformants were cultured to mid-log phase and total cellular extracts were prepared from the cultures. These were analysed for the presence of the Mad3p and Bub1p proteins by western blot analysis. Figure 5.1 shows proteins are produced from the *MAD3* and *BUB1* containing vectors and that the proteins produced by the ΔE5 constructs are approximately 7.3kDa smaller than those produced by the full-length constructs. The stability of the ΔE5 and full-length proteins is approximately equal suggesting the spindle checkpoint and segregation defects reported are not attributable to a reduction in the stability of the ΔE5 proteins.

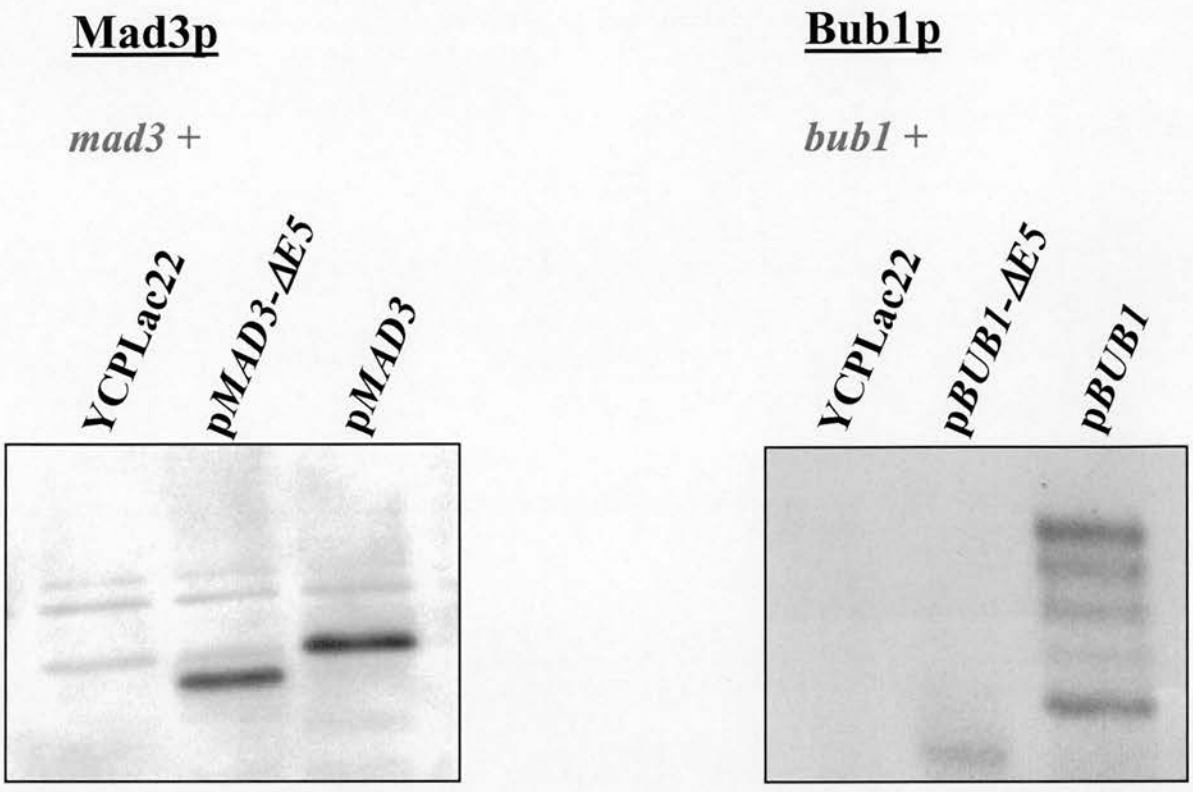

Figure 5.1 ΔE5 proteins are as stable as the full-length proteins

The proteins expressed by vectors YCPLac22, p*MAD3* and p*MAD3-ΔE5* in a null *mad3* strain and the YCPLac22, p*BUB1* and p*BUB1ΔE5* transformants in a null *bub1* strain. The proteins expressed by the ΔE5 constructs are approximately 7.3kilo daltons smaller than the full-length proteins due to the deletion of the 66amino acids. The additional bands shown in the vector lanes are additional non-specific antibody bands. The figure also shows that the stability of the ΔE5 and full-length proteins are approximately equal and therefore a reduction in stability is unlikely to be responsible for the checkpoint defective phenotypes described in chapter 4.

5.3.2 The Mad3ΔE5p Protein has a Reduced Affinity for Other Spindle Checkpoint Proteins Compared to the Full-length Protein

Co-immunoprecipitation experiments were used to determine the effects of the ΔE5 deletion on the interaction of Mad3p with Bub3p and Mad2p and also on the interaction between Mad3p and Cdc20p.

Strains null for *mad3* containing myc-tagged Bub3p were transformed with the over-expression constructs p*MAD3*, p*MAD3*-ΔE5 and p423MET. The resulting transformants were cultured to mid-log phase. These cultures were immunoprecipitated with anti-myc conjugated beads and resulting extracts were analysed for Mad3p, myc-tagged Bub3p and Mad2p. Three controls were used; the p423MET transformant and a *mad2* deletion strain acted as controls against non-specific bands in the western blot analysis, and a wild type strain in which Bub3p was not myc-tagged transformed with p*MAD3* ensured no non-specific complexes were immunoprecipitated.

Representative results of these co-immunoprecipitation experiments are shown in figure 5.2. The co-immunoprecipitation was repeated three times on fresh cultures for each repetition and similar results obtained.

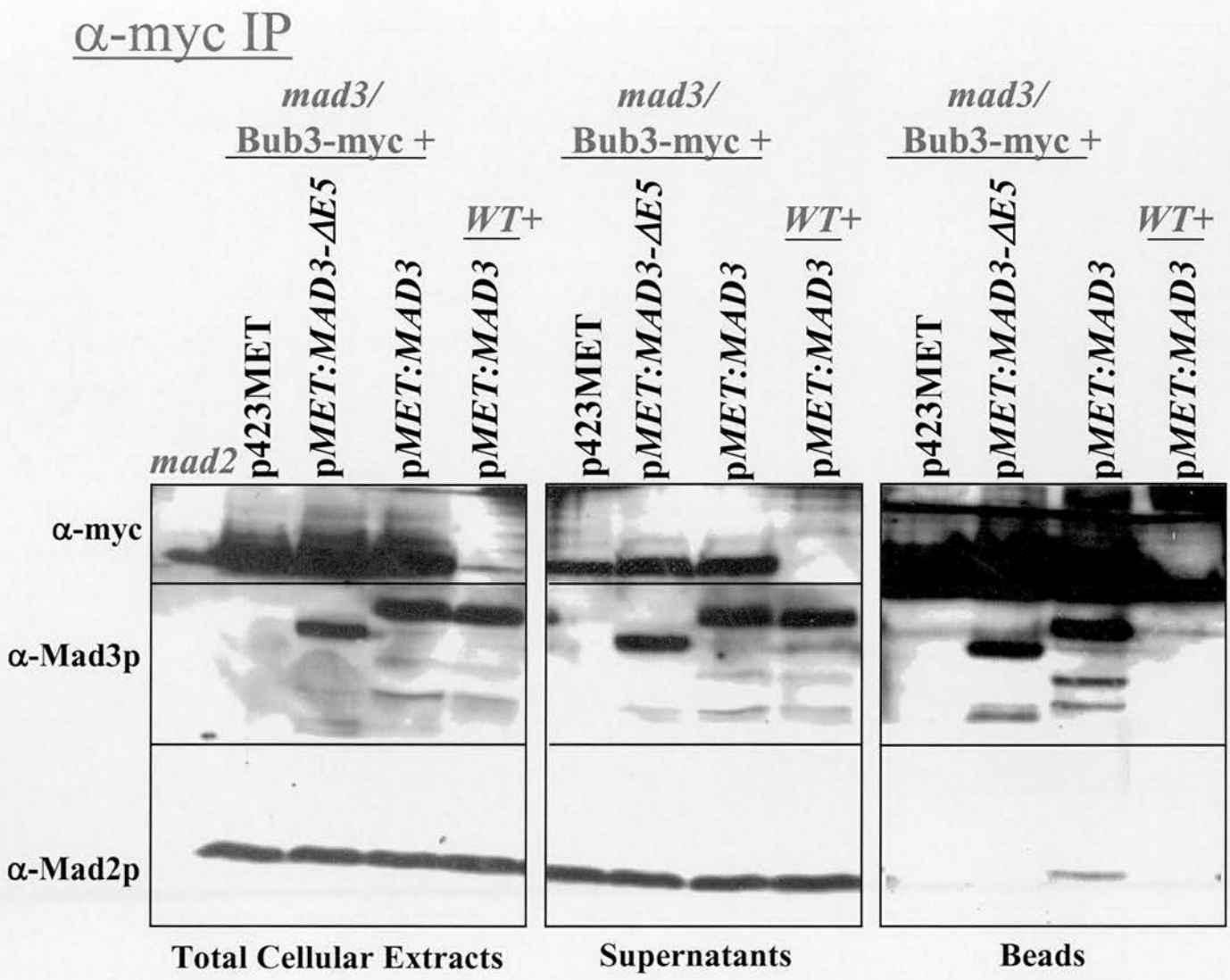

Figure 5.2 Mad3ΔE5p forms reduced interactions with Bub3p and the amount of Mad2p in this complex is also reduced

An equivalent amount of protein is expressed from p*MET:MAD3* and p*MET:MAD3-ΔE5*, supporting the previous evidence of their similar stability. However, the amount of Mad3p which immunoprecipitates with myc-tagged Bub3p, as indicated by the bead fraction, is slightly reduced in the ΔE5 mutant suggesting a reduction in the Bub3p binding activity of Mad3ΔE5p. Consistent with this, the amount of Mad3ΔE5p in the supernatant fraction is slightly raised compared to the amount of full-length Mad3p.

The amount of Mad2p immunoprecipitated by myc-tagged Bub3p is also reduced in the ΔE5 mutant. Similarly Mad2p does not immunoprecipitate with Bub3p in the *mad3* null strain transformed with vector alone, suggesting a trimer complex of Bub3p, Mad3p and Mad2p is formed in yeast and Mad3p is essential for the interaction between Bub3p and Mad2p in this complex. The ΔE5 deletion appears to reduce formation of this checkpoint complex.

The *mad2* null strain and non-myc wild type strain transformed with full-length p*MAD3* act as controls.

The results show the interaction between Mad3ΔE5p and Bub3p is reduced by approximately 35% compared to the full-length protein as determined by densitometry and serial dilution of three repetitions.

The amount of Mad2p associated with this Mad3p-Bub3p complex is also reduced in the ΔE5 mutant by approximately 75%. This may be a direct result of the reduction in the amount of Mad3p associated with Bub3p or may be due to deletion of the ΔE5 region disrupting a direct interaction between Mad3p and Mad2p. Bub3p does not immunoprecipitate Mad2p in the mad3 *null* strain transformed with vector alone suggesting Mad3p is required for the interaction between Bub3p and Mad2p. This may be due to a direct interaction between Mad3p and Mad2p which recruits Mad2p to the Mad3p-Bub3p complex. Alternatively, the interaction between Mad3p and Bub3p may induce a conformational change in the complex inducing its interaction with Mad2p. The removal of the ΔE5 region disrupts this interaction between Mad2p and the Mad3p-Bub3p complex, this could be achieved through a reduced ability of Mad3p to bind Mad2p or may be a down stream effect of the reduced interaction between Mad3p and Bub3p.

In addition the ability of Mad3p to interact with Cdc20p was investigated by co-immunoprecipitation experiments. This required production of a *mad3* deletion myc-tagged Cdc20p strain into which the three over-expression constructs were transformed. Nocodazole arrested cultures of the transformants were prepared and these were again immunoprecipitated using anti-myc conjugated beads. The resulting fractions were analysed for the presence of Mad3p and Cdc20p by western blotting. Again a wild type strain in which Cdc20p was not myc-tagged ensured the proteins pulled down were the result of specific interactions, and the *mad3* null strain transformed with the p423MET vector alone ensured anti-Mad3p antibody specificity. The results of this analysis are shown in figure 5.3. The mean densitometry of the three repetitions show the interaction between Mad3ΔE5p and Cdc20p is reduced by 50% compared to the full-length protein.

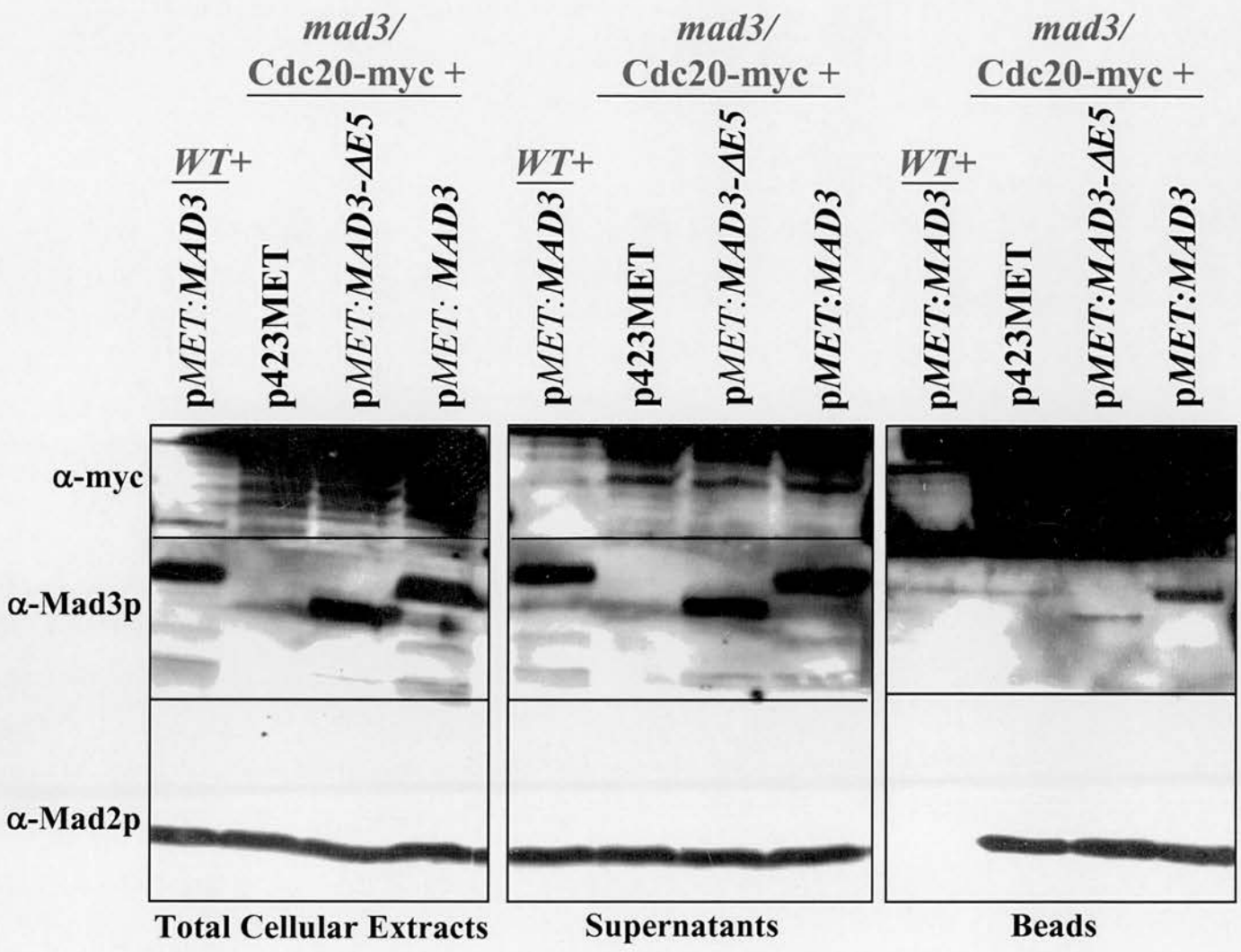

Figure 5.3 Mad3ΔE5p forms reduced interactions with Cdc20p

Similar amounts of the ΔE5 and full-length Mad3p proteins are isolated from total cellular extracts. However, the amount of Mad3p which immunoprecipitates with myc-tagged Cdc20p is slightly reduced (in bead fraction) in the ΔE5 mutant indicative of a reduction in the Cdc20p binding activity of Mad3ΔE5p.

The amount of Mad2p immunoprecipitated by myc-tagged Cdc20p is not reduced in the vector transformant suggesting Mad3p does not directly interact with Mad2p and that it is not required for an interaction between Mad2p and Cdc20p. Consistent with this hypothesis, the amount of Mad2p interacting with Cdc20p is unaffected by Mad3ΔE5p.

The non-myc wild type strain transformed with full-length p*MET:MAD3* is included as a control.

Mad2p is also associated with the Mad3p-Cdc20p complex and Mad2p is immunoprecipitated with Cdc20p in the *mad3* null mutant transformed with vector alone suggesting the Cdc20p-Mad2p complex is not dependent on Mad3p. The amount of Mad2p associated with Cdc20p is unaffected by Mad3ΔE5p, consistent with the independence of the Mad2p-Cdc20p interaction and suggests Mad2p does not interact with Mad3p directly in this complex.

This has relevance to the nature of the Mad3p-Mad2p interaction in the Mad3p-Bub3p-Mad2p complex. The hypothesis that the interaction between Mad3p and Bub3p recruits Mad2p to the complex, perhaps through a conformational change is supported by studies of the interaction between Mad3p, Cdc20p and Mad2p. Mad2p is immunoprecipitated with Cdc20p even in a *mad3* null strain transformed with vector alone, suggesting the interaction between Mad3p and Mad2p is not a direct one. However, if the reduced interaction between Mad2p and Bub3p is a result of the reduced interaction between Bub3p and Mad3p in the ΔE5 mutant, we might expect these interactions to be reduced by similar amounts. This phenomenon is not observed as the 35% reduced interaction between Bub3p and Mad3p corresponds to a 75% reduced interaction between Bub3p and Mad2p. However, this may be due to in part to a dimeric form of Mad2p associated with the complex. Thus perhaps both a reduced interaction between Mad3p and Bub3p and disruption of a direct interaction between Mad3p and Mad2p contribute to the loss of Mad2p in the Bub3p-Mad3p-Mad2p complex in the ΔE5 mutant.

In addition this suggests the reduced association between Bub3p and Mad2p seen in the Mad3ΔE5 mutant (figure 5.2) is not due to an effect on a direct interaction between Mad2p and Mad3p by ΔE5. It may in fact be a result of the reduced interaction between Bub3p and Mad3p in the ΔE5 mutant.

5.3.3 The Interaction Between Bub1p and Bub3p is Reduced in the BUB1ΔE5 Mutant

A null *bub1* strain containing myc-tagged Bub3p was used to compare the interaction between the ΔE5 and full-length Bub1p proteins with Bub3p using co-immunoprecipitation experiments. This strain was transformed with the over-expression vectors p*MET:BUB1* and *pMET:BUB1-ΔE5*, and p423MET as a control to ensure detection by the anti-Bub1p antibody is specific. Again a wild type strain transformed with p*MET:BUB1* ensured the co-immunoprecipitation specifically pulled down myc-tagged complexes. The results of these co-immunoprecipitation experiments are shown in figure 5.4 and indicate that the interaction between Bub1ΔE5p and Bub3p is reduced by approximately 60% when compared with the full-length protein and Bub3p. This was observed in three independent experiments, the quantitation includes densitometry results from the three repetitions and comparison of serial dilutions.

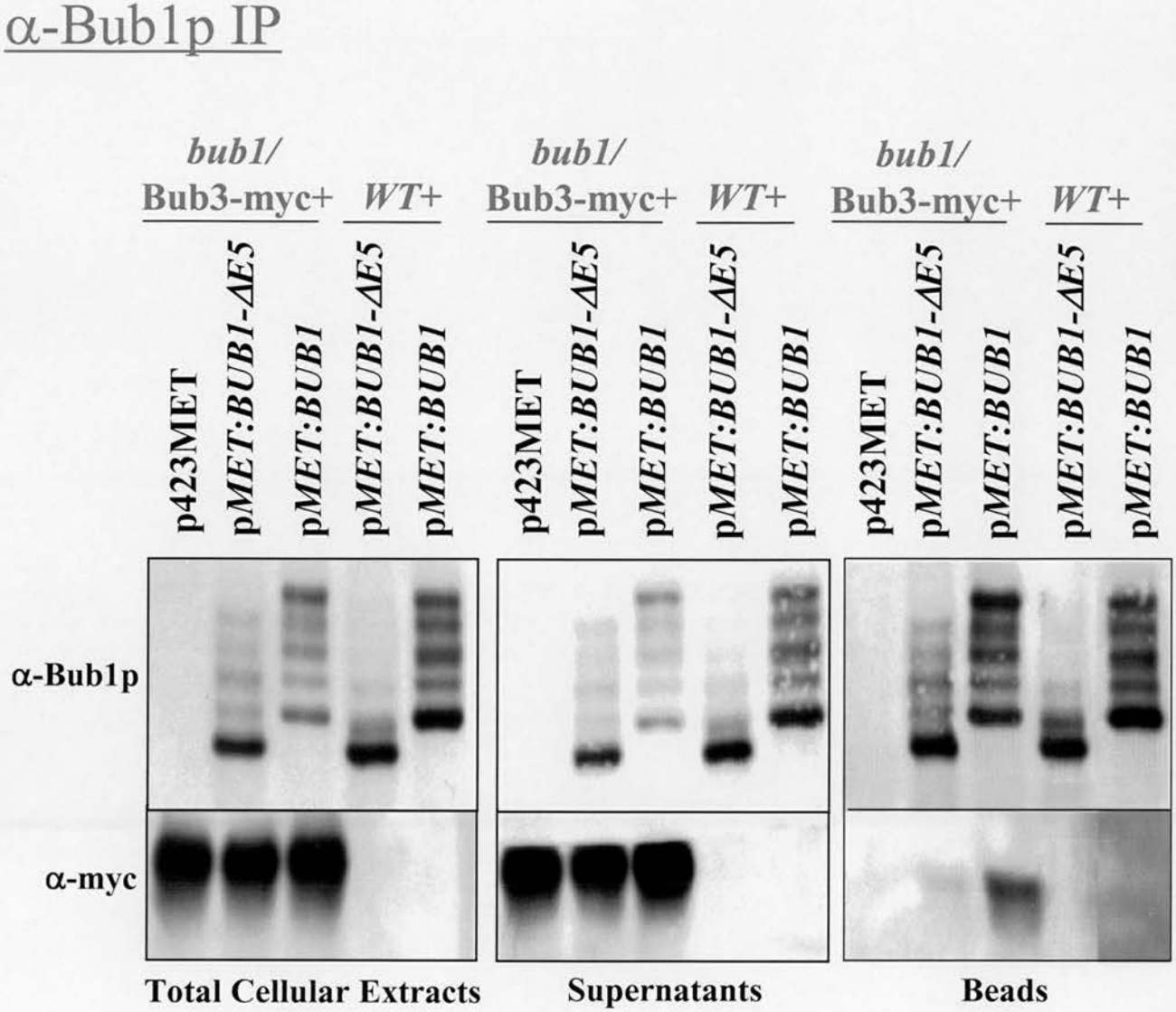

Figure 5.4 Bub1ΔE5p forms reduced interactions with Bub3p

An equivalent amount of protein is observed in the total cellular extracts isolated from both the ΔE5 and full-length transformants supporting the equivalent stability of the wild type and mutant proteins. However, the amount of myc-tagged Bub3p which immunoprecipitates with Bub1p in the bead fraction is reduced by 60% in the ΔE5 mutant indicative of a reduction in the Bub3p binding activity of Bub1ΔE5p compared to the full-length protein. Consistent with this, the amount of myc-Bub3p in the ΔE5 supernatant fraction is slightly raised compared to the full-length fraction. The vector transformant and non-myc wild type strain transformed with full-length p*MET:BUB1* and p*MET:BUB1-ΔE5* act as controls.

The interaction between Bub1p and Mad1p was also investigated in the ΔE5 mutant. However, despite numerous attempts, co-immunoprecipitation of Mad1p with anti-Bub1p antibodies and vice versa was unsuccessful and so the effect of ΔE5 on this interaction is uncertain. However, previous studies indicate Bub3p-Bub1p and Mad1p form a trimer complex and so abrogation of the interaction between Bub1p and Bub3p by ΔE5 is likely to affect the function of the Bub3p-Bub1p-Mad1p signalling complex and hence spindle checkpoint function.

A null *bub1* strain containing myc-tagged Cdc20p was constructed in order to investigate the interaction between Bub1p and Cdc20p in the ΔE5 mutant but unfortunately technical difficulties and time constraints prevented completion of this analysis. Some initial immunoprecipitations from nocodazole arrested cultures showed the interaction between Bub1p and Cdc20p to be reduced in ΔE5 using a wild type strain with myc-tagged Cdc20p as shown in figure 5.5. However, the absence of non-myc controls for this experiment made it difficult to draw firm conclusions from the data. The relevance of such a Bub1p-Cdc20p complex in a normal cell cycle is unclear as it has only been detected when Bub1p is over-expressed or in *mad3* mutants (Hardwick et al., 2000).

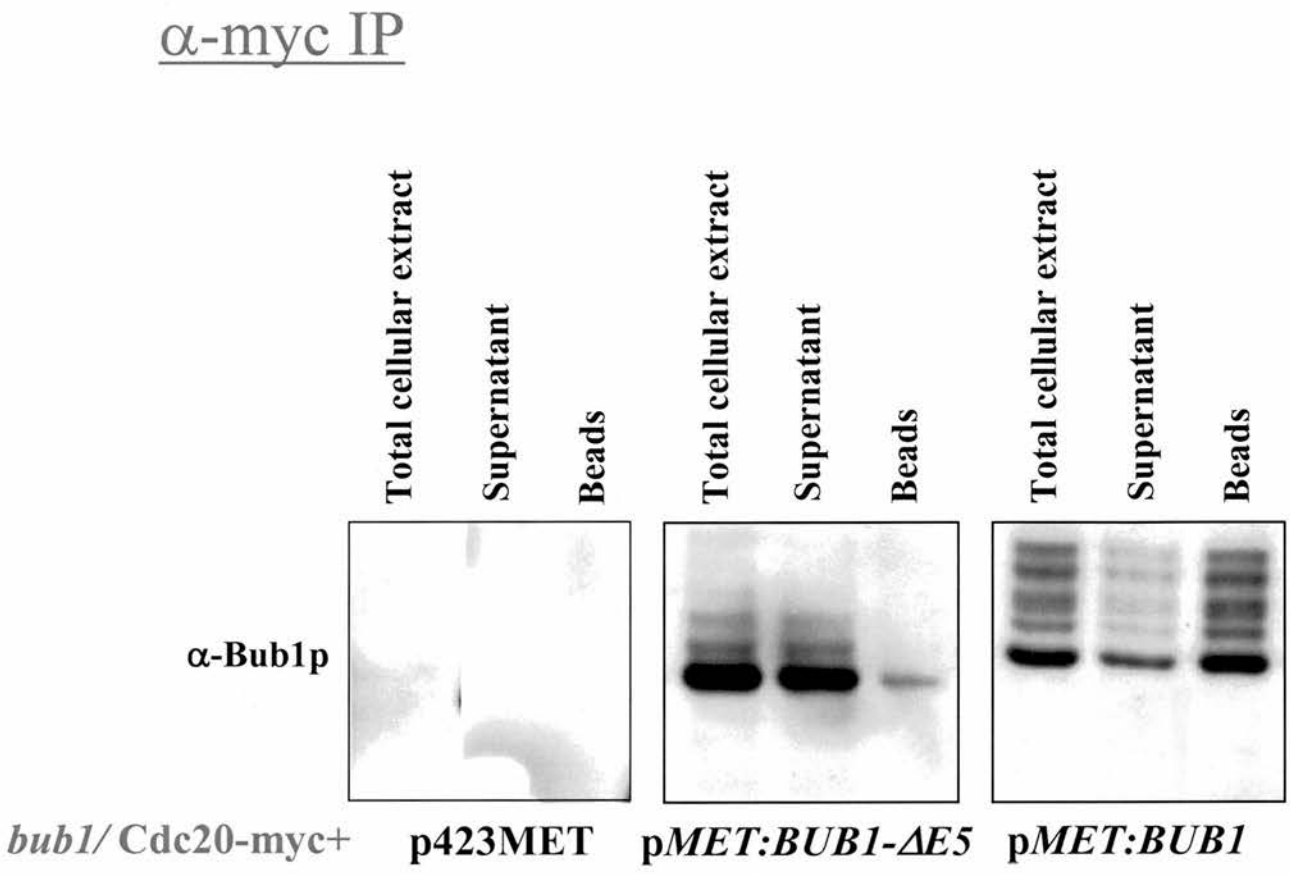

Figure 5.5 Initial data suggest Bub1ΔE5p may form reduced interactions with Cdc20p

A roughly equivalent amount of protein is observed in the total cellular extracts isolated from both the ΔE5 and full-length transformants. However, the amount of Bub1p which immunoprecipitates with myc-tagged Cdc20p is reduced in the ΔE5 mutant indicative of a reduction in the Cdc20p binding activity of Bub1ΔE5p compared to the full-length protein. Consistent with this, the amount of Bub1p in the ΔE5 supernatant fraction is raised compared to the full-length fraction.
These are very preliminary results with limitations as they were not performed in a *bub1* null strain, nor were non-myc controls included to check for the stickiness of the beads nor the amount of myc-Cdc20 analysed by western blotting to standardise amount of beads added.

5.3.4 Bub1ΔE5p is Aberrantly Phosphorylated

Western blot analysis of total cellular extracts from p*BUB1* and p*BUB1*-ΔE5 transformants showed they are extensively modified, producing at least 5 protein bands, one of which may be a doublet. This is shown in figure 5.6A and can also be seen in many of the other figures. Treatment of the extracts with lambda protein phosphatase removes these bands indicating the modification is due to the phosphorylation of Bub1p. The phosphorylation of Bub1ΔE5p is also altered compared to the full-length protein. While each of the individual bands appear to be present in Bub1ΔE5p, the relative intensities of the bands are altered. Thus it is unlikely that the phosphorylated residues are situated within the region deleted by ΔE5 as this would be predicted to result in fewer modified forms and less bands on the protein gel. Thus I hypothesised that the reduced interaction between Bub1p and Bub3p in the ΔE5 mutant may be responsible for the aberrant phosphorylation.

To address this hypothesis the full-length BUB1 construct, p*BUB1*, was transformed into a null *bub3* strain and the phosphorylation was analysed by western blotting analysis. The results shown in figure 5.6B indicate Bub1p was heavily phosphorylated in the *bub3Δ* strain and did not show the alternate pattern seen in the Bub1ΔE5p mutant. Thus we concluded that the aberrant phosphorylation of Bub1ΔE5p does not seem to be a result of it's reduced affinity for Bub3p and that Bub1p phosphorylation is not Bub3p dependent. The altered phosphorylation pattern appears to be an independent effect of ΔE5, perhaps due to disruption of other BUB1p interactions or its localisation.

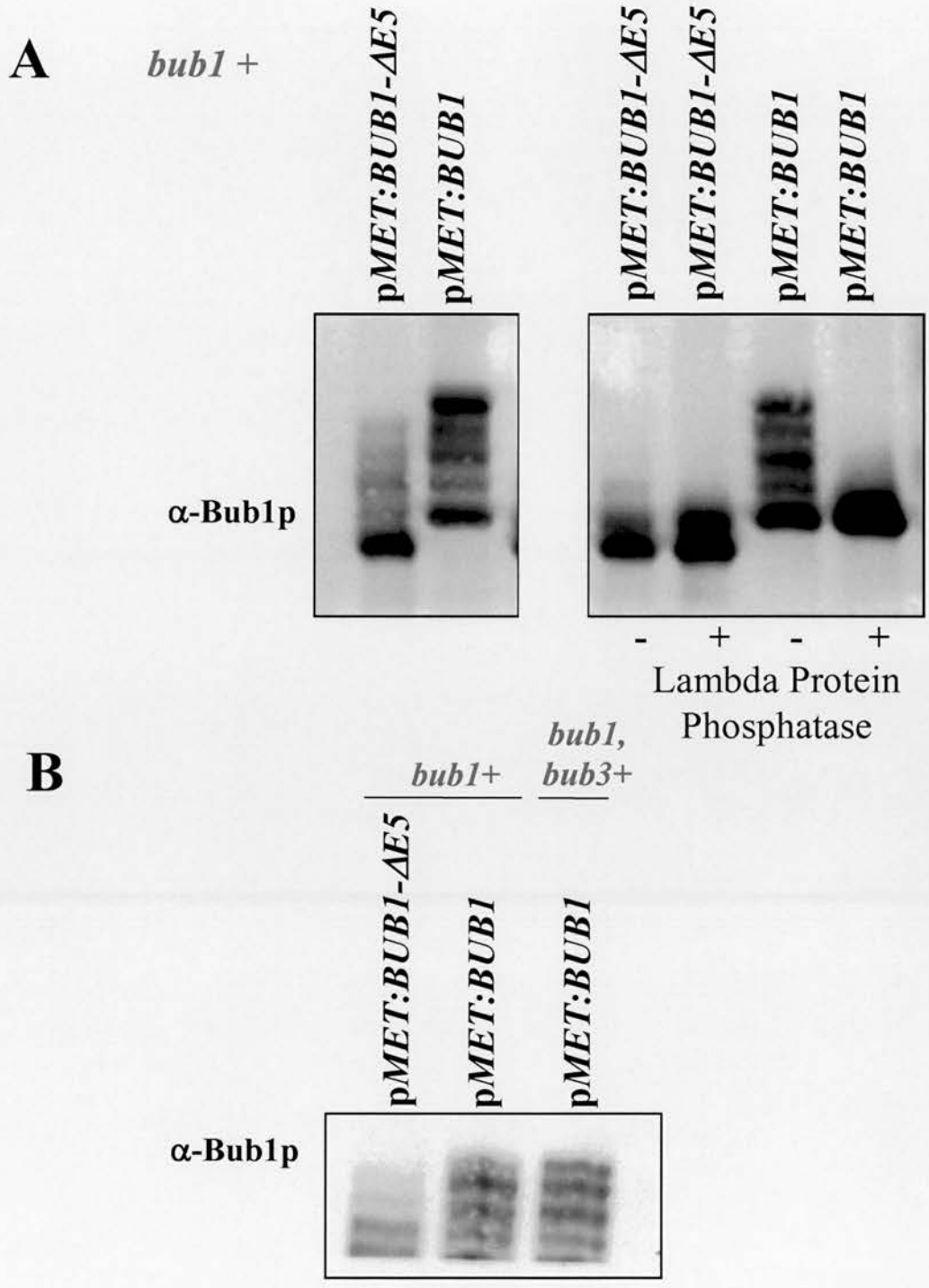

Figure 5.6 Bub1ΔE5p is aberrantly phosphorylated

A) Bub1p is heavily modified and this modification is reduced and altered in the ΔE5 mutant. The most heavily modified and slowly migrating bands are reduced in intensity relative to the other bands in Bub1ΔE5p compared to the full-length protein. This modification is removed upon treatment with phosphatase confirming it is a phosphorylation effect.

B) The phosphorylation of the full-length Bub1p protein is not altered in a *bub3* mutant strain. Thus the aberrant phosphorylation effect seen in Bub1ΔE5p is not a result of it's reduced interaction with Bub3p.

5.3.5 Mad3ΔE5 Confers a Mild Chromosome Loss Phenotype when Over-expressed

To further investigate the ability of Bub1ΔE5p to interact with Bub3p and to observe whether it acts in a dominant negative fashion Wild type strains were transformed with the over-expression constructs p*MET:MAD3*, p*MET:MAD3-ΔE5* and p423MET. The transformants were analysed using benomyl sensitivity and chromosome loss assays for checkpoint dysfunction and chromosome mis-segregation.

Benomyl sensitivity assays were unsuccessful, with the full-length control transformants showing no noticeable increased sensitivity to microtubule poisons than the wild type strain transformed with vector alone. This is thought to be due to technical difficulties in producing low methionine media to induce protein over-expression from the plasmids, which also contains benomyl.

The total results of the chromosome loss experiments are presented in tables 5.2 and 5.3 and presented graphically in figure 5.7. As previously reported an increased rate of chromosome loss was observed when full-length Mad3p was over-expressed compared to that seen in the vector transformant. This has previously been attributed to the ability of Mad3p to interact with and sequester Bub3p exerting a dominant negative effect (Warren et al., 2002). This increased loss was seen in two experimental repetitions and analysis showed this increased loss to be statistically significant ($t = 4.806$ $p<0.0001$). A similar increased chromosome loss phenotype was seen in the p*MET:MAD3-ΔE5* transformant suggesting Mad3ΔE5p is both able to bind Bub3p and to exert a dominant negative phenotype through retention of this binding. This loss phenotype is significantly elevated over the vector transformant ($t = 3.831$ $p = 0.0002$) but does not significantly differ from that seen in the full-length transformant ($t = 1.160$ $p = 0.246$). Thus there is no evidence from these assays that loss of Bub3p binding by Mad3ΔE5p is responsible for the spindle checkpoint defect and chromosome mis-segregation phenotype exhibited by MAD3ΔE5 mutants.

In addition, the ability of Mad3ΔE5p to interact with Bub3p may allow it to exert dominant negative effects when heterozygous in colorectal tumour cells. Such a

dominant negative phenotype has been observed in the colorectal tumour cell lines harbouring the equivalent BUB1 mutation V400 (Cahill et al., 1998).

Table 5.2 MAD3 over-expression chromosome loss assay

The number of half-sectored colonies observed in the MAD3 over-expression chromosome loss assay are listed below as a proportion of total non-red colonies. The results of two experimental repetitions are listed as well as the total of the two experiments

Experiment	Proportion of half sectored colonies		
	WT+ p423MET	*WT*+ p*MET:MAD3-ΔE5*	*WT*+ p*MET:MAD3*
A	3/7144	34/14603	19/6393
B	1/9562	5/5967	10/7567
Total	4/16706	39/20570	29/13960

Table 5.3 MAD3 over-expression chromosome loss assay

The rates of chromosome loss observed when mutant and full-length Mad3p are over-expressed in a wild type strain are shown below. The table shows results from two experimental repetitions and the total loss rate for these two experiments which is presented graphically in figure 5.7.

Experiment	Chromosome loss rate per thousand divisions		
	WT+ p423MET	*WT*+ p*MET:MAD3-ΔE5*	*WT*+ p*MET:MAD3*
A	0.420	2.328	2.972
B	0.105	0.838	1.322
Total	0.239	1.896	2.077

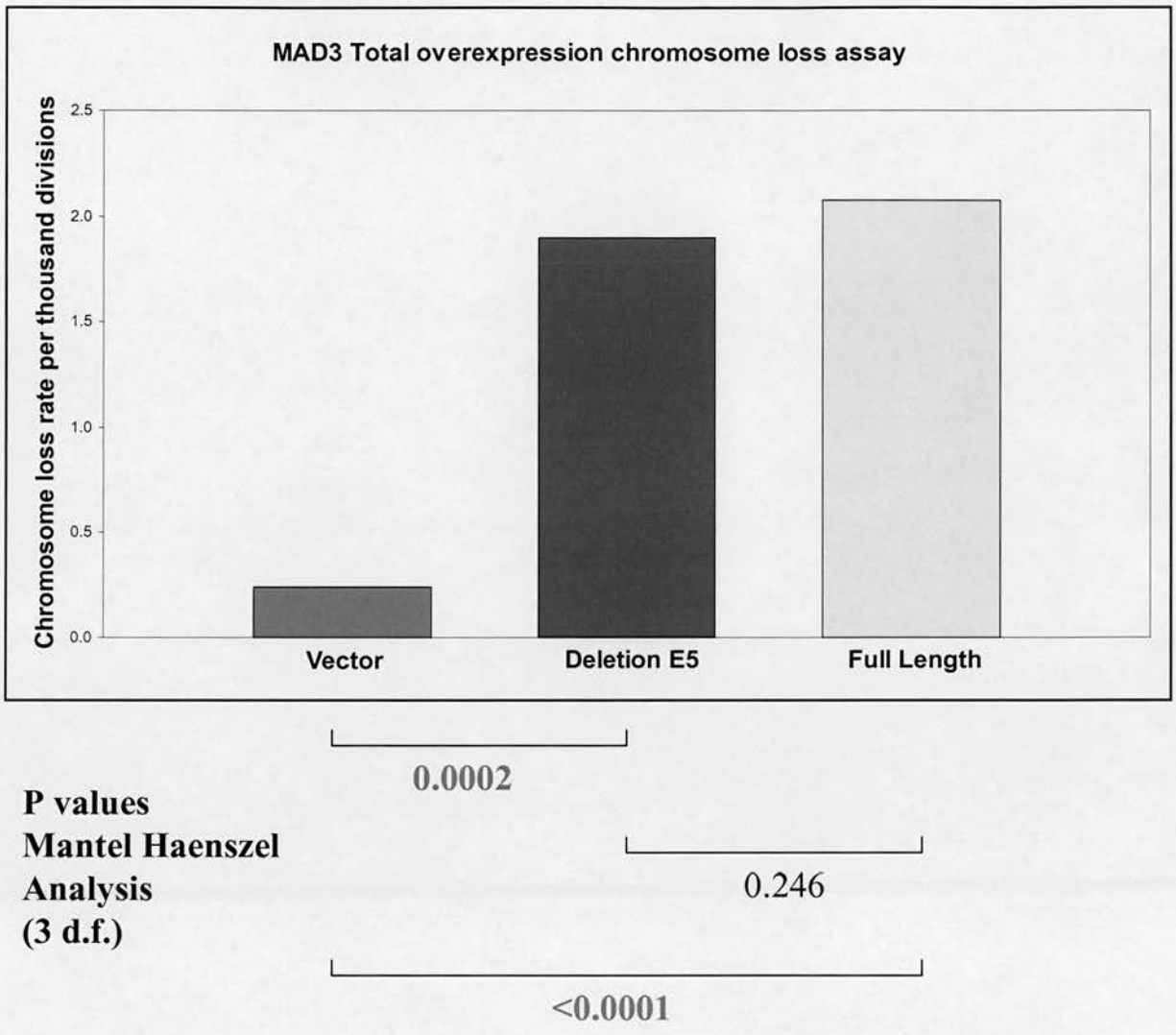

Figure 5.7 Over-expression of Mad3ΔE5p causes a chromosome loss phenotype

The graph above shows the chromosome loss rates observed when the over-expression constructs were expressed in a wild type strain. The p values resulting from Mantel Haenszel statistical analysis of the data from three experimental repetitions are shown below the graph with statistically significant values in red. Results of individual experimental repetitions and their individual analysis using chi-squared are presented in appendix 14.
The Mad3ΔE5p protein causes a chromosome loss phenotype similar to the full-length protein when over-expressed suggesting it is able to interact with Bub3p and exert dominant negative effects.

5.3.6 Over-expression of Bub1ΔE5 is Associated with an Intermediate Chromosome Loss Phenotype

The equivalent experiments were also used to analyse the ability of Bub1ΔE5p to interact with Bub3p and cause a dominant negative phenotype. The over-expression plasmids p*MET:BUB1*, p*MET:BUB1-ΔE5* and p423MET were transformed into wild type chromosome loss strains and transformants were used in benomyl sensitivity and chromosome loss assays. As in the MAD3 experiments, the benomyl sensitivity assays were unsuccessful with full-length and vector controls showing no difference in benomyl sensitivity. The total results of two repetitions of the chromosome loss experiments are shown in tables 5.4 and 5.5 and presented graphically in figure 5.8. Again over-expression of the full-length Bub1p protein produced an elevated rate of chromosome loss compared to the vector transformant ($t = 4.750$ $p < 0.0001$). However, a great deal of variation was observed in the loss rate of the full-length transformant. The results of the individual repetitions are shown in Appendix 15 and indicate the rate of loss in the full-length transformant is increased relative to the vector in both repetitions. The rate of chromosome loss observed in the BUB1ΔE5 mutant is also elevated compared to the vector alone ($t = 3.083$, $p = 0.0024$) but is intermediate between that and the full-length transformant from which it also significantly differs ($t = 2.907$ $p = 0.0018$). This is indicative of a reduced Bub1ΔE5p interaction with Bub3p. Thus, consistent with the previous data, Bub1ΔE5p seems to retain partial function but its interaction with Bub3p is compromised and may be causing a spindle checkpoint defect and chromosome segregation phenotype.

In addition there is substantial evidence from both the co-immunoprecipitation studies and the over-expression chromosome loss studies that while the interaction between Bub1ΔE5p and Bub3p is compromised, it is not entirely abolished. This is consistent with the dominant negative effect of BUB1ΔE5 as previously reported for the human V400 mutation in colorectal tumour cells (Cahill et al., 1996).

Table 5.4 BUB1 over-expression chromosome loss assay

The number of half-sectored colonies observed in the BUB1 over-expression chromosome loss assay are listed below as a proportion of total non-red colonies. The results of two experimental repetitions are listed as well as the total of the two experiments.

Experiment	Proportion of half sectored colonies		
	***WT*+ p423MET**	***WT*+ p*MET:BUB1-ΔE5***	***WT*+ p*MET:BUB1***
A	3/7144	11/13238	32/9815
B	1/9562	8/4760	12/13064
Total	4/16706	19/17998	44/22879

Table 5.5 BUB1 over-expression chromosome loss assay

The rates of chromosome loss observed when mutant and full-length Bub1p are over-expressed in a wild type strain are shown below. The table shows results from two experimental repetitions and the total of these two experiments. The total data are presented graphically in figure 5.7.
Loss rates from individual experiments and their chi-squared statistical analysis are presented in Appendix 15.

Experiment	Chromosome loss rate per thousand divisions		
	***WT*+ p423MET**	***WT*+ p*MET:BUB1-ΔE5***	***WT*+ p*MET:BUB1***
A	0.420	0.831	3.260
B	0.105	1.681	0.919
Total	0.239	1.056	1.923

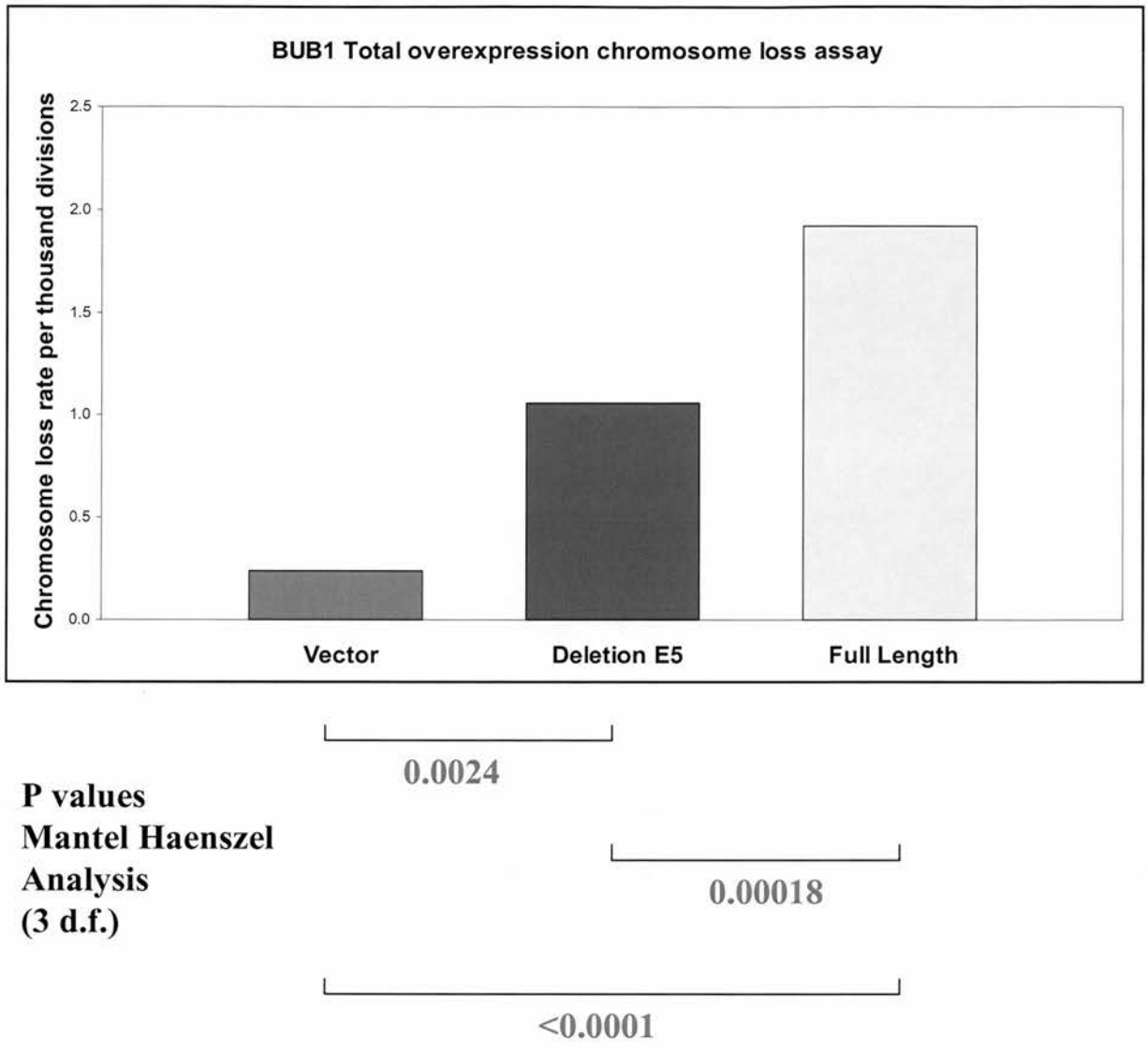

Figure 5.8 Over-expression of Bub1ΔE5p causes a chromosome loss phenotype

The graph above shows the total chromosome loss rates observed in two experiments when the over-expression constructs were expressed in a wild type strain. The data from the two individual data sets was analysed using Mantel Haenszel statistical analysis and the p values resulting from this are shown below the graph with statistically significant values in red.
The Bub1ΔE5p protein causes a chromosome loss phenotype similar to the full-length protein when over-expressed suggesting it is able to interact with Bub3p and exert dominant negative effects.

5.3.7 Mad3ΔE5 and Bub1ΔE5 Exert Mild Dominant Negative Effects

Next I wished to further investigate any dominant negative effects of the ΔE5 proteins. For this purpose the constructs in which BUB1 and MAD3 were under the control of their wild type promoters were transformed into a wild type strain and tested for benomyl sensitivity and chromosome loss phenotypes. These experiments were designed to partially mimic the heterozygous nature of the human mutations, as both full-length and mutant protein were present in the cell.

Unfortunately the results of the benomyl sensitivity assays were inconclusive and the sensitivities of the three populations could not be distinguished qualitatively. This could be due to the subtle nature of the phenotypes observed even in the full-length transformants and also previously discussed technical difficulties in observing these phenotypes. However, some conclusions can be drawn from the results of the chromosome loss studies, although it should be noted that due to time constraints these experiments were performed only once. Statistical analyses of these experiments used Chi-squared analysis due to the single repetition.

The results of the MAD3 studies are shown in figure 5.9 and indicate that a mild dominant negative phenotype is seen in the full-length transformant which significantly differs from that seen in the vector transformant (χ^2 = 9.770,p = 0.00177). This phenotype is thought to be due to a similar, but less severe, sequestering of Bub3p by Mad3p to that seen in the over-expression studies and indicates that dominant negative phenotypes can occur even when Mad3p is expressed only 2-fold. The ΔE5 transformant also shows an elevated chromosome loss phenotype compared to the vector transformant (χ^2 = 5.590, p = 0.0181, significant at the 2% confidence interval) and indistinguishable from the full-length phenotype (χ^2 = 0.915, p = 0.339) suggesting it can also exert a dominant negative effect. These results are consistent with the conclusions drawn from the over-expression experiments that Mad3ΔE5p retains a large proportion of Bub3p binding.

The results of similar expression of the BUB1 constructs are shown in figure 5.10. The full-length transformant produces a significant chromosome loss phenotype (χ^2 = 5.908, p = 0.0151) indicative of a dominant negative effect. The ΔE5 transformant shows a much milder chromosome loss phenotype which does not significantly differ

from the vector transformant ($\chi^2 = 0.661$, $p = 0.416$) but is different to the full-length transformant ($\chi^2 = 3.649$, $p = 0.0561$ significant only at 6% confidence interval), consistent with its greater reduced ability to interact with Bub3p. Thus it appears that if Bub1ΔE5p does exert a dominant negative effect, it is a very mild one and cannot be detected at 2-fold over-expression in *S.cerevisiae*.

This assay does however have limitations as it is actually performed in a haploid environment which is not truly representative of diploid tumour cells. The strains contain only haploid amounts of the spindle checkpoint proteins other than those transformed in on the extrinsic plasmids, which may affect the protein interactions and dominant negative effects displayed.

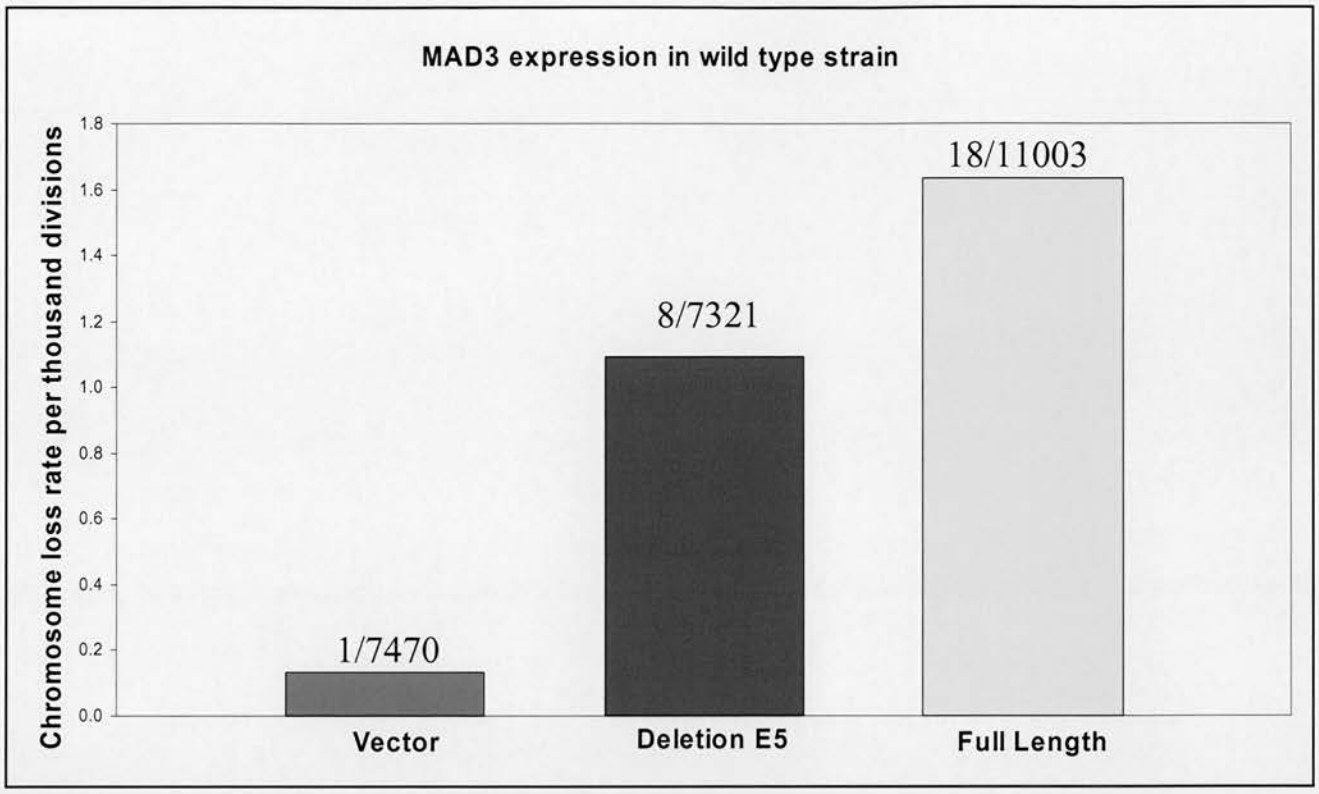

P values Chi-squared Analysis (1 d.f.)

0.0181

0.339

0.00177

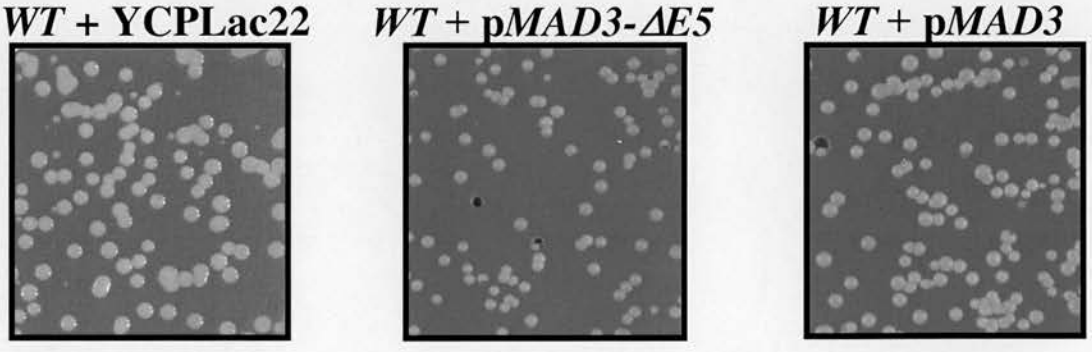

Figure 5.9 Expression of Mad3ΔE5p in a wild type strain causes a chromosome loss phenotype

The graph above shows the chromosome loss rates observed when the MAD3 constructs under the control of their wild type promoters were expressed in a wild type strain. The number of half sectored colonies as a proportion of total colony number are shown for each transformant population and p values resulting from statistical analysis of the counts are shown below the graph. The Mad3ΔE5p protein causes a chromosome loss phenotype similar to the full-length protein consistent with over-expression studies and suggesting it is able to exert a dominant negative effect.

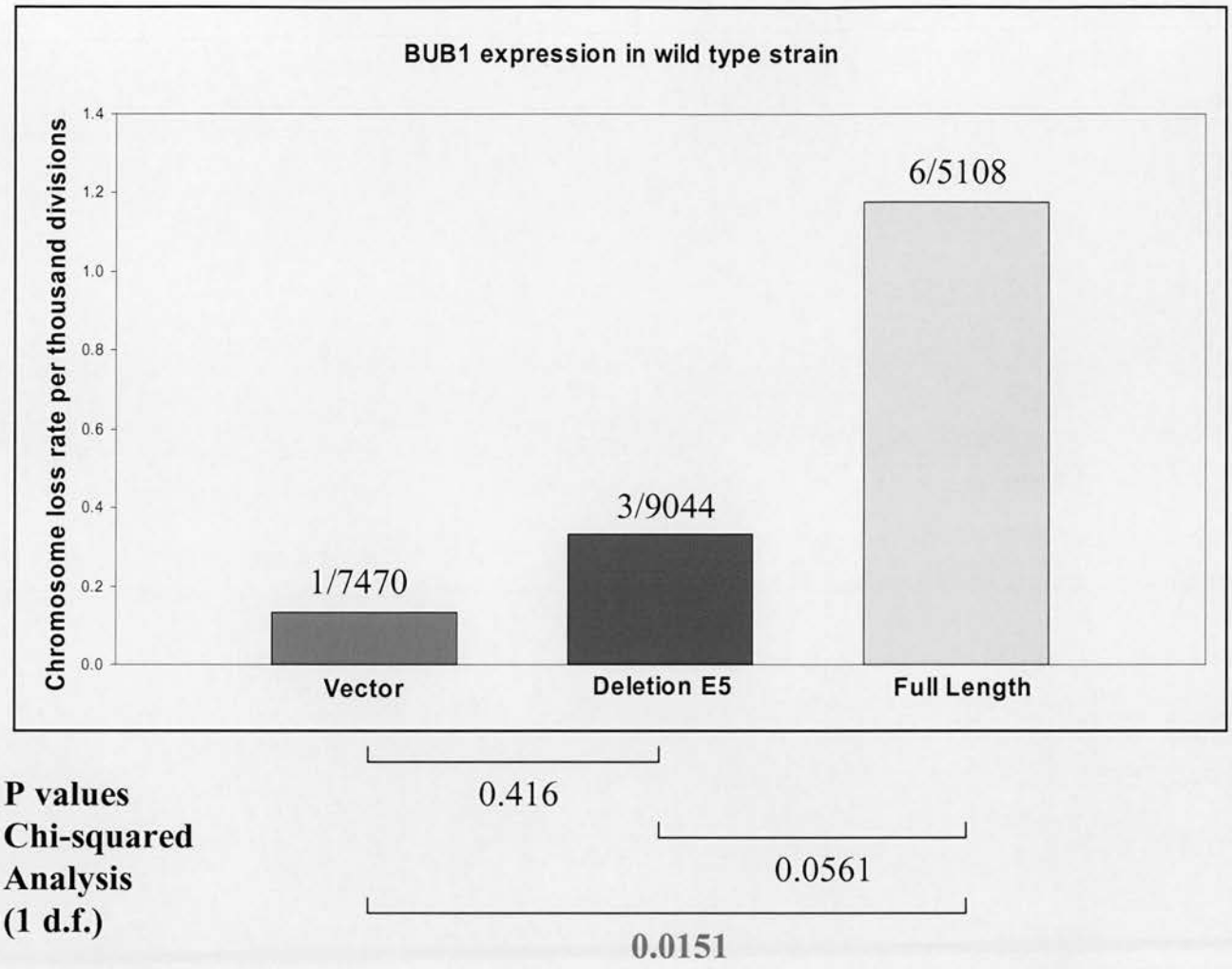

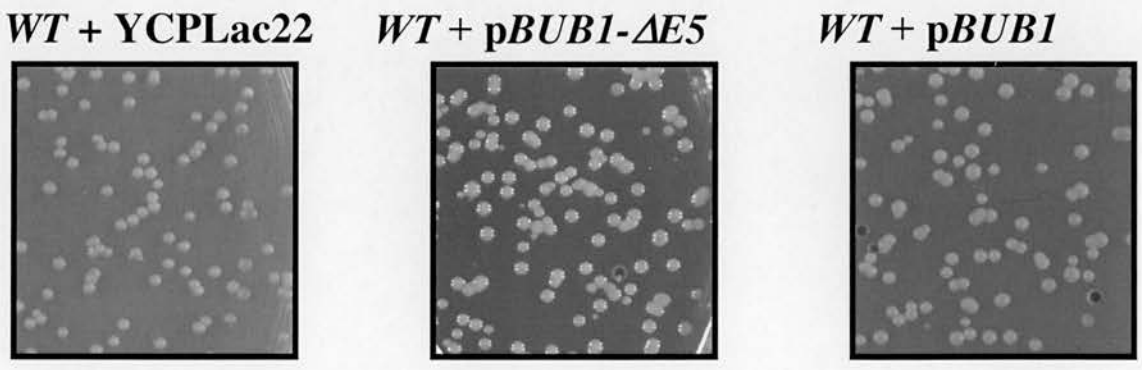

Figure 5.10 Expression of Bub1ΔE5p in a wild type strain does not cause a chromosome loss phenotype

The graph above shows the chromosome loss rates observed when the BUB1 constructs under the control of their wild type promoters were expressed in a wild type strain. The number of half sectored colonies as a proportion of total colony number are shown for each transformant population and p values resulting from statistical analysis of the counts are shown below the graph. The Bub1ΔE5p protein causes an intermediate chromosome loss phenotype suggesting it does not exert a dominant negative effect.

5.4 Discussion

The aim of this work was to assess the underlying cause of the checkpoint and mis-segregation defects associated with the ΔE5 mutations at the protein level. The results presented demonstrate that Mad3ΔE5p and Bub1ΔE5p proteins are as stable as the full-length proteins both at wild type and over-expression levels. Thus the defects in the ΔE5 mutants do not appear to be due to altered concentration of the deleted Mad3p or Bub1p proteins. Further investigation showed that Mad3ΔE5p has a reduced affinity for Cdc20p and Bub3p and the amount of Mad2p in a Mad3p-Bub3p-Mad2p complex is also reduced in the ΔE5 mutant. The Bub1ΔE5p protein forms interactions with Bub3p with a reduced affinity and is aberrantly phosphorylated compared to the full-length protein. Thus it appears that a reduction in specific protein complexes, known to be important in spindle checkpoint function, and altered protein modifications are responsible for the phenotypes observed in the MAD3ΔE5 and BUB1ΔE5 mutants.

The area removed by ΔE5 is predicted to mediate interactions with Cdc20p. This interaction between Mad3p and Cdc20p is disrupted in the ΔE5 mutant and there is initial evidence of its disruption in the Bub1ΔE5p protein but this requires further clarification using a *bub1Δ* CDC20-myc strain. The Bub1p-Cdc20p interaction has previously only been observed when Bub1p is over-expressed in a 2-hybrid system *in vitro* or in the absence of Mad3p, so the significance of this observed interaction *in vivo* is not clear (Hardwick et al., 2000).

The ability of the Bub1p and Mad3p proteins to interact with Bub3p is also altered in the ΔE5 mutants. This would not be expected from the amino acid sequence removed by ΔE5, as the domain predicted to interact with Bub3p remains intact. This suggests that there may be additional Bub3p interaction domains towards the N-terminals of the proteins. Alternatively, the removal of the E5 region may alter the tertiary structure of the Mad3p and Bub1p proteins and affect their ability to interact with Bub3p, although in both cases there is a reduction rather than an abolishment of interaction.

With respect to defective formation of the Bub1p-Bub3p complex, this is predicted to prevent formation of the Mad1p-Bub1p-Bub3p signalling complex, thought to be essential for effector complex formation and inhibition of the APC/C and chromosome segregation. This in turn could cause defects in chromosome segregation and loss effects if defective chromosome attachment is not detected and metaphase to anaphase transition continues. Defects in Cdc20p, Mad2p and Bub3p binding by Mad3p would be predicted to affect formation of the APC/C inhibitor complex causing spindle checkpoint and chromosome segregation defects through a similar mechanism.

The phosphorylation of Bub1p is reduced and altered in the ΔE5 mutant but Mad3p is normally phosphorylated. The significance of phosphorylation in the spindle checkpoint is not clear but both Mad3p and Bub1p are phosphorylated during mitosis. The aberrant phosphorylation of Bub1p is unlikely to be due to deletion of specific phosphorylated amino acids, as modified bands of equivalent sizes are observed in both the ΔE5 and full-length proteins. This effect is not related to the reduced interaction with Bub3p. The Bub3p protein kinase is thought to be involved in phosphorylation of Bub1p, however, over-expressed full-length Bub1p in a null *bub3* strain does not show the aberrant phosphorylation effect shown in the ΔE5 protein, suggesting the reduced Bub1p-Bub3p interaction is not causative of the aberrant phosphorylation effect. However, the reduced interaction between Bub1p and Bub3p may be a function of the reduced Bub1p phosphorylation. This could be further investigated using known *bub1* mutants which form defective interactions with Bub3p, such as *bub1-1*. I attempted to investigate the phosphorylation of Bub1p in these *bub1-1* mutants but the endogenous Bub1p protein in total cell extracts from the *bub1-1* strain could not be detected with current antibodies. Thus in order to confirm whether other Bub1p mutant proteins, with reduced Bub3p interactions, are also associated with aberrant phosphorylation, cloning of the mutants such as *bub1-1* into over-expression constructs would be required, or the development of more sensitive antibodies. These experiments were not within the scope of this thesis. A further possibility is that the aberrant phosphorylation of Bub1p is actually a result of its inability to arrest at the spindle checkpoint and the proportion of cells in each of the stages of the cell cycle and thus the extent of cell

cycle stage specific Bub1p phosphorylation may be altered in Bub1ΔE5. This is not consistent with our results which exhibit extensive phosphorylation of full-length Bub1p observed in extracts both in the presence of and the absence of nocodazole arrest.

Therefore it is likely that reduction in the protein interactions and/or in Bub1p phosphorylation contribute to the spindle checkpoint and chromosome segregation defects exhibited by the ΔE5 mutants. These protein alterations may be directly due to the ΔE5 deletion or may all be a result of aberrant kinetochore localisation of the proteins, induced by ΔE5. However, we would then expect all the interactions to be reduced to the same extent which is not consistent with the results obtained. However, the contribution of mislocalisation of the ΔE5 proteins to the spindle checkpoint deficient phenotype may be a topic for future investigation.

Bub1p and Mad3p are homologous and most of the area removed by ΔE5 falls into a functional domain conserved between Bub1p and Mad3p. Thus the effect of deletion of E5 on the protein function of Bub1p and Mad3p would be expected to be similar. The Bub1p and Mad3p mutants do both show a reduced ability to interact with Bub3p, although the reduction is greater in the BUB1 mutant. There are some further differences between the protein functions of Bub1ΔE5p and Mad3ΔE5p, in that Cdc20p interaction is reduced in Mad3ΔE5p but the effect on this interaction is not clear in Bub1ΔE5p. In addition the Bub1p mutant protein is aberrantly phosphorylated unlike Mad3ΔE5p.

The differences in protein function may be due to differences in the normal function of Mad3p and Bub1p in the checkpoint or may relate to differences in the primary structure of the proteins. Bub1p and Mad3p are homologous showing most similarity in the conserved domains, CD1 and CD2 however they do show sequence variations which may relate to their differing functions and phenotypes. The tertiary structures of Mad3p and Bub1p may also differ and these disparities may in part explain the diversities in the phenotypes of the ΔE5 mutants. Alternatively, the less severe phenotype exhibited in MAD3ΔE5 compared to BUB1ΔE5 may be due to the greater proportion of the Bub3p binding activity retained by the Mad3ΔE5p protein

(approximately 65%) as shown by both co-immunoprecipitation analysis and in the over-expression chromosome loss experiments.

The defects in Bub1ΔE5p function and the spindle checkpoint defects are unlikely to be attributable to the additional variations in the sequence of the ΔE5 plasmid out with the area of the deletion. As previously discussed in chapter 3, these alterations affect unconserved amino acids or result in conservative changes. An amino acid alteration in conserved domain 2 of Bub1p is altered from a Serine to a threonine. This may potentially affect the phosphorylation of Bub1p but as serine kinases also phosphorylate threonine residues, and this residue is actually a conserved threonine in several other species, this is unlikely to have a significant effect either on protein phosphorylation or checkpoint function. Thus the phenotypes exhibited by the BUB1ΔE5 mutant can be attributed to the ΔE5 mutation.

To investigate protein interactions, some of the experiments used over-expression of the full-length and ΔE5 proteins. These methods have previously been used to examine such protein interactions (Warren et al., 2002). The over-expression nature of the system may not directly reflect the interactions seen at wild type expression levels, but they do clarify the ability of the mutant proteins to form these interactions. In addition the use of the full-length proteins as controls with which to compare the intensity of the interactions increases the validity of the results.

In addition to clarifying the Bub3p binding defects in the ΔE5 mutants, the over-expression chromosome loss experiments provide information about the ability of the ΔE5 mutants to convey dominant negative phenotypes through interaction with and sequestering of Bub3p. Mad3ΔE5p retains much of its ability to interact with Bub3p in the chromosome loss assays, exhibiting a similar dominant negative phenotype to the full-length protein. The expression of Mad3ΔE5p from its wild type promoter to mimic heterozygosity of the human mutations, results in a similar increased chromosome loss phenotype to the full-length transformant. This indicates that the Mad3ΔE5p protein could potentially exert a dominant negative effect on the spindle checkpoint in heterozygous cells, abrogating the spindle checkpoint and leading to chromosomal instability.

Over-expression of the Bub1ΔE5p protein also leads to a chromosome loss phenotype consistent with its ability to bind some Bub3p. This phenotype is intermediate between the vector and full-length transformants and is less severe than in the Mad3ΔE5p mutant, presumably due to the greater reduction in Bub3p binding of Bub1ΔE5p as shown in co-immunoprecipitation experiments. This intermediate phenotype was also observed in the second set of experiments, where the heterozygous nature of the mutations are investigated. However, analysis of the vector and BUB1ΔE5 transformants results showed no statistically significantly differences. This suggests that Bub1ΔE5p does not exert dominant negative effects, which is not consistent with the over-expression assays or Cahill analysis of the human V400 mutation. However, the wild type level assays assessing the Bub1p proteins were repeated only once and do not fully reflect the diploid nature of the heterozygous cells in a human system and therefore have their limitations. The mild nature of the chromosome loss phenotypes exhibited in the over-expression and dominant negative experiments indicate that very large sample sizes would be required to clarify the data. Further repetition of these assays may be undertaken in the future to confirm these effects.

Thus to summarise the yeast functional work indicates the ΔE5 mutations are associated with a benomyl sensitivity phenotype indicative of a mitotic defect. Further analysis shows this to be due to aberrant spindle checkpoint function and that the mutations also confer a chromosome segregation defect. These phenotypes are attributable to the disruption of specific protein interactions and aberrant phosphorylation in the case of Bub1p. Mad3ΔE5p forms reduced interactions with Cdc20p and with a Bub3p-Mad2p complex. The interaction between Bub3p and Bub1p is also compromised in the ΔE5 mutants. There is some evidence that the mutant proteins are able to exert mild dominant negative effects.

Future directions for this yeast functional analysis could investigate the interactions of the ΔE5 mutants using yeast 2-hybrid analyses, particularly those interactions which have proved difficult to observe with co-immunoprecipitation experiments, for example, interactions between Bub1p and Mad1p and Bub1p and Cdc20p. A 1-hybrid assay has previously been used to investigate the ability of

mutants to localise to the kinetochore in budding yeast. Localisation to the kinetochore may be important for formation of important interactions and for correct phosphorylation and therefore may have relevance to the effects and phenotypes shown by the ΔE5 mutants. Further analysis of protein localisation and interactions using fluorescently tagged proteins could be investigated in *S.pombe* which are larger in size and have larger chromosomes, centromeres and kinetochores. Additionally, *in silico* or *in vitro* work such as X-ray crystallography could investigate the effects of the ΔE5 mutations on the structure of the Mad3p and Bub1p proteins and whether this relates to the defective interactions shown.

The ability of the ΔE5 proteins to retain some Bub3p binding and the mild phenotype seen in the over-expression and dominant negative experiments may suggest that the checkpoint defects conferred by the ΔE5 mutations in humans are minor and would lead to a slightly increased chromosomal instability rate. This may well explain the high frequency of detection of the BUBR1ΔE5 mutations in tumours, whereas other studies aiming to identify mutations in spindle checkpoint genes in tumours have revealed few variants. The ΔE5 mutants may alter the chromosomal stability of the cell to a level which is tolerated, whereas other mutations may produce such severe defects that they induce apoptosis and lethality.

To further our knowledge of the ΔE5 mutations in the human system we wished to further investigate the effect of BUBR1ΔE5 in human cell lines. The aim was to determine whether BUBR1ΔE5 causes a mitotic checkpoint defect and chromosome instability in diploid colon cancer cell lines. In addition we wished to investigate the effect of BUBR1ΔE5 and BUB1V400 on the formation of spindle checkpoint complexes using immunofluorescence and co-immunoprecipitation experiments. These experiments are discussed in further detail in chapter 6.

Chapter 6: The Functional Analysis of BUBR1ΔE5 in Human Cell Lines

6.1 Introduction

The findings from the functional analysis in budding yeast indicated that ΔE5 affected chromosome segregation and the spindle checkpoint. Thus it was important to investigate the consequences of the ΔE5 mutations in a human system as this has a wider relevance to colorectal cancer. The effect of the BUB1 V400 mutation was previously analysed in human diploid tumour cell lines and shown to induce phenotypes similar to those observed in aneuploid cell lines (Cahill et al., 1998).

Specifically, Cahill et al showed that aneuploid cell lines exhibit an abnormal cell phenotype upon nocodazole induced mitotic arrest compared to diploid cell lines. The diploid cells were shown to arrest at the G2/M transition, with large numbers of cells showing condensed chromosomes, indicative of a sustained mitotic block. Fewer aneuploid cell lines maintained this block and in general they showed a reduced mitotic index with a less defined peak, indicative of defective mitotic arrest. In addition, the aneuploid cell lines show a similar defective response to treatment with colcemid and a large proportion of the aneuploid cells continued to synthesise DNA after treatment with either drug, unlike the diploid cell lines. Two of these aneuploid cell lines were shown to harbour mutations in the spindle checkpoint gene *BUB1*. V429 contained a missense mutation resulting in the substitution of a tyrosine for a conserved serine and V400 showed an alteration of a splice donor site leading to a 197 base pair deletion homologous to BUBR1ΔE5. Both mutations were heterozygous with the other allele being wild type and occurred only in somatic tumour tissue (Cahill et al., 1998).

Subsequent expression of these mutant proteins was achieved by Cahill et al via an inducible expression system using the Tet-On strategy (Clontech). A stable Tet-On cell line is generated by transfection of the pTet-On plasmid, based on the *E.coli* tetracycline-resistance operon, encoding the reverse tetracycline repressor, rTetR and

integrants are selected using the neomycin resistance marker on the plasmid. These stable cell lines can then express the reverse tetracycline-controlled transactivator, rtTA. This consists of the N-terminal of the Tetracycline repressor, providing the control by tetracycline and doxycycline, fused to the C-terminal of the Herpes simplex virus VP16 activation domain, converting the repressor to an activator. In addition, the pTet-On plasmid contains 4 amino acid changes in the tetracycline repressor domain resulting in expression of the rtTA in the presence of doxycycline rather than in its absence. The response plasmids, pBI-GFP in these experiments, are transfected into the pTet-On stable cell lines, which can be induced to produce rtTA by addition of the antibiotic, doxycycline, to the culture media. The target plasmids contain the gene of interest (in this case *BUB1*) under the control of a promoter containing a Tetracycline Responsive Element (TRE) and, within it, seven copies of the tetracycline operator sequence. Thus expression from this promoter is induced in the presence of the rtTA and hence in the presence of doxycycline. The promoter region in the pBI-GFP plasmids, P_{bi-1}, is bi-directional allowing co-expression of BUB1 and GFP and easy recognition and selection of BUB1 expressing cells through their fluorescence. Overall, this provides a system in which expression of the BUB1 and GFP proteins from the P_{bi-1} promoter can be induced by addition of antibiotics. In addition, expression from this promoter can be altered in a dose dependent manner producing over-expression of the target protein up to 10,000 fold. This system is summarised in figure 6.1.

Figure 6.1: An inducible over-expression system used to analyse the effect of BUB1 mutations on mitotic checkpoint arrest

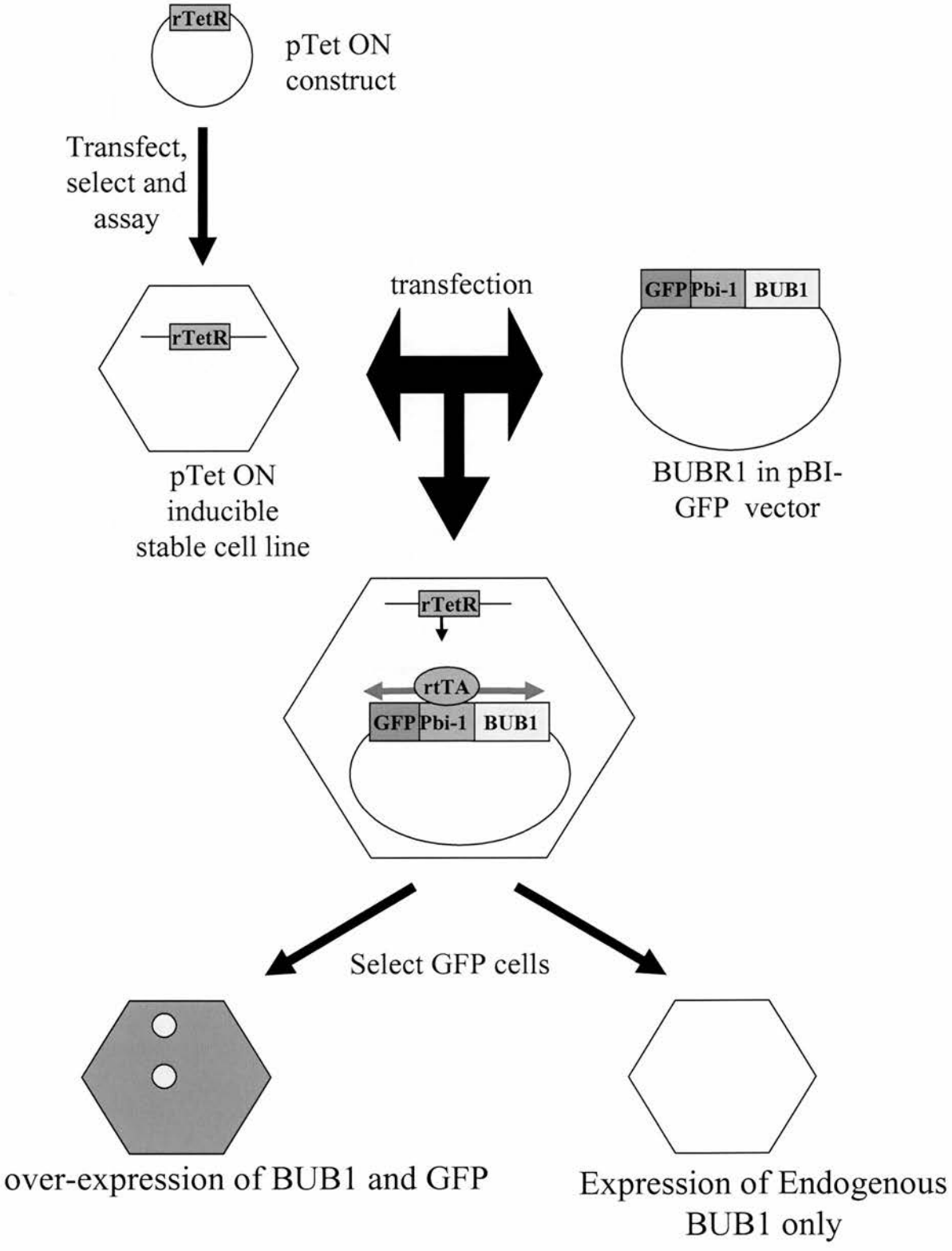

In Cahill et al., the system was used to express the mutant BUB1 proteins in diploid cell lines using the wild type *BUB1* plasmid as a control. Cells successfully transfected with mutant plasmids were isolated by Fluorescence Activated Cell Sorting (FACS) on the basis of GFP expression. The phenotypes of the cells were analysed after nocodazole treatment and the cells transformed with the mutant plasmids exhibited similar phenotypes to the aneuploid cell lines previously analysed including a reduced mitotic index and increased S-phase re-entry compared to those transfected with the wild type plasmid. Thus these mutant BUB1 proteins do appear to confer checkpoint defects when introduced into diploid cell lines. In addition, co-transfection of the mutant plasmid with the wild type plasmid produces a similar phenotype, suggesting the mutant BUB1 proteins exert dominant negative effects.

These phenotypes are similar to the checkpoint defects exhibited by the yeast BUB1ΔE5 and MAD3ΔE5 mutants and we wished to further establish the effects of the BUBR1ΔE5 mutant in the human system using similar experiments. This required the construction of pTet-On stable cell lines in a diploid colon cancer cell line background and also construction of the wild type and mutant ΔE5 *BUBR1* coding sequences in the pBI-GFP plasmids. The wild type and mutant BUB1 constructs described above form suitable controls for experimental verification. Thus the BUB1 mutant plasmids were also required to be transformed into pTet-On inducible diploid cell lines and the effect of the mutants proteins on mitotic arrest, mitotic index and bromodeoxyuridine (BrdU) incorporation, indicative of DNA synthesis, were to be examined following mitotic arrest with microtubule poisons.

The aim was to demonstrate checkpoint deficiency of the mutant proteins and to assess the formation of spindle checkpoint complexes using immunofluorescence and co-immunoprecipitation experiments. Previously published antibodies were raised to the C-terminal or a large part of the N terminal of BUB1 and BUBR1. It was necessary to construct antibodies to the very N terminal sequences of BUB1 and BUBR1 as the tertiary structure of this area of the proteins was unlikely to be disrupted by the deletion of E5 and thus N terminal antibodies should be able to recognise both the wild type and mutant proteins. We also aimed to construct GFP fusion BUB1 and BUBR1 constructs to use in immunofluorescence experiments to investigate the localisation and interactions of the mutant and wild type proteins.

This provides advantages over the budding yeast system in that the localisation of the mutant proteins to kinetochores can be visualised. Finally, some proteins thought to interact with BUB1 and BUBR1 have no known homologues in yeast such as CENP-E and CENP-F and the effect of these interactions could be investigated using immunofluorescence in human cell lines.

6.2 Methodological Overview

6.2.1 Chemical Transformation into *E.coli*

A full-length construct of BUBR1 was obtained from Dr Stephen Taylor (Taylor et al., 2001). The full-length and mutant BUB1 plasmids previously analysed were obtained from Professor Bert Vogelstein (Cahill et al., 1998). These were transformed into *E.coli* TOP 10 cells as described in 2.5.2 and plated on selective media containing ampicillin.

6.2.2 Colony Selection and Plasmid Identification

Positive transformants were selected as described in 2.5.3 and analysed by colony PCR (2.4.3). Positive transformants were cultured (2.5.5), their DNA isolated by miniprep analysis as described in 2.33 and sequenced to confirm the identity of the insert as described in 2.6.

6.2.3 Polymerase Chain Reaction

Expand Hi fidelity PCR as described in 2.4.2 was used to amplify the two sections of coding sequence flanking the area of ΔE5 sec1 and sec2 using the human BUBR1 section primers. The pcDNA-3 Myc hMad3 plasmid (2.2.2) was used as a template. Correct amplification of the sections was confirmed by agarose gel electrophoresis, as described in 2.4.4 and sequencing of the PCR reactions, as described in 2.6, to determine accuracy of the PCR.

In addition Expand Hi fidelity PCR was used to amplify the full coding sequence of wild type BUB1 and BUBR1 for construction of the GFP fusion plasmids.

6.2.4 Restriction Digestion

Restriction sites for cloning inserts were carefully designed to be compatible with the plasmids while retaining the reading frame of any tags or promoters and to ensure they were single cutters and the fragments were inserted in the correct orientation.

Restriction digestions were performed on the amplified sections to construct the ΔE5 sequence and on the ligated sections to prepare them for ligation with the vector backbone. They were also used to switch the full-length coding sequences between different plasmids and to digest full-length PCR products for insertion into new

vectors. Various enzymes were used and these are discussed with cloning strategies in the results section. Digestion reactions were carried out as described in 2.5.4 and resulting fragments were purified using gel purification as described in 2.5.5.

Digests with two enzymes were performed sequentially with an ethanol precipitation step in between, to remove incompatible buffers.

6.2.5 Ligation

The digested fragments of sec1 and sec2 for BUBR1 were ligated together as described in 2.5.6 to produce the insert for the cassette. The insert of sec1 and sec2 and the appropriate vector were then appropriately digested with restriction enzymes at external sites. The gel purified insert was then ligated into the gel purified vector as described in 2.5.6. Restriction and then ligation reactions were used to switch inserts between different vectors ensuring the vectors were in frame for correct translation.

6.2.6 Generation of pTet-On Stable Cell Lines

Stable pTet-On cell lines were generated with DLD1 and HCT116 and LoVo diploid colorectal carcinoma cell lines. The cell lines were maintained as described in 2.11.2. They were transfected with the pTet-On plasmid using FuGene reagent as described in 2.11.3 and stable integration of the plasmid was selected using Geneticin. The populations of transfected cells underwent serial dilutions to allow isolation of single cell clones as described in 2.11.3.

The single cell clones were tested for pTet-On activity using luciferase assays as described in 2.11.4. β-galactosidase assays were used to normalise for cell number and these two assays were used to identify the clones with greatest inducibility. This was necessary as the pTet-On plasmid may have integrated into a silent site and thus would not be expressed or induce the test plasmids. Clones with at least 2-fold inducibility were grown on a large scale and frozen down for use in subsequent assays to test the effect of the BUBR1ΔE5 mutant.

6.2.7 Generation of Double Stable Cell Lines

The inducible cell lines were transfected with the test and control BUBR1 and BUB1 pBI constructs using FuGene reagent as described in 2.11.3 and double stable cell lines were selected with Geneticin and Hygromycin.

6.3 Results

6.3.1 Construction of *BUB1* and *BUBR1* Plasmids

The BUB1 wild type and mutant vectors obtained from Professor Vogelstein and the BUBR1 vector obtained from Dr Taylor were manipulated to form various BUB1 and BUBR1 constructs for analysis. To provide a renewable source of the coding sequences in a more extensive multiple cloning site (MCS) than that present in the functional vectors the inserts were placed into pBluescript. This provided increased options for construction of the required vectors. Initial sequencing indicated that some of the cloning sites in the pBI vectors were altered which limited the cloning possibilities. The coding sequence of BUBR1 was also transferred to a pBI-GFP vector. This construct was important for investigation of the effect of BUBR1ΔE5 on mitotic checkpoint function. It allows us to differentiate the specific effects attributable to the BUBR1ΔE5 mutant protein from any effects produced due to the over-expression of the BUBR1 protein in general. The mutant and coding sequences were also transferred into Enhanced Green Fluorescent Protein vectors (EGFP) in order to produce GFP-fusion proteins for use in immunofluorescence experiments.

Restriction maps of each of the coding sequences and restriction maps/diagrams of the vectors were obtained and created. These were used to identify appropriate single cutter restriction enzymes whose recognition sites were present in the MCS of the vectors and which cleaved at the termini of the insert but not within the coding sequence. The selected enzymes were also checked for compatibility with the all new vector to ensure a single suitable site was present. The orientation of the insert considerably narrowed the scope of suitable restriction sites. Once suitable restriction enzymes had been identified, these were used to excise the insert and digest the vector before both were purified and ligated together.

The coding sequences of *BUB1*, *BUB1V400*, *BUB1V429* and *BUBR1* were removed from their original vector background and transferred into pBluescript to allow for easy manipulation of the coding sequences and to provide maximum compatible restriction sites for future cloning. The wild type and mutant *BUB1*

coding sequences were excised from the pBI-GFP vectors by digestion with Not1 and Sal1 unique restriction sites and purified using gel purification. The pBluescript vector was digested with the same enzymes and purified using a PCR purification method. These were ligated together and transformed into chemically competent *E.coli* strain. A map of one of the BUB1 pBluescript constructs generated is shown in figure 6.2.

Figure 6.2 BUB1 and BUBR1 coding sequences were transferred into pBluescript vectors

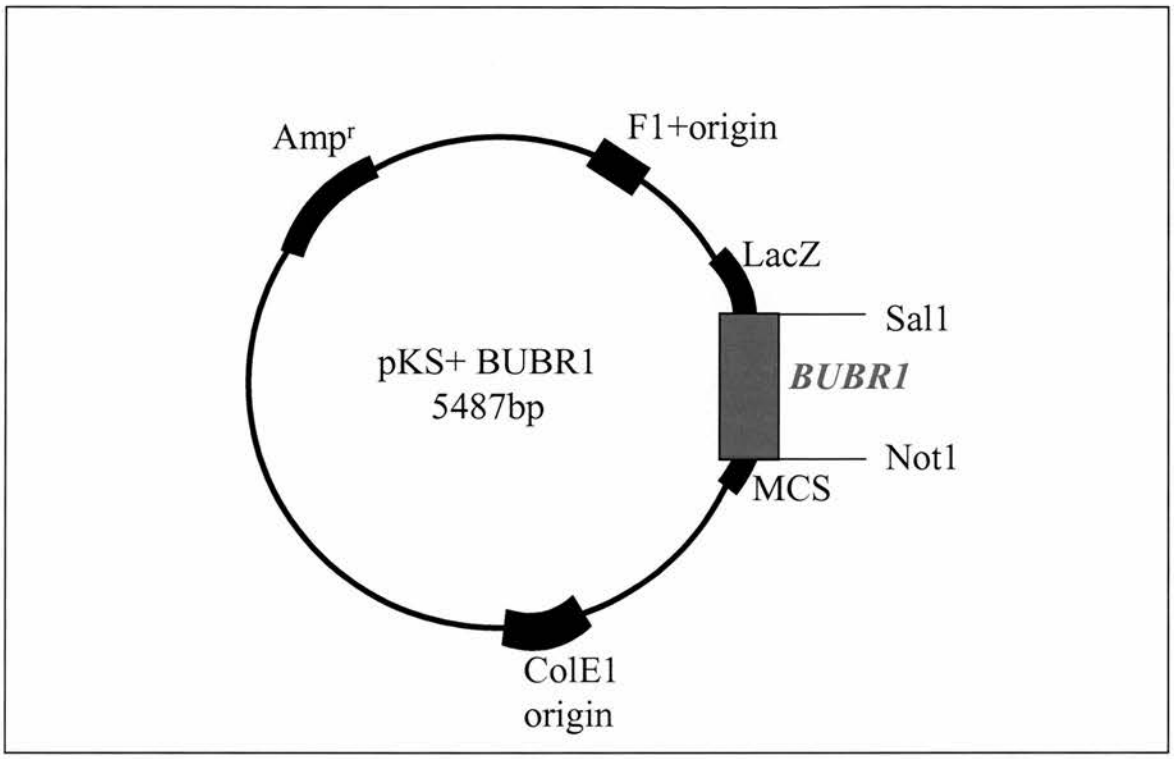

BUBR1 was similarly cloned into pBluescript using Not1 and Sal1 restriction sites. These sites were also used to excise the full-length BUBR1 for cloning into pBI-GFP. A BUBR1 pBI-GFP construct was required as a control for investigating the effect of BUBR1ΔE5 on mitotic checkpoints. The pBI-GFP vector was gel purified from the digested BUB1 pBI-GFP construct and the Not1/Sal1 BUBR1 fragment was ligated with it. Colony PCR and sequencing analysis of 94 clones identified 6 containing *BUBR1*, a recovery of 6.4%. A map of one of the constructs generated is shown in figure 6.3.

Figure 6.3 BUBR1 coding sequences were transferred into pBI-GFP vectors for use in an inducible expression system

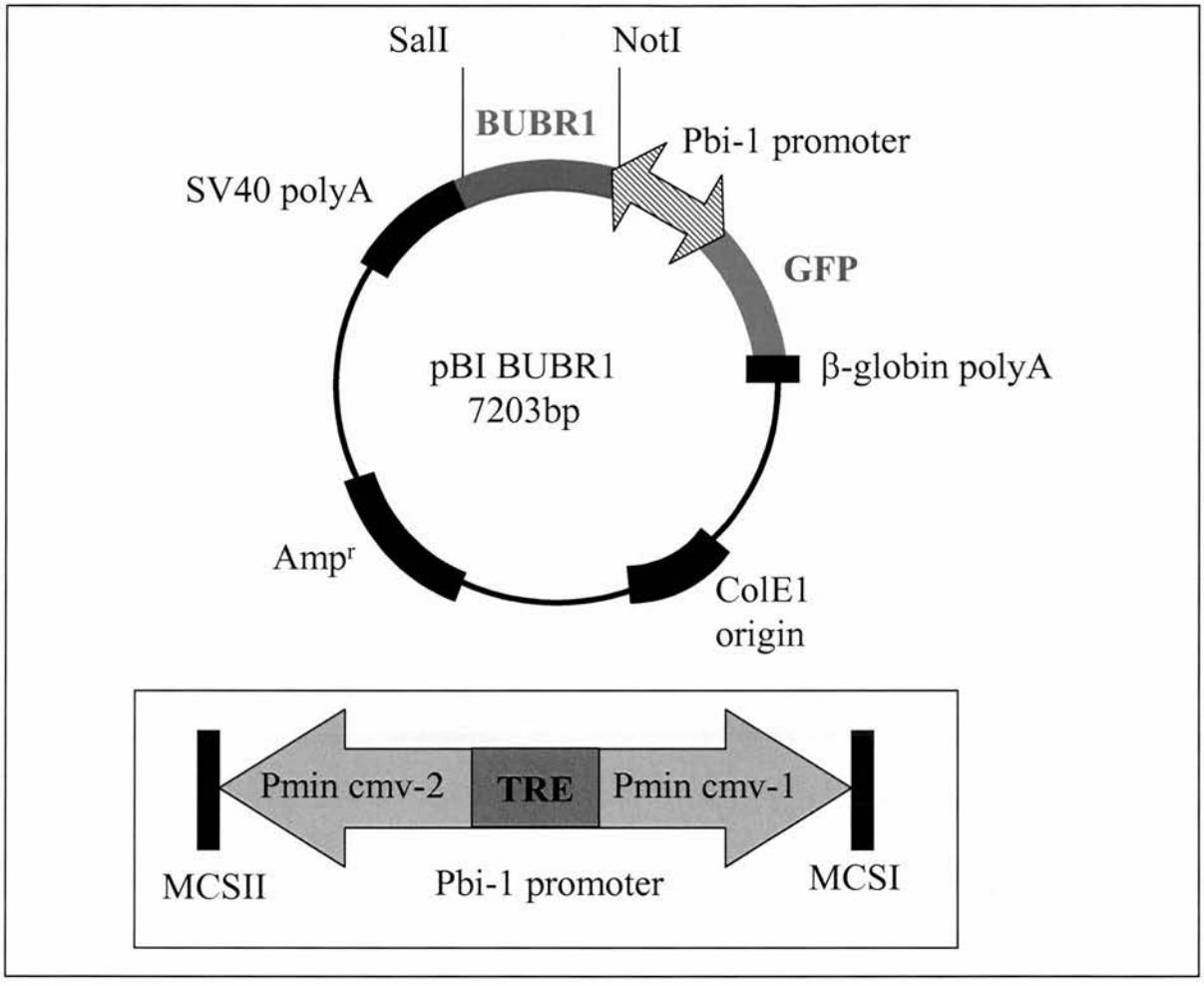

The wild type and mutant *BUB1* and *BUBR1* coding sequences were cloned into EGFP constructs in order to generate GFP-fusion proteins for use in localisation and interaction studies. We decided to construct these so that the GFP tag was situated at the N-terminal of the BUB1 and BUBR1 proteins as any effect on the primary structure translation or folding of the protein would be less likely to affect an N-terminal tag.

Unfortunately, due to the absence of compatible unique restriction sites between the vector MCS and the gene sequences this has proved difficult. Initially the method involved the PCR amplification of the entire coding sequence from the pBluescript construct using primers with restriction sites complimentary to those in the MCS of EGFP-C1; BspEI and BamHI for *BUB1* and SacII and SmaI for *BUBR1*. These primers did not amplify very successfully and optimisation of the PCR was difficult and time consuming. However, eventually products were obtained and these were digested and ligated into the similarly digested EGFP vector. Analysis of 93 potential *BUB1* wild type clones identified 2 containing the wild type sequence and a map of this construct is shown in figure 6.4, but analyses of 186 *BUB1V429* clones and 186 deletion clones for *BUB1V400* and 93 clones for *BUBR1* were all negative. Thus a new strategy was employed for cloning these.

Figure 6.4 Construction of BUB1 and BUBR1 EGFP fusion vectors

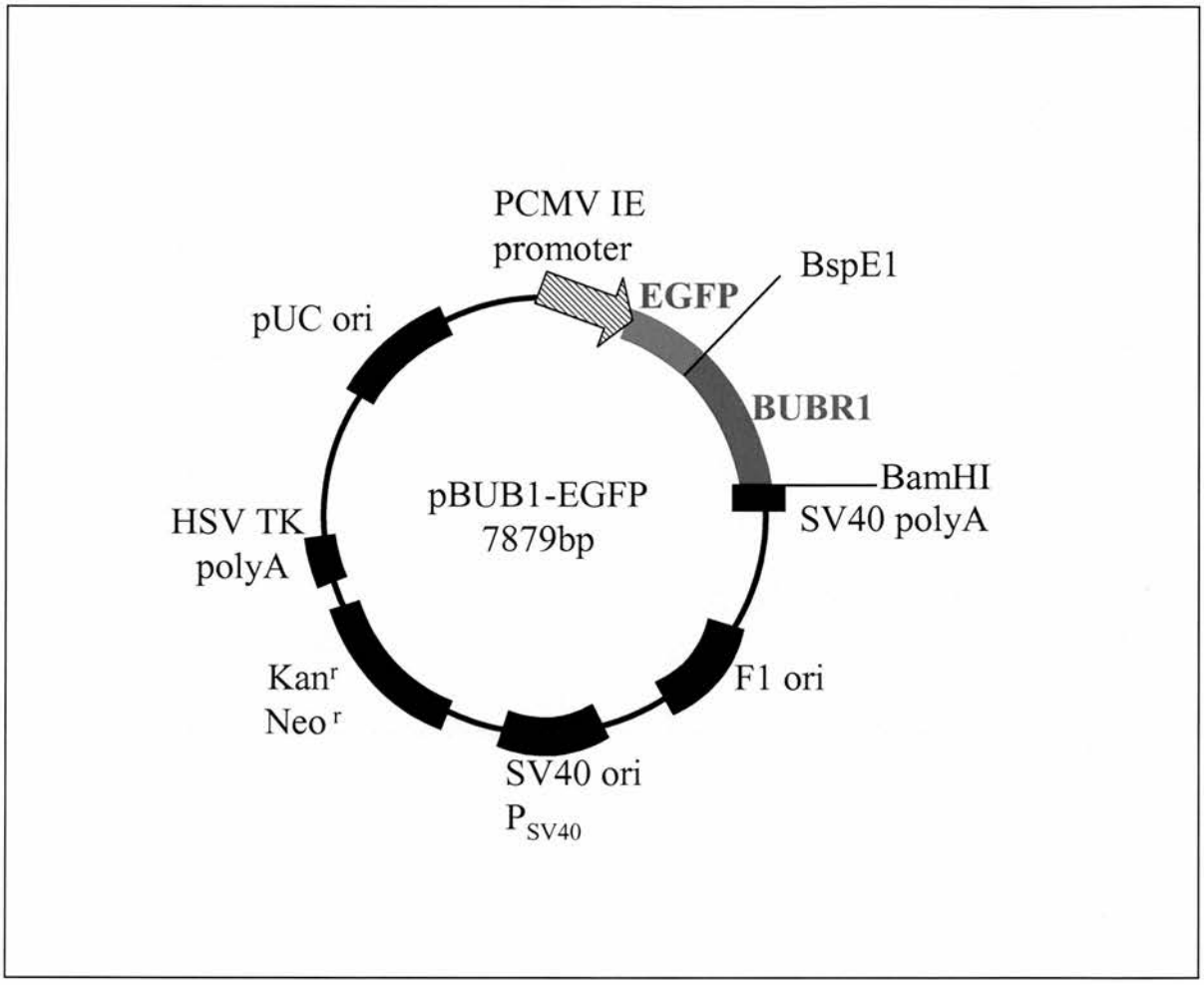

The new method involved using Sac1 and Sal1 restriction enzymes to digest the pBluescript constructs. This produced a vector fragment and two insert fragments that were ligated together before the total insert was ligated into digested EGFP-C1 and the ligation site within the coding sequence and orientation were confirmed by sequencing. Analysis of approximately 300 colonies for each of *BUB1V400* and *BUB1V429* and *BUBR1* revealed none containing appropriate sequence.

The constructs which were successfully isolated were sequenced fully and stored at –70°C as glycerol stocks for future use in functional assays.

These cloning strategies are summarised in figure 6.5.

Figure 6.5 Cloning strategies for the BUB1 and BUBR1 constructs

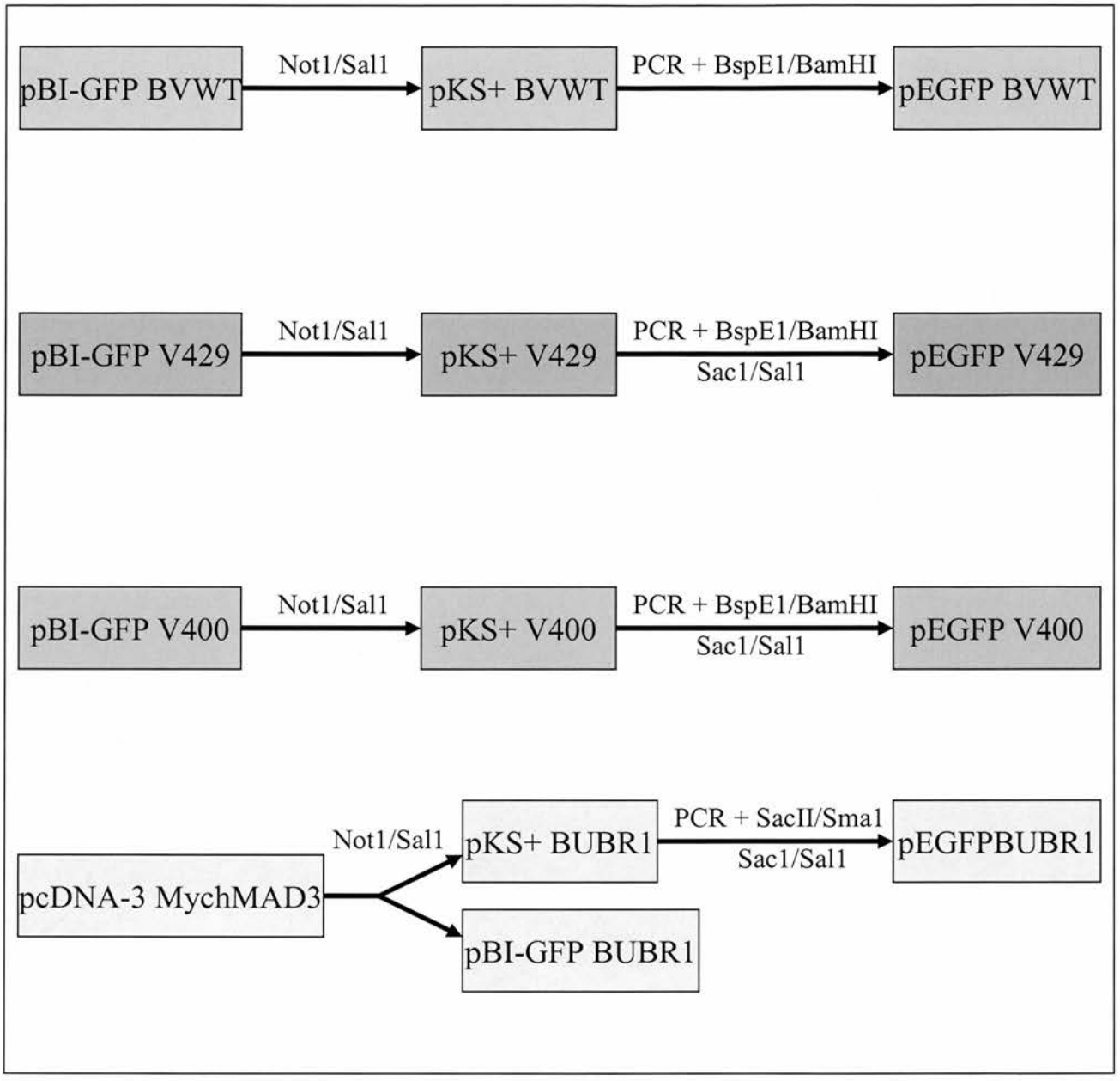

6.3.2 A Strategy for Construction of the BUBR1ΔE5 Coding Sequence

Unfortunately the *BUBR1ΔE5* mutant coding sequence could not be isolated from the tumour samples in which it was initially identified as the RNA was of poor quality and thus the initial analysis PCR amplified the tumour RNA in sections. Thus we attempted to construct the *BUBR1ΔE5* coding sequence using PCR based methods.

The initial attempts to construct the *BUBR1* deletion used the same restriction strategy as that used for the yeast deletion clones. The two sections flanking the ΔE5 deletion were PCR amplified using the pBluescript and original *BUBR1* constructs as templates. The internal primers used contained Bts1 recognition sequences and external primers contained sites for Not1 and Sal1 enzymes. Attempts to digest these and ligate them together did not produce a product of appropriate size even after a further round of PCR amplification. Nor did transformation experiments and analysis of 281 colonies, from 4 separate experiments, yield any positive deletion clones.

A new strategy was employed in which overlapping PCR methods were used. This involved PCR amplification of the same flanking sections with internal primers containing no restriction enzyme recognition sequences. The products from these PCRs are then utilised as a template in a secondary PCR using the external primers with unique Not1 and Sal1 restriction sites. This cloning strategy is summarised in figure 6.6. Analysis of 93 clones revealed only full-length *BUBR1* constructs. This strategy was then altered to include a gel purification of the primary PCR products before use as a template. Unfortunately, analysis of 186 clones revealed no sequences containing *BUBR1ΔE5*.

Figure 6.6 Cloning strategy for BUBR1ΔE5

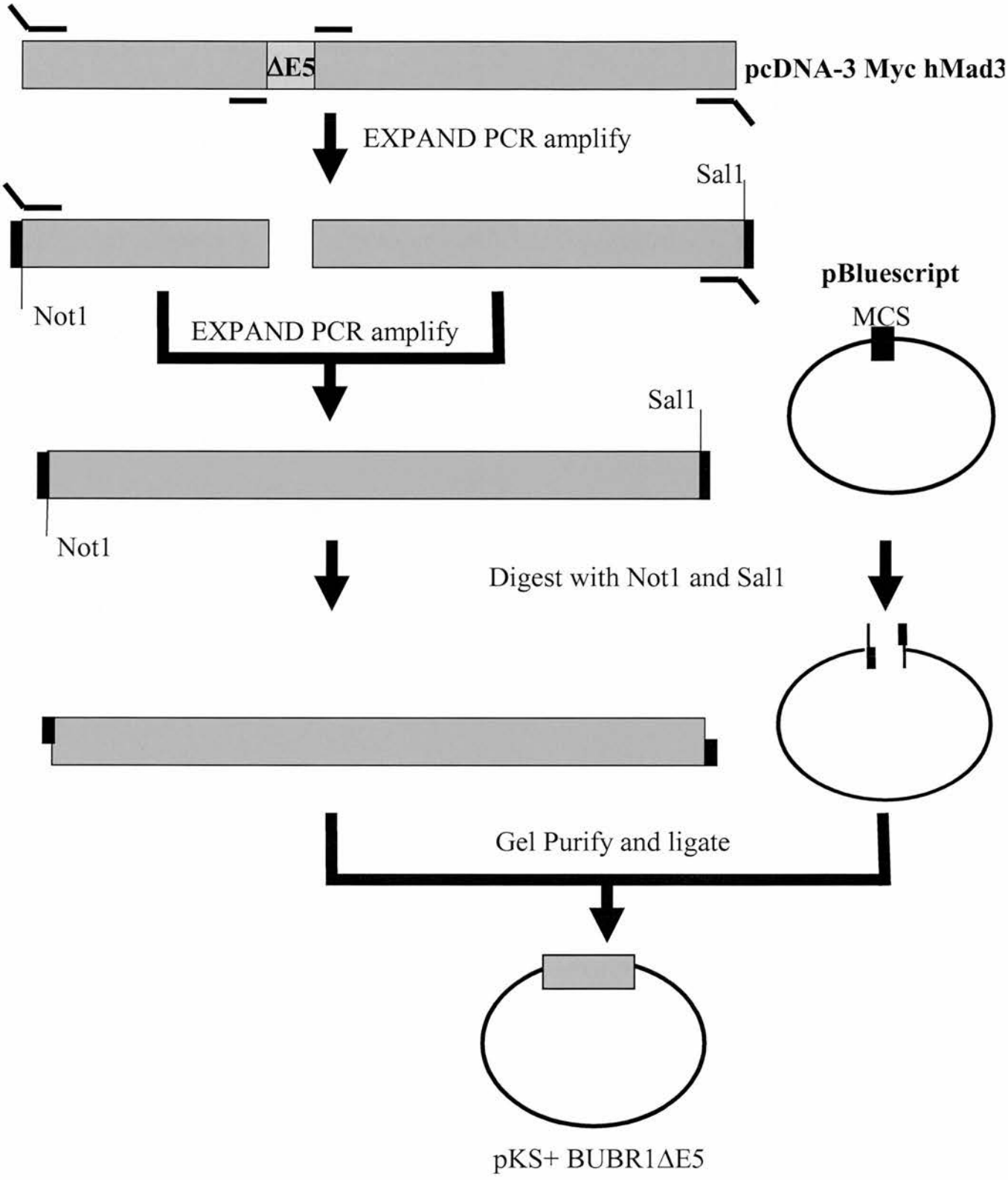

6.3.3 Production of pTet-On stable cell lines

The pBI-GFP constructs will be used to analyse the effect of the mutations on the spindle checkpoint response of mammalian cell lines when over-expressed. The principal for this experiment is shown in figure 6.1 and requires the generation of pTet-On stable cell lines. This produces a system in which expression of the BUBR1 protein can be controlled by the addition of antibiotics to the cell culture media. The mammalian cell lines to be used, DLD1, HCT116 and LoVo, were transfected with the pTet-On plasmid using Fu-Gene reagent. The transfectants were treated with Geneticin to select for incorporation of the plasmid and the surviving cells were diluted to obtain single cell clones. These were tested for expression of pTet-On by co-transfection using lipofectin with pCMVβ, a control vector which allows standardisation through β-galactosidase assays, and pTRELuc, which contains a luciferase gene under the control of Tet-responsive promoter. The cells were induced with doxycycline for 48hours before luciferase and β-galactosidase assays were carried out to determine the inducibility of the cell populations.

A great deal of variation was observed in the induction levels of the luciferase plasmid between clones. Transfection of a large flask of cultured cells yielded only 1-2 clones with inducible luciferase activity. In fact, many transfections produced no clones with inducible activity at all. From these three cell line populations, at least 35 geneticin resistant single cell clones were identified from at least 2 transfection procedures. From these only one clone of each of LoVo, HCT116 and DLD1 were identified with inducibility at levels ranging from 6 to 11.7 fold when corrected for cell number. Further investigation of these most responsive clones revealed the inducibility to be highly variable and unreliable. The LoVo and DLD1 clones were both found to have little inducibility in experimental repetitions and the HCT116 clone showed inconsistent levels of inducibility varying from 0.97 to 5.5 fold. These results are summarised in figure 6.7 and table 6.1.

Table 6.1: Variability in Induction Levels of pTet-On Stable Cell Lines

Cell Line	Number of Single Cell Clones Analysed	Maximum Induction	Inducibility of individual experimental repetitions (fold)
HCT116	48	6 fold	2.40, 5.50, 0.97
DLD1	36	11.7 fold	1.96, 0.07, 0.48, 3.20
LoVo	41	6.8 fold	1.54, 1.13, 0.95, 0.19

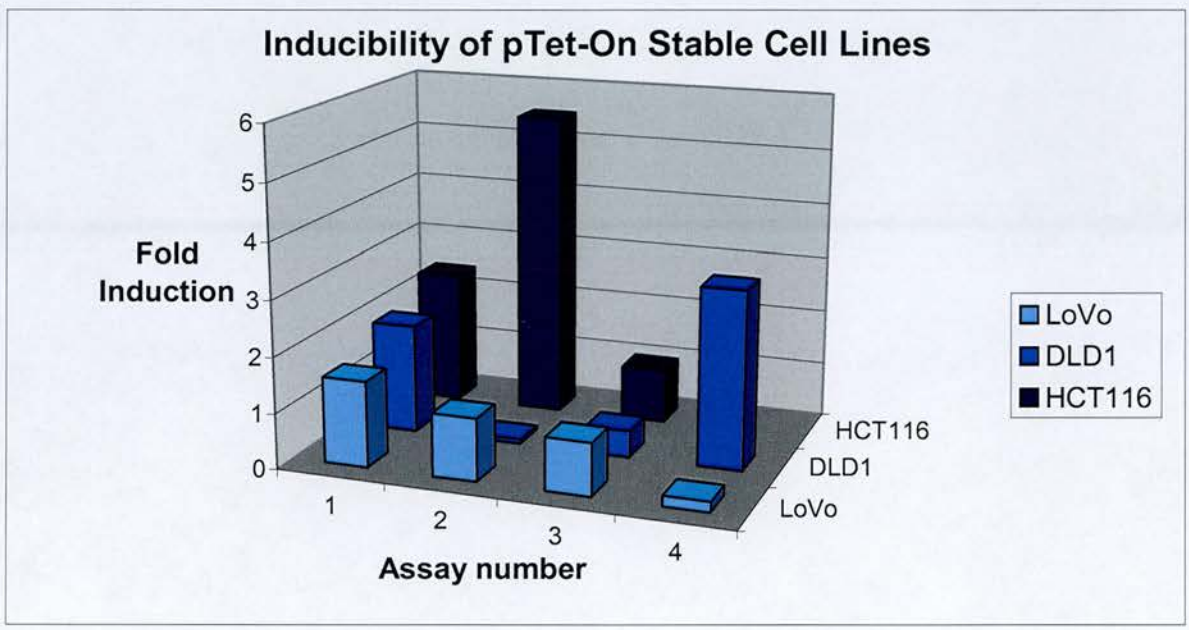

Figure 6.7 Inducibility of pTet-On Stable Cell Lines

Identical repetitions of luciferase assays on single cell clone populations show a dramatic variability in the induction of the pTet-On stable cell lines.

The pTet-On HCT116 cell line was used in further pilot experiments to generate pTet-On / BUB1 stable cell lines by co-transfection with the BUB1 pBI-GFP vector and a pTK-Hyg plasmid to confer hygromycin resistance. Positive transformants were then selected by adding hygromycin to the cell culture media at concentrations shown to cause death in over 90% of untransfected HCT116 control populations. Unfortunately, the transfected populations were unaffected by the hygromycin and positive transfectants could not be isolated. Further experiments showed the untransfected HCT116 pTet-On stable cell line was resistant to hygromycin even at extremely high levels suggesting integration of the pTet-On plasmid had somehow conferred a hygromycin resistant phenotype to the HCT116 cells. An alternative drug resistance plasmid would be required for future experiments.

6.3.4 Generation of BUB1 and BUBR1 N Terminal Antibodies

In combination with the localisation studies of the GFP-fusion proteins, I wished to use immunofluorescence techniques and co-immunoprecipitation experiments to explore the biochemistry of spindle checkpoint proteins. No N-terminal antibodies were available for BUB1 or BUBR1 at the time of these experiments and N-terminal antibodies were specifically required as the deletions being studied are likely to cause truncations or alterations in tertiary structure which may remove any C-terminal or central antibody epitopes. To this end we identified a string of 25 amino acids at the N terminus of BUB1 and 21 amino acids at the N terminus of BUBR1 which, according to the UK HGMP resource centre and the BLAST facility, http://www.ncbi.nlm.nih.gov/blast, shares little homology with other proteins. In addition these motifs are not conserved between BUB1 and BUBR1 reducing the possibility of cross reactivity. Initially I tried to PCR amplify these regions from wild type constructs but the small product produced was difficult to isolate and clone so an alternative technique was used. The oligomers encoding the entire peptide sequence were obtained (MWG Biotech) and annealed together before inserting into a Glutathione-S Transferase (GST)-fusion vector, pGEX4T1. The peptide sequences to which the antibodies were raised and a map of the GST construct generated is shown in figure 6.8. This plasmid was transformed into TOP10 *E.coli* cells and stored as a glycerol stock. Sequencing analysis of 24 clones of each identified 3 positive BUB1 clones and 5 positive BUBR1 clones, an efficiency of 12.5% and 20.8% respectively. These were transformed into *E.coli* M15 (pRep4) for expression of the fusion proteins and pilot induction experiments were successful. Two clones were selected for mass induction experiments and affinity purification of the GST-fusion proteins were performed using glutathione coupled sepharose beads. The protein eluted mostly in the 2nd and 3rd fractions and fractions 2-4 were concentrated by dialysis to finally yield 4mg of BUB1-GST and 8mg of BUBR1-GST (figure 6.9). This protein was to be used to generate polyclonal antibodies for use in biochemical studies. However, shortly after production of the GST-fusion protein, the initial plasmids were found to be altered in sequence. This is thought to be due to the cells used for cloning and storage of the recombinant plasmids. Thus we could not be sure

that the sequences of the GST fused peptides generated were correct. To avoid any potential error in the antibodies generated, peptides of the N-terminal sequences were commissioned from an external manufacturer and these were used for antibody generation.

Figure 6.8 Construct for generation of BUB1 and BUBR1 N-terminal antibodies

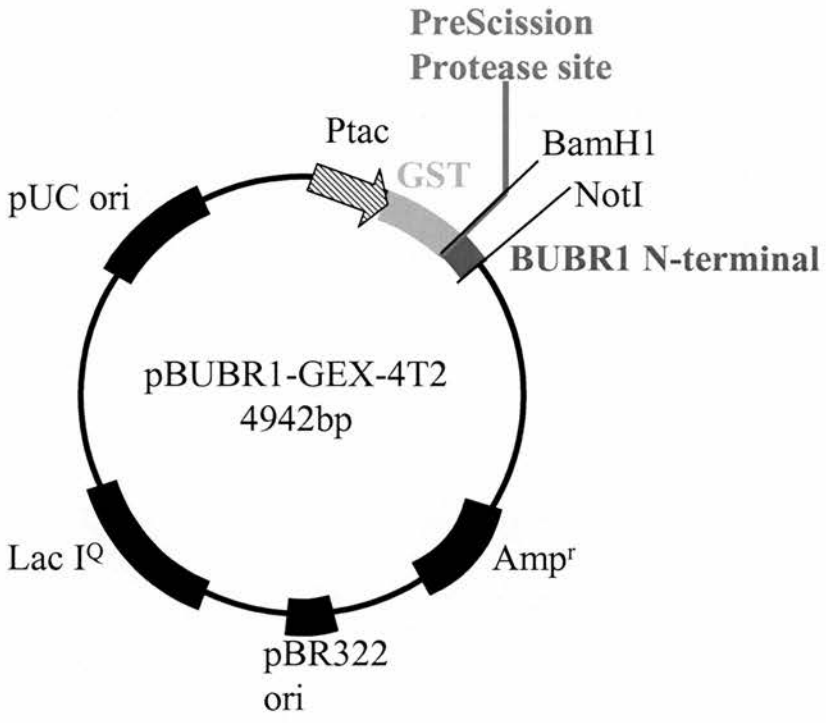

Peptide sequences for Antibodies

BUB1	MDTPENVLQMLEAHMQSYKGNDPLG
BUBR1	MAAVKKEGGALSLANSLEDGEWELS

Figure 6.9: Expression and Purification of BUB1 and BUBR1 GST-fusion Proteins

A) Pilot Study of Inducibility

Total protein extracts with and without induction by IPTG.
Clones B2 and A6 were selected for mass induction experiments

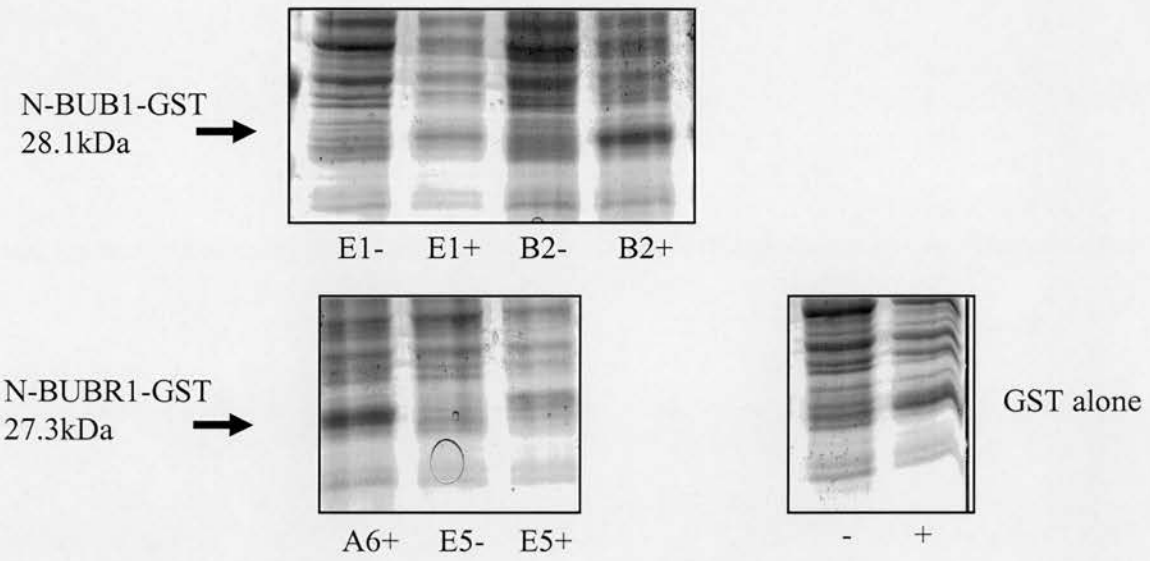

B) Large-Scale Expression and Protein Purification

8mg of BUB1-GST and 4mg of BUBR1-GST was isolated from fractions 2,3 and 4 and concentrated to 2 and 4mg/ml respectively.

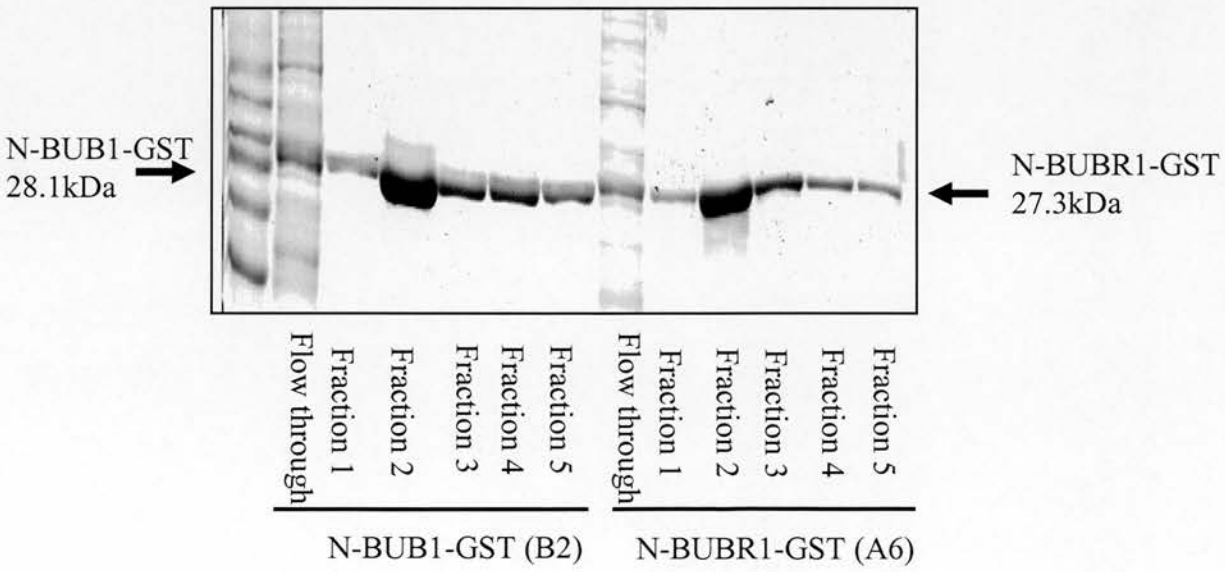

6.4 Discussion

The functional analysis in *S.cerevisiae* clarifies the effect of the V400 and ΔE5 mutations on specific functions including checkpoint arrest, chromosome segregation and protein complex formation. However, it is important to verify these effects in the human system. The *BUB1*V400 mutation has been shown to abrogate the spindle checkpoint in diploid cell lines using an inducible expression system. The work described in this chapter aimed to construct tools to be used in similar functional analyses in human cell lines. Time constraints indicated these experiments were beyond the scope of this thesis but these tools will be vital in future investigations into the role of *BUBR1ΔE5* and *BUB1V400* on the spindle checkpoint and protein function. In addition, the antibodies and GFP-fusion constructs can be used in immunofluorescence experiments to further investigate the roles of BUB1 and BUBR1 in the spindle checkpoint.

The primary aim of the functional analysis was to determine whether *BUBR1ΔE5* induced an abnormal mitotic checkpoint arrest, similar to that seen in CIN cell lines, when over-expressed. Such an effect has previously been shown for the BUB1V400 mutant protein. This required construction of *BUBR1* full-length and ΔE5 coding sequences in pBI-GFP inducible plasmids. Several attempts at cloning have isolated a *BUBR1* pBI-GFP construct which can be used in future checkpoint assays. This construct can be used as a positive control to ensure over-expression of the wild type protein in diploid cell lines does not abrogate the mitotic checkpoint. Unfortunately, multiple attempts to construct *BUBR1ΔE5* in a pBluescript plasmid have been unsuccessful. These techniques could be adapted in future attempts perhaps by further optimisation of the PCR techniques. In addition the PCR products of the sections could be PCR cloned with a TOPO PCR cloning kit for example which has the added advantage of using topoisomerase and does not require the TA overhang and would thus be suitable for use with a Hi Fidelity Taq polymerase such as that from an Expand kit. This would provide a renewable source of the section PCRs and may allow the DNA to be concentrated, aiding future digestion and cloning attempts. A similar PCR amplification and cloning technique can be used to concentrate the recombinant PCR before cloning into the functional vectors.

This functional work also requires pTet-On stable cell lines in which expression from the pBI promoter is induced in the presence of doxycycline. This inducible system allows the specific effects of the mutant proteins to be investigated at a certain time point. By generating double pTet-On, *BUBR1* pBI-GFP stable cell lines, a renewable source for future analyses can be produced, minimising the number of future transfection procedures. For these experiments pTet-On stable cell lines were generated from several diploid tumour cell lines. These were found to have a great deal of variability in their levels of induction even between individual repetitions using aliquots of cells derived from the same single cell clone transfectant. Ideally the induction levels would require some optimisation and confirmation before these cells could be used in checkpoint assays. This could be done by varying the conditions of the luciferase assays to obtain consistent luminescence in experimental repeats. Although the experimental repetitions carried out here maintained external conditions they may have been subtly affected by other factors such as cell number. Alternatively, a sub-population of these cells may have undergone additional alterations, which have caused a reduction in the induction levels and further dilution cloning may help to identify and isolate a more consistent population. In addition, preliminary experiments suggest that some of the HCT116 pTet-On cells are resistant to hygromycin and thus an alternative resistance plasmid would be required for co-transfection with and selection for stable integration of the pBI-GFP plasmids, for example puromycin. Neither geneticin nor doxycycline can be used for this selection as they are used in the selection for pTet-On stables and induction of target gene expression respectively. Alternatively, positive transfectants could be isolated by FACS.

Additionally, the range of Tet-On cell lines available commercially are increasing and although they do not include any colorectal carcinoma cell lines, these may be available in the future (http://www.clontech.com/products/cat/HTML/1193.shtml).

In order to assess the effect of the mutant BUB1 and BUBR1 proteins on spindle checkpoint function, the checkpoint function in the untreated diploid CRC cell lines must be established. The HCT116 cell line has previously been shown to be checkpoint proficient by Dr Farrington but insertion of the pTet-On plasmid may

have potentially disrupted the checkpoint. This involves blocking the cells in mitosis by treatment with nocodazole and harvesting them at several time points before scoring the proportion of metaphase cells to determine the efficiency of the mitotic block. If the cells have a functional mitotic checkpoint, a high proportion of the cells will arrest at the metaphase transition. The cell lines from which the stable *BUBR1* cell lines are to be generated must have functional checkpoints in order to ascertain the effect of ΔE5 on these checkpoints.

The *BUB1* pBI-GFP plasmids act as controls for the experimental strategy as the effects of these mutant and wild type proteins on checkpoint function has already been reported. Thus the assay can be optimised using these constructs before testing the effect of *BUBR1* full-length and *BUBR1ΔE5*.

The effect of the *BUBR1ΔE5* and *BUB1 V400* mutations on protein function can ultimately be investigated using GFP-fusion constructs and the N-terminal antibodies. Immunofluorescence analyses will be used to clarify the localisation of the mutant proteins and to investigate their interactions under different conditions and during different stages of the cell cycle. This will aid our understanding of the relevance of the yeast functional analyses and also provide information about conservation between the human and yeast spindle checkpoints.

The full-length GFP-fusion plasmids can be used in these assays both as controls for determining the specific influences of the mutant proteins and to further investigate wild type protein function in the mitotic processes such as checkpoint arrest, chromosome segregation and kinetochore assembly. In addition the antibodies generated can be used in co-immunoprecipitation experiments to see if the ΔE5 and V400 mutations have a similar effect on spindle checkpoint complex formation in human cells to that seen in yeast.

These antibodies will also be useful in extending our knowledge of the impact of the ΔE5 mutations on colorectal tumours. Unfortunately, the tumours in which the mutation was originally identified are of poor quality and cannot be used for further RNA and protein expression anlaysis. We are currently collecting a panel of tumours for further mutation analysis in order to identify tumours containing the *BUBR1* variant. The protein and genomic tumour DNA from this sample can then be

further analysed to determine the genomic change associated with the deletion and the effect of this at the protein level. It will be particularly interesting to determine the expression levels, stability and truncation status of the mutant protein compared to that expressed from the wild type allele. This could be compared with the yeast functional work which investigated an in frame form of the deletion.

These antibodies could also be used for immunohistochemistry on tumour sample cohorts to identify any changes in expression levels in tumour tissue. Altered expression levels of spindle checkpoint proteins have previously been observed in a variety of tumours and associated with checkpoint defects (Wang et al., 2000a; Wang et al., 2002) and are probably an important aspect by which loss of checkpoint control may be implemented.

In summary, the yeast functional analyses have shown the ΔE5 and V400 mutations have a detrimental effect on the spindle checkpoint and chromosome segregation. The full effect of the mutations on tumourigenesis will ultimately require analysis in human cell lines. This initial work has achieved the construction of important plasmids, cell lines and antibodies which are an important resource and vital for use in the functional analysis of BUBR1ΔE5 and BUB1V400. These results can be compared with the yeast results to expand our knowledge of the conservation between the yeast and human spindle checkpoints and further our insight of the influence of the *BUBR1ΔE5* mutation on colorectal tumourigenesis.

Chapter 7: Summary and Discussion

The work presented in this thesis aimed to clarify the importance of spindle checkpoint mutations in colorectal tumours. This was approached in two ways. Firstly, a yeast model system was used to investigate the effects of cancer associated deletions in MAD3 and BUB1, the yeast homologues of BUBR1 and BUB1, on spindle checkpoint function, chromosome segregation and checkpoint protein complex formation. Secondly, molecular biological tools were developed to address the effect of the mutations on checkpoint activity in human cell lines.

The mutations investigated in these analyses were the BUBR1ΔE5 mutation observed in 20% of a panel of aneuploid colorectal tumours during previous work by this laboratory and the BUB1 V400 mutation, previously identified in CIN colorectal tumour cell lines (Cahill et al., 1998). Alignments of the sequences of these two related proteins revealed the area removed in these two deletions was identical and also showed that this area is highly conserved between species (Hardwick et al., 2000). The mutations remove part of a functional domain thought to interact with Cdc20p (Hardwick et al., 2000) an interaction important for checkpoint function.

The functional analysis in the yeast system involved the construction of plasmid forms of the ΔE5 and V400 mutations in the MAD3 and BUB1 coding sequences, the yeast homologues of BUBR1 and BUB1 respectively. These were transformed into strains null for either BUB1 or MAD3 and the ability of the mutant plasmids to rescue phenotypes associated with the null mutants was examined. These experiments effectively examined the effect of the ΔE5 mutations on spindle checkpoint function and chromosome segregation. The *mad3* and *bub1* null mutants exhibit a sensitivity to the microtubule poison benomyl indicative of a mitotic defect (Warren et al., 2002). Further phenotypic analyses demonstrated that the *mad3* null mutant is associated with an altered pattern of growth in microcolony assays and *bub1* mutants exhibit a multi-budded phenotype when arrested with nocodazole. These additional studies aimed to dissect the mitotic defect producing the benomyl sensitivity phenotypes, and identified that the defect is a result of abrogation of spindle checkpoint arrest. Additionally both the *mad3* and *bub1* null mutants exhibit

an elevated chromosome mis-segregation rate. These assays also demonstrated that the MAD3 and BUB1 ΔE5 mutants exhibit increased benomyl sensitivity, spindle checkpoint abrogation and chromosome loss phenotypes, indicating that the function of the protein is compromised by the ΔE5 mutation. In the MAD3 mutant these phenotypes are as severe as the null mutant suggesting the protein is fully compromised. However, the BUB1ΔE5 mutant shows an intermediate phenotype between that of the null mutant and wild type strains suggesting the Bub1ΔE5p protein, while defective in its checkpoint and segregation roles, does retain some of its function. The null and ΔE5 BUB1 mutants exhibit more severe phenotypes than the MAD3 mutants consistent with previous reports that in yeast Bub1p has a greater function in the spindle checkpoint and additional roles in mitosis compared to Mad3p.

These defects were further investigated at the protein level using co-immunoprecipitation experiments and over-expression studies. The ΔE5 mutant proteins were found to be expressed at equivalent levels to their full-length counterparts both when expressed from wild type promoters and from methionine-inducible over-expression promoters. Thus a reduced stability or expression of the mutant protein does not seem to be responsible for the phenotypes exhibited by the ΔE5 mutants. Further investigations showed specific interactions important in checkpoint function are disrupted in the ΔE5 proteins. Mad3ΔE5p forms interactions with both Cdc20p and Bub3p with a reduced affinity compared to the full-length proteins (reduced by 50% and 35% respectively) and the interaction between Bub3p and Mad2p is also reduced by 75% in the presence of the ΔE5 mutant protein, probably through an indirect effect of the reduced Mad3p-Bub3p complex formation. Over-expression of the full-length Mad3p protein causes an elevated chromosome loss phenotype due to sequestering of Bub3p which is also exhibited by the ΔE5 mutant although at a slightly reduced level. This is consistent with the co-immunoprecipitation experiments which indicate Mad3ΔE5p retains a large proportion of Bub3p binding. The reduced formation of these complexes is hypothesised to interfere with the formation of the constitutive Mad3p-Bub3p complex, important for Mad3p localisation to the kinetochore; the Mad3p-Cdc20p complex, involved in APC/C inhibition and thus the Mad3p-Bub3p-Mad2p complex

which may also be involved in APC/C inhibition through sequestering of Cdc20p. Preliminary experiments suggest Mad3ΔE5p is normally phosphorylated. Thus the phenotypes exhibited by the MAD3ΔE5 mutants can be attributed to the disruption of these three checkpoint complexes.

The BUB1ΔE5 mutant also shows a reduced affinity for Bub3p (by 60%), which is a complex which is important for Bub1p localisation to the kinetochore and also in the formation of a Bub1p-Bub3p-Mad1p signalling complex from which Mad2p is released in an activated form to inhibit the APC/C. This is supported in experiments analysing the chromosome loss phenotype, when the full-length and mutant proteins are over-expressed. Over-expression of the full-length protein induces a chromosome loss phenotype due to sequestering of Bub3p. This phenotype is far less severe in the ΔE5 mutant due to a much reduced ability to interact with Bub3p. In addition, Bub1ΔE5p shows aberrant phosphorylation, the importance of which is not yet clear. The effect of the ΔE5 deletion on the interactions between Bub1p and Mad1p and Bub1p and Cdc20p is also not clear, although preliminary evidence suggests ΔE5 may compromise an interaction between Bub1p and Cdc20p. Thus the spindle checkpoint and mis-segregation defects exhibited by the BUB1ΔE5 mutant can be attributed, at least in part to this reduced protein function, possibly via phosphorylation effects and reduced protein complex formation.

The interactions are compromised in the MAD3 and BUB1ΔE5 mutants by between 35 and 75% suggesting the checkpoint and segregation defects in the mutants should be compromised but not equivalent to the null mutant. Although this is consistent with the phenotype observed in the BUB1ΔE5 mutant, this is not the case for the MAD3ΔE5 mutant which in fact exhibits phenotypes as severe as those seen in the null *mad3* strain. This may be due to an additive effect of the disruption of multiple interactions or may be due to the reduction of the concentration of important complexes below a threshold level required for correct spindle checkpoint function. However, the BUB1ΔE5 mutant exhibits a compromised checkpoint complex formation with a more extreme disruption of the interaction with Bub3p, but a phenotype intermediate between the null and wild type strains is observed in the ΔE5 mutant. Perhaps this total loss of Mad3p protein function is an additive effect of

compromisation of several of Mad3p's protein interactions, whereas in Bub1p only the interaction with Bub3p is known to be specifically disrupted, producing an intermediate phenotype between the full-length and vector transformants. Alternatively this may be due to the limitations of the assays used, which require large sample sizes to accurately and statistically distinguish between the null *mad3* mutant and wild type strain in the chromosome loss assay in particular. Thus to distinguish between these and an intermediate mutant may be difficult. The more severe mis-segregation phenotype observed in the *bub1* mutants would allow intermediate phenotypes to be distinguished statistically even with smaller sample numbers.

The area removed by ΔE5 removes a functional domain conserved between Bub1p and Mad3p (Hardwick et al., 2000) and thus the effect of the ΔE5 mutation would be expected to be similar in both BUB1 and MAD3. However, BUB1ΔE5 produces a far more severe phenotype than MAD3 and also shows a partial defect in chromosome segregation and mitosis, whereas these functions of Mad3p are entirely abrogated in MAD3ΔE5. This variation in the phenotypes of the BUB1 and MAD3 mutants probably partially reflects the greater role of Bub1p in the spindle checkpoint and in other functions in mitosis, consistent with the similar multi-budded phenotype of the *bub1* null and ΔE5 mutants. Variations in the primary sequence and tertiary structure may also be reflected in the differing phenotypes of the MAD3 and BUB1 mutants. In addition, the mild nature of the MAD3 mutant phenotype may reflect redundancy in the inhibitory complex. Both Mad3p (and it's homologue BUBR1) and Mad2p have been shown to be involved in complexes able to inhibit the APC/C (Sudakin et al., 2001; Fraschini et al., 2001; Fang et al., 1998) and some studies especially in vertebrates, indicate these form two separate inhibitory complexes (Tang et al., 2001). The severity of the phenotype in the BUB1 mutants may partly reflect the greatly reduced interaction between Bub1p and Bub3p. This is supported by the high levels of chromosome loss exhibited by *bub3* null mutants and upon over-expression of Bub1p, resulting in the sequestering of Bub3p. The defect in Bub3p binding in the MAD3ΔE5 mutant is less severe as demonstrated by co-immunoprecipitation and over-expression experiments, consistent with the milder phenotype of the MAD3ΔE5 mutant. However, the difference in the severity of the

defect in the interaction with Bub3p is not entirely responsible for the milder phenotypes of the MAD3ΔE5 mutant, as abolishment of the interaction between Mad3p and Bub3p in the *mad3* null mutant is still associated with a milder phenotype than the *BUB1* mutants. The interaction of Bub1p and Mad3p with Bub3p is thought to be important for the kinetochore localisation of (Roberts et al., 1994; Hardwick et al., 2000) both proteins and thus the ΔE5 proteins may be mislocalised. The milder phenotype of the MAD3 mutant may be due to the involvement of Mad3p in APC/C inhibitory complexes away from the kinetochore. The Mad2p-Mad3p-Cdc20p complex is thought to be involved in APC/C inhibition in a soluble pool as well as at the kinetochore (Fang, 2002) and the association with this complex may occur despite minor defects in Bub3p binding and therefore kinetochore localisation. However, the localisation of Bub1p to the kinetochore through interaction with Bub3p is important for the formation of the Mad1p-Bub1p-Bub3p signalling complex at the kinetochore (Brady and Hardwick, 2000) and disruption and mislocalisation of this is hypothesised to produce the severe checkpoint defects observed here. Thus the reduced interaction between Mad3p and Cdc20p in the ΔE5 mutant may be a greater contributor to the phenotype of the MAD3 mutant, whereas the defect in Bub3p binding is the major cause of the severe BUB1 mutant phenotype. This hypothesis would be consistent with the different phenotypes seen in the two mutants as the importance of an interaction between Bub1p and Cdc20p is not clear and the effect of ΔE5 on this interaction has not been fully elucidated.

The effect of the ΔE5 mutation on the Bub1p- Mad1p complex has not been fully investigated. Co-immunoprecipitation experiments to investigate this have been inconclusive and this is an area for future investigation by optimisation of the assays or using yeast 2-hybrid assays. This interaction is important in the formation of a Bub1p-Bub3p-Mad1p signalling complex (Brady and Hardwick, 2000), although it is likely to be defective in the ΔE5 mutant due to a reduced interaction between Bub1p and Bub3p but this could be confirmed in further analyses.

Other future work could investigate the different phenotypes observed, with a view to separating the individual interactions and the residues which affect them. Previous mutation analysis of Bub1p has identified two main functional domains

CD1 and CD2 which are involved in Cdc20p and Bub3p interactions respectively (Hardwick et al., 2000). Similar analysis of Mad3p involving mutation of conserved amino acids and domains could aid the understanding of the interactions of Mad3p and clarify the phenotypes associated with the defects in complex formation seen here. The areas deleted by ΔE5 in both the MAD3 and the BUB1 mutants remove a large proportion of CD1 and thus would be expected to effect the protein interaction with Cdc20p. However, CD2 is not directly altered by the deletion ΔE5 and thus the effect on Bub3p binding is probably due to an alteration of the tertiary structure of the protein through removal of a large section. This is difficult to confirm in functional assays but could be further investigated using an *in silico* approach or using structural analyses such as X-ray crystallography. There is also the possibility that Bub3p binding sites are present in CD1.

In addition the defects in individual protein interactions could be further investigated to relate them to the specific phenotypes shown by the mutants. This again could involve mutating individual amino acids and domains and analysing their effect on spindle checkpoint function and chromosome segregation using the benomyl sensitivity, checkpoint and chromosome loss assays. Further information would also be provided by mutational analysis of the Mad3p and Bub1p proteins with regard to individual protein interactions, using co-immunoprecipitation experiments and two hybrid assays. Mutational analysis of the interaction partners Cdc20p, Bub3p and Mad1p to identify residues involved in the interactions with Bub1p and Bub3p is of importance and some analysis has already identified important amino acids involved in protein interactions (Hardwick et al., 2000; Warren et al., 2002). Comparison of any mutant phenotypes produced may aid in identifying the specific defective interactions involved in the checkpoint defect and chromosome mis-segregation phenotypes of the MAD3 and BUB1ΔE5 mutants.

The relationship between the individual phenotypes and the defective interactions can also be investigated by complementation of the mutant strains with a plasmid over-expressing that protein. For example, by addition of a plasmid over-expressing Bub3p to the BUB1ΔE5 mutant, the increased concentration of Bub3p should restore the interaction between Bub1p and Bub3p to normal levels. If the disruption of this interaction was the major contributing defect to the phenotypes observed in the

mutants, then this complementation should restore the chromosome loss rates and spindle checkpoint function to wild type levels. This has previously been used to confirm the importance of interactions (Warren et al., 2002) and the same theory could be used for each of the interactions with Cdc20p, Bub3p and Mad2p. In addition the phosphorylation of Bub1ΔE5p in this complemented mutant, could be investigated to determine whether the aberrant phosphorylation is a result of the reduced Bub3p-Bub1p interaction. Preliminary experiments of this nature were undertaken involving transformation of a Bub3p overexpression plasmid into the BUB1 and MAD3ΔE5 transformants in order to restore the interaction with Bub3p. The relative contribution of the Bub3p binding defect to the mutant phenotypes could then be investigated using chromosome loss and benomyl sensitivity assays. Unfortunately time constraints prevented the optimisation and completion of these experiments.

The aberrant phosphorylation of Bub1ΔE5p has been further investigated to clarify whether it is a result of the reduced interaction between Bub1p and Bub3p. Full-length Bub1p is normally phosphorylated in a *bub3* null strain suggesting Bub1p phosphorylation is not Bub3p dependent. This could be further investigated using other mutants which are defective in Bub3p binding such as *bub1-1*. The bub1-1 mutant strain harbours the mutation in E333K and has been shown to be suppressible by an increased dosage of Bub3p and thus is thought to form a defective interaction with Bub3p (Hoyt et al., 1991; Roberts et al., 1994). This *bub1-1* strain could also be used in co-immunoprecipitation experiments with anti-Bub3p or anti-myc (in a Bub3p-myc strain) beads to investigate the relationship between the phosphorylation of Bub1p and its interaction with Bub3p. Alternatively, co-immunoprecipitation experiments with phosphatase treated extracts could be used to determine whether the interaction with Bub3p is dependent on the phosphorylation of Bub1p.

The aberrant phosphorylation of Bub1ΔE5p may in fact be unrelated to the reduced interaction with Bub3p. It may be a specific effect of removal of the E5 domain, perhaps due to alterations in tertiary structure masking the amino acids to be phosphorylated, or may reflect a mis-localisation of the protein. The localisation of the Bub1p and Mad3p proteins are difficult to assess in budding yeast due to their small size but their localisation to the kinetochore can be investigated using a one

hybrid assay (Warren et al., 2002). In this assay the ability of the mutant protein fused to a Gal4 activation domain to activate transcription of a centromere reporter gene, HIS3 indicative of centromere localisation, is assessed by analysing cell growth on media lacking histidine (Warren et al., 2002).

The chromosome loss phenotypes associated with over-expression of Mad3p and Bub1p provide information about the interaction with Bub3p and have additional relevance to colorectal cancer in two ways. Firstly, variations in the expression levels of spindle checkpoint proteins have been observed in various cancers (see table 1.4) and these phenotypes suggest a mechanism by which the over-expression of these proteins may contribute to tumourigenesis. Secondly, the over-expression of the mutant proteins in a wild type background produces a mis-segregation phenotype, suggesting they may exert dominant negative effects. This is thought to be mediated by the interaction with and sequestering of spindle checkpoint proteins such as Bub3p by the mutant proteins, preventing the formation of important spindle checkpoint protein complexes. This dominant negative effect is consistent with a mitotic defect observed upon over-expression of BUB1V400 in human colorectal cancer cell lines (Cahill et al., 1998a). The dominant negative effect observed in these over-expression experiments was further investigated by expression of the mutant proteins from their wild type promoters in a wild type strain, mimicking the heterozygous nature of the mutations. Preliminary data from my experiments indicated Mad3ΔE5p can exert dominant negative effects whereas the effect of Bub1ΔE5p appears to be milder. The difficulties discussed above in interpreting milder phenotypes in chromosome loss assays are also evident here and are confounded by the small sample sizes and single repetition in these pilot experiments. In addition, these experiments are not truly indicative of the human system as the other checkpoint proteins are expressed only at haploid levels and thus there must be a degree of caution in these interpretations.

In summary, this functional analysis in yeast has been extremely important in our understanding of the phenotypic effects of the ΔE5 mutations of spindle checkpoint function and chromosome segregation. They have revealed that the mutations are associated with a spindle checkpoint defect and chromosome mis-segregation phenotype consistent with the CIN frequently observed in colorectal tumours. These

defects are more severe in the BUB1ΔE5 mutant than in MAD3ΔE5 consistent with a greater role for BUB1 in mitosis. The ΔE5 mutation also appears to abolish Mad3p checkpoint function whereas Bub1p function is only compromised. Furthermore, defects in specific protein interactions appear to mediate these mitotic defects and may allow the mutant proteins to exert dominant negative effects. These experiments have contributed significantly to our knowledge of both the control of the spindle checkpoint in *S.cerevisiae* and the ΔE5 mutations and how they may be influencing tumourigenesis.

The functional assays used in these experiments are important to examine the effect of the mutation on checkpoint and mitotic function in *S.cerevisiae*. However, they do have limitations. The benomyl sensitivity assays are most useful in qualitative analysis which is less informative than a quantitative assay due to the error margin introduced through human interpretation, although this is reduced through repetition of the experiments and the analysis of several separate transformants. The benomyl media used does not select for the transformed plasmids due to technical constraints in plate preparation. However, the rate of spontaneous plasmid loss should be consistent for both the mutant and full-length transformants. In addition this assay does not directly analyse spindle checkpoint function but represents defects in a sum of mitotic processes. For this reason further checkpoint assays were carried out; the microcolony assay and the liquid culture assay. These assays have similar technical limitations in that they are carried out in a benomyl (or nocodazole) containing media which does not contain nutrient selection for the exogenous plasmids, the use of the full-length transformants acts as controls. In performing the microcolony assay, a proportion of cells die during the experimental set up and this can result in different sample sizes for each transformant which is not ideal for comparison. However, in each repetition at least 20 cells remained viable during the early divisions and the use of appropriate controls compensates for this error. The chromosome loss experiments also incorporate a lack of selection during the actual assay (although the overnight cultures are prepared in selective media) however the use of full-length controls standardises for this. Some of these technical difficulties could be removed through integration of the mutant sequences into the yeast genome. This would also ensure equal expression of the mutant proteins as the

plasmid nature of the system may allow alterations in plasmid copy number and expression levels. However, protein analysis has not revealed any such problems in our experiments and indeed integration of mutant sequences has its own technical problems, can be more time consuming and has been associated with reduced protein stability. Additionally the use of plasmids allows the easy transfer of the mutant sequences to new strains without the need for crosses which can also be both problematic and time consuming. As discussed previously, the chromosome loss assays are limiting in the analysis of mild phenotypes such as those exhibited by the over-expression transformants, the *mad3* mutants and in the dominant negative assays. The sample size for the MAD3 mutants was much greater than for the BUB1 mutants and this was important to obtain consistent phenotypes for statistical analysis. The assay is fairly time consuming, particularly the scoring of colonies (with nearly 280,000 colonies counted during the course of this thesis!) and thus may not be the most suitable for routinely investigating the effect of mutations on chromosome segregation. Certainly the checkpoint assays are practically easier for analysing checkpoint function and alternative assays analysing chromosome segregation may prove more suitable in future mutational analyses.

The co-immunoprecipitation experiments provided important information on interactions but were limited due to the robust nature of the antibodies. The antibodies used here did not easily recognise proteins expressed at wild type levels and hence the over-expression plasmids were used for this analysis. The production of new antibodies could improve these results or an alternative could involve the use of yeast 2-hybrid systems to investigate the protein interactions. This assay still relies on over-expression of the proteins and is an *in vitro* assay, but could be used for those interactions where the antibodies were too poor for co-immunoprecipitation assays, for example the Mad1p-Bub1p interaction.

However, *S.cerevisiae* has its limitations as a model system. The cells are small in size and thus cannot easily be used to analyse the localisation of the proteins or view their interactions microscopically using immunofluorescence. This could be done in the fission yeast *S.pombe* on construction of the homologous *S.pombe* mutant plasmids. However, the organism with most relevance to the colorectal tumours is the human system itself. Human cell lines can be used to confirm whether the effects

of the BUBR1ΔE5 mutation are consistent with the phenotypes observed in the BUB1ΔE5 and MAD3ΔE5 mutants in *S.cerevisiae*. Both the MAD3 and BUB1 ΔE5 mutants are likely to have relevance to the BUBR1ΔE5 mutation in humans. BUBR1 was initially identified as a BUB1 related protein (Cahill et al., 1998a) but is now generally considered to be the MAD3 homologue. The protein sequence of BUBR1 is more homologous to MAD3 (Millband and Hardwick, 2002) and the functions described for BUBR1, in the inhibition of the APC/C by direct binding of CDC20 are similar to those described for MAD3 (Sudakin et al., 2001; Fraschini et al., 2001). Thus the phenotype of the MAD3 mutant may be the most relevant to BUBR1ΔE5. However, BUBR1 does contain a BUB1-like C-terminal kinase domain, absent from MAD3, which is thought to have additional functions in mitosis (Warren et al., 2002) suggesting the more severe phenotype and intermediate phenotype between that of a null mutant and the wild type protein exhibited by BUB1ΔE5 in *S.cerevisiae* may be relevant. Thus it appears both the BUB1 and MAD3 mutants may be pertinent to the phenotype of BUBR1ΔE5. To clarify this, investigation of BUBR1 in higher organisms is required. For this reason, the aim of further investigations was to analyse BUBR1ΔE5 function using human cell lines.

The functional analysis in human cell lines is based upon previous investigations of the BUB1 V400 mutation (Cahill et al., 1998a). Over-expression of this mutant protein in MIN colorectal tumour cell lines induced a mitotic checkpoint phenotype similar to that seen in CIN colorectal tumour cell lines. This included a reduced mitotic index peak and incomplete arrest at mitosis in the presence of nocodazole with a high proportion of cells re-entering S-phase. These experiments utilised an inducible expression system involving pTet-On cell lines and tetracycline responsive vectors expressing the mutant or wild type BUB1 coding sequence and GFP. Thus similar experiments to investigate the effect of BUBR1ΔE5 required the construction of stable pTet-On colorectal tumour cell lines and full-length and mutant BUBR1 inducible pBI-GFP plasmids. These would then be used to generate double stable cell lines in which both the pTet-On inducer, rTetR and the appropriate BUBR1 coding sequence under the control of a tetracycline responsive promoter, were integrated into the genome. Then by addition of the tetracycline derivative doxycycline to the culture media, the expression of the target BUBR1 gene is turned

on, with expression being switched off in the absence of the antibiotic. Thus the double transformants can be induced using doxycycline and the effect of the mutant protein on mitotic checkpoints analysed by examining the mitotic index and BrdU incorporation of the mutant and full-length transfected populations. This would indicate whether BUBR1ΔE5 induces a mitotic defect in human cell lines and thus whether it is likely to be a major contributor to CIN in colorectal cancer. The work described in this thesis attempted to construct the cell line and plasmid tools required for this analysis. I successfully managed to isolate clones of diploid colorectal tumour cell lines with the pTet-On plasmid stably integrated into the genome. However, luciferase assays revealed this cell line showed variable levels of induction of target genes and this would require optimisation before use in further assays. In addition, construction of plasmid forms of the mutant and wild type BUBR1 sequences was undertaken. The wild type pBI-GFP BUBR1 plasmid was successfully constructed but unfortunately, numerous attempts at constructing BUBR1ΔE5 did not yield any plasmids containing the mutant sequence and the cloning strategy may require further development or optimisation for isolation of the deleted plasmid. These will however be useful resources for future analysis of the function of BUBR1ΔE5 in colorectal tumourigenesis.

The effect of the mutations on the localisation and interactions of BUBR1 and BUB1 would also be a good direction for future investigation. Chen et al., have previously reported that BUBR1 is required for the kinetochore localisation of BUB1, MAD1, MAD2 and CENP-E (Chen et al., 2002) and also that BUB1 may be required as a scaffold to recruit BUB3, MAD1, MAD2 and CENP-E (Sharp-Baker and Chen, 2001) and the effect of the ΔE5 mutation on these functions could be investigated in human cell lines. For this analysis, antibodies to the N-terminal of BUB1 and BUBR1 were developed as currently available antibodies were raised to sequences predicted to be removed or altered by the ΔE5 and V400 deletions. In addition molecular biology techniques were utilised to construct EGFP fusion vectors of the BUB1 and BUBR1 mutant and wild type proteins. These are to be utilised in future immunofluorescence and co-immunoprecipitation experiments to investigate the effects of ΔE5 and V400 on the localisation and interactions of BUBR1 and BUB1.

These antibodies could also be used to investigate the effect and occurrence of the BUBR1ΔE5 mutation in tumours through western blot analysis of tumour protein samples. The mutation was initially identified through a mutant RNA transcript in colorectal tumours and is predicted to cause a frameshift and truncation of the BUBR1 protein, but the effect at the protein level is unknown and it would be useful to clarify this. The antibodies may aid further investigation of the size and nature of the protein expressed by the BUBR1ΔE5 allele. This may also help to solve hypotheses that ΔE5 may represent an alternative splicing affect as it deletes the entire exon 5 of BUBR1.

The genomic change associated with the ΔE5 deletion has been investigated using long-range genomic PCR techniques and sequencing of the surrounding introns, but as yet no genomic change has been identified and other deletion mapping strategies are being employed. Much of these difficulties are believed to be due to poor quality DNA and protein material from the original tumours and thus we are also currently attempting to identify the change in a new panel of tumours from which higher quality DNA and protein material can be isolated and used in further analysis.

This will be important for clarifying the relevance of the results from the yeast studies. The yeast assays investigated the effect of the ΔE5 mutations on the assumption that they did not cause truncation of the BUB1 or BUBR1 proteins. If this is not valid and the ΔE5 and V400 proteins are truncated, the phenotypes associated with them might be expected to be more severe.

One of the interesting outcomes of the yeast functional analyses was the suggestion that the phenotypes exhibited by tumours with spindle checkpoint mutations may vary in their severity according to the gene which is mutated and the type of mutation. In human tumour studies, mutations in spindle checkpoint genes are fairly rare but combinations of polymorphisms and variations in levels of spindle checkpoint protein expression may contribute to the CIN observed frequently in tumours(see table 1.4) (Sato et al., 2000; Seike et al., 2002). Polymorphic variants of MAD1 which are associated with cancer cell lines have been demonstrated to disrupt its interactions with MAD2 and are thus thought to compromise spindle checkpoint function. In addition a polymorphic variant of STK15 (an auroraB homologue) is associated with increased levels of aneuploidy in colorectal tumours and confers an

increased cancer risk in mice (Ewart-Toland, 2003). It appears the contribution of spindle checkpoint defects to tumours is widespread and very variable, with a great deal of variation between tumour types. Several spindle checkpoint mutations have been identified in colorectal tumours but extensive analysis of other tumour types, including those specifically associated with aneuploidy have not identified many spindle checkpoint mutations, but some polymorphisms and variations in protein expression (Saeki et al., 2002). Thus it appears the contribution of mutations in spindle checkpoint genes to aneuploidy may be a colorectal tumour specific effect. The explanation for this is not clear but perhaps the high turnover rate of colorectal cells or the driving influence of faecal carcinogens may be contributory factors, perhaps by accelerating the rate of mutations in apoptotic genes to allow checkpoint mutant cells to avoid lethality. Studies of multiple tumour types suggest mild spindle checkpoint mutations, polymorphisms and variations in expression levels may be responsible for a proportion of all aneuploid cancers and these may act in combination with similar minor defects in other mitotic genes to produce CIN and accelerate tumourigenesis. It is likely that a broad range of mitotic genes, some of which are listed in table 1.2, each contribute to a subset of tumours by producing CIN and allowing aneuploidy to develop.

The two conflicting theories regarding the driving force behind tumourigenesis are selection versus growth advantage. Early mutation of genes involved in protecting the stability of the genome would invoke a mutator phenotype necessary for tumour progression (Loeb, 2001) but Tomlinson and Bodmer argue that selection for growth advantage is the initiator and accelerator of tumourigenesis (Tomlinson and Bodmer, 1999) Defects in mitotic genes and proteins may provide a solution to the selection for mutation versus growth advantage paradox. They are envisaged to induce a mutator phenotype by the development of CIN and thus accelerate tumourigenesis. Cells with mutations in checkpoint genes, which prevent mitotic arrest at mitosis in the presence of defects, may also impart a growth advantage on the cell and thus the cell cycle would be shorter, further accelerating tumourigenesis. The p53 protein is involved in both the maintenance of genomic stability through cell cycle checkpoints and also in apoptosis and would thus confer a growth advantage

when mutated. Mutations in p53 are common in tumours, occurring in at least 50%, and in colorectal tumours p53 mutations are generally late events (Molinari, 2000).

So where do spindle checkpoint defects fit into the established order of mutations in colorectal tumours? Current evidence suggests CIN and aneuploidy are early events in tumourigenesis (Fischbach et al., 1991). Assuming that this is true we would expect spindle checkpoint defects to also be early events in colorectal tumourigenesis providing a chromosomal instability and growth advantage to drive later stages of tumour progression. For the CIN to allow the accumulation of multiple gene alterations, through mutation, gene rearrangements and the loss and gain of chromosomes, it is likely there must also be at least one mutation in the apoptosis pathway to allow survival of the mutant cells and their subsequent selection to tumourigenesis. This apoptotic mutation may be an earlier event than the development of the mitotic defect, thus allowing the survival of a sub-population of cells with defects in chromosome segregation. Alternatively, it may develop as a result of the accelerated mutator phenotype produced by CIN and occur downstream of it. The population of cells with a mitotic defect would be expected to accumulate a wide range of different mutations through chromosome segregation. By chance, a proportion of these cells may develop mutations in apoptotic genes, allowing them to survive the accumulation of numerous genetic alterations and accelerating their tumourigenic potential. This hypothesis could be further addressed by examining colorectal tumours with mitotic defects for mutations and variable expression of apoptotic genes and other key contributors to colorectal tumourigenesis such as K-Ras, p53 and APC. The examination of tumours at different stages of tumourigenesis would also provide important information when determining the order of mutations in tumour progression. The BUB1 and BUBR1 antibodies developed during the work described in this thesis could be used for example to examine the expression of these spindle checkpoint proteins in tumours and adenomas at different stages. Understanding the order of mutations in carcinogenesis, can aid diagnosis and treatment of patient tumours.

The relatively rare identification of spindle checkpoint mutations in tumours may reflect the wide range of mitotic genes potentially involved in generating aneuploidy. However, studies in mice suggest mutations in spindle checkpoint genes may be

lethal (Dobles et al., 2001) and thus mutations which abolish checkpoint function may be selected against in tumourigenesis. This is interesting in the context of the checkpoint mutations described here, where the yeast functional analysis shows that the identified mutations induce compromisation but not full abolition of checkpoint function and checkpoint protein complex formation, at least in the case of BUB1. This would impart the advantageous mutator and growth advantage phenotypes on the cell but may allow them to escape the lethality associated with full abolishment of protein function. Thus only those mutations which compromise checkpoint function without fully abolishing it may be observed in tumours, with full 'knock-out' mutations being lethal to the cell, reducing the frequency of such mutations. This is supported by evidence from microcolony and benomyl sensitivity assays which demonstrate that the ΔE5 mutants are more viable than the null *bub1* and *mad3* mutants. In summary, it is likely that there is a small range of spindle checkpoint mutations which impart growth advantages and mutator phenotypes while avoiding the lethality associated with null mutants.

This is further supported by the hypothesis that the known checkpoint mutations, which are heterozygous in nature, exert dominant negative effects, preventing the protein expressed from the wild type allele from functioning correctly. If the mutant allele produced a protein whose function was abolished this would produce a near null phenotype, which may be lethal to the cell. In addition, only one germline defect in spindle checkpoint proteins has been identified in BUB1 (Cahill et al., 1998) and the effect of this has not been studied, supporting the hypothesis that they may be lethal during development, even in heterozygous form. Thus spindle checkpoint mutations may contribute to sporadic colorectal tumours but not to an inherited susceptibility to aneuploid colorectal tumours. However, spindle checkpoint polymorphisms may confer a familial susceptibility to aneuploid colorectal tumours through more subtle defects in mitotic processes.

Future directions for this work could focus on further analysis of the effects of the ΔE5 mutations using *S.pombe* and human systems. This would allow more intricate investigation of the effects of the mutations on the localisation and interactions of the proteins. Analysis in the human system also has increased relevance to the BUBR1 ΔE5 mutation, as the protein does differ in sequence from the yeast Mad3p and

Bub1p proteins and BUBR1 is suggested to have a prominent role in mitosis (Ditchfield et el., 2003) and thus the relevance of the BUB1 and MAD3ΔE5 phenotypes is not clear.

In addition, the genomic change associated with the mutant transcript and nature of the protein defect will be examined in future work. The development of the antibodies generated during this work will aid these investigations into the effect of the ΔE5 change at the protein level and may also be utilised in immunohistochemistry experiments to examine expression levels of BUB1 and BUBR1 at different stages of tumourigenesis.

Ultimately, the effect of the BUBR1ΔE5 mutation could be further determined by development of a mutant mouse. The conservation between human and mouse proteins is greater than that between yeast and human and thus the relevance to tumourigenesis is greater than that of the yeast functional analysis. In addition, the physiological effect and impact on tumourigenesis can be examined in mice, while the mouse embryonic stem cells provide a renewable source for similar functional analysis to that planned in the human cell lines, including the effect of protein complex formation, mitotic checkpoint function and protein localisation. The interaction with other important spindle checkpoint and chromosome segregation genes could easily be investigated with appropriate strain crosses.

In conclusion, spindle checkpoint mutations such as BUBR1ΔE5 and BUB1V400 make a significant contribution to spindle checkpoint dysfunction and mis-segregation of chromosomes. The work presented in this thesis, using a yeast model system, demonstrated that these mutations abrogate spindle checkpoint function and induce a chromosome mis-segregation phenotype which is associated with the CIN observed in the majority of colorectal tumours. These phenotypes are attributable to specific defects in spindle checkpoint protein complex formation and tools have been developed to further investigate these effects in a human system. These investigations will aid our understanding of the significant contribution of spindle checkpoint mutations to aneuploid tumour formation.

Chapter 8: Bibliography

Aaltonen,L.A., Peltomaki,P., Leach,F.S., Sistonen,P., Pylkkanen,L., Mecklin,J.P., Jarvinen,H., Powell,S.M., Jen,J., and Hamilton,S.R. (1993). Clues to the pathogenesis of familial colorectal cancer [see comments]. Science *260*, 812-816.

Aaltonen,L.A., Salovaara,R., Kristo,P., Canzian,F., Hemminki,A., Peltomaki,P., Chadwick,R.B., Kaariainen,H., Eskelinen,M., Jarvinen,H., Mecklin,J.P., and de la Chapelle,A. (1998). Incidence of hereditary nonpolyposis colorectal cancer and the feasibility of molecular screening for the disease [see comments]. N. Engl. J Med *338*, 1481-1487.

Abrieu,A., Kahana,J.A., Wood,K.W., and Cleveland,D.W. (2000) CENP-E as an essential component of the mitotic checkpoint in vitro. *102*, 817-826.

Abrieu,A., Magnaghi-Jaulin,L., Kahana,J.A., Peter,M., Castro,A., Vigneron,S., Lorca,T., Cleveland,D.W., and Labbe,J.C. (2001). Mps1 is a kinetochore-associated kinase essential for the vertebrate mitotic checkpoint. Cell *106*, 83-93.

Adams,R.R., Eckley,D.M., Vagnarelli,P., Wheatley,S.P., Gerloff,D.L., Mackay,A.M., Svingen,P.A., Kaufmann,S.H., and Earnshaw,W.C. (2001). Human INCENP colocalizes with the Aurora-B/AIRK2 kinase on chromosomes and is overexpressed in tumour cells. Chromosoma *110*, 65-74.

Al Tassan,N., Chmiel,N.H., Maynard,J., Fleming,N., Livingston,A.L., Williams,G.T., Hodges,A.K., Davies,D.R., David,S.S., Sampson,J.R., and Cheadle,J.P. (2002). Inherited variants of MYH associated with somatic G:C-->T:A mutations in colorectal tumors. Nat. Genet. *30*, 227-232.

Alexandru,G., Uhlmann,F., Mechtler,K., Poupart,M.A., and Nasmyth,K. (2001). Phosphorylation of the cohesin subunit Scc1 by Polo/Cdc5 kinase regulates sister chromatid separation in yeast. Cell *105*, 459-472.

Alexandru,G., Zachariae,W., Schleiffer,A., and Nasmyth,K. (1999). Sister chromatid separation and chromosome re-duplication are regulated by different mechanisms in response to spindle damage. EMBO J *18*, 2707-2721.

Amon,A. (1999). The spindle checkpoint. Curr Opin Genet Dev *9*, 69-75.

Amon,A. (2001). Together until separin do us part. Nat. Cell Biol. *3*, E12-E14.

Baba,H., Korenaga,D., Kakeji,Y., Haraguchi,M., Okamura,T., and Maehara,Y. (2002). DNA ploidy and its clinical implications in gastric cancer. Surgery *131*, S63-S70.

Bardelli,A., Cahill,D.P., Lederer,G., Speicher,M.R., Kinzler,K.W., Vogelstein,B., and Lengauer,C. (2001). Carcinogen-specific induction of genetic instability. Proc. Natl. Acad. Sci. U. S. A *98*, 5770-5775.

Bardin,A.J. and Amon,A. (2001). Men and sin: what's the difference? Nat. Rev. Mol. Cell Biol. *2*, 815-826.

Basto,R., Gomes,R., and Karess,R.E. (2000). Rough deal and Zw10 are required for the metaphase checkpoint in Drosophila. Nat. Cell Biol 2000. Dec. ;2. (12.):939. - 43. *2*, 939-943.

Basu,J., Bousbaa,H., Logarinho,E., Li,Z., Williams,B.C., Lopes,C., Sunkel,C.E., and Goldberg,M.L. (1999). Mutations in the essential spindle checkpoint gene bub1 cause chromosome missegregation and fail to block apoptosis in Drosophila. J Cell Biol *146*, 13-28.

Basu,J., Logarinho,E., Herrmann,S., Bousbaa,H., Li,Z., Chan,G.K., Yen,T.J., Sunkel,C.E., and Goldberg,M.L. (1998). Localization of the Drosophila checkpoint control protein Bub3 to the kinetochore requires Bub1 but not Zw10 or Rod. Chromosoma *107*, 376-385.

Bernard,P., Hardwick,K., and Javerzat,J.P. (1998). Fission yeast bub1 is a mitotic centromere protein essential for the spindle checkpoint and the preservation of correct ploidy through mitosis. J Cell Biol *143*, 1775-1787.

Berrueta,L., Kraeft,S.K., Tirnauer,J.S., Schuyler,S.C., Chen,L.B., Hill,D.E., Pellman,D., and Bierer,B.E. (1998). The adenomatous polyposis coli-binding protein EB1 is associated with cytoplasmic and spindle microtubules. Proc Natl Acad Sci U S A *95*, 10596-10601.

Biggins,S. and Murray,A.W. (1999). Sister chromatid cohesion in mitosis. Curr Opin Genet Dev *9*, 230-236.

Biggins,S. and Murray,A.W. (2001). The budding yeast protein kinase Ipl1/Aurora allows the absence of tension to activate the spindle checkpoint. Genes Dev. *15*, 3118-3129.

Bingham,S.A., Day,N.E., Luben,R., Ferrari,P., Slimani,N., Norat,T., Clavel-Chapelon,F., Kesse,E., Nieters,A., Boeing,H., Tjonneland,A., Overvad,K., Martinez,C., Dorronsoro,M., Gonzalez,C.A., Key,T.J., Trichopoulou,A., Naska,A., Vineis,P., Tumino,R., Krogh,V., Bueno-de-Mesquita,H.B., Peeters,P.H., Berglund,G., Hallmans,G., Lund,E., Skeie,G., Kaaks,R., and Riboli,E. (2003). Dietary fibre in food and protection against colorectal cancer in the European Prospective Investigation into Cancer and Nutrition (EPIC): an observational study. Lancet *361*, 1496-1501.

Birkenbihl,R.P. and Subramani,S. (1995). The rad21 gene product of Schizosaccharomyces pombe is a nuclear, cell cycle-regulated phosphoprotein. J. Biol. Chem. *270*, 7703-7711.

Bischoff,J.R., Anderson,L., Zhu,Y., Mossie,K., Ng,L., Souza,B., Schryver,B., Flanagan,P., Clairvoyant,F., Ginther,C., Chan,C.S., Novotny,M., Slamon,D.J., and

Plowman,G.D. (1998). A homologue of Drosophila aurora kinase is oncogenic and amplified in human colorectal cancers. EMBO J. *17*, 3052-3065.

Bisgaard,M.L., Fenger,K., Bulow,S., Niebuhr,E., and Mohr,J. (1994). Familial adenomatous polyposis (FAP): frequency, penetrance, and mutation rate. Hum Mutat *3*, 121-125.

Boland,C.R. (2000). Molecular genetics of hereditary nonpolyposis colorectal cancer. Ann N Y Acad Sci *910*, 50-59.

Borresen,A.L., Lothe,R.A., Meling,G.I., Lystad,S., Morrison,P., Lipford,J., Kane,M.F., Rognum,T.O., and Kolodner,R.D. (1995). Somatic mutations in the hMSH2 gene in microsatellite unstable colorectal carcinomas. Hum Mol Genet *4*, 2065-2072.

Brady,D.M. and Hardwick,K.G. (2000). Complex formation between Mad1p, Bub1p and Bub3p is crucial for spindle checkpoint function. Curr. Biol. *10*, 675-678.

Brinkley,B.R. (2001). Managing the centrosome numbers game: from chaos to stability in cancer cell division. Trends Cell Biol *11*, 18-21.

Buonomo,S.B., Clyne,R.K., Fuchs,J., Loidl,J., Uhlmann,F., and Nasmyth,K. (2000). Disjunction of homologous chromosomes in meiosis I depends on proteolytic cleavage of the meiotic cohesin Rec8 by separin. Cell *103*, 387-398.

Burkitt,D.P. (1971). Epidemiology of cancer of the colon and rectum. Cancer *28*, 3-13.

Cahill,D.P., da Costa,L.T., Carson-Walter,E.B., Kinzler,K.W., Vogelstein,B., and Lengauer,C. (1999). Characterization of MAD2B and other mitotic spindle checkpoint genes. Genomics *58*, 181-187.

Cahill,D.P., Lengauer,C., Yu,J., Riggins,G.J., Willson,J.K., Markowitz,S.D., Kinzler,K.W., and Vogelstein,B. (1998). Mutations of mitotic checkpoint genes in human cancers [see comments]. Nature *392*, 300-303.

Campbell,L. and Hardwick,K.G. (2003). Analysis of Bub3 spindle checkpoint function in Xenopus egg extracts. J. Cell Sci. *116*, 617-628.

Campbell,M.S., Chan,G.K., and Yen,T.J. (2001). Mitotic checkpoint proteins HsMAD1 and HsMAD2 are associated with nuclear pore complexes in interphase. J. Cell Sci. *114*, 953-963.

Campbell,M.S. and Gorbsky,G.J. (1995). Microinjection of mitotic cells with the 3F3/2 anti-phosphoepitope antibody delays the onset of anaphase. J. Cell Biol. *129*, 1195-1204.

Chan,G.K., Jablonski,S.A., Starr,D.A., Goldberg,M.L., and Yen,T.J. (2000). Human Zw10 and ROD are mitotic checkpoint proteins that bind to kinetochores. Nat. Cell Biol 2000. Dec. ;2. (12.):944. -7. *2*, 944-947.

Chan,G.K., Jablonski,S.A., Sudakin,V., Hittle,J.C., and Yen,T.J. (1999). Human BUBR1 is a mitotic checkpoint kinase that monitors CENP-E functions at kinetochores and binds the cyclosome/APC. J Cell Biol *146*, 941-954.

Chan,G.K., Schaar,B.T., and Yen,T.J. (1998). Characterization of the kinetochore binding domain of CENP-E reveals interactions with the kinetochore proteins CENP-F and hBUBR1. J Cell Biol *143*, 49-63.

Chaturvedi,P., Sudakin,V., Bobiak,M.L., Fisher,P.W., Mattern,M.R., Jablonski,S.A., Hurle,M.R., Zhu,Y., Yen,T.J., and Zhou,B.B. (2002). Chfr regulates a mitotic stress pathway through its RING-finger domain with ubiquitin ligase activity. Cancer Res. *62*, 1797-1801.

Chen,J. and Fang,G. (2001). MAD2B is an inhibitor of the anaphase-promoting complex. Genes Dev. *15*, 1765-1770.

Chen,R.H. (2002). BubR1 is essential for kinetochore localization of other spindle checkpoint proteins and its phosphorylation requires Mad1. J. Cell Biol. *158*, 487-496.

Chen,R.H., Brady,D.M., Smith,D., Murray,A.W., and Hardwick,K.G. (1999). The spindle checkpoint of budding yeast depends on a tight complex between the Mad1 and Mad2 proteins. Mol. Biol Cell *10*, 2607-2618.

Chen,R.H., Shevchenko,A., Mann,M., and Murray,A.W. (1998). Spindle checkpoint protein Xmad1 recruits Xmad2 to unattached kinetochores. J Cell Biol *143*, 283-295.

Chen,R.H., Waters,J.C., Salmon,E.D., and Murray,A.W. (1996). Association of spindle assembly checkpoint component XMAD2 with unattached kinetochores. Science *274*, 242-246.

Chung,E. and Chen,R.H. (2002). Spindle checkpoint requires Mad1-bound and Mad1-free Mad2. Mol. Biol. Cell *13*, 1501-1511.

Chung,E and Chen,R.H. (2003). Phosphorylation of Cdc20 is required for its inhibition by the spindle checkpoint. Nat. Cell Biol *5*, 748-53.

Ciosk,R., Shirayama,M., Shevchenko,A., Tanaka,T., Toth,A., Shevchenko,A., and Nasmyth,K. (2000). Cohesin's binding to chromosomes depends on a separate complex consisting of Scc2 and Scc4 proteins. Mol. Cell *5*, 243-254.

Ciosk,R., Zachariae,W., Michaelis,C., Shevchenko,A., Mann,M., and Nasmyth,K. (1998). An ESP1/PDS1 complex regulates loss of sister chromatid cohesion at the metaphase to anaphase transition in yeast. Cell *93*, 1067-1076.

Clarke,D.J. (2002). Spotlight on mitosis: introduction. Cell Cycle *1*, 298-299.

Clarke,D.J. and Gimenez-Abian,J.F. Checkpoints controlling mitosis. (2000). Bioessays. *22*, 351-363.

Cohen-Fix,O., Peters,J.M., Kirschner,M.W., and Koshland,D. (1996). Anaphase initiation in Saccharomyces cerevisiae is controlled by the APC-dependent degradation of the anaphase inhibitor Pds1p. Genes Dev. *10*, 3081-3093.

Corn,P.G., Summers,M.K., Fogt,F., Virmani,A.K., Gazdar,A.F., Halazonetis,T.D., and El Deiry,W.S. (2003). Frequent hypermethylation of the 5' CpG island of the mitotic stress checkpoint gene Chfr in colorectal and non-small cell lung cancer. Carcinogenesis *24*, 47-51.

Cortez,D. and Elledge,S.J. (2000). Conducting the mitotic symphony. Nature 2000. *406*, 354-356.

Dawson,I.A., Roth,S., Akam,M., and Artavanis-Tsakonas,S. (1993). Mutations of the fizzy locus cause metaphase arrest in Drosophila melanogaster embryos. Development *117*, 359-376.

Dawson,I.A., Roth,S., and Artavanis-Tsakonas,S. (1995). The Drosophila cell cycle gene fizzy is required for normal degradation of cyclins A and B during mitosis and has homology to the CDC20 gene of Saccharomyces cerevisiae. J. Cell Biol. *129*, 725-737.

Delattre,O., Olschwang,S., Law,D.J., Melot,T., Remvikos,Y., Salmon,R.J., Sastre,X., Validire,P., Feinberg,A.P., and Thomas,G. (1989). Multiple genetic alterations in distal and proximal colorectal cancer. Lancet *2*, 353-356.

Delhommeau,F., Vasseur-Godbillon,C., Leclerc,P., Schischmanoff,P.O., Croisille,L., Rince,P., Moriniere,M., Benz,E.J., Jr., Tchernia,G., Tamagnini,G., Ribeiro,L., Delaunay,J., and Baklouti,F. (2002). A splicing alteration of 4.1R pre-mRNA generates 2 protein isoforms with distinct assembly to spindle poles in mitotic cells. Blood *100*, 2629-2636.

Ditchfield,C., Johnson,V.L., Tighe,A., Ellston,R., Haworth,C., Johnson,T., Mortlock,A., Keen,N., and Taylor,S.S. (2003). Aurora B couples chromosome alignment with anaphase by targeting BubR1, Mad2, and Cenp-E to kinetochores. J. Cell Biol. *161*, 267-280.

Dobles,M., Liberal,V., Scott,M.L., Benezra,R., and Sorger,P.K. (2000). Chromosome missegregation and apoptosis in mice lacking the mitotic checkpoint protein Mad2. Cell. *101*, 635-645.

Doherty,F.J., Dawson,S., and Mayer,R.J. (2002). The ubiquitin-proteasome pathway of intracellular proteolysis. Essays Biochem. *38:51-63.*, 51-63.

Duesberg,P. and Li,R. (2003). Multistep carcinogenesis: a chain reaction of aneuploidizations. Cell Cycle *2*, 202-210.

Dunlop,M.G., Farrington,S.M., Carothers,A.D., Wyllie,A.H., Sharp,L., Burn,J., Liu,B., Kinzler,K.W., and Vogelstein,B. (1997). Cancer risk associated with germline DNA mismatch repair gene mutations. Hum Mol Genet *6*, 105-110.

Dunlop,M.G., Farrington,S.M., Nicholl,I., Aaltonen,L., Petersen,G., Porteous,M., and Carothers,A. (2000). Population carrier frequency of hMSH2 and hMLH1 mutations. Br J Cancer *83*, 1643-1645.

Elledge,S.J. (1996). Cell cycle checkpoints: preventing an identity crisis. Science *274*, 1664-1672.

Ewart-Toland,A.; Briassouli,P.; de Koning,J.P.; Mao,J.H.; Yuan,J.; Chan,F.; MacCarthy-Morrogh,L.; Ponder,B.A.; Nagase,H.; Burn,J.; Ball,S.; Almeida,M.; Linardopoulos,S.; Balmain,A. (2003). Identification of Stk6/STK15 as a candidate low-penetrance tumor-susceptibility gene in mouse and human. Nat.Genet. *34* 403-412.

Ewen,M.E., Sluss,H.K., Whitehouse,L.L., and Livingston,D.M. (1993). TGF beta inhibition of Cdk4 synthesis is linked to cell cycle arrest. Cell *74*, 1009-1020.

Fang,G. (2002). Checkpoint protein BubR1 acts synergistically with Mad2 to inhibit anaphase-promoting complex. Mol. Biol. Cell *13*, 755-766.

Fang,G., Yu,H., and Kirschner,M.W. (1998). The checkpoint protein MAD2 and the mitotic regulator CDC20 form a ternary complex with the anaphase-promoting complex to control anaphase initiation. Genes Dev. *12*, 1871-1883.

Farr,K.A. and Hoyt,M.A. (1998). Bub1p kinase activates the Saccharomyces cerevisiae spindle assembly checkpoint. Mol Cell Biol *18*, 2738-2747.

Farrington,S.M. (2003). The Genetics of familial Colon Cancer. In Genetic Predisposition to Cancer, (Chapman and Hall) Edition 2, Chapter 21.

Farrington,S.M. and Dunlop,M.G. (2001). Familial colon cancer syndromes and their genes.

Fearon,E.R. and Vogelstein,B. (1990). A genetic model for colorectal tumorigenesis. Cell *61*, 759-767.

Fischbach,W., Rubsam,B., Mossner,J., Wunsch,H.P., Seyschab,H., and Hohn,H. (1991). DNA aneuploidy and proliferation in spontaneous human and dimethylhydrazine-induced murine colorectal carcinogenesis. Z. Gastroenterol. *29*, 533-537.

Fisk,H.A. and Winey,M. (2001). The mouse Mps1p-like kinase regulates centrosome duplication. Cell *106*, 95-104.

Fodde,R., Kuipers,J., Rosenberg,C., Smits,R., Kielman,M., Gaspar,C., van Es,J.H., Breukel,C., Wiegant,J., Giles,R.H., and Clevers,H. (2001). Mutations in the APC tumour suppressor gene cause chromosomal instability. Nat. Cell Biol. *3*, 433-438.

Franceschi,S., Favero,A., La Vecchia,C., Negri,E., Conti,E., Montella,M., Giacosa,A., Nanni,O., and Decarli,A. (1997). Food groups and risk of colorectal cancer in Italy. Int J Cancer *72*, 56-61.

Fraschini,R., Beretta,A., Sironi,L., Musacchio,A., Lucchini,G., and Piatti,S. (2001). Bub3 interaction with Mad2, Mad3 and Cdc20 is mediated by WD40 repeats and does not require intact kinetochores. EMBO J. *20*, 6648-6659.

Fukasawa,K., Choi,T., Kuriyama,R., Rulong,S., and Vande Woude,G.F. (1996). Abnormal centrosome amplification in the absence of p53. Science *271*, 1744-1747.

Funabiki,H., Kumada,K., and Yanagida,M. (1996a). Fission yeast Cut1 and Cut2 are essential for sister chromatid separation, concentrate along the metaphase spindle and form large complexes. EMBO J. *15*, 6617-6628.

Funabiki,H., Yamano,H., Kumada,K., Nagao,K., Hunt,T., and Yanagida,M. (1996b). Cut2 proteolysis required for sister-chromatid seperation in fission yeast. Nature *381*, 438-441.

Furuta,T., Tuck,S., Kirchner,J., Koch,B., Auty,R., Kitagawa,R., Rose,A.M., and Greenstein,D. (2000). EMB-30: an APC4 homologue required for metaphase-to-anaphase transitions during meiosis and mitosis in Caenorhabditis elegans. Mol Biol Cell *11*, 1401-1419.

Gachet,Y., Tournier,S., Millar,J.B., and Hyams,J.S. (2001). A MAP kinase-dependent actin checkpoint ensures proper spindle orientation in fission yeast. Nature 2001. Jul. *412*, 352-355.

Garcia,M.A., Vardy,L., Koonrugsa,N., and Toda,T. (2001). Fission yeast ch-TOG/XMAP215 homologue Alp14 connects mitotic spindles with the kinetochore and is a component of the Mad2-dependent spindle checkpoint. EMBO J. *20*, 3389-3401.

Gascoyne,D.M., Hixon,M.L., Gualberto,A., and Vivanco,M.D. (2003). Loss of Mitotic Spindle Checkpoint Activity Predisposes to Chromosomal Instability at Early Stages of Fibrosarcoma Development. Cell Cycle *2*, 238-245.

Gertig,D.M. and Hunter,D.J. (1998). Genes and environment in the etiology of colorectal cancer. Semin. Cancer Biol. *8*, 285-298.

Ghigna,C., Moroni,M., Porta,C., Riva,S., and Biamonti,G. (1998). Altered expression of heterogenous nuclear ribonucleoproteins and SR factors in human colon adenocarcinomas. Cancer Res. *58*, 5818-5824.

Giovannucci,E., Rimm,E.B., Stampfer,M.J., Colditz,G.A., Ascherio,A., and Willett,W.C. (1994). Intake of fat, meat, and fiber in relation to risk of colon cancer in men. Cancer Res *54*, 2390-2397.

Goel,A., Arnold,C.N., Niedzwiecki,D., Chang,D.K., Ricciardiello,L., Carethers,J.M., Dowell,J.M., Wasserman,L., Compton,C., Mayer,R.J., Bertagnolli,M.M., and Boland,C.R. (2003). Characterization of sporadic colon cancer by patterns of genomic instability. Cancer Res. *63*, 1608-1614.

Goldbohm,R.A., van den Brandt,P.A., van,'., V, Brants,H.A., Dorant,E., Sturmans,F., and Hermus,R.J. (1994). A prospective cohort study on the relation between meat consumption and the risk of colon cancer. Cancer Res *54*, 718-723.

Gorbsky,G.J. and Ricketts,W.A. (1993). Differential expression of a phosphoepitope at the kinetochores of moving chromosomes. J. Cell Biol. *122*, 1311-1321.

Groden,J., Thliveris,A., Samowitz,W., Carlson,M., Gelbert,L., Albertsen,H., Joslyn,G., Stevens,J., Spirio,L., and Robertson,M. (1991). Identification and characterization of the familial adenomatous polyposis coli gene. Cell *66*, 589-600.

Guacci,V., Koshland,D., and Strunnikov,A. (1997). A direct link between sister chromatid cohesion and chromosome condensation revealed through the analysis of MCD1 in S. cerevisiae. Cell *91*, 47-57.

Haenszel,W. (1961). Cancer mortality among the foreign-born in the united states. J Natl Cancer Inst. *26*, 37-132.

Hagting,A., den Elzen,N., Vodermaier,H.C., Waizenegger,I.C., Peters,J.M., and Pines,J. (2002). Human securin proteolysis is controlled by the spindle checkpoint and reveals when the APC/C switches from activation by Cdc20 to Cdh1. J. Cell Biol. *157*, 1125-1137.

Halford,S.E., Rowan,A.J., Lipton,L., Sieber,O.M., Pack,K., Thomas,H.J., Hodgson,S.V., Bodmer,W.F., and Tomlinson,I.P. (2003). Germline mutations but not somatic changes at the MYH locus contribute to the pathogenesis of unselected colorectal cancers. Am. J. Pathol. *162*, 1545-1548.

Hardwick,K.G. (1998). The spindle checkpoint. Trends Genet *14*, 1-4.

Hardwick,K.G., Johnston,R.C., Smith,D.L., and Murray,A.W. (2000). MAD3 encodes a novel component of the spindle checkpoint which interacts with Bub3p, Cdc20p, and Mad2p. J Cell Biol *148*, 871-882.

Hardwick,K.G. and Murray,A.W. (1995). Mad1p, a phosphoprotein component of the spindle assembly checkpoint in budding yeast. J Cell Biol *131*, 709-720.

Hardwick,K.G., Weiss,E., Luca,F.C., Winey,M., and Murray,A.W. (1996). Activation of the budding yeast spindle assembly checkpoint without mitotic spindle disruption. Science *273*, 953-956.

Hartman,T., Stead,K., Koshland,D., and Guacci,V. (2000). Pds5p Is an Essential Chromosomal Protein Required for both Sister Chromatid Cohesion and Condensation in Saccharomyces cerevisiae. J Cell Biol *151*, 613-626.

Hartwell,L.H. and Kastan,M.B. (1994). Cell cycle control and cancer. Science *266*, 1821-1828.

Haruki,N., Saito,H., Harano,T., Nomoto,S., Takahashi,T., Osada,H., Fujii,Y., and Takahashi,T. (2001). Molecular analysis of the mitotic checkpoint genes BUB1, BUBR1 and BUB3 in human lung cancers. Cancer Lett. *162*, 201-205.

He,X., Jones,M.H., Winey,M., and Sazer,S. (1998). Mph1, a member of the Mps1-like family of dual specificity protein kinases, is required for the spindle checkpoint in S. pombe. J Cell Sci *111*, 1635-1647.

He,X., Patterson,T.E., and Sazer,S. (1997). The Schizosaccharomyces pombe spindle checkpoint protein mad2p blocks anaphase and genetically interacts with the anaphase-promoting complex. Proc. Natl. Acad. Sci. U. S. A *94*, 7965-7970.

Heaney,A.P., Singson,R., McCabe,C.J., Nelson,V., Nakashima,M., and Melmed,S. (2000). Expression of pituitary-tumour transforming gene in colorectal tumours. Lancet *355*, 716-719.

Hempen,P.M., Kurpad,H., Calhoun,E.S., Abraham,S., and Kern,S.E. (2003). A double missense variation of the BUB1 gene and a defective mitotic spindle checkpoint in the pancreatic cancer cell line Hs766T. Hum. Mutat. *21*, 445.

Hieter,P., Mann,C., Snyder,M., and Davis,R.W. (1985). Mitotic stability of yeast chromosomes: a colony color assay that measures nondisjunction and chromosome loss. Cell *40*, 381-392.

Hilioti,Z., Chung,Y.S., Mochizuki,Y., Hardy,C.F., and Cohen-Fix,O. (2001). The anaphase inhibitor Pds1 binds to the APC/C-associated protein Cdc20 in a destruction box-dependent manner. Curr. Biol. *11*, 1347-1352.

Hoffman,D.B., Pearson,C.G., Yen,T.J., Howell,B.J., and Salmon,E.D. (1995). Microtubule-dependent changes in assembly of microtubule motor proteins and mitotic spindle checkpoint proteins at ptk1 kinetochores. Mol. Biol Cell 2001. Jul. ;12. (7.):1995. -2009. *12*, 1995-2009.

Homfray,T.F., Cottrell,S.E., Ilyas,M., Rowan,A., Talbot,I.C., Bodmer,W.F., and Tomlinson,I.P. (1998). Defects in mismatch repair occur after APC mutations in the pathogenesis of sporadic colorectal tumours. Hum Mutat. *11*, 114-120.

Howe,J.R., Roth,S., Ringold,J.C., Summers,R.W., Jarvinen,H.J., Sistonen,P., Tomlinson,I.P., Houlston,R.S., Bevan,S., Mitros,F.A., Stone,E.M., and Aaltonen,L.A. (1998). Mutations in the SMAD4/DPC4 gene in juvenile polyposis. Science *280*, 1086-1088.

Howell,B.J., Hoffman,D.B., Fang,G., Murray,A.W., and Salmon,E.D. (2000). Visualization of Mad2 dynamics at kinetochores, along spindle fibers, and at spindle poles in living cells. J Cell Biol *150*, 1233-1250.

Howell,B.J., McEwen,B.F., Canman,J.C., Hoffman,D.B., Farrar,E.M., Rieder,C.L., and Salmon,E.D. (2001). Cytoplasmic dynein/dynactin drives kinetochore protein transport to the spindle poles and has a role in mitotic spindle checkpoint inactivation. J. Cell Biol. *155*, 1159-1172.

Hoyt,M.A., Stearns,T., and Botstein,D. (1990). Chromosome instability mutants of Saccharomyces cerevisiae that are defective in microtubule-mediated processes. Mol. Cell Biol. *10*, 223-234.

Hoyt,M.A., Totis,L., and Roberts,B.T. (1991). S. cerevisiae genes required for cell cycle arrest in response to loss of microtubule function. Cell *66*, 507-517.

Huang,J., Papadopoulos,N., McKinley,A.J., Farrington,S.M., Curtis,L.J., Wyllie,A.H., Zheng,S., Willson,J.K., Markowitz,S.D., Morin,P., Kinzler,K.W., Vogelstein,B., and Dunlop,M.G. (1996). APC mutations in colorectal tumors with mismatch repair deficiency. Proc. Natl. Acad. Sci. U. S. A *20;93*, 9049-9054.

Huang,J.Y. and Raff,J.W. (2002). The dynamic localisation of the Drosophila APC/C: evidence for the existence of multiple complexes that perform distinct functions and are differentially localised. J. Cell Sci. *115*, 2847-2856.

Hwang,L.H., Lau,L.F., Smith,D.L., Mistrot,C.A., Hardwick,K.G., Hwang,E.S., Amon,A., and Murray,A.W. (1998). Budding yeast Cdc20: a target of the spindle checkpoint. Science *279*, 1041-1044.

Ikui,A.E., Furuya,K., Yanagida,M., and Matsumoto,T. (2002). Control of localization of a spindle checkpoint protein, Mad2, in fission yeast. J. Cell Sci. *115*, 1603-1610.

Iouk,T., Kerscher,O., Scott,R.J., Basrai,M.A., and Wozniak,R.W. (2002). The yeast nuclear pore complex functionally interacts with components of the spindle assembly checkpoint. J. Cell Biol. *159*, 807-819.

Irniger,S., Piatti,S., Michaelis,C., and Nasmyth,K. (1995). Genes involved in sister chromatid separation are needed for B-type cyclin proteolysis in budding yeast. Cell *81*, 269-278.

Iwanaga,Y. and Jeang,K.T. (2002). Expression of mitotic spindle checkpoint protein hsMAD1 correlates with cellular proliferation and is activated by a gain-of-function p53 mutant. Cancer Res. *62*, 2618-2624.

Iwanaga,Y., Kasai,T., Kibler,K., and Jeang,K.T. (2002). Characterization of regions in hsMAD1 needed for binding hsMAD2. A polymorphic change in an hsMAD1 leucine zipper affects MAD1-MAD2 interaction and spindle checkpoint function. J. Biol. Chem. *277*, 31005-31013.

Jablonski,S.A., Chan,G.K., Cooke,C.A., Earnshaw,W.C., and Yen,T.J. (1998). The hBUB1 and hBUBR1 kinases sequentially assemble onto kinetochores during prophase with hBUBR1 concentrating at the kinetochore plates in mitosis. Chromosoma *107*, 386-396.

Jaffrey,R.G., Pritchard,S.C., Clark,C., Murray,G.I., Cassidy,J., Kerr,K.M., Nicolson,M.C., and McLeod,H.L. (2000). Genomic instability at the BUB1 locus in colorectal cancer, but not in non-small cell lung cancer. Cancer Res *60*, 4349-4352.

Jallepalli,P.V. and Lengauer,C. (2001). Chromosome segregation and cancer: cutting through the mystery. Nat. Rev. Cancer *1*, 109-117.

Jensen,S., Segal,M., Clarke,D.J., and Reed,S.I. (2001). A novel role of the budding yeast separin Esp1 in anaphase spindle elongation: evidence that proper spindle association of Esp1 is regulated by Pds1. J. Cell Biol. *152*, 27-40.

Jin,D.Y., Spencer,F., and Jeang,K.T. (1998). Human T cell leukemia virus type 1 oncoprotein Tax targets the human mitotic checkpoint protein MAD1. Cell *93*, 81-91.

Jones,S., Emmerson,P., Maynard,J., Best,J.M., Jordan,S., Williams,G.T., Sampson,J.R., and Cheadle,J.P. (2002). Biallelic germline mutations in MYH predispose to multiple colorectal adenoma and somatic G:C-->T:A mutations. Hum. Mol. Genet. *11*, 2961-2967.

Jorgensen,P.M., Graslund,S., Betz,R., Stahl,S., Larsson,C., and Hoog,C. (2001). Characterisation of the human APC1, the largest subunit of the anaphase-promoting complex. Gene *262*, 51-59.

Joslyn,G., Carlson,M., Thliveris,A., Albertsen,H., Gelbert,L., Samowitz,W., Groden,J., Stevens,J., Spirio,L., and Robertson,M. (1991). Identification of deletion mutations and three new genes at the familial polyposis locus. Cell *66*, 601-613.

Kalitsis,P., Earle,E., Fowler,K.J., and Choo,K.H. (2000). Bub3 gene disruption in mice reveals essential mitotic spindle checkpoint function during early embryogenesis. Genes Dev. *14*, 2277-2282.

Kallio,M., Weinstein,J., Daum,J.R., Burke,D.J., and Gorbsky,G.J. (1998). Mammalian p55CDC mediates association of the spindle checkpoint protein Mad2 with the cyclosome/anaphase-promoting complex, and is involved in regulating anaphase onset and late mitotic events. J Cell Biol *141*, 1393-1406.

Kang,D., Chen,J., Wong,J., and Fang,G. (2002). The checkpoint protein Chfr is a ligase that ubiquitinates Plk1 and inhibits Cdc2 at the G2 to M transition. J. Cell Biol. *156*, 249-259.

Kaplan,K.B., Burds,A.A., Swedlow,J.R., Bekir,S.S., Sorger,P.K., and Nathke,I.S. (2001). A role for the Adenomatous Polyposis Coli protein in chromosome segregation. Nat. Cell Biol. *3*, 429-432.

Karelia,N.H., Patel,D.D., Desai,N.S., Mehta,H.V., Yadav,P.K., Patel,S.M., Kothari,K.C., and Shah,P.M. (2001). Prognostic significance of DNA aneuploidy and p21 ras oncoprotein expression in colorectal cancer and their role in the determination of treatment modalities. Int. J. Biol. Markers *16*, 97-104.

Kasai,T., Iwanaga,Y., Iha,H., and Jeang,K.T. (2002). Prevalent loss of mitotic spindle checkpoint in adult T-cell leukemia confers resistance to microtubule inhibitors. J. Biol. Chem. *277*, 5187-5193.

Kawamura,K., Moriyama,M., Shiba,N., Ozaki,M., Tanaka,T., Nojima,T., Fujikawa-Yamamoto,K., Ikeda,R., and Suzuki,K. (2003). Centrosome hyperamplification and chromosomal instability in bladder cancer. Eur. Urol. *43*, 505-515.

Kikuchi,H., Takata,A., Akasaka,Y., Fukuzawa,R., Yoneyama,H., Kurosawa,Y., Honda,M., Kamiyama,Y., and Hata,J. (1998). Do intronic mutations affecting splicing of WT1 exon 9 cause Frasier syndrome? J Med Genet *35*, 45-48.

King,R.W., Peters,J.M., Tugendreich,S., Rolfe,M., Hieter,P., and Kirschner,M.W. (1995). A 20S complex containing CDC27 and CDC16 catalyzes the mitosis-specific conjugation of ubiquitin to cyclin B. Cell *81*, 279-288.

Kinzler,K.W., Nilbert,M.C., Su,L.K., Vogelstein,B., Bryan,T.M., Levy,D.B., Smith,K.J., Preisinger,A.C., Hedge,P., and McKechnie,D. (1991). Identification of FAP locus genes from chromosome 5q21. Science *253*, 661-665.

Kinzler,K.W. and Vogelstein,B. (1996). Lessons from hereditary colorectal cancer. Cell *87*, 159-170.

Kitaeva,M.N., Grogan,L., Williams,J.P., Dimond,E., Nakahara,K., Hausner,P., DeNobile,J.W., Soballe,P.W., and Kirsch,I.R. (1997). Mutations in beta-catenin are uncommon in colorectal cancer occurring in occasional replication error-positive tumors. Cancer Res *57*, 4478-4481.

Kitagawa,K., Abdulle,R., Bansal,P.K., Cagney,G., Fields,S., and Hieter,P. (2003). Requirement of skp1-bub1 interaction for kinetochore-mediated activation of the spindle checkpoint. Mol. Cell *11*, 1201-1213.

Kitagawa,R. and Rose,A.M. (1999). Components of the spindle-assembly checkpoint are essential in Caenorhabditis elegans. Nat Cell Biol *1*, 514-521.

Kitamura,K., Maekawa,H., and Shimoda,C. (1998). Fission yeast Ste9, a homolog of Hct1/Cdh1 and Fizzy-related, is a novel negative regulator of cell cycle progression during G1-phase. Mol. Biol. Cell *9*, 1065-1080.

Klamt,B., Koziell,A., Poulat,F., Wieacker,P., Scambler,P., Berta,P., and Gessler,M. (1998). Frasier syndrome is caused by defective alternative splicing of WT1 leading to an altered ratio of WT1 +/-KTS splice isoforms. Hum Mol Genet *7*, 709-714.

Kolodner,R.D., Putnam,C.D., and Myung,K. (2002). Maintenance of genome stability in Saccharomyces cerevisiae. Science *297*, 552-557.

Kominami,K., Seth-Smith,H., and Toda,T. (1998). Apc10 and Ste9/Srw1, two regulators of the APC-cyclosome, as well as the CDK inhibitor Rum1 are required for G1 cell-cycle arrest in fission yeast. EMBO J. *17*, 5388-5399.

Kotani,S., Tanaka,H., Yasuda,H., and Todokoro,K. (1999). Regulation of APC activity by phosphorylation and regulatory factors. J. Cell Biol. *146*, 791-800.

Kramer,A., Neben,K., and Ho,A.D. (2002). Centrosome replication, genomic instability and cancer. Leukemia *16*, 767-775.

Kruse,R., Rutten,A., Lamberti,C., Hosseiny-Malayeri,H.R., Wang,Y., Ruelfs,C., Jungck,M., Mathiak,M., Ruzicka,T., Hartschuh,W., Bisceglia,M., Friedl,W., and Propping,P. (1998). Muir-Torre phenotype has a frequency of DNA mismatch-repair-gene mutations similar to that in hereditary nonpolyposis colorectal cancer families defined by the Amsterdam criteria. Am J Hum Genet *63*, 63-70.

La Vecchia,C., Negri,E., Franceschi,S., Conti,E., Montella,M., Giacosa,A., Falcini,A., and Decarli,A. (1997). Aspirin and colorectal cancer. Br J Cancer *76*, 675-677.

Lanzi,C., Cassinelli,G., Cuccuru,G., Supino,R., Zuco,V., Ferlini,C., Scambia,G., and Zunino,F. (2001). Cell cycle checkpoint efficiency and cellular response to paclitaxel in prostate cancer cells. Prostate *48*, 254-264.

Le Marchand,L., Wilkens,L.R., Kolonel,L.N., Hankin,J.H., and Lyu,L.C. (1997). Associations of sedentary lifestyle, obesity, smoking, alcohol use, and diabetes with the risk of colorectal cancer. Cancer Res *57*, 4787-4794.

Lee,S.B. and Haber,D.A. . (2001). Wilms tumor and the WT1 gene. Exp. Cell Res. *264*, 74-99.

Leismann,O., Herzig,A., Heidmann,S., and Lehner,C.F. (2000). Degradation of Drosophila PIM regulates sister chromatid separation during mitosis. Genes Dev. *14*, 2192-2205.

Lengauer,C., Kinzler,K.W., and Vogelstein,B. (1997). Genetic instability in colorectal cancers. Nature *386*, 623-627.

Lengauer,C., Kinzler,K.W., and Vogelstein,B. (1998). Genetic instabilities in human cancers. Nature *396*, 643-649.

Levi,F., Pasche,C., La Vecchia,C., Lucchini,F., and Franceschi,S. (1999). Food groups and colorectal cancer risk. Br J Cancer *79*, 1283-1287.

Li,R. and Murray,A.W. (1991). Feedback control of mitosis in budding yeast. Cell *66*, 519-531.

Li,R., Sonik,A., Stindl,R., Rasnick,D., and Duesberg,P. (2000). Aneuploidy vs. gene mutation hypothesis of cancer: recent study claims mutation but is found to support aneuploidy. Proc Natl Acad Sci U S A *97*, 3236-3241.

Li,W., Lan,Z., Wu,H., Wu,S., Meadows,J., Chen,J., Zhu,V., and Dai,W. (1999). BUBR1 phosphorylation is regulated during mitotic checkpoint activation. Cell Growth Differ *10*, 769-775.

Li,X. and Nicklas,R.B. (1995). Mitotic forces control a cell-cycle checkpoint. Nature *373*, 630-632.

Li,Y. and Benezra,R. (1996). Identification of a human mitotic checkpoint gene: hsMAD2. Science *274*, 246-248.

Li,Y., Gorbea,C., Mahaffey,D., Rechsteiner,M., and Benezra,R. (1997). MAD2 associates with the cyclosome/anaphase-promoting complex and inhibits its activity. Proc Natl Acad Sci U S A *94*, 12431-12436.

Liao,H., Winkfein,R.J., Mack,G., Rattner,J.B., and Yen,T.J. (1995). CENP-F is a protein of the nuclear matrix that assembles onto kinetochores at late G2 and is rapidly degraded after mitosis. J. Cell Biol. *130*, 507-518.

Liaw,D., Marsh,D.J., Li,J., Dahia,P.L., Wang,S.I., Zheng,Z., Bose,S., Call,K.M., Tsou,H.C., Peacocke,M., Eng,C., and Parsons,R. (1997). Germline mutations of the PTEN gene in Cowden disease, an inherited breast and thyroid cancer syndrome. Nat Genet *16*, 64-67.

Liu,S.T., Chan,G.K., Hittle,J.C., Fujii,G., Lees,E., and Yen,T.J. (2003a). Human MPS1 kinase is required for mitotic arrest induced by the loss of CENP-E from kinetochores. Mol. Biol. Cell *14*, 1638-1651.

Liu,S.T., Hittle,J.C., Jablonski,S.A., Campbell,M.S., Yoda,K., and Yen,T.J. (2003b). Human CENP-I specifies localization of CENP-F, MAD1 and MAD2 to kinetochores and is essential for mitosis. Nat. Cell Biol. *5*, 341-345.

Loeb,L.A. (2001). A mutator phenotype in cancer. Cancer Res *61*, 3230-3239.

Loeb,L.A., Springgate,C.F., and Battula,N. (1974). Errors in DNA replication as a basis of malignant changes. Cancer Res *34*, 2311-2321.

Longnecker,M.P., Orza,M.J., Adams,M.E., Vioque,J., and Chalmers,T.C. (1990). A meta-analysis of alcoholic beverage consumption in relation to risk of colorectal cancer. Cancer Causes Control *1*, 59-68.

Losada,A., Hirano,M., and Hirano,T. (1998). Identification of Xenopus SMC protein complexes required for sister chromatid cohesion. Genes Dev. *12*, 1986-1997.

Losada,A., Yokochi,T., Kobayashi,R., and Hirano,T. (2000). Identification and characterization of SA/Scc3p subunits in the Xenopus and human cohesin complexes. J. Cell Biol. *150*, 405-416.

Luo,X., Fang,G., Coldiron,M., Lin,Y., Yu,H., Kirschner,M.W., and Wagner,G. (2000). Structure of the Mad2 spindle assembly checkpoint protein and its interaction with Cdc20. Nat. Struct. Biol. *7*, 224-229.

Luo,X., Tang,Z., Rizo,J., and Yu,H. (2002). The Mad2 spindle checkpoint protein undergoes similar major conformational changes upon binding to either Mad1 or Cdc20. Mol. Cell *9*, 59-71.

Lynch,E.D., Ostermeyer,E.A., Lee,M.K., Arena,J.F., Ji,H., Dann,J., Swisshelm,K., Suchard,D., MacLeod,P.M., Kvinnsland,S., Gjertsen,B.T., Heimdal,K., Lubs,H.,

Moller,P., and King,M.C. (1997). Inherited mutations in PTEN that are associated with breast cancer, cowden disease, and juvenile polyposis. Am J Hum Genet *61*, 1254-1260.

Lynch,H.T. and de la Chapelle,A. (1999). Genetic susceptibility to non-polyposis colorectal cancer. J Med Genet *36*, 801-818.

Ma,A.H., Xia,L., Littman,S.J., Swinler,S., Lader,G., Polinkovsky,A., Olechnowicz,J., Kasturi,L., Lutterbaugh,J., Modrich,P., Veigl,M.L., Markowitz,S.D., and Sedwick,W.D. (2000). Somatic mutation of hPMS2 as a possible cause of sporadic human colon cancer with microsatellite instability. Oncogene *19*, 2249-2256.

Malkhosyan,S., Rampino,N., Yamamoto,H., and Perucho,M. (1996). Frameshift mutator mutations [letter]. Nature *382*, 499-500.

Mao,Y., Abrieu,A. and Cleveland,D.W. (2003). Activating and Silencing the mitotic checkpoint through CENP-E-Dependent activation/inactivation of BubR1. Cell *114* 87-98.

Martinez-Exposito,M.J., Kaplan,K.B., Copeland,J., and Sorger,P.K. (1999). Retention of the BUB3 checkpoint protein on lagging chromosomes. Proc. Natl. Acad. Sci. U. S. A *20;96*, 8493-8498.

Masuda,T.A., Inoue,H., Sonoda,H., Mine,S., Yoshikawa,Y., Nakayama,K., Nakayama,K., and Mori,M. (2002). Clinical and biological significance of S-phase kinase-associated protein 2 (Skp2) gene expression in gastric carcinoma: modulation of malignant phenotype by Skp2 overexpression, possibly via p27 proteolysis. Cancer Res. *62*, 3819-3825.

Matsumoto,T. (1997). A fission yeast homolog of CDC20/p55CDC/Fizzy is required for recovery from DNA damage and genetically interacts with p34cdc2. Mol. Cell Biol. *17*, 742-750.

Matsuura,S., Ito,E., Tauchi,H., Komatsu,K., Ikeuchi,T., and Kajii,T. . (2000)Chromosomal instability syndrome of total premature chromatid separation with mosaic variegated aneuploidy is defective in mitotic-spindle checkpoint. Am. J. Hum. Genet. *67*, 483-486.

McCollum,D. and Gould,K.L. (2001). Timing is everything: regulation of mitotic exit and cytokinesis by the MEN and SIN. Trends. Cell Biol *11*, 89-95.

McEwen,B.F., Chan,G.K., Zubrowski,B., Savoian,M.S., Sauer,M.T., and Yen,T.J. (2001). CENP-E is essential for reliable bioriented spindle attachment, but chromosome alignment can be achieved via redundant mechanisms in mammalian cells. Mol. Biol. Cell *12*, 2776-2789.

McMichael,A.J. and Giles,G.G. (1988). Cancer in migrants to Australia: extending the descriptive epidemiological data. Cancer Res *48*, 751-756.

Mecklin,J.P., Jarvinen,H.J., Hakkiluoto,A., Hallikas,H., Hiltunen,K.M., Harkonen,N., Kellokumpu,I., Laitinen,S., Ovaska,J., and Tulikoura,J. (1995). Frequency of hereditary nonpolyposis colorectal cancer. A prospective multicenter study in Finland. Dis Colon Rectum *38*, 588-593.

Michaelis,C., Ciosk,R., and Nasmyth,K. (1997). Cohesins: chromosomal proteins that prevent premature separation of sister chromatids. Cell *91*, 35-45.

Michel,L.S., Liberal,V., Chatterjee,A., Kirchwegger,R., Pasche,B., Gerald,W., Dobles,M., Sorger,P.K., Murty,V.V., and Benezra,R. (2001). MAD2 haplo-insufficiency causes premature anaphase and chromosome instability in mammalian cells. Nature *409*, 355-359.

Millband,D.N., Campbell,L., and Hardwick,K.G. (2002). The awesome power of multiple model systems: interpreting the complex nature of spindle checkpoint signaling. Trends Cell Biol. *12*, 205-209.

Millband,D.N. and Hardwick,K.G. (2002). Fission yeast Mad3p is required for Mad2p to inhibit the anaphase-promoting complex and localizes to kinetochores in a Bub1p-, Bub3p-, and Mph1p-dependent manner. Mol. Cell Biol. *22*, 2728-2742.

Miyoshi,Y., Iwao,K., Egawa,C., and Noguchi,S. (2001). Association of centrosomal kinase STK15/BTAK mRNA expression with chromosomal instability in human breast cancers. Int. J. Cancer *92*, 370-373.

Modrek,B., Resch,A., Grasso,C., and Lee,C. (2001). Genome-wide detection of alternative splicing in expressed sequences of human genes. Nucleic. Acids. Res *29*, 2850-2859.

Molinari,M. (2000). Cell cycle checkpoints and their inactivation in human cancer [In Process Citation]. Cell Prolif *33*, 261-274.

Muir,E.G., Bell,A.J., and Barlow,K.A. (1967). Multiple primary carcinomata of the colon, duodenum, and larynx associated with kerato-acanthomata of the face. Br J Surg *54*, 191-195.

Munemitsu,S., Souza,B., Muller,O., Albert,I., Rubinfeld,B., and Polakis,P. (1994). The APC gene product associates with microtubules in vivo and promotes their assembly in vitro. Cancer Res *54*, 3676-3681.

Murray,A.W. (1995). The genetics of cell cycle checkpoints. Curr. Opin. Genet. Dev. *5*, 5-11.

Musacchio,A. and Hardwick,K.G. (2002). The spindle checkpoint: structural insights into dynamic signalling. Nat. Rev. Mol. Cell Biol. *3*, 731-741.

Muscat,J.E., Stellman,S.D., and Wynder,E.L. (1994). Nonsteroidal antiinflammatory drugs and colorectal cancer. Cancer *74*, 1847-1854.

Nabetani,A., Koujin,T., Tsutsumi,C., Haraguchi,T., and Hiraoka,Y. (2001). A conserved protein, Nuf2, is implicated in connecting the centromere to the spindle during chromosome segregation: a link between the kinetochore function and the spindle checkpoint. Chromosoma *110*, 322-334.

Nakamura,M., Zhou,X.Z., and Lu,K.P. (2001). Critical role for the EB1 and APC interaction in the regulation of microtubule polymerization. Curr Biol *11*, 1062-1067.

Nakayama,K., Nagahama,H., Minamishima,Y.A., Matsumoto,M., Nakamichi,I., Kitagawa,K., Shirane,M., Tsunematsu,R., Tsukiyama,T., Ishida,N., Kitagawa,M., and Hatakeyama,S. (2000). Targeted disruption of Skp2 results in accumulation of cyclin E and p27(Kip1), polyploidy and centrosome overduplication. EMBO J *19*, 2069-2081.

Nasmyth,K. (1996). At the heart of the budding yeast cell cycle. Trends Genet. *12*, 405-412.

Nicklas,R.B. (1997). How cells get the right chromosomes. Science *275*, 632-637.

Nicklas,R.B., Ward,S.C., and Gorbsky,G.J. (1995). Kinetochore chemistry is sensitive to tension and may link mitotic forces to a cell cycle checkpoint. J. Cell Biol. *130*, 929-939.

Nigg,E.A. (2001). Cell cycle regulation by protein kinases and phosphatases. Ernst. Schering. Res. Found. Workshop 19-46.

Nishisho,I., Nakamura,Y., Miyoshi,Y., Miki,Y., Ando,H., Horii,A., Koyama,K., Utsunomiya,J., Baba,S., and Hedge,P. (1991). Mutations of chromosome 5q21 genes in FAP and colorectal cancer patients. Science *253*, 665-669.

Nowak,M.A., Komarova,N.L., Sengupta,A., Jallepalli,P.V., Shih,I., Vogelstein,B., and Lengauer,C. (2002). The role of chromosomal instability in tumor initiation. Proc. Natl. Acad. Sci. U. S. A *99*, 16226-16231.

Nowell,P.C. (1976). The clonal evolution of tumor cell populations. Science *194*, 23-28.

O'Driscoll,M. and Jeggo,P.A. (2003). Clinical Impact of ATR Checkpoint Signalling Failure in Humans. Cell Cycle *2*, 194-195.

Ohshima,K., Haraoka,S., Yoshioka,S., Hamasaki,M., Fujiki,T., Suzumiya,J., Kawasaki,C., Kanda,M., and Kikuchi,M. (2000). Mutation analysis of mitotic checkpoint genes (hBUB1 and hBUBR1) and microsatellite instability in adult T-cell leukemia/lymphoma. Cancer Lett *158*, 141-150.

Olesen,S.H., Thykjaer,T., and Orntoft,T.F. (2001). Mitotic checkpoint genes hBUB1, hBUB1B, hBUB3 and TTK in human bladder cancer, screening for mutations and loss of heterozygosity. Carcinogenesis *22*, 813-815.

Orr-Weaver,T.L. and Weinberg,R.A. (1998). A checkpoint on the road to cancer [news; comment]. Nature *392*, 223-224.

Ouyang,B., Knauf,J.A., Ain,K., Nacev,B., and Fagin,J.A. (2002). Mechanisms of aneuploidy in thyroid cancer cell lines and tissues: evidence for mitotic checkpoint dysfunction without mutations in BUB1 and BUBR1. Clin. Endocrinol. (Oxf) *56*, 341-350.

Ouyang,B., Lan,Z., Meadows,J., Pan,H., Fukasawa,K., Li,W., and Dai,W. (1998). Human Bub1: a putative spindle checkpoint kinase closely linked to cell proliferation. Cell Growth Differ *9*, 877-885.

Pangilinan,F., Li,Q., Weaver,T., Lewis,B.C., Dang,C.V., and Spencer,F. (1997). Mammalian BUB1 protein kinases: map positions and in vivo expression. Genomics *46*, 379-388.

Pangilinan,F. and Spencer,F. (1996). Abnormal kinetochore structure activates the spindle assembly checkpoint in budding yeast. Mol. Biol. Cell *7*, 1195-1208.

Parkin,D.M., Pisani,P., and Ferlay,J. (1999). Global cancer statistics. CA Cancer J Clin *49*, 33-64, 1.

Paulovich,A.G., Toczyski,D.P., and Hartwell,L.H. (1997). When checkpoints fail. Cell *88*, 315-321.

Peinado,M.A., Malkhosyan,S., Velazquez,A., and Perucho,M. (1992). Isolation and characterization of allelic losses and gains in colorectal tumors by arbitrarily primed polymerase chain reaction. Proc Natl Acad Sci U S A *89*, 10065-10069.

Peltomaki,P. (2001). Deficient DNA mismatch repair: a common etiologic factor for colon cancer. Hum Mol Genet *10*, 735-740.

Peltomaki,P. (2001). DNA mismatch repair and cancer. Mutat Res *488*, 77-85.

Percy,M.J., Myrie,K.A., Neeley,C.K., Azim,J.N., Ethier,S.P., and Petty,E.M. (2000). Expression and mutational analyses of the human MAD2L1 gene in breast cancer cells. Genes Chromosomes Cancer *29*, 356-362.

Peter,M., Castro,A., Lorca,T., Le Peuch,C., Magnaghi-Jaulin,L., Doree,M., and Labbe,J.C. (2001). The APC is dispensable for first meiotic anaphase in Xenopus oocytes. Nat. Cell Biol. *3*, 83-87.

Peters,J.M. (2002). The anaphase-promoting complex: proteolysis in mitosis and beyond. Mol. Cell *9*, 931-943.

Pfleger,C.M., Salic,A., Lee,E., and Kirschner,M.W. (2001). Inhibition of Cdh1-APC by the MAD2-related protein MAD2L2: a novel mechanism for regulating Cdh1. Genes Dev. *15*, 1759-1764.

Philips,A.V. and Cooper,T.A. (2000). RNA processing and human disease. Cell Mol Life Sci. *57*, 235-249.

Pihan,G.A., Purohit,A., Wallace,J., Malhotra,R., Liotta,L., and Doxsey,S.J. (2001). Centrosome defects can account for cellular and genetic changes that characterize prostate cancer progression. Cancer Res. *61*, 2212-2219.

Pihan,G.A., Wallace,J., Zhou,Y., and Doxsey,S.J. (2003). Centrosome abnormalities and chromosome instability occur together in pre-invasive carcinomas. Cancer Res. *63*, 1398-1404.

Pines,J. and Rieder,C.L. (2001). Re-staging mitosis: a contemporary view of mitotic progression. Nat. Cell Biol. *3*, E3-E6.

Potter,J.D. (1999). Colorectal cancer: molecules and populations. J. Natl. Cancer Inst. *91*, 916-932.

Raff,J.W., Jeffers,K., and Huang,J.Y. (2002). The roles of Fzy/Cdc20 and Fzr/Cdh1 in regulating the destruction of cyclin B in space and time. J. Cell Biol. *157*, 1139-1149.

Rieder,C.L. and Khodjakov,A. (1997). Mitosis and checkpoints that control progression through mitosis in vertebrate somatic cells. Prog. Cell Cycle Res. *3:301-12.*, 301-312.

Rieder,C.L. and Salmon,E.D. (1998). The vertebrate cell kinetochore and its roles during mitosis. Trends Cell Biol. *8*, 310-318.

Risques,R.A., Moreno,V., Marcuello,E., Petriz,J., Cancelas,J.A., Sancho,F.J., Torregrosa,A., Capella,G., and Peinado,M.A. (2001). Redefining the significance of aneuploidy in the prognostic assessment of colorectal cancer. Lab Invest *81*, 307-315.

Roberts,B.T., Farr,K.A., and Hoyt,M.A. (1994). The Saccharomyces cerevisiae checkpoint gene BUB1 encodes a novel protein kinase. Mol. Cell Biol *14*, 8282-8291.

Rosin-Arbesfeld,R., Townsley,F., and Bienz,M. (2000). The APC tumour suppressor has a nuclear export function. Nature. *406*, 1009-1012.

Ru,H.Y., Chen,R.L., Lu,W.C., and Chen,J.H. (2002). hBUB1 defects in leukemia and lymphoma cells. Oncogene *21*, 4673-4679.

Rudner,A.D. and Murray,A.W. (1996). The spindle assembly checkpoint. Curr Opin Cell Biol *8*, 773-780.

Sablina,A.A., Chumakov,P.M., Levine,A.J., and Kopnin,B.P. (2001). p53 activation in response to microtubule disruption is mediated by integrin-Erk signaling. Oncogene *20*, 899-909.

Saeki,A., Tamura,S., Ito,N., Kiso,S., Matsuda,Y., Yabuuchi,I., Kawata,S., and Matsuzawa,Y. (2002). Frequent impairment of the spindle assembly checkpoint in hepatocellular carcinoma. Cancer *94*, 2047-2054.

Salisbury,J.L., Whitehead,C.M., Lingle,W.L., and Barrett,S.L. (1999). Centrosomes and cancer. Biol Cell *91*, 451-460.

Sankila,R., Aaltonen,L.A., Jarvinen,H.J., and Mecklin,J.P. (1996). Better survival rates in patients with MLH1-associated hereditary colorectal cancer. Gastroenterology *110*, 682-687.

Sarafan-Vasseur,N., Lamy,A., Bourguignon,J., Pessot,F.L., Hieter,P., Sesboue,R., Bastard,C., Frebourg,T., and Flaman,J.M. (2002). Overexpression of B-type cyclins alters chromosomal segregation. Oncogene *21*, 2051-2057.

Sato,M., Sekido,Y., Horio,Y., Takahashi,M., Saito,H., Minna,J.D., Shimokata,K., and Hasegawa,Y. (2000). Infrequent mutation of the hBUB1 and hBUBR1 genes in human lung cancer. Jpn. J Cancer Res. *91*, 504-509.

Sato,N., Mizumoto,K., Nakamura,M., Maehara,N., Minamishima,Y.A., Nishio,S., Nagai,E., and Tanaka,M. (2001). Correlation between centrosome abnormalities and chromosomal instability in human pancreatic cancer cells. Cancer Genet. Cytogenet. *126*, 13-19.

Schaar,B.T., Chan,G.K., Maddox,P., Salmon,E.D., and Yen,T.J. (1997). CENP-E function at kinetochores is essential for chromosome alignment. J Cell Biol *139*, 1373-1382.

Schneider,S., Wildhardt,G., Ludwig,R., and Royer-Pokora,B. (1993). Exon skipping due to a mutation in a donor splice site in the WT-1 gene is associated with Wilms' tumor and severe genital malformations. Hum Genet *91*, 599-604.

Schwab,M.S., Roberts,B.T., Gross,S.D., Tunquist,B.J., Taieb,F.E., Lewellyn,A.L., and Maller,J.L. (2001). Bub1 is activated by the protein kinase p90(Rsk) during Xenopus oocyte maturation. Curr. Biol. *11*, 141-150.

Scolnick,D.M. and Halazonetis,T.D. (2000). Chfr defines a mitotic stress checkpoint that delays entry into metaphase [see comments]. Nature *406*, 430-435.

Seeley,T.W., Wang,L., and Zhen,J.Y. (1999). Phosphorylation of human MAD1 by the BUB1 kinase in vitro. Biochem. Biophys. Res. Commun. *257*, 589-595.

Seike,M., Gemma,A., Hosoya,Y., Hosomi,Y., Okano,T., Kurimoto,F., Uematsu,K., Takenaka,K., Yoshimura,A., Shibuya,M., Ui-Tei,K., and Kudoh,S. (2002). The promoter region of the human BUBR1 gene and its expression analysis in lung cancer. Lung Cancer *38*, 229-234.

Shannon,K.B., Canman,J.C., and Salmon,E.D. (2002). Mad2 and BubR1 function in a single checkpoint pathway that responds to a loss of tension. Mol. Biol. Cell *13*, 3706-3719.

Sharp-Baker,H. and Chen,R.H. (2001). Spindle checkpoint protein Bub1 is required for kinetochore localization of Mad1, Mad2, Bub3, and CENP-E, independently of its kinase activity. J. Cell Biol. *153*, 1239-1250.

Shonn,M.A., McCarroll,R., and Murray,A.W. (2000). Requirement of the spindle checkpoint for proper chromosome segregation in budding yeast meiosis. Science *289*, 300-303.

Sieber,O.M., Lipton,L., Crabtree,M., Heinimann,K., Fidalgo,P., Phillips,R.K., Bisgaard,M.L., Orntoft,T.F., Aaltonen,L.A., Hodgson,S.V., Thomas,H.J., and Tomlinson,I.P. (2003). Multiple colorectal adenomas, classic adenomatous polyposis, and germ-line mutations in MYH. N. Engl. J. Med. *348*, 791-799.

Signoretti,S., Di Marcotullio,L., Richardson,A., Ramaswamy,S., Isaac,B., Rue,M., Monti,F., Loda,M., and Pagano,M. (2002). Oncogenic role of the ubiquitin ligase subunit Skp2 in human breast cancer. J. Clin. Invest *110*, 633-641.

Sigrist,S., Jacobs,H., Stratmann,R., and Lehner,C.F. (1995). Exit from mitosis is regulated by Drosophila fizzy and the sequential destruction of cyclins A, B and B3. EMBO J. *14*, 4827-4838.

Sironi,L., Mapelli,M., Knapp,S., De Antoni,A., Jeang,K.T., and Musacchio,A. (2002). Crystal structure of the tetrameric Mad1-Mad2 core complex: implications of a 'safety belt' binding mechanism for the spindle checkpoint. EMBO J. *21*, 2496-2506.

Skoufias,D.A., Andreassen,P.R., Lacroix,F.B., Wilson,L., and Margolis,R.L. (2001). Mammalian mad2 and bub1/bubR1 recognize distinct spindle-attachment and kinetochore-tension checkpoints. Proc. Natl. Acad. Sci. U. S. A *98*, 4492-4497.

Smith,A.P., Gimenez-Abian,J.F., and Clarke,D.J. (2002). DNA-damage-independent checkpoints: yeast and higher eukaryotes. Cell Cycle *1*, 16-33.

Smith,K.J., Levy,D.B., Maupin,P., Pollard,T.D., Vogelstein,B., and Kinzler,K.W. (1994). Wild-type but not mutant APC associates with the microtubule cytoskeleton. Cancer Res *54*, 3672-3675.

Spencer,F., Gerring,S.L., Connelly,C., and Hieter,P. (1990). Mitotic chromosome transmission fidelity mutants in Saccharomyces cerevisiae. Genetics *124*, 237-249.

Stark,L.A., Din,F.V., Zwacka,R.M., and Dunlop,M.G. (2001). Aspirin-induced activation of the NF-kappaB signaling pathway: a novel mechanism for aspirin-mediated apoptosis in colon cancer cells. FASEB J *15*, 1273-1275.

Stearns,T. and Botstein,D. (1988). Unlinked noncomplementation: isolation of new conditional-lethal mutations in each of the tubulin genes of Saccharomyces cerevisiae. Genetics *119*, 249-260.

Stearns,T., Hoyt,M.A., and Botstein,D. (1990). Yeast mutants sensitive to antimicrotubule drugs define three genes that affect microtubule function. Genetics *124*, 251-262.

Stemmermann,G.N. (1970). Patterns of disease among Japanese living in Hawaii. Arch Environ Health *20*, 266-273.

Stern,B.M. and Murray,A.W. (2001). Lack of tension at kinetochores activates the spindle checkpoint in budding yeast. Curr. Biol. *11*, 1462-1467.

Strunnikov,A.V., Larionov,V.L., and Koshland,D. (1993). SMC1: an essential yeast gene encoding a putative head-rod-tail protein is required for nuclear division and defines a new ubiquitous protein family. J. Cell Biol. *123*, 1635-1648.

Stucke,V.M., Sillje,H.H., Arnaud,L., and Nigg,E.A. (2002). Human Mps1 kinase is required for the spindle assembly checkpoint but not for centrosome duplication. EMBO J. *21*, 1723-1732.

Sudakin,V., Chan,G.K., and Yen,T.J. (2001). Checkpoint inhibition of the APC/C in HeLa cells is mediated by a complex of BUBR1, BUB3, CDC20, and MAD2. J Cell Biol. *154*, 925-936.

Sudakin,V., Ganoth,D., Dahan,A., Heller,H., Hershko,J., Luca,F.C., Ruderman,J.V., and Hershko,A. (1995). The cyclosome, a large complex containing cyclin-selective ubiquitin ligase activity, targets cyclins for destruction at the end of mitosis. Mol. Biol. Cell *6*, 185-197.

Sullivan,M., Lehane,C., and Uhlmann,F. (2001). Orchestrating anaphase and mitotic exit: separase cleavage and localization of Slk19. Nat. Cell Biol. *3*, 771-777.

Takahashi,T., Haruki,N., Nomoto,S., Masuda,A., Saji,S., and Osada,H. (1999). Identification of frequent impairment of the mitotic checkpoint and molecular analysis of the mitotic checkpoint genes, hsMAD2 and p55CDC, in human lung cancers. Oncogene *18*, 4295-4300.

Takahashi,T., Sano,B., Nagata,T., Kato,H., Sugiyama,Y., Kunieda,K., Kimura,M., Okano,Y., and Saji,S. (2003). Polo-like kinase 1 (PLK1) is overexpressed in primary colorectal cancers. Cancer Sci. *94*, 148-152.

Tanaka,T., Fuchs,J., Loidl,J., and Nasmyth,K. (2000). Cohesin ensures bipolar attachment of microtubules to sister centromeres and resists their precocious separation. Nat Cell Biol *2*, 492-499.

Tanaka,T.U. (2002). Bi-orienting chromosomes on the mitotic spindle. Curr. Opin. Cell Biol. *14*, 365-371.

Tang,Z., Bharadwaj,R., Li,B., and Yu,H. (2001). Mad2-Independent inhibition of APCCdc20 by the mitotic checkpoint protein BubR1. Dev Cell *1*, 227-237.

Taylor,S.S., Ha,E., and McKeon,F. (1998). The human homologue of Bub3 is required for kinetochore localization of Bub1 and a Mad3/Bub1-related protein kinase. J Cell Biol *142*, 1-11.

Taylor,S.S., Hussein,D., Wang,Y., Elderkin,S., and Morrow,C.J. (2001). Kinetochore localisation and phosphorylation of the mitotic checkpoint components Bub1 and BubR1 are differentially regulated by spindle events in human cells. J. Cell Sci. *114*, 4385-4395.

Taylor,S.S. and McKeon,F. (1997). Kinetochore localization of murine Bub1 is required for normal mitotic timing and checkpoint response to spindle damage. Cell *89*, 727-735.

Teraoka,S.N., Telatar,M., Becker-Catania,S., Liang,T., Onengut,S., Tolun,A., Chessa,L., Sanal,O., Bernatowska,E., Gatti,R.A., and Concannon,P. (1999). Splicing defects in the ataxia-telangiectasia gene, ATM: underlying mutations and consequences. Am. J. Hum. Genet. *64*, 1617-1631.

Tighe,A., Johnson,V.L., Albertella,M., and Taylor,S.S. (2001) Aneuploid colon cancer cells have a robust spindle checkpoint. EMBO Rep. 2001. Jul. ;2. (7.):609. - 14. *2*, 609-614.

Tomlinson,I. and Bodmer,W. (1999). Selection, the Mutation rate and cancer: ensuring that the tail does not wag the dog. Nature Medicine *5*, 11-12.

Tomlinson,I.P., Novelli,M.R., and Bodmer,W.F. (1996). The mutation rate and cancer. Proc Natl Acad Sci U S A *93*, 14800-14803.

Tomonaga,T., Nagao,K., Kawasaki,Y., Furuya,K., Murakami,A., Morishita,J., Yuasa,T., Sutani,T., Kearsey,S.E., Uhlmann,F., Nasmyth,K., and Yanagida,M. (2000). Characterization of fission yeast cohesin: essential anaphase proteolysis of Rad21 phosphorylated in the S phase. Genes Dev. *14*, 2757-2770.

Torrance,C.J., Agrawal,V., Vogelstein,B., and Kinzler,K.W. (2001). Use of isogenic human cancer cells for high-throughput screening and drug discovery. Nat. Biotechnol. *19*, 940-945.

Torre,D. (1968). Multiple sebaceous tumors. Arch Dermatol *98*, 549-551.

Toyoda,Y., Furuya,K., Goshima,G., Nagao,K., Takahashi,K., and Yanagida,M. (2002). Requirement of chromatid cohesion proteins rad21/scc1 and mis4/scc2 for normal spindle-kinetochore interaction in fission yeast. Curr. Biol. *12*, 347-358.

Trock,B., Lanza,E., and Greenwald,P. (1990). Dietary fiber, vegetables, and colon cancer: critical review and meta-analyses of the epidemiologic evidence. J. Natl. Cancer Inst. *82*, 650-661.

Tsukasaki,K., Miller,C.W., Greenspun,E., Eshaghian,S., Kawabata,H., Fujimoto,T., Tomonaga,M., Sawyers,C., Said,J.W., and Koeffler,H.P. (2001). Mutations in the mitotic check point gene, MAD1L1, in human cancers. Oncogene. *20*, 3301-3305.

Tunquist,B.J., Schwab,M.S., Chen,L.G., and Maller,J.L. (2002). The spindle checkpoint kinase bub1 and cyclin e/cdk2 both contribute to the establishment of meiotic metaphase arrest by cytostatic factor. Curr. Biol. *12*, 1027-1033.

Turcot,J.T., Despres,J.-P., and St.Pierre,F. (1959). Malignant tumours of the central nervous system associated with familial polyposis of the colon: report of two cases. Dis Colon Rectum *2*, 465-468.

Uhlmann,F., Lottspeich,F., and Nasmyth,K. (1999). Sister-chromatid separation at anaphase onset is promoted by cleavage of the cohesin subunit Scc1. Nature *400*, 37-42.

Uhlmann,F., Wernic,D., Poupart,M.A., Koonin,E.V., and Nasmyth,K. (2000). Cleavage of cohesin by the CD clan protease separin triggers anaphase in yeast [In Process Citation]. Cell *103*, 375-386.

Uzawa,S., Samejima,I., Hirano,T., Tanaka,K., and Yanagida,M. (1990). The fission yeast cut1+ gene regulates spindle pole body duplication and has homology to the budding yeast ESP1 gene. Cell *62*, 913-925.

Vanoosthuyse,V. and Hardwick,K.G. (2003). The complexity of Bub1 regulation--phosphorylation, phosphorylation, phosphorylation. Cell Cycle *2*, 118-119.

Viallard,J.F., Lacombe,F., Belloc,F., Pellegrin,J.L., and Reiffers,J. (2001). [Molecular mechanisms controlling the cell cycle: fundamental aspects and implications for oncology]. Cancer Radiother. *5*, 109-129.

Visintin,R., Prinz,S., and Amon,A. (1997). CDC20 and CDH1: a family of substrate-specific activators of APC-dependent proteolysis. Science *278*, 460-463.

Vogelstein,B., Fearon,E.R., Hamilton,S.R., Kern,S.E., Preisinger,A.C., Leppert,M., Nakamura,Y., White,R., Smits,A.M., and Bos,J.L. (1988). Genetic alterations during colorectal-tumor development. N. Engl. J Med *319*, 525-532.

Waizenegger,I., Gimenez-Abian,J.F., Wernic,D., and Peters,J.M. (2002). Regulation of human separase by securin binding and autocleavage. Curr. Biol. *20;12*, 1368-1378.

Waizenegger,I., Hauf,S., Meinke,A., and Peters,J. (2000). Two distinct pathways remove mammalian cohesion from chromosome arms in prophase and from centromeres in anaphase. Cell *103*, 399-410.

Wang,Q., Moyret-Lalle,C., Couzon,F., Surbiguet-Clippe,C., Saurin,J.C., Lorca,T., Navarro,C., and Puisieux,A. (2003a). Alterations of anaphase-promoting complex genes in human colon cancer cells. Oncogene *22*, 1486-1490.

Wang,X., Jin,D.Y., Ng,R.W., Feng,H., Wong,Y.C., Cheung,A.L., and Tsao,S.W. (2002). Significance of MAD2 expression to mitotic checkpoint control in ovarian cancer cells. Cancer Res. *62*, 1662-1668.

Wang,X., Jin,D.Y., Wong,H.L., Feng,H., Wong,Y.C., and Tsao,S.W. (2003b). MAD2-induced sensitization to vincristine is associated with mitotic arrest and Raf/Bcl-2 phosphorylation in nasopharyngeal carcinoma cells. Oncogene *22*, 109-116.

Wang,X., Jin,D.Y., Wong,Y.C., Cheung,A.L., Chun,A.C., Lo,A.K., Liu,Y., and Tsao,S.W. (2000a). Correlation of defective mitotic checkpoint with aberrantly reduced expression of MAD2 protein in nasopharyngeal carcinoma cells. Carcinogenesis *21*, 2293-2297.

Wang,Y., Cortez,D., Yazdi,P., Neff,N., Elledge,S.J., and Qin,J. (2000b). BASC, a super complex of BRCA1-associated proteins involved in the recognition and repair of aberrant DNA structures. Genes Dev *14*, 927-939.

Wang,Y., Hu,F., and Elledge,S.J. (2000c). The Bfa1/Bub2 GAP complex comprises a universal checkpoint required to prevent mitotic exit [In Process Citation]. Curr Biol *10*, 1379-1382.

Warren,C.D., Brady,D.M., Johnston,R.C., Hanna,J.S., Hardwick,K.G., and Spencer,F.A. (2002). Distinct chromosome segregation roles for spindle checkpoint proteins. Mol. Biol. Cell *13*, 3029-3041.

Wassmann,K., Liberal,V., and Benezra,R. (2003). Mad2 phosphorylation regulates its association with Mad1 and the APC/C. EMBO J. *22*, 797-806.

Waters,J.C., Chen,R.H., Murray,A.W., and Salmon,E.D. (1998). Localization of Mad2 to kinetochores depends on microtubule attachment, not tension. J Cell Biol *141*, 1181-1191.

Weinstein,J. (1997). Cell cycle-regulated expression, phosphorylation, and degradation of p55Cdc. A mammalian homolog of CDC20/Fizzy/slp1. J Biol Chem *272*, 28501-28511.

Weiss,E. and Winey,M. (1996). The Saccharomyces cerevisiae spindle pole body duplication gene MPS1 is part of a mitotic checkpoint. J Cell Biol *132*, 111-123.

Weitzel,D.H. and Vandre,D.D. (2000). Differential spindle assembly checkpoint response in human lung adenocarcinoma cells. Cell Tissue Res. *300*, 57-65.

Willett,W. (1989). The search for the causes of breast and colon cancer. Nature *338*, 389-394.

Willett,W.C., Stampfer,M.J., Colditz,G.A., Rosner,B.A., and Speizer,F.E. (1990). Relation of meat, fat, and fiber intake to the risk of colon cancer in a prospective study among women. N Engl J Med *323*, 1664-1672.

Williams,C.S., Mann,M., and DuBois,R.N. (1999). The role of cyclooxygenases in inflammation, cancer, and development. Oncogene *18*, 7908-7916.

Winey,M., Goetsch,L., Baum,P., and Byers,B. (1991). MPS1 and MPS2: novel yeast genes defining distinct steps of spindle pole body duplication. J. Cell Biol. *114*, 745-754.

Wojcik,E., Basto,R., Serr,M., Scaerou,F., Karess,R., and Hays,T. (2001). Kinetochore dynein: its dynamics and role in the transport of the Rough deal checkpoint protein. Nat. Cell Biol. *3*, 1001-1007.

Wolf,D.A. and Jackson,P.K. (1998). Cell cycle: oiling the gears of anaphase. Curr Biol *8*, R636-R639.

Wu,H., Lan,Z., Li,W., Wu,S., Weinstein,J., Sakamoto,K.M., and Dai,W. (2000). p55CDC/hCDC20 is associated with BUBR1 and may be a downstream target of the spindle checkpoint kinase. Oncogene *19*, 4557-4562.

Wu,X., Zhao,H., Wei,Q., Amos,C.I., Zhang,K., Guo,Z., Qiao,Y., Hong,W.K., and Spitz,M.R. (2003). XPA polymorphism associated with reduced lung cancer risk and a modulating effect on nucleotide excision repair capacity. Carcinogenesis *24*, 505-509.

Yam,C.H., Fung,T.K., and Poon,R.Y. (2002). Cyclin A in cell cycle control and cancer. Cell Mol. Life Sci. *59*, 1317-1326.

Yamaguchi,S., Decottignies,A., and Nurse,P. (2003). Function of Cdc2p-dependent Bub1p phosphorylation and Bub1p kinase activity in the mitotic and meiotic spindle checkpoint. EMBO J. *22*, 1075-1087.

Yamaguchi,S., Murakami,H., and Okayama,H. (1997). A WD repeat protein controls the cell cycle and differentiation by negatively regulating Cdc2/B-type cyclin complexes. Mol. Biol. Cell *8*, 2475-2486.

Yamashita,Y.M., Nakaseko,Y., Samejima,I., Kumada,K., Yamada,H., Michaelson,D., and Yanagida,M. (1996). 20S cyclosome complex formation and proteolytic activity inhibited by the cAMP/PKA pathway. Nature *384*, 276-279.

Yao,X., Abrieu,A., Zheng,Y., Sullivan,K.F., and Cleveland,D.W. (2000). CENP-E forms a link between attachment of spindle microtubules to kinetochores and the mitotic checkpoint [In Process Citation]. Nat Cell Biol *2*, 484-491.

Ye,X. and Adams,P.D. (2003). Coordination of s-phase events and genome stability. Cell Cycle *2*, 185-187.

Yen,T.J. (2002). The complexity of APC/C regulation: location, location, location. Cell Cycle *1*, 260-261.

Yen,T.J., Compton,D.A., Wise,D., Zinkowski,R.P., Brinkley,B.R., Earnshaw,W.C., and Cleveland,D.W. (1991). CENP-E, a novel human centromere-associated protein required for progression from metaphase to anaphase. EMBO J *10*, 1245-1254.

Yoon,D.S., Wersto,R.P., Zhou,W., Chrest,F.J., Garrett,E.S., Kwon,T.K., and Gabrielson,E. (2002). Variable levels of chromosomal instability and mitotic spindle checkpoint defects in breast cancer. Am. J. Pathol. *161*, 391-397.

Yu,H. (2002). Regulation of APC-Cdc20 by the spindle checkpoint. Curr. Opin. Cell Biol. *14*, 706-714.

Yu,J., Zhang,L., Hwang,P.M., Rago,C., Kinzler,K.W., and Vogelstein,B. (1999). Identification and classification of p53-regulated genes [In Process Citation]. Proc Natl Acad Sci U S A *96*, 14517-14522.

Zhang,F., White,R.L., and Neufeld,K.L. (2001). Cell density and phosphorylation control the subcellular localization of adenomatous polyposis coli protein. Mol. Cell Biol. *21*, 8143-8156.

Zhou,H., Kuang,J., Zhong,L., Kuo,W.L., Gray,J.W., Sahin,A., Brinkley,B.R., and Sen,S. (1998). Tumour amplified kinase STK15/BTAK induces centrosome amplification, aneuploidy and transformation [see comments]. Nat Genet *20*, 189-193.

Zhou,J., Panda,D., Landen,J.W., Wilson,L., and Joshi,H.C. (2002a). Minor alteration of microtubule dynamics causes loss of tension across kinetochore pairs and activates the spindle checkpoint. J. Biol. Chem. *277*, 17200-17208.

Zhou,J., Yao,J., and Joshi,H.C. (2002b). Attachment and tension in the spindle assembly checkpoint. J. Cell Sci. *115*, 3547-3555.

Zou,H., McGarry,T.J., Bernal,T., and Kirschner,M.W. (1999). Identification of a vertebrate sister-chromatid separation inhibitor involved in transformation and tumorigenesis. Science *285*, 418-422.

Zumbrunn,J., Kinoshita,K., Hyman,A.A., and Nathke,I.S. (2001). Binding of the adenomatous polyposis coli protein to microtubules increases microtubule stability and is regulated by GSK3 beta phosphorylation. Curr. Biol. *11*, 44-49.

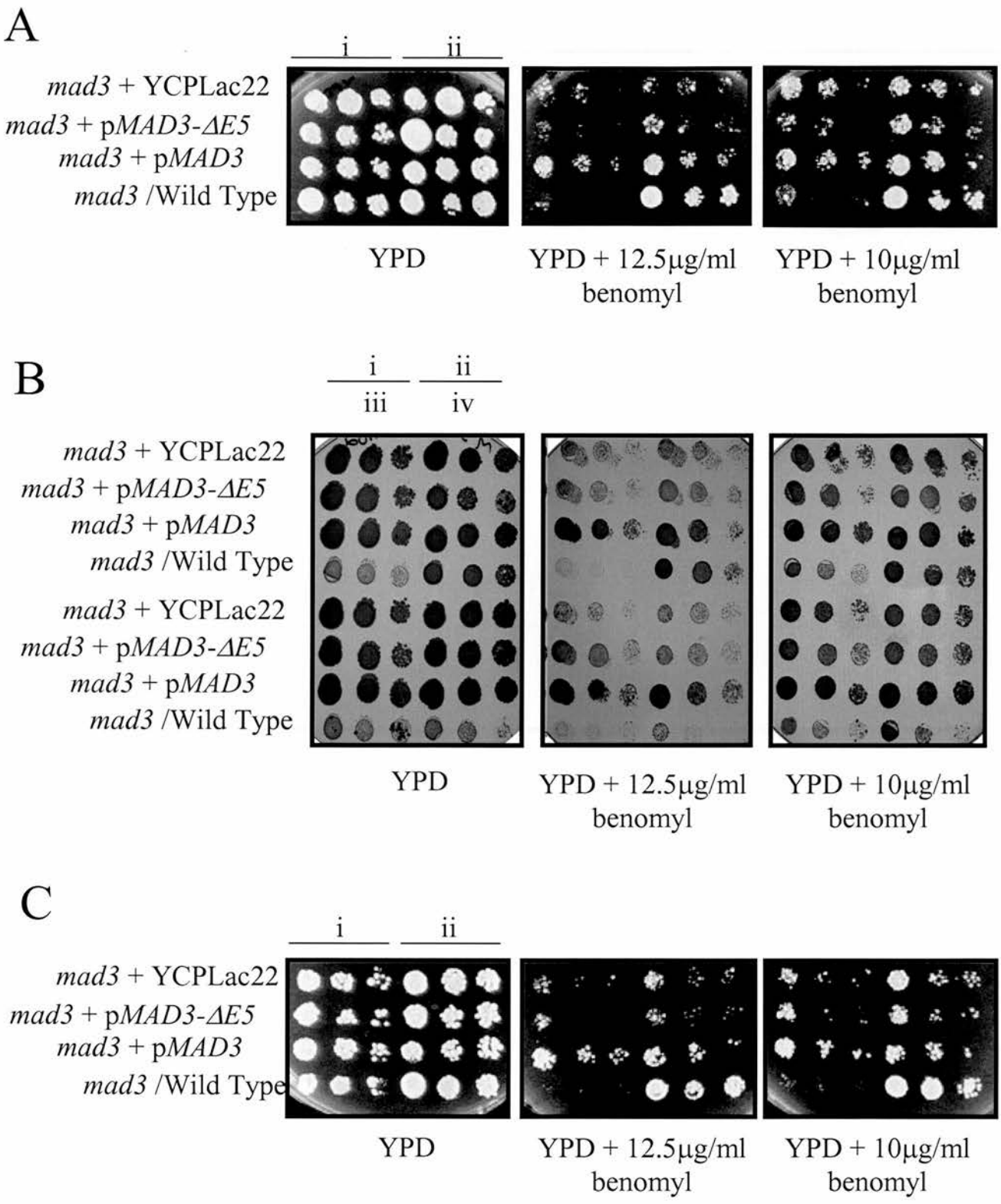

Appendix 1: MAD3 benomyl sensitivity assay

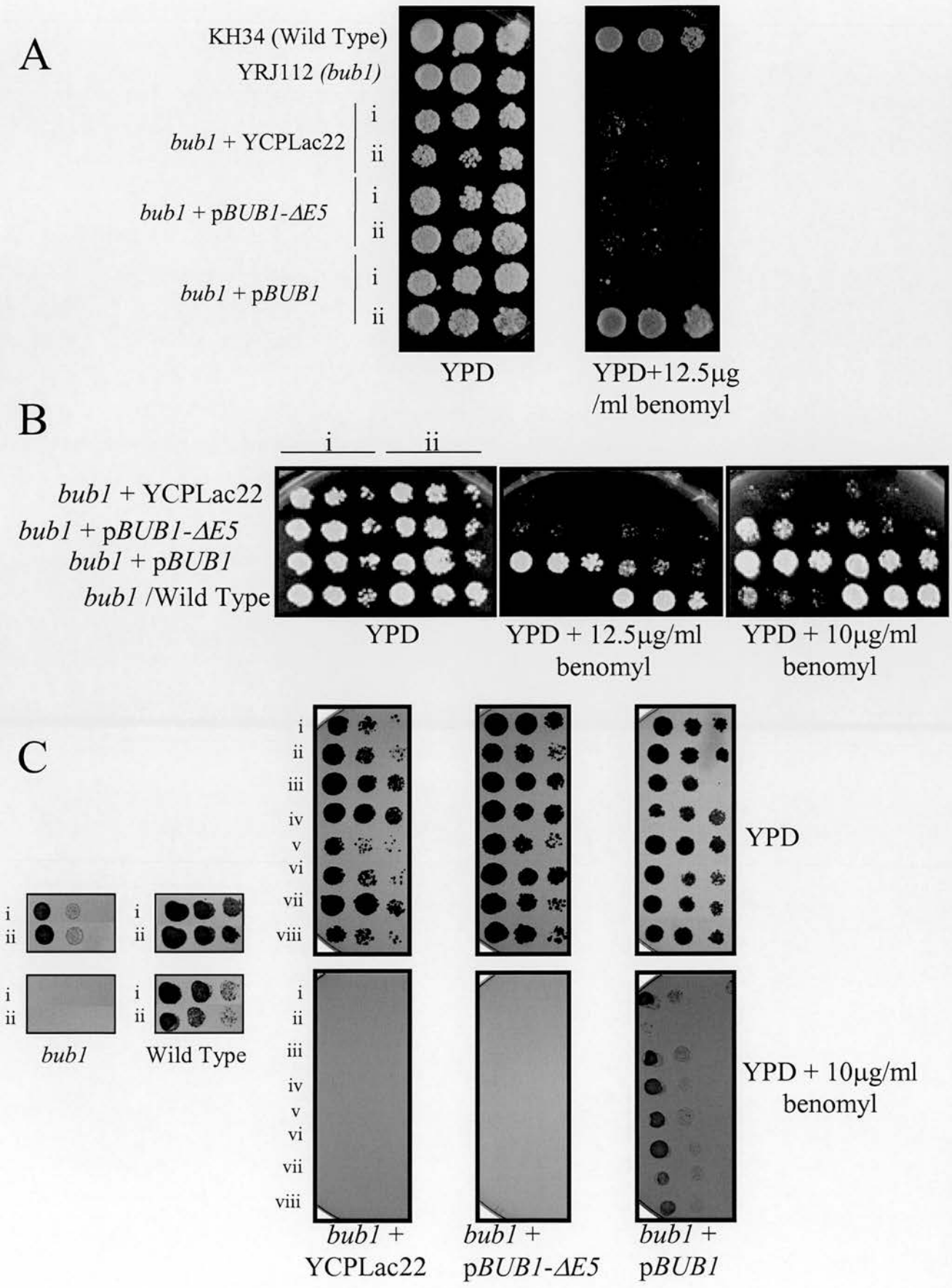

Appendix 2: BUB1 benomyl sensitivity assay

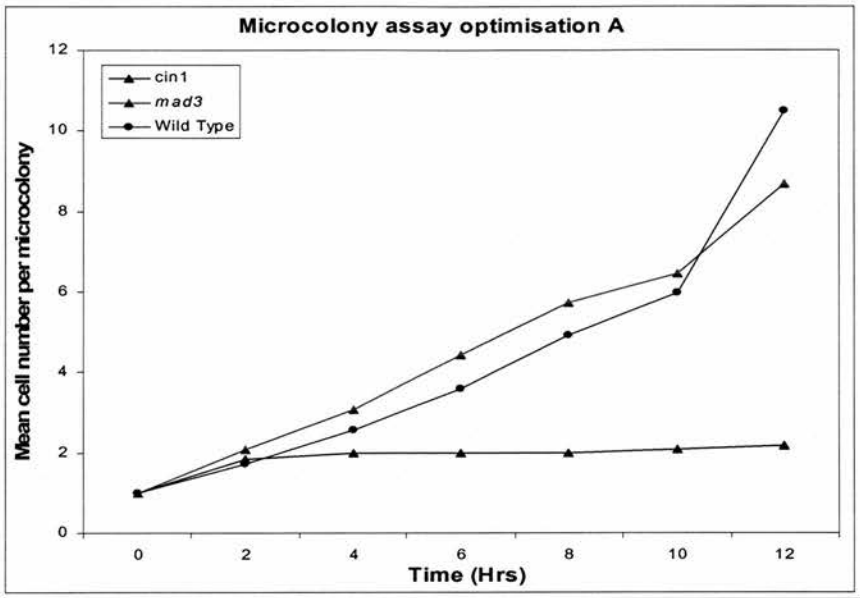

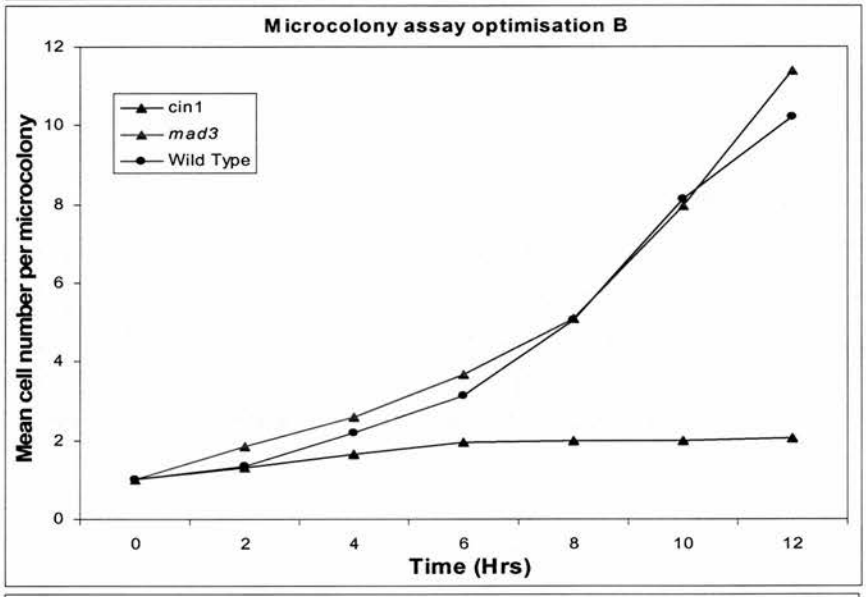

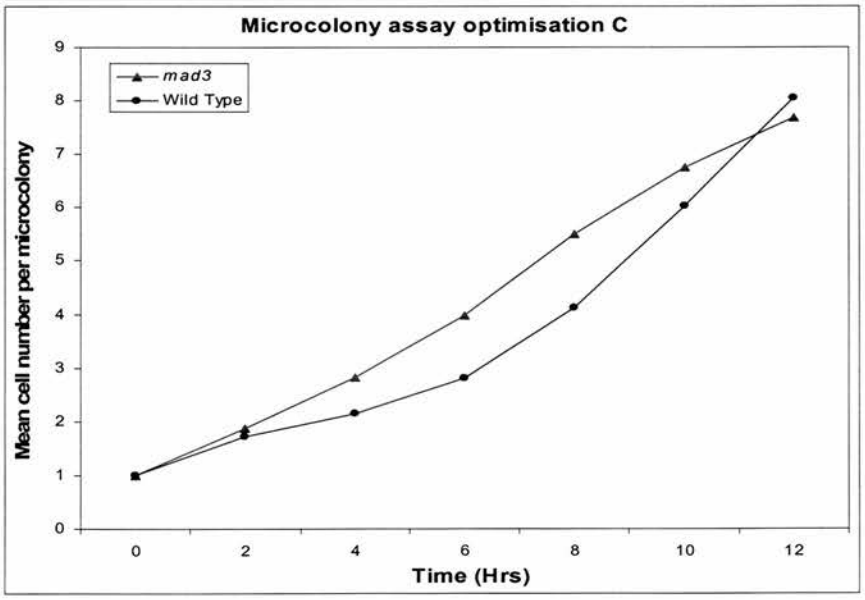

Appendix 3 Microcolony assay optimisation

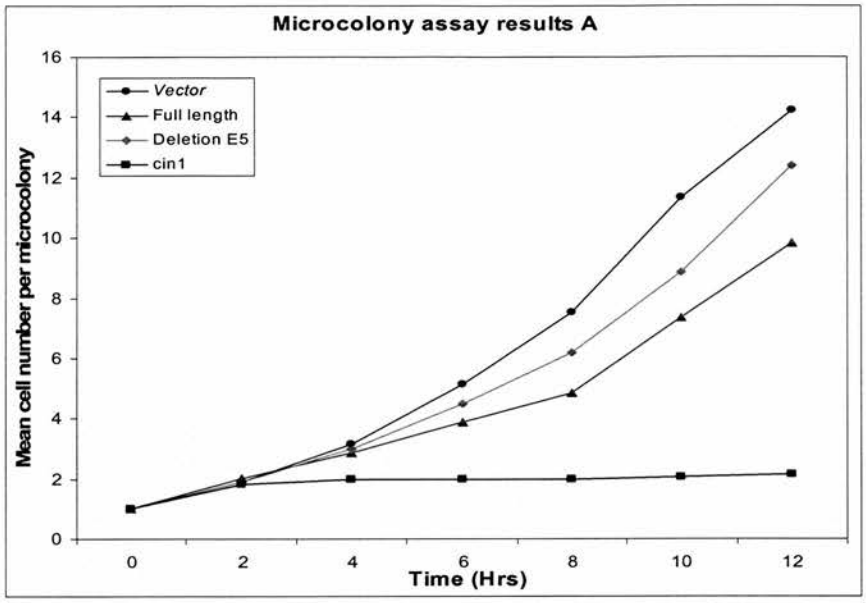

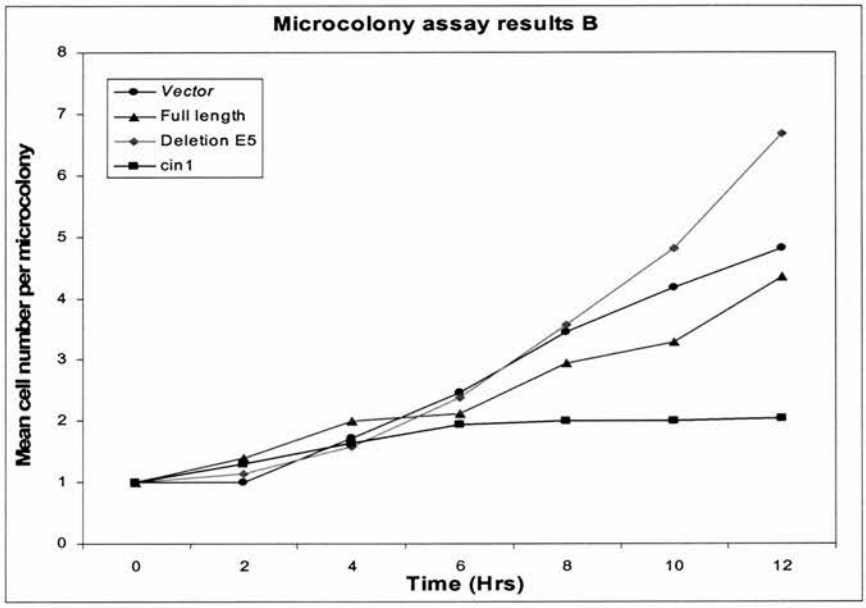

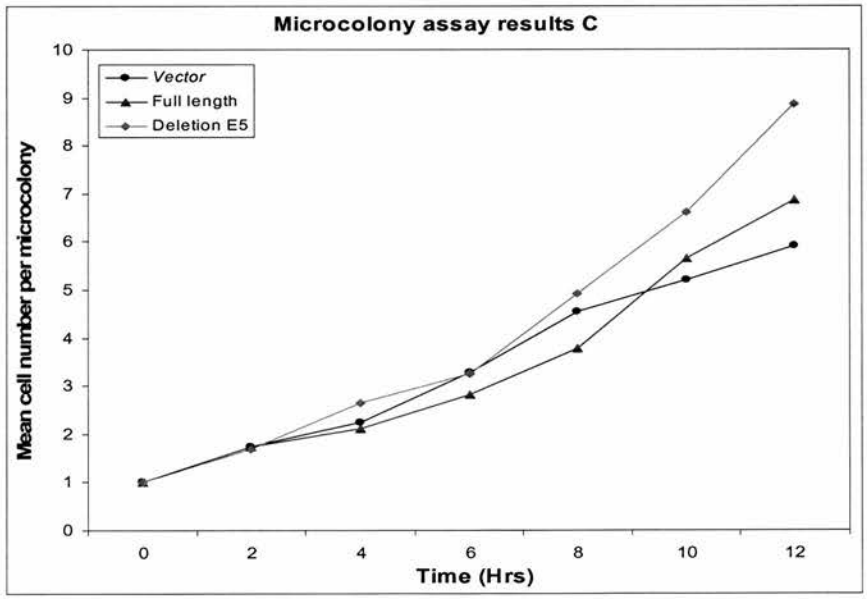

Appendix 4 MAD3 microcolony assay results

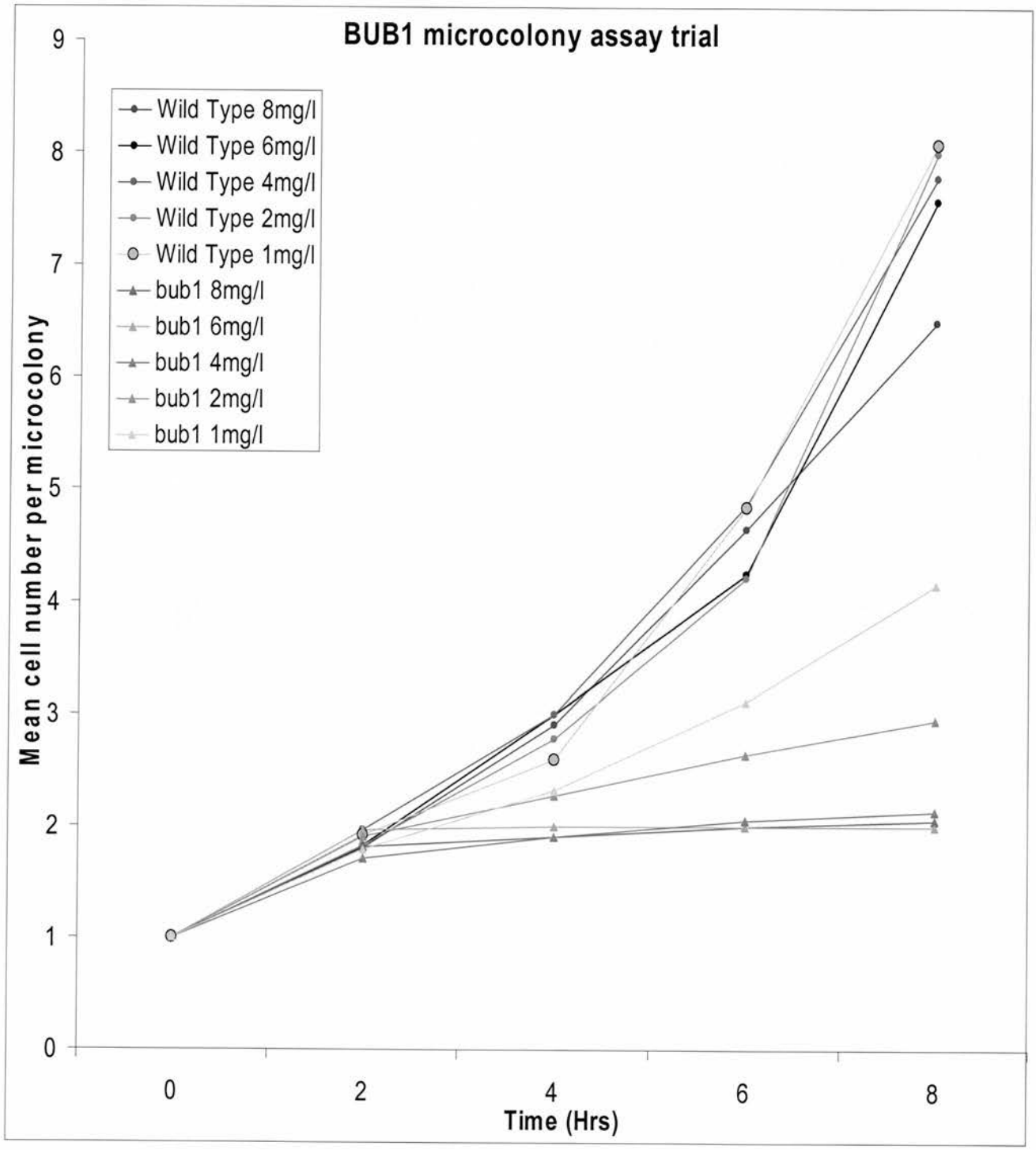

Appendix 5 BUB1 microcolony assay trial

The bub1 null strain shows an extreme sensitivity to benomyl, even at low concentrations. Thus it was decided that the microcolony assay is unable to differentiate between spindle checkpoint defects and other defects causing a benomyl sensitivity phenotype in BUB1 mutants making it unsuitable for assessing Bub1p spindle checkpoint function.

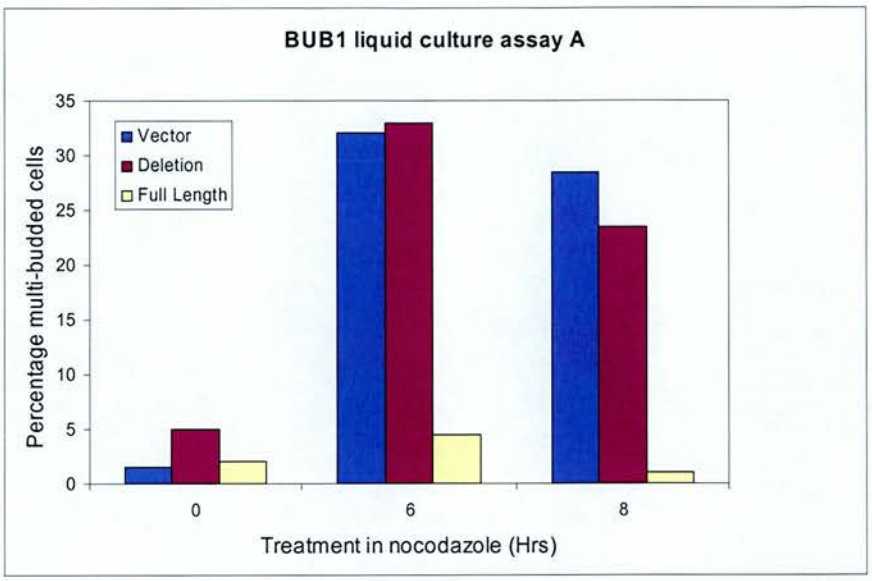

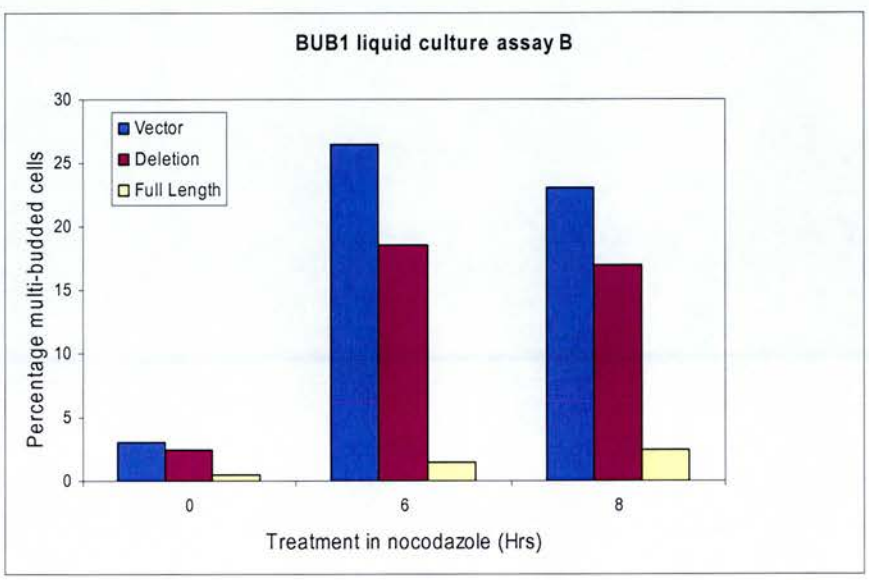

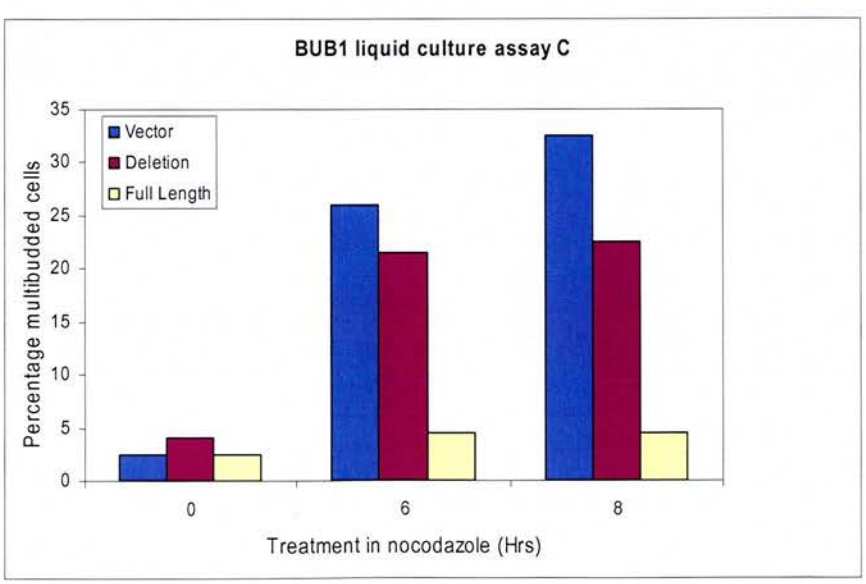

Appendix 6: BUB1 liquid culture assay results

Experiment	Time (Hrs)	Comparison	χ^2 / t	Probability
Liquid Culture A	0	Vector/Full length	0.148	0.700
	0	Vector/ΔE5	**4.031**	**0.0447**
	0	ΔE5/ Full length	2.765	0.0963
	6	Vector/Full length	**65.257**	**$6.573*10^{-16}$**
	6	Vector/ΔE5	0.0879	0.767
	6	ΔE5/ Full length	**69.312**	**$8.406*10^{-17}$**
	8	Vector/Full length	**72.725**	**$1.490*10^{-17}$**
	8	Vector/ΔE5	2.003	0.157
	8	ΔE5/ Full length	**54.737**	**$1.378*10^{-13}$**
Liquid Culture B	0	Vector/Full length	3.701	0.0544
	0	Vector/ΔE5	0.0962	0.756
	0	ΔE5/ Full length	2.749	0.0973
	6	Vector/Full length	**62.004**	**$3.428*10^{-15}$**
	6	Vector/ΔE5	**5.172**	**0.0230**
	6	ΔE5/ Full length	**36.125**	**$1.851*10^{-9}$**
	8	Vector/Full length	**44.243**	**$2.901*10^{-11}$**
	8	Vector/ΔE5	3	0.0833
	8	ΔE5/ Full length	**26.788**	**$2.271*10^{-7}$**
Liquid Culture C	0	Vector/Full length	0	1
	0	Vector/ΔE5	0.740	0.390
	0	ΔE5/ Full length	0.740	0.390
	6	Vector/Full length	**43.614**	**$4.000*10^{-11}$**
	6	Vector/ΔE5	1.624	0.203
	6	ΔE5/ Full length	**30.042**	**$4.229*10^{-8}$**
	8	Vector/Full length	**67.267**	**$2.371*10^{-16}$**
	8	Vector/ΔE5	**8.081**	**0.00447**
	8	ΔE5/ Full length	**32.877**	**$9.819*10^{-9}$**
Mantel Haenszel analysis of A, B and C	0	Vector/Full length	0.346	0.729
	0	Vector/ΔE5	0.5161	0.606
	0	ΔE5/ Full length	0.8347	0.404
	6	Vector/Full length	**2.2819**	**0.0224**
	6	Vector/ΔE5	0.3159	0.752
	6	ΔE5/ Full length	**2.120**	**0.034**
	8	Vector/Full length	**2.397**	**0.0166**
	8	Vector/ΔE5	0.567	0.571
	8	ΔE5/ Full length	**2.030**	**0.0424**

Appendix 7: BUB1 liquid culture assay Chi-squared analysis

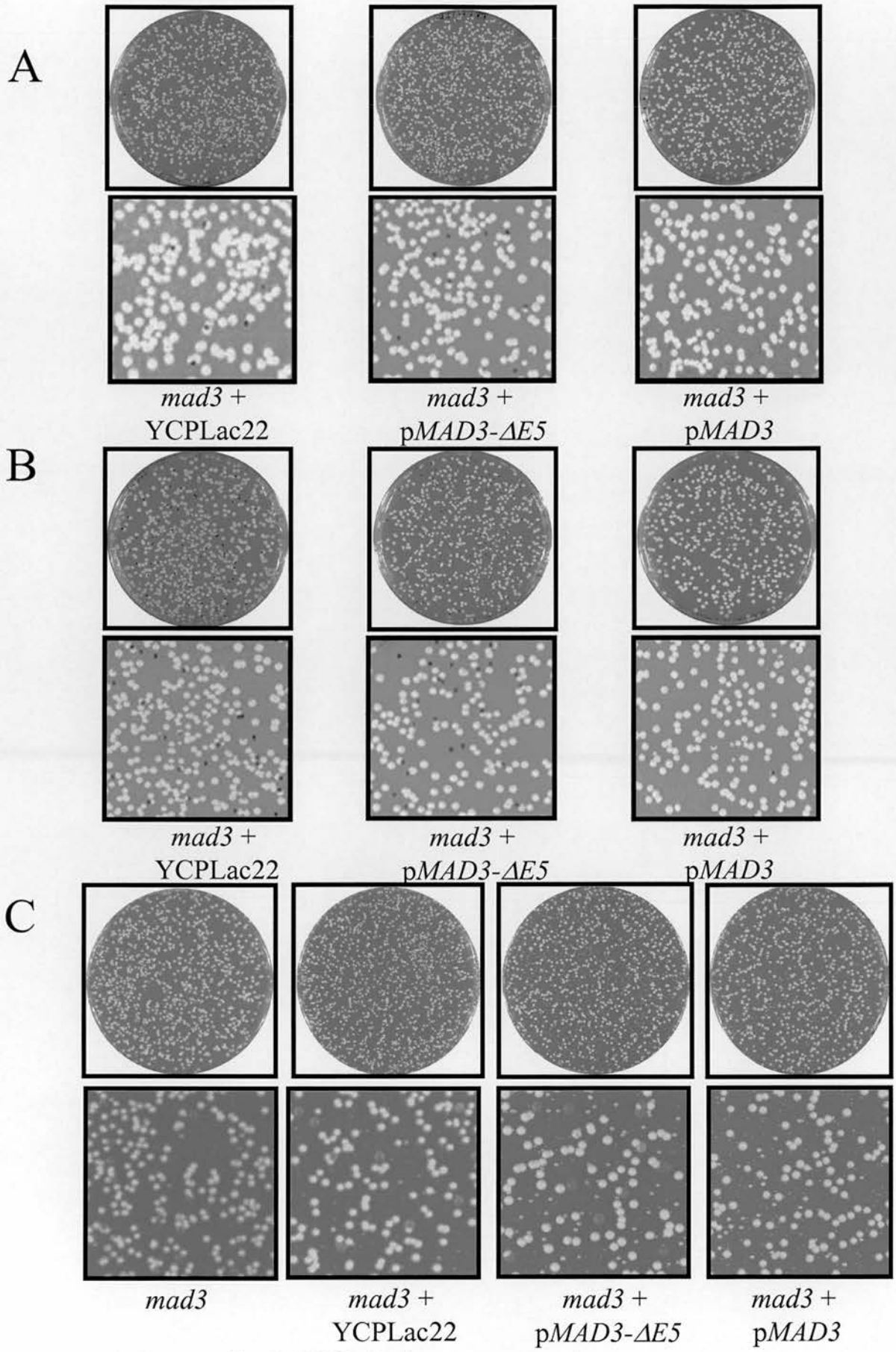

Appendix 8: MAD3 chromosome loss assay

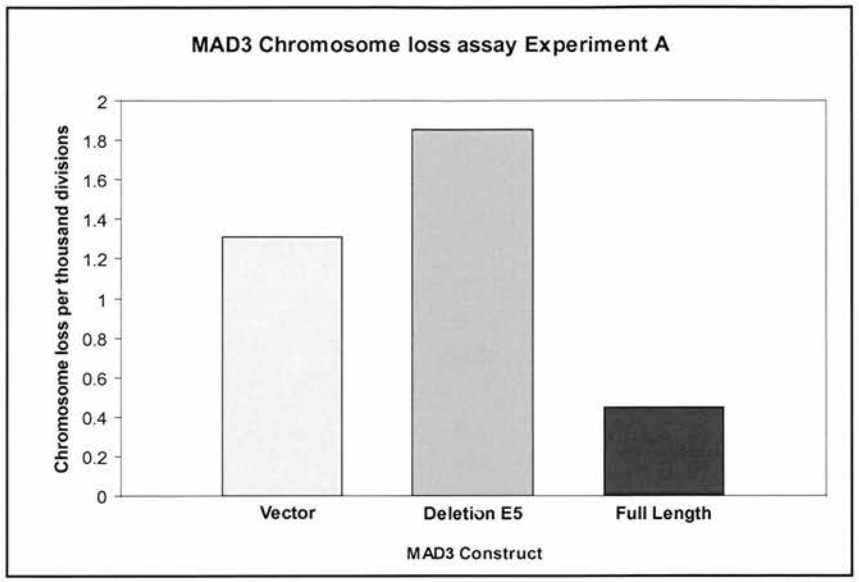

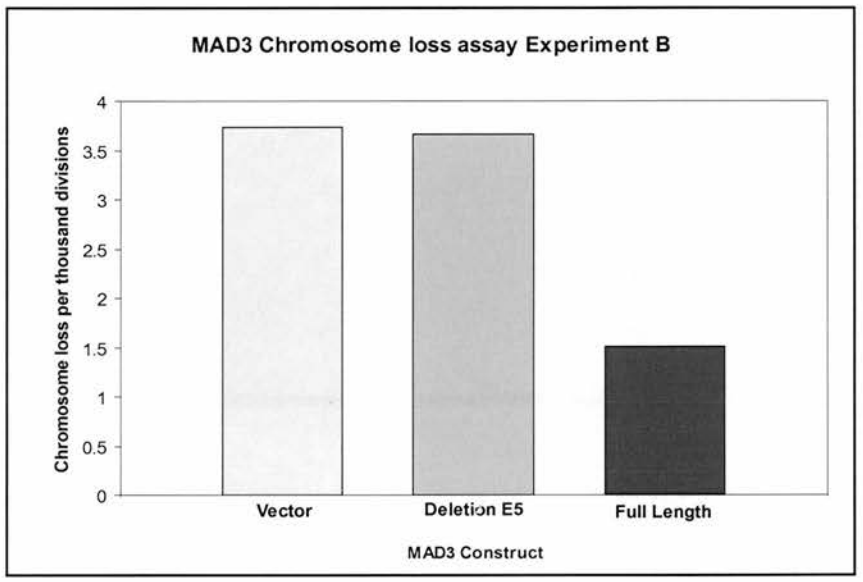

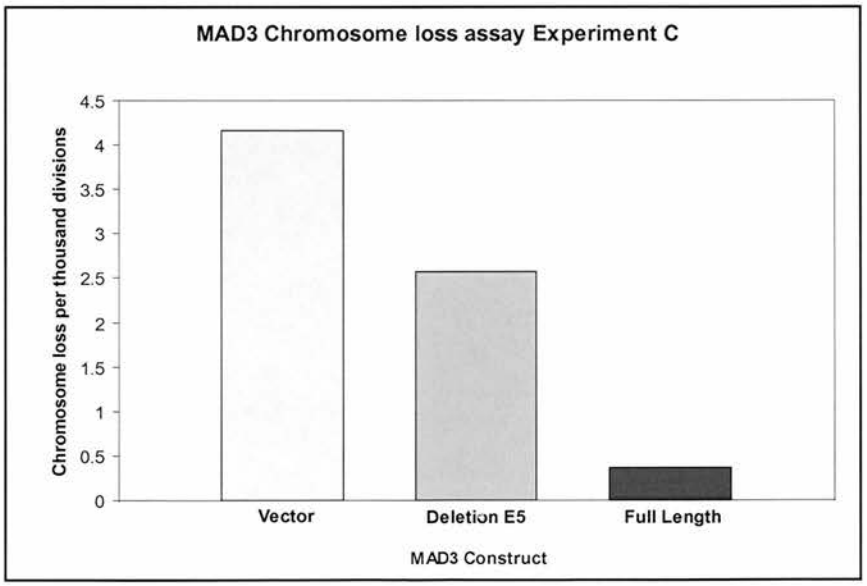

Appendix 9: MAD3 Chromosome loss assay results

Experiment	Comparison	χ^2 / t	Probability
Chromosome loss A	Vector/Full length	3.056	0.0804
	Vector/ΔE5	1.009	0.315
	ΔE5/ Full length	6.259	0.0124
Chromosome loss B	Vector/Full length	**12.579**	**0.000390**
	Vector/ΔE5	0.0137	0.907
	ΔE5/ Full length	**11.838**	**0.000580**
	Wild type/Full length	2.088	0.148
	mad3/vector	0.844	0.358
Chromosome loss C	Vector/Full length	**25.637**	**$4.120*10^{-7}$**
	Vector/ΔE5	2.315	0.128
	ΔE5/ Full length	**13.216**	**0.000278**
Mantel Haenszel analysis of A, B and C	Vector/Full length	**5.854**	**<0.0001**
	Vector/ΔE5	0.357	0.721
	ΔE5/ Full length	**5.303**	**<0.0001**

Appendix 10: MAD3 chromosome loss assay Chi-squared analysis

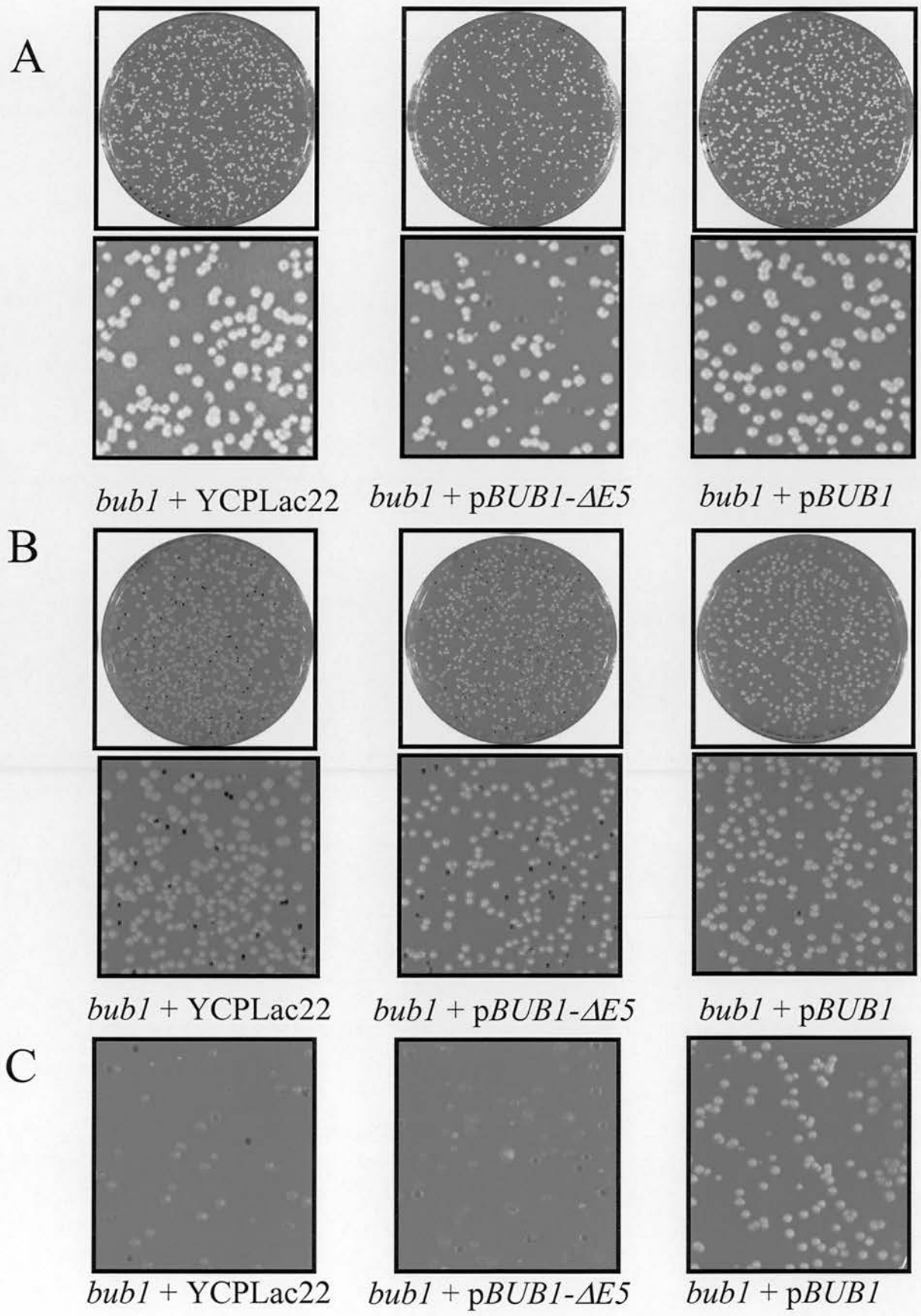

Appendix 11: BUB1 chromosome loss assays

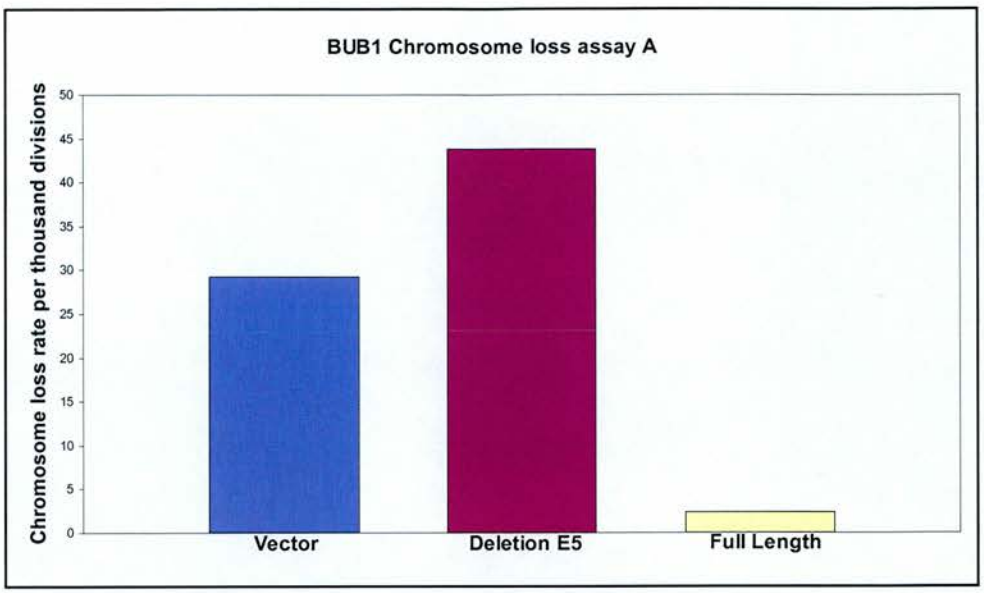

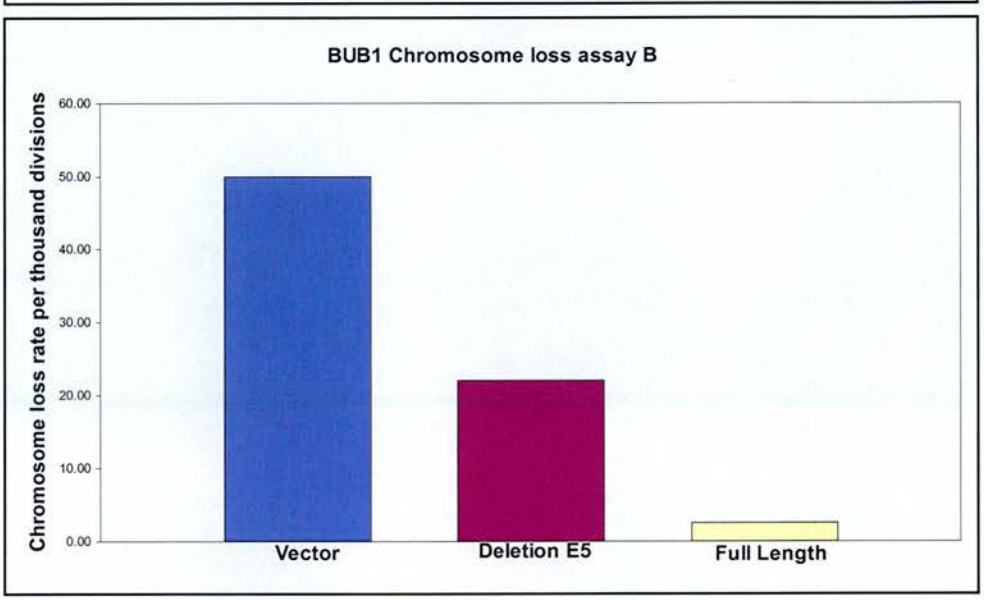

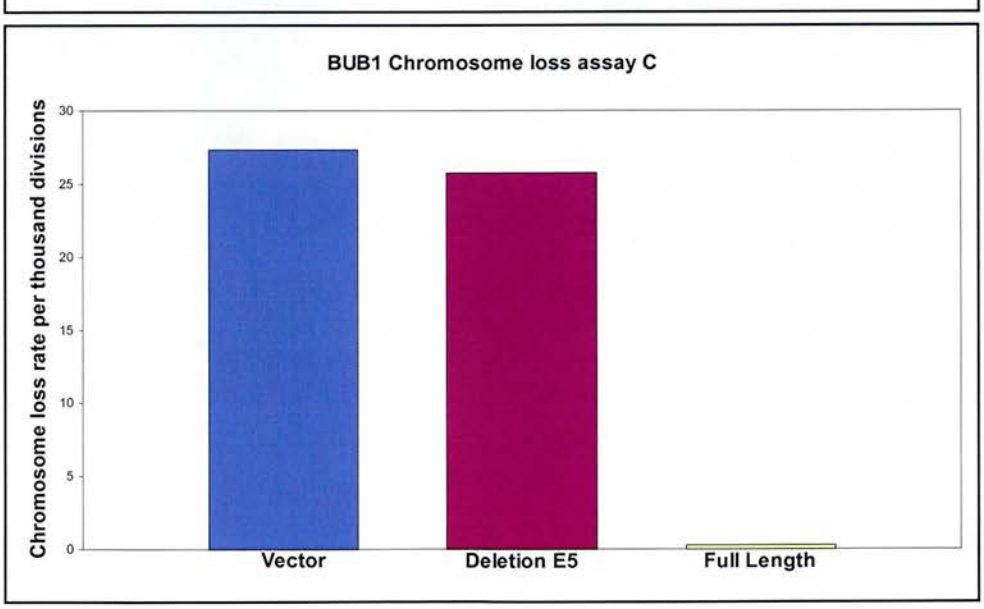

Appendix 12: BUB1 Chromosome loss assay results

Experiment	Comparison	χ^2 / t	Probability
Chromosome loss A	Vector/Full length	**94.219**	**$2.824*10^{-22}$**
	Vector/ΔE5	5.228	0.0222
	ΔE5/ Full length	**147.471**	**$6.191*10^{-34}$**
Chromosome loss B	Vector/Full length	**298.010**	**$8.940*10^{-67}$**
	Vector/ΔE5	**32.088**	**$1.474*10^{-08}$**
	ΔE5/ Full length	**114.737**	**$8.985*10^{-27}$**
Chromosome loss C	Vector/Full length	**182.833**	**$1.167*10^{-41}$**
	Vector/ΔE5	0.143	0.7058
	ΔE5/ Full length	**175.290**	**$5.176*10^{-40}$**
Mantel Haenszel analysis of A, B and C	Vector/Full length	**23.181**	**<0.0001**
	Vector/ΔE5	**2.332**	**0.0198**
	ΔE5/ Full length	**17.692**	**<0.0001**

Appendix 13: BUB1 chromosome loss assay Chi-squared analysis

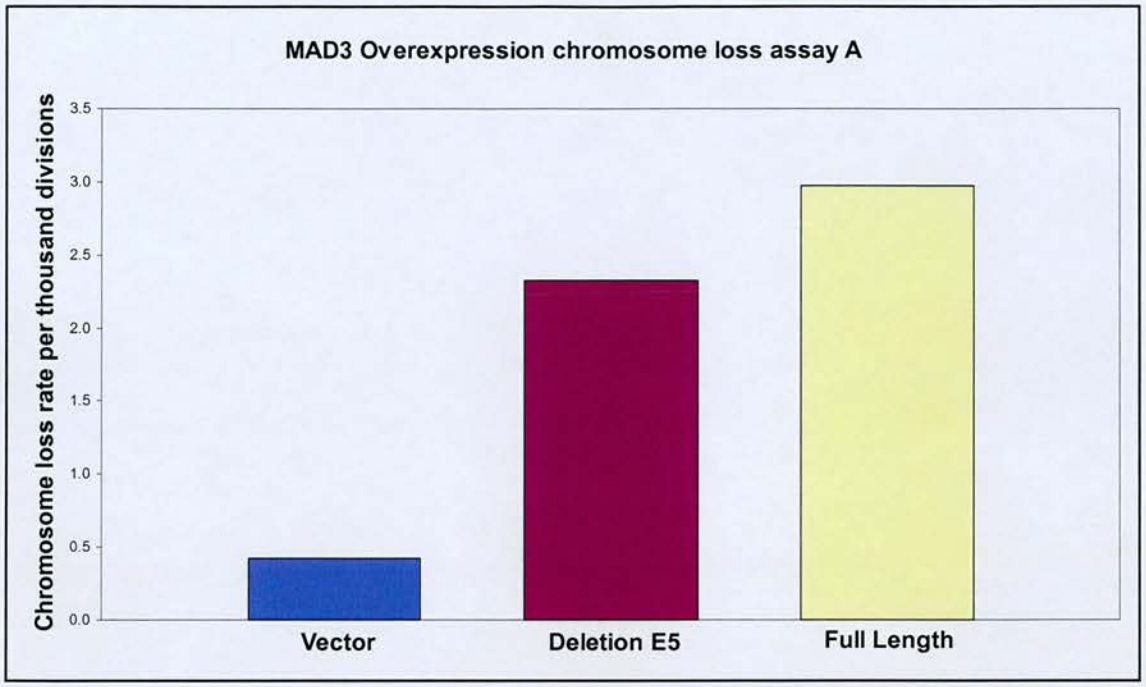

0.00134

0.392

0.000233

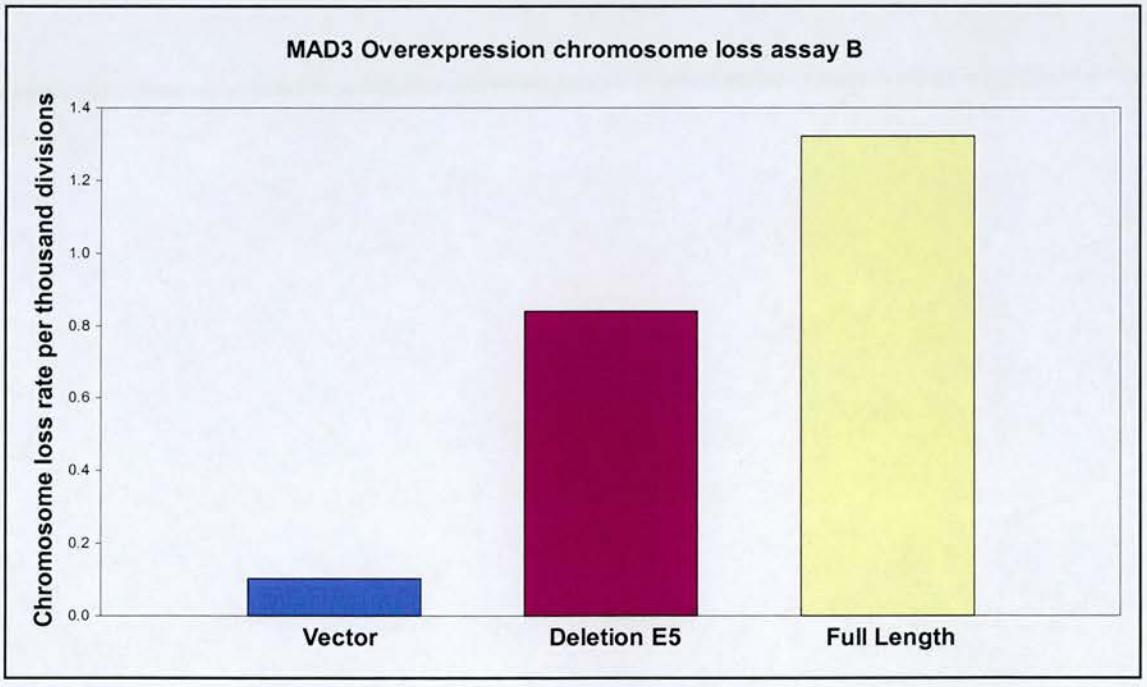

0.0237

0.41

0.00180

Appendix 14: MAD3 overexpression chromosome loss assays

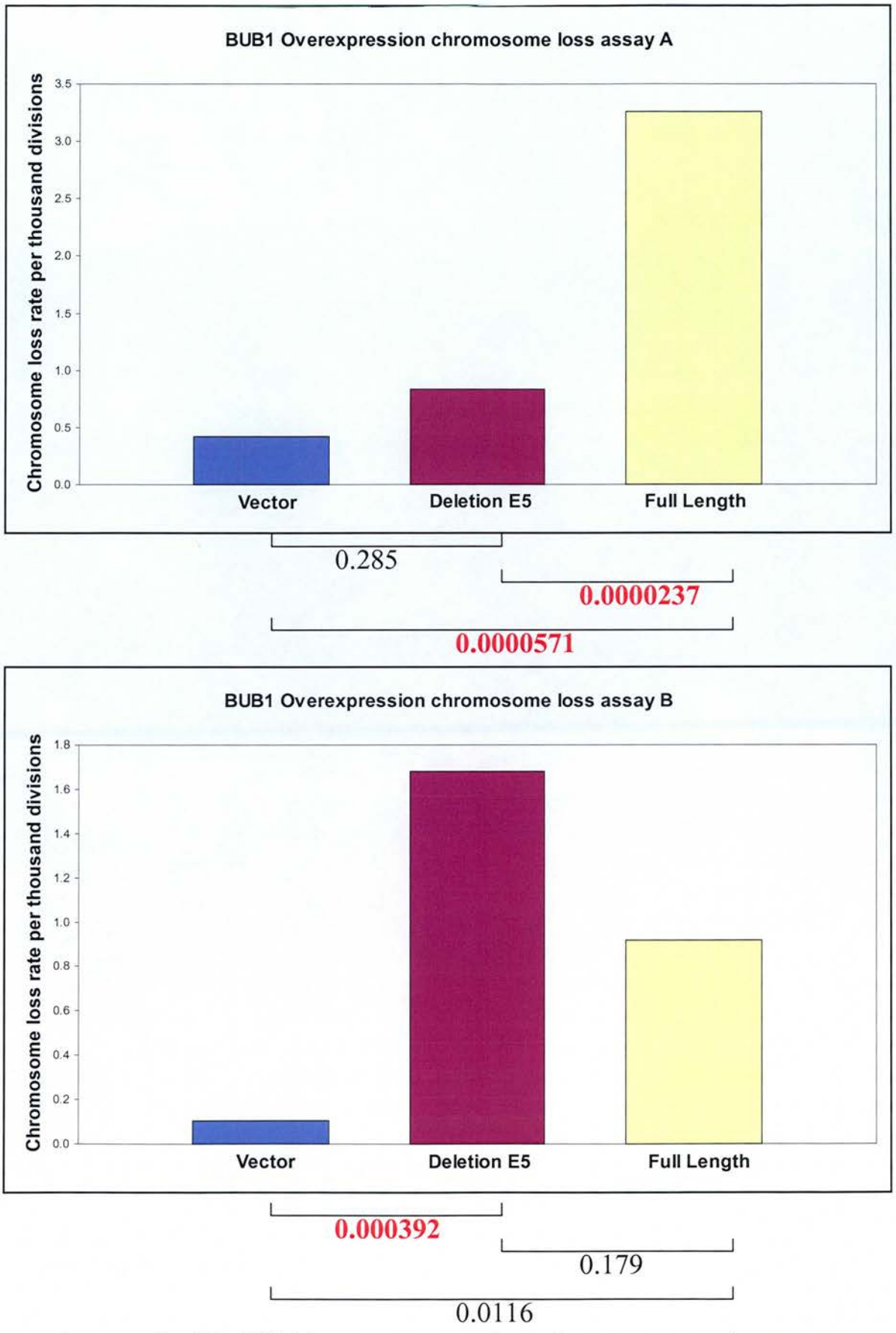

Appendix 15: BUB1 overexpression chromosome loss assays